PERMEATION THROUGH POLYMER LATEX FILMS

MALCOLM CHAINEY

A thesis submitted in partial fulfilment of the requirements for the degree of Doctor of Philosophy of the Council for National Academic Awards. The work reported in this thesis was carried out in the Department of Physical Sciences, Trent Polytechnic, Nottingham and in Physical Protection Division, Chemical Defence Establishment, Porton Down, Salisbury.

Parts of the work reported in this thesis have been presented at the Fourth International Conference on Surface and Colloid Science, Jerusalem, Israel, July 1981, the NATO Advanced Study Institute Conference on Polymer Colloids, University of Bristol, UK, July 1982 and the International Symposium on Emulsion copolymerisation and copolymers, Lyon, France, March 1984, and published in the British Polymer Journal, and Industrial and Engineering Chemistry, Product Research and Development.

March 1984

PERMEATION THROUGH POLYMER LATEX FILMS

by

MALCOLM CHAINEY

ABSTRACT

The permeation characteristics of films formed from polymer latices have been studied. Three areas of work were involved, namely preparation of polymer latices, preparation of films from these latices and determination of the film permeabilities.

A wide range of polymer latices were produced by surfactant-free emulsion polymerisation, which is known to produce a monodisperse product of controllable particle size. The kinetics of the styrene reaction were determined and compared with the predictions of several published theories.

Film forming core-shell latices were prepared by a novel 'shot-growth' technique, in which the core particles are polymerised in situ. This technique was found to produce a monodisperse product at a lower number density of core particles than required by conventional seeded growth techniques.

A freshly prepared latex contains impurities such as unreacted monomer and reaction biproducts. The traditional methods of purification, namely dialysis and ion-exchange are inefficient in the removal of some of these impurities, and can lead to further contamination. The microfiltration technique devised during this study proved to be rapid and efficient in removing contaminants.

Several techniques for preparing thin films from polymer solutions or latex dispersions reported in the literature were evaluated. After extensive trials all were rejected, as the minimum thickness of film which it was possible to cast was at least an order of magnitude larger than that required. A flash casting technique was devised and successfully employed to prepare a wide variety of thin films. Polymer films prepared by this method were characterised by scanning electron microscopy.

The gas permeabilities of homopolymer films cast from solution and latex dispersions were measured. The permeabilities of solvent cast films remained constant for the period of several months over which they were examined. The permeability coefficients of most latex films started off at a value considerably higher than that of the corresponding solvent cast film and then dropped at a rate dependent on the polymer concerned. This reduction is attributed to ageing processes occurring within the film after casting. Latex film permeability coefficients are always higher than those of solvent cast films, and this suggests that latex films never become completely homogeneous.

The permeabilities of heterogeneous films cast from blends of two homopolymer latices and from core-shell latices also diminish after casting. The rate and extent of this reduction decreases with increasing content of hard, undeformable dispersed phase.

D 58241/85

ACKNOWLEDGEMENTS

The author wishes to express his gratitude to the many people who have contributed to the work described in this thesis. First and foremost to Dr J. Hearn and Dr M.C. Wilkinson for their continued guidance during the course of their work. Thanks are also due to Trent Polytechnic and the Chemical Defence Establishment for provision of facilities and financial support. The author is grateful to the academic, technical and program advisory staff at Trent Polytechnic for advice and practical help and to the design and engineering staff at CDE who designed and built much of the equipment used. The authors thanks go also to Mrs Lyn Hart and Miss Valerie Bowden for typing this thesis and to Mrs Jill Alford who drew the diagrams.

PERMEATION THROUGH POLYMER LATEX FILMS

by

MALCOLM CHAINEY

ABSTRACT

The permeation characteristics of films formed from polymer latices have been studied. Three areas of work were involved, namely preparation of polymer latices, preparation of films from these latices and determination of the film permeabilities.

A wide range of polymer latices were produced by surfactant-free emulsion polymerisation, which is known to produce a monodisperse product of controllable particle size. The kinetics of the styrene reaction were determined and compared with the predictions of several published theories.

Film forming core-shell latices were prepared by a novel 'shot-growth' technique, in which the core particles are polymerised in situ. This technique was found to produce a monodisperse product at a lower number density of core particles than required by conventional seeded growth techniques.

A freshly prepared latex contains impurities such as unreacted monomer and reaction biproducts. The traditional methods of purification, namely dialysis and ion-exchange are inefficient in the removal of some of these impurities, and can lead to further contamination. The microfiltration technique devised during this study proved to be rapid and efficient in removing contaminants.

Several techniques for preparing thin films from polymer solutions or latex dispersions reported in the literature were evaluated. After extensive trials all were rejected, as the minimum thickness of film which it was possible to cast was at least an order of magnitude larger than that required. A flash casting technique was devised and successfully employed to prepare a wide variety of thin films. Polymer films prepared by this method were characterised by scanning electron microscopy.

The gas permeabilities of homopolymer films cast from solution and latex dispersions were measured. The permeabilities of solvent cast films remained constant for the period of several months over which they were examined. The permeability coefficients of most latex films started off at a value considerably higher than that of the corresponding solvent cast film and then dropped at a rate dependent on the polymer concerned. This reduction is attributed to ageing processes occurring within the film after casting. Latex film permeability coefficients are always higher than those of solvent cast films, and this suggests that latex films never become completely homogeneous.

The permeabilities of heterogeneous films cast from blends of two homopolymer latices and from core-shell latices also diminish after casting. The rate and extent of this reduction decreases with increasing content of hard, undeformable dispersed phase.

CONTENTS

CHAPTER I

INTRODUCTION

One of the more important features of polymeric materials is their ability to dissolve molecules of gas, vapour or liquid and allow the transport of these molecules through the solid phase. This property has many practical applications, and sometimes unwelcome repercussions.

Polymer films are widely employed as protective barriers, when, for example, metals are painted to prevent corrosion, paper is coated to render it moisture resistant, or foodstuffs are packaged to reduce their rate of deterioration. In these applications, the permeability of the film can be a major consideration. The plastics industry, in particular, has devoted considerable research to improving the barrier properties of packaging materials[1].

In the field of chemical engineering, polymer films are sometimes used to effect the separation of mixtures, e.g. the extraction of helium from natural gas, the drying of organic solvents and the desalination of seawater[2]. More recently, the feasibility of using fluorinated polymers in pollution control systems has been examined. Promising results for the removal of hydrocarbons have been obtained[3]. The degree of selectivity achieved by a polymer depends on its ability to discriminate between dissolved molecules on the basis of size, shape, polarity, charge or other factors, and this is often highly dependent on preparation, conditioning and operating conditions.

Polymer films may be used to control the rate at which a substance is released into its environment. This property is exploited by the pharmaceutical industry in the production of sustained release dosage forms[4]. A typical example is the 'cold cure' capsule, which contains tiny drug-containing polymer particles. The thickness of polymer coat controls the rate at which the drug is released from the particle. By this means, several components can be included in one capsule, and each can be released at varying rates to give the optimum therapeutic effect.

Sometimes, a polymer film may be present in situations where its limited permeability is a hindrance. This arises, for instance, when a charcoal adsorbent is coated by the binder attaching it to the fabric of protective clothing, or when

it must be coated with a hydrophilic material to make it biocompatible and hence suitable for use in clinical haemoperfusion[5]. In these cases, the polymers used must have a high permeability to the adsorbates for the charcoal to be utilised efficiently.

Polymers are manufactured by many different processes, depending on the type of polymer and the polymerisation mechanism involved. One method which has become increasingly important over the last decade or so, is emulsion polymerisation[6]. In this process, a monomer emulsion is produced by agitation, normally in the presence of surfactants, and is then polymerised by a free radical initiator. The suspending medium is almost always water. The principal advantage of this process over other means of addition polymerisation is that the usual inverse relationship between the rate of reaction and molecular weight does not apply. Other benefits include easier thermal control of the reaction and a final product of low viscosity: problems of handling and disposing of toxic and flammable organic solvents are also reduced.

The product of the reaction is a latex, i.e. a colloidal dispersion of polymer in water. In some cases, the latex finds direct application in its liquid state, for example, paint formulations, or in adhesives and binders[7]. However, the more usual route is for the latex to be coagulated to recover the solid polymer. After washing and drying, the polymer can be extruded, moulded or otherwise processed, like any other polymer.

The transmission (and other) properties of a polymer will be affected by both the method of preparation and the subsequent processing. Characteristics such as molecular weight, degree of dispersity, extent of chain branching, and degree of crystallinity are determined principally by the polymerisation process. Changes in these characteristics usually has some effect on the permeability of the polymer. These effects have been systematically studied by many workers,[8-13] and the use of permeating molecules as molecular "probes" is a promising technique in the study of polymer morphology. However, the subsequent treatment received by a polymer has a much more subtle influence on its properties. Annealing a polymer film, for example, may produce no detectable change in any of the characteristics likely to affect the transmission properties, but the annealed film will almost certainly have a different permeability.

A. EMULSION POLYMERISATION

The first reported attempts at polymerising monomers in aqueous suspension were made in the years 1909-1915[14-16]. The process, which was intended to mimic the production of isoprene latex by the rubber tree, involved the use of protective colloids, such as gelatin, egg albumin or starch to stabilise the emulsions. The reactions were carried out at ambient temperatures and in the absence of initiators. These conditions led to long reaction times, of the order of six weeks, which were hopelessly impractical. With the introduction of soap and initiator in 1926, the production of synthetic rubber latex became a practical possibility[17,18]. A wartime shortage of natural rubber prompted intensive investigation of the preparation of synthetic styrene/butadiene latex. The results of these studies were reported by Harkins[19], whose qualitative theory of particle formation in systems containing surfactant above its critical micelle concentration, has become generally accepted. The quantitative treatment of Smith and Ewart[20] has been successful in explaining the kinetics of emulsion polymerisation in a limited number of cases, the most widely reported being that of styrene. However, in other situations, particularly those involving the more water soluble monomers, the agreement between theory and experiment is poor[21].

The initial reaction mixture of an emulsion polymerisation consists of four components, namely:-

(i) Water

(ii) Monomer(s)

(iii) Surfactant (usually anionic, and often mixtures of impure commercial products)

(iv) Water soluble initiator (usually an inorganic peroxide)

Sometimes, other materials may be added to influence the course of the reaction or the characteristics of the resulting polymer; these include chain transfer agents and buffers.

The polymer characteristics are also influenced by the way in which the polymerisation is conducted. In the batch process, the reactancts are added to a stirred tank, which is heated to the decomposition temperature of the initiator; after the reaction is complete, the product is pumped away. Alternatively, the reactants are added continuously to a stirred tank. Partly reacted latex is pumped into one or more tanks, where the reaction proceeds to completion. This is termed the continuous process. A third alternative, known either as the semi batch or semi continuous process involves adding the monomer(s) to the

remaining reactants in a stirred tank. This method is normally employed when it is required to operate under monomer starved conditions.

Monomers commonly encountered in industrial applications include:

(i) acrolein
(ii) acrylonitrile
(iii) butadiene and its derivatives
(iv) esters of acrylic and methacrylic acids
(v) ethylene
(vi) isoprene
(vii) styrene and its derivatives
(viii) vinyl acetate and other vinyl esters
(ix) vinyl chloride
(x) vinylidene chloride

The mechanisms of polymerisation vary from monomer to monomer. Some form polymer in which the monomer is soluble (e.g. styrene) and others form precipitating polymers (e.g. acrylonitrile).

The product of such a reaction is typically a polydisperse latex of small average particle size typically ca.300 nm and high solids content (40 - 60% w/w). The amount of surfactant included in the recipe is normally more than adequate to give complete surface coverage of the particles, so that the latex is stable to coagulation under a wide range of conditions. Where this is not the case extra stabiliser may be added after the reaction to assure stability.

By carefully controlling the reaction conditions, and in particular the types and concentration of surfactant, it is possible to produce latices having very narrow size distributions. The Dow Chemical Company (Dow Chemical Company, Midland, Michigan, U.S.A.) has commercially produced monodispersed polystyrene and poly (vinyl toluene) latices since 1947 [22]. Such latices have been widely used as calibrants for apparatus such as Coulter counters, light scattering instruments, ultracentrifuges, etc.

Emulsion polymerisation in the absence of surfactant has been known since 1946[23]. It achieved prominance in 1965 when Matsumoto and Ochi[24] used the process to prepare monodisperse latices easily and reproducibly, where before, in the presence of surfactant, this had required careful control of the reaction mixture composition and conditions[25].

Industrially, the omission of surfactant has considerable disadvantages, the rate of polymerisation is lower and the solids content must be kept low (less than 20%) to avoid coagulation. However, the process is of considerable academic interest[26-47]. Kinetic studies become more precise, because the effects of

surfactant on initiator decomposition and as a chain transfer agent are avoided. The surface characterisation of the resulting latex is uncomplicated by the presence of adsorbed surfactant, which is difficult, if not impossible, to remove completely. A wide range of particle sizes (100 nm - 1 μm) can be prepared in a single stage process,[48] and these are now widely used as particle standards and calibrants.

One of the main reasons for the interest in surfactant free polymer latices lies in their potential utility as 'model' colloids for use in fundamental studies of colloidal properties and stability. The properties required of a model colloid are that it should be a monodisperse dispersion of hard, undeformable spheres, stabilised entirely by surface charges, whose type and distribution are known. Potassium persulphate initiated polystyrene latices were widely acclaimed as satisfying these criteria. It was thought that the remaining impurities (electrolyte, residual monomer and reaction by-products such as benzaldehyde) could be readily removed by the existing cleaning techniques of dialysis and ion-exchange. However, several unforeseen problems arose. The use of peroxy initiators, such as potassium persulphate, at elevated temperatures provided an oxidising medium in which styrene was readily converted to benzaldehyde and benzoic acid[44,49]. It was realised that existing cleaning techniques were not always completely effective in the removal of these or other impurities, and furthermore, often themselves contaminated the latex.[47]. The surface sulphate groups proved susceptible to hydrolysis on storage, making the exact nature of the charge stablising groups uncertain.[44]. Bacterial contamination caused significant changes in the surface characteristics of polystyrene latices[50].

Recent advances have overcome some of these problems. Several new initiators have been reported which avoid the problems of oxidiation side reactions and/or provide stable endgroups. Amongst these are peroxy compounds giving rise to sulphonate endgroups[51], and water soluble analogues of azobisisobutyronitrile[6]. Of these, azo initiators producing endgroups of a single type offer the greatest promise[52]. New cleaning techniques are also available (these are discussed in Chapter II).

However, several fundamental problems remain. The most serious of these is the occurrence of anomalous regions[53] in the particles. These are presumed to arise from the low molecular weight material formed in the early stages of the reaction[34]. Since the number of endgroups is greater in the anomolous regions, the distribution of charge around the particle surface will be uneven. Another problem has been revealed by recent studies of latex compressibility[54] and particle deposition on collector surfaces[55], which suggest that a steric contribution to stability is not entirely absent. Thus, the goal of preparing

polymer latices satisfying the criteria required of a model coloid is still some way from fulfilment.

1. Kinetics and Mechanisms of Emulsion Polymerisation

Since the early theories of Harkins[19] and Smith and Ewart[20], the kinetics and mechanism of emulsion polymerisation have been studied by many workers, of whom Blackley[6], Gardon[56,57], Napper[58] and Ugelstad[59] are prominent. There are many detailed discussions of these topics[6,21,54,60] and only a summary of the main points will be given here.

In common with other free radical mechanisms, the three basic processes in emulsion polymerisation are initiation, propagation and termination. Initiation involves the production of free radicals by the thermal decomposition of an initiator

$$I \xrightarrow{k_i} 2R^{\cdot}$$

and these react with monomer molecules to give monomer radicals, which in turn add more and more monomer units to form polymeric radicals of increasing chain length.

$$R^{\cdot} + M \xrightarrow{k_p} RM^{\cdot}$$

$$RM^{\cdot} + nM \xrightarrow{k_p} R(M)_n M^{\cdot}$$

Polymeric radicals can react with one another to terminate the chain: this may be by combination

$$R(M)_m M^{\cdot} + R(M)_n M^{\cdot} \xrightarrow{k_t} R(M)_{m+n+2} R$$

or disproportionation

$$R(M)_m M^{\cdot} + R(M)_n M^{\cdot} \xrightarrow{k_t'} R(M)_m M' + R(M)_n M''$$

Termination with a primary radical is also possible.

$$R(M)_n M^{\cdot} + R^{\cdot} \rightarrow R(M)_{n+1} R$$

Termination can also occur via a number of chain transfer reactions:

transfer to monomer

$$R(M)_n M^{\cdot} + M \rightarrow R(M)_n M' + M^{\cdot}$$

transfer to initiator

$$R(M)_n M^{\cdot} + I \rightarrow R(M)_n M' + I^{\cdot}$$

transfer to polymer

$$R(M)_n M^{\cdot} + P \rightarrow R(M)_n M' + P^{\cdot}$$

This last reaction will result in branching and cross linking in the final product. In mass, solution and suspension polymerisation reactions, the polymerisation rate and the polymer molecular weight are inversely related. An increased rate of radical production results not only in an increased initiation rate, but also an increased rate of termination, and hence a shortening of the polymer chain. In the emulsion system, due to the discrete nature of the loci of polymerisation, it is possible for the molecular weight and polymerisation rate to increase simultaneously, especially at high surfactant concentrations.

That emulsion polymerisation involves more than mere polymerisation of monomer droplets is shown by the fact that, while the monomer droplets are rarely smaller than 1 μm, the resulting polymer particles can be much smaller (down to 10 nm).

a) Mechanism in the presence of surfactant micelles

Prior to initiation, the monomer and surfactant are dispersed in the aqueous phase. Each can be considered to be present in three loci:

(i) dissolved in the aqueous phase

(ii) monomer solubilised in surfactant micelles

(iii) monomer emulsion droplets stabilised by adsorbed surfactant

Typically, a micelle consists of approximately 100 surfactant ions aggregated into a spherical structure with a diameter of around 5 nm. At the concentrations usually employed, there will be 10^{18} micelles per cubic centimetre of water. These become swollen to twice their original diameter by solubilisation of sparingly soluble monomer. The size of monomer droplets will depend on the intensity of agitation, but are at least 1 μm in diameter. For a typical formulation, these would number 10^{10} cm^{-3}.

When the initiator is added, it decomposes in the aqueous phase at a rate dependent on its type and the temperature of the reaction. The free radicals thus formed react with the small amount of solute monomer to form oligomeric ion radicals. Each monomer unit added causes the ion radical to become more hydrophobic, and, when 4-6 units have been added, surface active.

The next stage of the reaction is particle nucleation, which leads to the formation of a separate polymer phase. Several mechanisms of particle

nucleation have been proposed. These mechanisms fall into four classes[60] depending on the site at which the oligomeric ion radicals initiate polymerisation; namely

(i) micelles,

(ii) the aqueous phase,

(iii) monomer droplets, and

(iv) any adsorbed surfactant layer[61].

Only (i) and (ii) are normally important. The characteristics of the monomer is the principal factor in determining which mechanism prevails.

(i) Initiation in micelles: The oligomeric ion radicals are captured by monomer swollen micelles, presumably by exchange with surfactant ions. Initiator radicals are unlikely to be captured, since this would require transfer of an inorganic species from a polar to a non-polar environment. For the usual case of persulphate ion initiator and anionic surfactant, the repulsion between like charges provides a further barrier to capture. Since the core of the micelle consists entirely of monomer, the polymerisation proceeds at a rapid rate until terminated by entry of a second radical. Polymerisation is re-initiated by capture of a third radical, terminated by a fourth and so on. Only 0.1 - 1% of the micelles originally present capture an oligomeric radical. Those that do absorb monomer from the aqueous phase to continue growth. It is also possible that particles are formed by irreversible association of the oligomeric ion radicals, a mechanism which has been proposed for the surfactant free reaction. In order to minimise the surface free energy of the system, surfactant adsorbs on the ever increasing surface area of the particles, and thereby augments their stability. Those micelles which have not captured a radical lose monomer and surfactant to the aqueous phase to replace that removed by the particles: ultimately these micelles disband. When all the micelles have disappeared, no new particles can be formed.

(ii) Initiation in the aqueous phase: This mechanism, more commonly known as homogeneous nucleation[62], involves the oligomeric ion radicals growing to an extent that they become insoluble and precipitate on themselves. The more water soluble monomers will favour this route, since they will be able to polymerise more rapidly and become insoluble before being captured by a micelle.

The precipitated particles then absorb monomer and adsorb surfactant. If sufficiently stable, the particles will maintain their discrete identities: otherwise coagulation with other particles occurs.

(iii) Initiation in monomer droplets. For the polymerisation recipes and conditions usually employed, monomer droplets are unlikely to capture radicals, despite their larger individual surface areas. This is simply due to there being 10^6 times as many micelles, which enjoy a 60 fold advantage in total surface area. The absence of polymerisation within the droplets has been verified experimentally by quenching a reaction, separating the remaining monomer droplets and analysing for polymer[63]. The amount detected was less than 0.1% of the total polymer during the reaction. Only if the monomer droplets can be made very small will there be significant polymerisation within them.

(iv) Initiation in adsorbed surfactant layers: According to this mechanism, the oligomeric ion radicals generated in the aqueous phase diffuse to an adsorbed surfactant layer, which could be on the surface of a micelle, polymer particle or monomer droplet. At the beginning of the reaction, it is likely to be the micelles, given their much larger total surface area. Once formed, the polymer particles will compete with micelles on the basis of surface area, and this is qualitatively similar to the initiation in micelles mechanism.

Whichever mechanism operates, it should be noted that nucleation may take place over an appreciable length of time, which will result in the latex having a broad particle size distribution.

It is usual to divide the course of an emulsion polymerisation into three intervals. During Interval I, an initially two phase system (water and monomer) becomes a three phase system, due to the formation of polymer particles. Interval I is complete when the total number of polymer particles present in the system becomes constant. Interval II lasts from the end of Interval I until the system again consists of two phases, monomer swollen polymer particles and water. During Interval II, the number of particles and the monomer concentration within the particles remains constant. The polymerising monomer in the growing particles is replaced from the monomer droplets via solution in the aqueous phase, until these are exhausted. Interval III is the final stage of the reaction, during which the monomer remaining within the particles is polymerised.

b) Kinetics of the Surfactant Present System

The kinetics of emulsion polymerisation have been widely studied both theoretically and experimentally. The results provide much of the evidence for the mechanisms described above.

The first theoretical treatment was developed by Smith and Ewart[20]. They devised a general recursion equation, in terms of the number of particles containing n free radicals, N_n, to describe Interval II, the region in which the total number of particles has become constant. Particles containing n free radicals, are created by three processes:

(i) the entry of a free radical into particles containing n-1 radicals;

(ii) the exit of a free radical from particles containing n + 1 radicals, and;

(iii) the termination of two free radicals in particles containing n + 2 radicals.

Similar processes occuring in particles already containing n free radicals result in their disappearance.

By assuming that the concentration of primary free radicals remains constant and that the rate of appearance and disappearance of particles containing n free radicals is equal, i.e. that N_n is constant, they obtained the following steady state equation:

$$N_{n-1}\ \frac{\rho}{N} + N_{n-1}\ k_o S\left(\frac{N+1}{V}\right) + N_{n+2}\ k_t\left[\frac{(n+1)\ (n+2)}{V}\right]$$
$$= N_n\left\{\frac{\rho}{N} + k_o S\left(\frac{n}{V}\right) + k_t\left[\frac{n(n+1)}{V}\right]\right\} \qquad (I:1)$$

This equation relates N_n to the rates of radical entry into the particles, ρ, radical transfer out of the particles, k_o, and termination, k_t; the particles having volume V and surface area S.

Smith and Ewart did not attempt a general solution to the equation, but solved it for three limiting cases depending on the average number of free radicals per particle, $\bar{n}$.

(i) Case 1, $\bar{n} << 0.5$. Here the rate of radical entry is much less than the rate of disappearance, usually due to a rapid rate of transfer out. This case would be favoured by more water soluble monomers giving hydrophilic polymers.

(ii) Case 2, $\bar{n} = 0.5$. This situation is realised if termination of a propagating radical in the particle occurs immediately after the acquisition of a

second free radical, and the rate of radical transfer out of the particle is negligible. Application of these conditions gives the result that approximately equal numbers of particles will contain one or no propagating radicals and that almost no particles will contain more than one radical. This can be visualised as a particle being struck by a succession of free radicals with an average time interval between collisions. The first radical intitiates polymerisation, which proceeds at a rate governed by the propagation rate constant, k_p, until terminated by the entry of the second free radical. The particle remains dormant until the entry of a third free radical, and so on. The particles are thus active for half their lifetime, which is statistically equivalent to saying they contain half a radical.

By making further assumptions, expressions linking observed variables such as particle number density, rate of polymerisation and average degree of polymerisation with reactant concentrations and various rate constants may be obtained, which provide a means of testing the theory. There is considerable experimental evidence[21] to confirm that Case 2 kinetics are obeyed by the emulsion polymerisation of styrene in the presence of surfactant, provided that the particle diameter is less than 150 nm and that the rate of primary free radical generation is relatively low. Agreement between theory and experiment is poor, however, when more water soluble monomers (such as vinyl acetate and the lower aliphatic esters of acrylic and methacrylic acid) are considered.

(iii) Case 3, $n \gg 0.5$. The rate of entry of free radicals is greater than the rate of loss. Systems producing large particles would be expected to obey Case 3 kinetics, since more than one radical could exist in the particle for significant periods of time, without initial termination occuring. Since emulsion polymerisation of styrene in the absence of surfactant produces fewer and larger particles than in its presence (typically 10^{12} cm^{-3} of 500 nm compared with 10^{15} cm^{-3} of average 50 nm) it is likely that Case 3 rather than Case 2 would be a better representation.

The Smith-Ewart theory has been extended by many authors. Stockmeyer[64] obtained a general solution of the recursion equation. O'Toole[65] treated the case in which radical transfer out of the particles was not insignificant, and Ugelstad and Hansen[59] considered reabsorption of these

radicals. Gardon[56,57] examined emulsion polymerisation in the presence of surfactant, from initiation to the end of interval II. General equations were derived which predicted conversion as a function of time, particle size and molecular weight as a function of conversion and the influence of monomer, initiator and surfactant. However, as Vanderhoff[66] has pointed out, several of these theoretical works have yet to be corroborated by experiment.

c) Core-Shell Morphology in Single Stage Reactions

One of the features of styrene polymerisation is that the monomer and polymer are miscible in all proportions. It would, therefore, be expected that, during particle growth, polymerisation would occur in any region within the particle. However, in a series of papers by Williams and co-workers[67,73], it was postulated that polymerisation occurs at or near the surface of the monomer swollen latex particles. This behaviour was attributed to a monomer concentration gradient, the concentration being low at the centre of the particle and high at its periphery. The resulting particles were alleged to display a core-shell morphology.

Williams presented a thermodynamic argument to justify the existence of a monomer concentration gradient, and experimental evidence supporting its occurrence. Gardon[74] disputed these, and Napper[75] proposed an alternative hypothesis. The arguments and experimental evidence have been reviewed by Vanderhoff[66], who also proposed a hypothesis to account for Williams' observations. Recently, Löhr and Reinecke[76] repeated Williams' experiments in an attempt to resolve the controversy.

The arguments cited by Williams in favour of the core-shell morphology model for styrene/polystyrene were based on evidence in four areas:

(i) Small amounts of butadiene were added to styrene monomer which was polymerised in the first, second and third stages of seeded emulsion polymerisation. The polymer was embedded, microtomed, stained with osmium tetroxide and examined by electron microscopy. It was postulated that 99.3/0.7 styrene butadiene copolymer would be compatible with polystyrene. When butadiene was added to the second stage, it was found that a dark shell appeared, whereas when it was added to the first stage a dark core resulted.

(ii) Tritiated styrene was added to the first or second stages of polymerisation and the latex diluted, placed on a TEM substrate, covered with photographic emulsion and left in the dark for up to three months.

β-particles travelling over short distances developed the silver halide grains to give silver easily visible in the TEM. It was shown that if the shell was sufficiently thick then tritiated units in the core did not develop the film.

(iii) Since the random coil configuration in the monomer swollen particle cannot be maintained near the surface due to the particle/water interface, it was argued that the polymer molecules would be located far enough from the surface for the random coil configuration to be maintained and that this polymer concentration gradient would be balanced by a monomer concentration gradient.

(iv) The classical equation for the rate of emulsion polymerisation is:

$$R_P = k_p [M]_p N \bar{n}/N_A \qquad (I:)$$

where k_p is the propogation constant

$[M]$ is the monomer concentration at the locus of polymerisation in the latex particles

N is the particle number density

$\bar{n}$ is the average number of radicals per particle

Grancio and Williams[67] presented conversion time curves which were linear up to 60% conversion. They found that N was constant during their reactions, and assumed that $\bar{n}$ was also constant and equal to $\frac{1}{2}$, corresponding to Smith-Ewart Case 2 kinetics. However, the weight fraction of monomer in the particles decreased by a factor of two in the conversion range 0 - 60%. In order for the rate to remain constant whilst the overall monomer concentration was halved, it was argued that the monomer concentration at the site of polymerisation must remain constant, i.e. that polymerisation occurs in a polymer rich shell.

Gardon[74] criticised Williams' case on the following points:

(i) Williams' data could be replotted and interpreted to show positive deviations from the linear conversion/time relationship.

(ii) It was unlikely that the distribution of 'tagging' comonomers in a swollen latex particle could be frozen by their conversion to copolymers in a seeded growth reaction. The second stage polymer might well be incompatible with the seed polymer, even if the monomer was freely

soluble. Also, tritiated and normal monomers would have different copolymerisation characteristics if there was a significant kinetic isotope effect.

(iii) There was no basis for the assumption that the hydrophobic middle segments of the polymer chain could not be situated at the polymer/water interface. Gardon drew attention to the observation that polystyrene preferentially adsorbs onto glass and metals from dilute solution in benzene or cyclohexane giving a higher concentration at the interface than in the bulk solution. There was no reason to suppose that polystyrene segments could not similarly be located at the particle/water interface of a styrene swollen particle.

(iv) The diffusive mean free path of a monomer molecule over the time period required for high conversion was several times the particle radius. This would tend to even out any inhomogeneities in the monomer concentration.

Napper[75] considered that a core-shell morphology did occur, but felt that this was because the centre of the particle was inaccessible to the free radicals which initiated polymerisation of the monomer. Since monomer is consumed at the periphery of the particle, this is the region of low concentration, being replenished from the monomer swollen core of the particle.

Vanderhoff[66] reviewed the foregoing arguments and made the following comments:

(i) Although the conversion/time curves presented by Williams were generally linear, they could also be interpreted as showing slight positive deviations. However, the large variation in monomer concentration in the region in which the conversion/time curve was linear would be expected to produce much greater deviations. Furthermore, slight deviations from linearity were to be expected, since the reaction conditions used by Williams were outside the range in which Smith-Ewart Case 2 kinetics are considered applicable.

This conclusion is supported by the work of Friis and Hamielec[77]. They attributed the positive deviation from linearity in Williams' conversion/time curves to a decrease in the value of the termination rate constant, k_t, as the particle size increased, since in larger particles

the entry of a second free radical would not be expected to produce instantaneous termination. This view was supported by k_t values obtained from bulk polymerisation.

(ii) A comparison of the number of sulphate endgroups determined by conductometric titration and the Palit dye partition technique (which involves dissolving the polystyrene in benzene and shaking with an aqueous solution of a suitable dye) suggested that non-polar polystyrene molecules do tend to retract from the polymer/water interface, i.e. that the polymer segment density is lower at the particle surface - contrary to Gordon's view.

Vanderhoff then proposed an alternative hypothesis to explain Williams' results. The starting point is a particle of 15 nm diameter comprising a single polymer molecule of molecular weight 5.10^5 and an equal amount of monomer. The polymer molecule is said to adopt a random coil configuration with both sulphate endgroups located on the surface. Each subsequent cycle of initiation and termination results in the formation of additional polymer molecules, all of which have the same configuration. There is, however, little or no interpenetration of the chains, except at their surfaces, in accordance with the hypothesis of Vollmert[78]. Hence, each new molecule forces a previously formed molecule into the interior of the particle: the ends of the molecule stretch in order to allow the endgroups to remain at the surface. Eventually, for polymer molecules formed in the early stages of the reaction, the strain becomes too great, and the endgroups are buried beneath freshly formed polymer. This mechanism is in accord with Williams' experimental results, but avoids the contentious postulate of a non-uniform monomer distribution within the particle.

Löhr and Reinecke[76] made a further experimental study of the emulsion polymerisation of styrene, including repeats of some of Williams' original work, and obtained the following results:

(i) Williams' observations were essentially correct.

(ii) Determination of the particle size distribution by laser aerosol spectroscopy, at various stages of the reaction showed that particle growth is surface dependent this is contrary to Smith-Ewart case 2 kinetics which predict that particle growth is independent of particle size.

(iii) Measurement of the monomer concentration within the particles at various degrees of conversion showed that thermodynamic equilibrium between the monomer phase and the latex particles is not always attained, so that the polymerisation is partially diffusion controlled. This was ascribed to coalescence of monomer droplets arising from a poor emulsifier.

(iv) The observed molecular weight distributions were too broad, even at low conversions, to support a core-shell polymerisation.

(v) Electron microscope examination of samples containing 5% dimethyl butadiene, prepared by methods intended to encourage a core-shell structure, failed to reveal such a morphology.

They concluded, rather perversely in view of the literature to be discussed in Section 2, that even in a two-stage process, a core-shell morphology was unlikely to result with amorphous uncross-linked polymers.

d) Mechanism of the Surfactant-free Reaction

In the absence of surfactant, the monomer will be present in only two loci, namely in solution and in emulsion droplets, which for a given rate of agitation will be much larger than in the presence of surfactant. Radical generation and formation of oligomeric ion radicals take place as described earlier. Primary nuclei are thought to be produced in one or more of three ways:

(i) the growing free radicals terminate: primary nuclei are formed by coagulation of these dead species;

(ii) the growing free radicals achieve a size and concentration at which they become surface active, and associate by a process akin to micellisation (unlike true micellisation, the aggregation is irreversible since the free radical species terminate on association);

(iii) the oligomeric free radicals continue to grow in length until they become insoluble and precipitate.

Any of the above mechanisms would lead to particles consisting of low molecular weight polymer and having a high surface charge density. These particles are then considered to imbibe monomer, which is subsequently

polymerised by oligomeric free radicals and accompanied by an increase in size. The polymer thus generated will be of high molecular weight, so that few new charged end groups are incorporated into the particle. Thus the surface charge density decreases rapidly during the initial growth of the particles. These then coagulate until the surface charge density is increased to a level sufficient to confer stability. Compared with the surfactant present mechanism, this process of nucleation and coagulation takes place over a short period of time and hence the resulting latex is monodisperse.

Examination of multisampled surfactant-free styrene emulsion polymerisation reactions, by transmission electron microscopy, has shown that the particle size distribution remains monodisperse from the stage when particles can first be observed (diameter ca. 10 nm) to completion of the reaction[34]. Similar results have been obtained for surfactant-present systems where a monodisperse product is obtained[79].

The early stages of the surfactant-free emulsion polymerisation of styrene has been examined by a combination of light scattering techniques (photon correlation spectroscopy and total intensity light scattering) together with transmission electron microscopy[40,41]. Since the light scattered by the polymer particles would be swamped by the much larger monomer droplets, the reactions were unstirred. The reaction vessel contained either a saturated solution of styrene or a separate styrene layer above the aqueous phase. The light scattering results were interpreted by dividing the reaction into three intervals, A, B and C. During interval A, the light scattered did not increase above the dark count of the photomultiplier tube. It was thought that formation of initial particle nuclei took place during this interval, but that these nuclei were too small to be detected. During Interval B, the amount of scattered light increased rapidly. This was attributed to both particle growth (by polymer formation and subsequent monomer absorption) and to particle aggregation. Transmission electron microscopy showed the particle size distribution to be polydisperse at this point. Addition of inhibitor to halt polymerisation during the early stages of Interval B indicated that smaller particles were aggregating and coalescing. During Interval C, the number of particles aggregating was considerably reduced. The particles were quite large at this stage, but the rate of growth had dropped, presumably due to monomer starvation in the aqueous phase.

The processes thought to be occurring during the early stages of the surfactant free emulsion polmyerisation of styrene are summarised schematically in Fig. I:1[41]. As the initial nuclei grow they become unstable and coagulate and coalesce both with each other and with other particles which

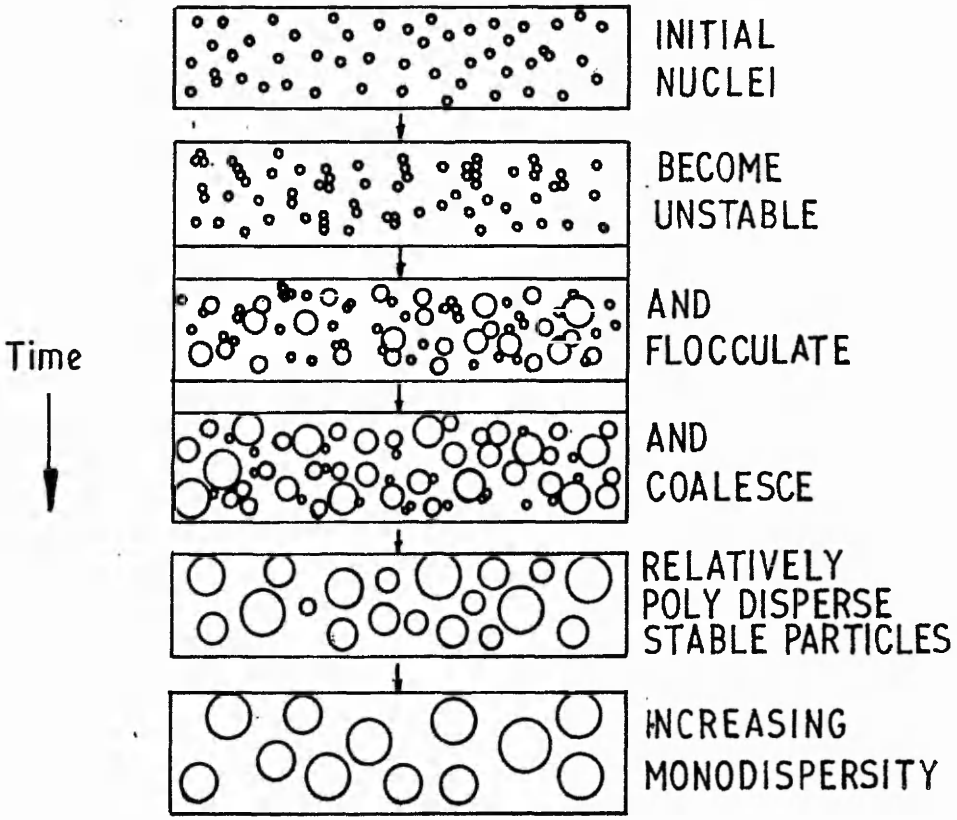

FIGI:1 SCHEMATIC DIAGRAM OF THE PROCESSES THOUGHT TO BE OCCURING DURING THE EARLY STAGES OF REACTION (NOT TO SCALE WITH REGARD TO EITHER SIZE OR IMPLIED NUMBER DENSITY) (FROM GOODALL et al (41))

are by themselves stable. This process continues until all the small particles have disappeared and thereafter, the number density remains constant. The particle size distribution is initially polydisperse, but narrows, as the reaction proceeds, due to competitive growth[80,81].

e) Kinetics of the Surfactant Free Reaction

The kinetics of the emulsion polymerisation of styrene in the presence of surfactant have been widely studied (see Section 1b). There is considerable experimental evidence[21] which confirms the validity of Smith-Ewart case 2 kinetics for particle sizes of less than 100 nm. After the nucleation stage of the polymerisation is complete, the surfactant plays only a minor role in the reaction. It might therefore be expected that particle growth in the presence and absence of surfactant would be essentially the same. However, the reactions differ in the size and number density of the particles produced (typically 10^{15} particles/cm^3 of average diameter 50 nm in the presence of surfactant compared with 10^{12} cm^{-3} of 500 nm in its absence). Furthermore, surfactant free reactions take longer to complete (typically 12 compared with 3 hours) and produce polymer of molecular weight an order of magnitude lower. Another possible difference is the influence of the adsorbed surfactant layer on the solubility of monomer in the polymer particles[61].

One contentious aspect of the mechanisms of emulsion polymerisation concerns the location of free radicals within the polymer particles and the way in which monomer is transported to the polymerisation sites. The arguments over the core-shell morphology, postulated by Williams and co-workers[67-73] to occur in homopolymer systems due to polymerisation in a monomer rich shell, have been reviewed in Section 1c. The role of particle swelling by monomer, which is relevant to this problem, has also been the subject of debate.

Chung-Li et al.[82] measured the rate of swelling of large (ca. 2 μm), freshly formed polystyrene particles in monomer saturated water, using a Coulter Counter. They found that this swelling rate was too low to explain the observed polymerisation rate in seeded growth experiments. In order to explain the higher growth rate, they proposed a heterocoagulation mechanism, whereby new and unstable monomer swollen particles were formed in the aqueous phase, which subsequently coagulated with the core particles. A recent study by Goodwin et al.[83], using small angle neutron scattering to monitor the swelling rate of smaller polystyrene particles, found that the swelling rates were adequate to explain the particle growth rate without recourse to a heterocoagulation mechanism. Similar results were obtained by proton correlation spectroscopy, during the study of the shot growth technique for core-

shell latex preparations (see Chapter III, Section C).

The direct relevance of swelling rates to polymerisation conditions can be questioned on several grounds. The monomer diffusion rate is presumably enhanced in the presence of free radicals, which, by polymerising the monomer in or on the particles, maintain a higher concentration gradient. Indeed, the need for appreciable dynamic swelling is in some doubt in view of the work of Wessling and Harrison[84]. These authors studied the polymerisation of vinylidene chloride, a monomer substantially insoluble in both aqueous and polymer phases, and the copolymerisation of vinylidine chloride and n-butyl acrylate, which produces swellable particles. Similar kinetics were observed for both systems, although in the former case, polymerisation could not take place in the particle. Wessling and Harrison proposed that the reaction zone was an adsorbed monomer layer, 2.5 nm thick, on the particle surface.

Of the various quantitative theories which have been derived to explain emulsion polymerisation kinetics, four are likely to apply to the surfactant-free emulsion polymerisation of styrene.

(i) Smith-Ewart Case 3[20]. This is preferred to Case 2, which best explains the emulsion polymerisation of styrene in the presence of surfactant, because of the much lower particle number density with respect to the number of free radicals. The rate of polymerisation is given by

$$R_p = \frac{k_p [M]_p}{N_A} \left(\frac{\rho_A V_p}{2k_t} \right)^{\frac{1}{2}} \qquad (I:3)$$

where k_p and k_t are the propogation and termination rate constants, $[M]_p$ is the monomer concentration in the particles, ρ_A is the rate of radical absorption, V_p is the volume of particles per dm^3 and N_A is Avogadro's number. The number average molecular weight, $\bar{M}_n$, is given by

$$\bar{M}_n = 100\, k_p [M]_p \quad (k_t \rho_A V_p/2)^{-\frac{1}{2}} \qquad (I:4)$$

(ii) Smith-Ewart Case 3 applied to the core-shell model[59]. This predicts

$$R_p = \frac{k_p [M]_s}{N_A} \left(\frac{\rho_A A L}{2k_{ts}} \right)^{\frac{1}{2}} \qquad (I:5)$$

and

$$\bar{M}_n = 100\, k_p [M]_s \quad (k_{ts} \rho_A A L/2)^{-\frac{1}{2}} \qquad (I:6)$$

where the subscript s applies to the shell, L is the shell thickness and A is the surface area of particles per dm^3

(iii) The surface phase polymerisation model[84] involving polymerisation in an adsorbed monomer layer and referred to above. This theory is quantitatively similar to (ii).

(iv) The Gardon theory[56,57], in which general equations are derived to describe the emulsion polymerisation in the presence of surfactant, from initiation to the end of Interval II, in terms of variables which can be independently determined. These equations can be readily adapted to surfactant-free systems after the nucleation stage by replacing the term involving the surfactant concentration by the observed value of the particle number density. The Gardon treatment might reasonably be expected to apply, since it allows for the average number of free radicals per particle, $\bar{n}$, to be much greater than unity, as expected for a system containing fewer, larger particles. Gardon's theory predicts:

$$P_v = At^2 + Bt \qquad (I:7)$$

where P is the conversion in terms of volume of polymer formed per unit volume of water, and

$$\bar{M}_n = \frac{(4 \cdot AN_A \cdot d_p)/(B \cdot \rho_A) \quad V_p}{\left[1 + (4 \cdot AN_A/B^2) \; V_p\right]^{\frac{1}{2}} - 1} \qquad (I:8)$$

A and B are defined by

$$A = 0.102 \; \frac{k_p^{1.94} \, \phi_m^{1.94} \, d_m \, \rho_A}{k_t^{0.94} \, (1-\phi_m)^{0.94} \, d_p \, N_A}$$

and

$$B = \frac{k_p \, \phi_m \, N}{2N_A} \qquad (I:9)$$

ϕ_m is the volume fraction of monomer in the particles and d_m and d_p are the densities of monomer and polymer respectively.

2. Preparation of Core-Shell Latices

The production of core-shell latices is an important industrial process and many examples are to be found in the patent literature[86-99]. This topic has also attracted the attention of workers in the field of emulsion polymerisation, as a means of producing either larger particles than can be produced in a single stage reaction[48] or controlled surface charge densities in model systems[33].

A variety of methods have been used for preparing core-shell latices. These fall into four categories:

(i) 'Initial charge', where the comonomers are both present at the beginning of the reaction;

(ii) 'Semi-continuous addition', where one monomer is present at the start, and the second monomer is added slowly throughout the course of the reaction;

(iii) 'Seeded growth', where the second monomer is added at the start of a reaction to a mixture containing a previously fully polymerised core latex;

(iv) 'Shot addition', where the core latex is polymerised 'in situ', being allowed to reach a fairly high conversion before the second monomer is charged (either in bulk or continuously).

The seeded and shot growth methods differ in that particles polymerised in situ will contain more monomer and hence swell more rapidly. A recent development is the power feed process[98,100], in which a monomer mixture of continuously varying composition is added. The resulting particles have a gradient of composition from the core to the periphery, which can be controlled by varying the rate(s) of monomer addition.

The locus of the polymerised second monomer, i.e. aqueous phase, bulk polymer or the interface between them, has been shown to be dependent in part on the reactivity of the monomer and its affinity for these loci[101]. It may be further influenced by the core-shell mechanism believed by Williams and co-workers[68-73] to operate even for compatible comonomers (see Section 1c). These factors will greatly influence the morphology of the particles in the final product. For a given combination of reactants, the particle morphology will also

be affected by variations in the polymerisation conditions, e.g. mode of monomer addition (flooded or starved), extent (if any) of particle pre-swelling, etc.[102].

The various types of particle morphology reported in the literature for seeded growth systems have been summarised by Lee and Ishikawa[103] as follows. A monomer or mixture of monomers II is polymerised in the presence of homopolymer or copolymer latex particles I. Depending on the properties of I and II, the product will fall into one of six classes.

(i) If polymer I is insoluble in monomer II, polymer II will form surface layers like onion skins, e.g. poly(vinyldene chloride)/(poly(n-butyl acrylate)[84].

(ii) If polymer II is miscible with polymer I and there is no difference in hydrophobicity between them, polymer II rich outside layers will be formed, resulting in a core-shell morphology, e.g. polystyrene/polystyrene[67]. This morphology also results when polymer II is more hydrophilic than polymer I, e.g. poly(methyl acrylate)/poly(methyl methacrylate)[104].

(iii) If monomer II swells polymer I, but polymer II is immiscible with polymer I, phase separation can take place, and many different structures are possible, e.g. polystyrene/styrene-butadiene copolymer[102].

(iv) If polymer I is cross-linked and immiscible with polymer II, polymer II can be trapped to form two interpenetrating continuous phases surrounded by polymer II rich shells.

(v) If polymer II is more hydrophilic than polymer I, a core-shell structure results, e.g. polystyrene/poly(ethyl acrylate)[105].

(vi) If polymer I is more hydrophilic than polymer II, polymer phase II separates into polymer phase I and many different structures result, e.g. 90:10 ethyl acrylate - methacrylic acid copolymer/60:40 styrene-butadiene copolymer which formed an inverted core shell morphology while 50:40:10 ethyl acrylate-styrene-methacrylic acid copolymer/polystyrene formed particles in which the second component was dispersed in the first[103] (see Fig. I:2).

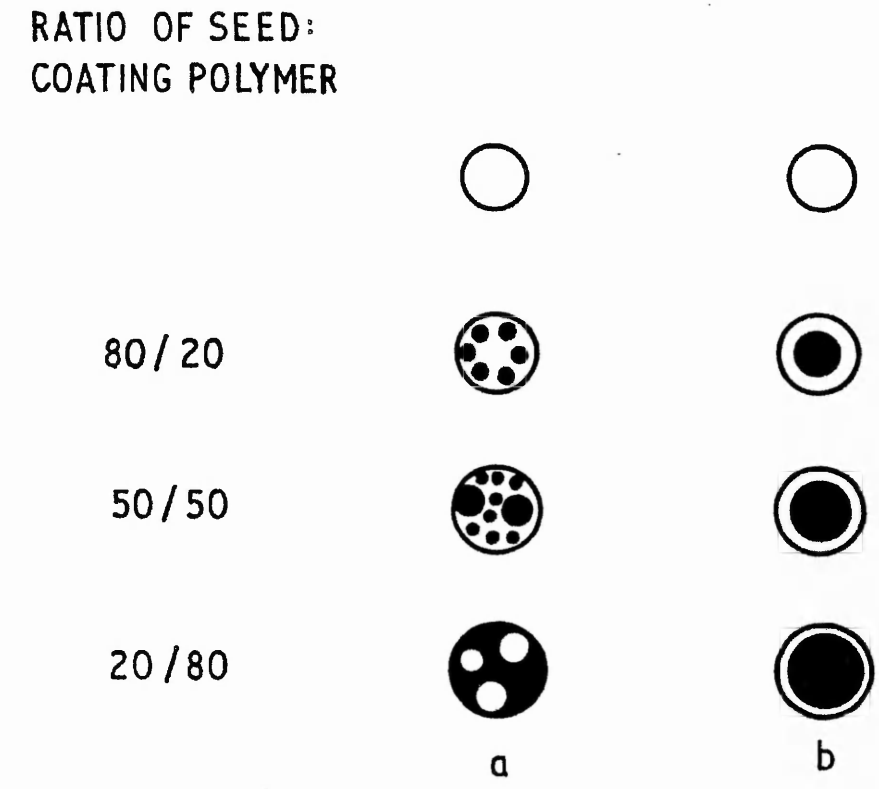

FIG I:2 MORPHOLOGY OF PARTICLES

PRODUCED BY SEEDED GROWTH REACTION WHERE COATING POLYMER IS HYDROPHOBIC AND SEED POLYMER IS (a) LESS HYDROPHILIC AND/OR OF HIGH MOLECULAR WEIGHT, OR (b) MORE HYDROPHILIC (b) (FROM LEE AND ISHIKAWA (103))

These systems have been extensively studied by Okubo and co-workers[106-109] who have observed what they describe as "raspberry" and "confetti" like morphologies together with voids and other anomalies when polymerising a hydrophobic monomer in the presence of a hydrophilic seed. These morphologies were attributed to the hydrophobic monomer polymerising in separate domains. At high volume fractions of second polymer, particle inversion occurred (see Fig. I:2a), leaving the seed polymer fragmented and dispersed in the second.

A further complication in the preparation of core-shell latices is the occurrence of a second crop of particles, resulting in a latex with a bimodal size distribution. It has been shown by Hearn[30] that the number density of seed particles at constant temperature, ionic strength and monomer and initiator concentrations is an important parameter in determining whether or not these secondary growth particles form. Chung-Li et al.[82] have discussed the occurrence of secondary nucleation in terms of heterocoagulation of new polymer, formed in the aqueous phase, with the seed particles, relative to its homocoagulation which can result in stable nuclei.

For reactions carried out in the presence of surfactant, the occurrence of secondary growth particles has been controlled by maintaining the concentration of surfactant at a value below its critical micelle concentration, so that micelles are absent from the aqueous phase[80,92,93,96,110]. However, under these conditions, surfactant coverage of the particle surface is less than complete and stability problems frequently ensue. The solution to this problem is to use a mixture of anionic and non-ionic surfactants[99,111].

In seeded growth processes, the particles intended to form the core of the final latex particles are prepared prior to the coating reaction. A variation on this method is to polymerise the core particles in situ and add the second monomer at a point when the first reaction is substantially complete. This 'shot-growth' technique was used by Sakota and Okaya[112] as a means of incorporating carboxyl groups from acrylic, methacrylic or itaconic acids on the surface of styrene-isoprene copolymer latices. They found that 60% incorporation of carboxyl groups could be achieved by addition at 80% conversion, increasing to 80% incorporation at 95% conversion.

B. LATEX FILM CASTING

Traditionally, polymer samples for diffusion studies are obtained by bulk or solution polymerisation. Film specimens are prepared by casting from solution in a suitable solvent[113] or by industrial processes, such as extrusion[114] or compression moulding[115]. Polymer films can also be prepared from latex dispersions by casting processes similar to those used for polymer solutions. However, film casting from latices is much less straightforward, for several reasons. The principle stricture is that the temperature at which the film is cast must be above the minimum film formation temperature (MFT) of the polymer, if a continuous film is to be obtained. This temperature is roughly comparable with the glass transition temperature of the polymer. Polymer latices dried below their MFT form friable, discontinuous films, which crumble to a powder when disturbed. A latex is said to be soft if it forms a film at or below room temperature (e.g. poly(ethyl acrylate) and poly (vinyl acetate)) or hard if it does not (e.g. poly (methyl methacrylate) and polystyrene).

Practical difficulties arise from the physical properties (e.g. latent heat of vaporisation) of water (the dispersion medium), and the fact that polymer latices often contain extraneous materials (e.g. surfactants and buffers from the polymerisation process, fungicides to prevent microbial contamination, etc.). The latter applies particularly to commercial latices. These problems are discussed later.

When a latex dispersion is dried by evaporation of water from its surface, the polymer particles are driven closer together until the stabilising forces (electrostatic and/or steric) keeping them apart are overcome. A soft latex (i.e. one above its minimum film formation temperature) then forms a continuous film by coalescence of the polymer particles.

The drying of latex dispersions has been studied by several workers including Myers and Schultz[116], Sheetz[117] and Vanderhoff et al.[118]. The techniques employed ranged from simple gravimetric determination of water loss to the use of sophisticated apparatus such as an ultrasonic impedometer. The results of these studies were all broadly similar; the polymer volume fraction plotted as a function of time giving a sigmoidal curve (Fig. I:3).

Vanderhoff et al.[118] interpreted these curves by dividing the drying process into three stages, which are illustrated in Fig. I:4. During the first stage, which lasts until the particles come into irreversible contact with each other, water evaporates from the surface of the latex. The rate of evaporation from the latex was shown to be the same, within experimental error, as that

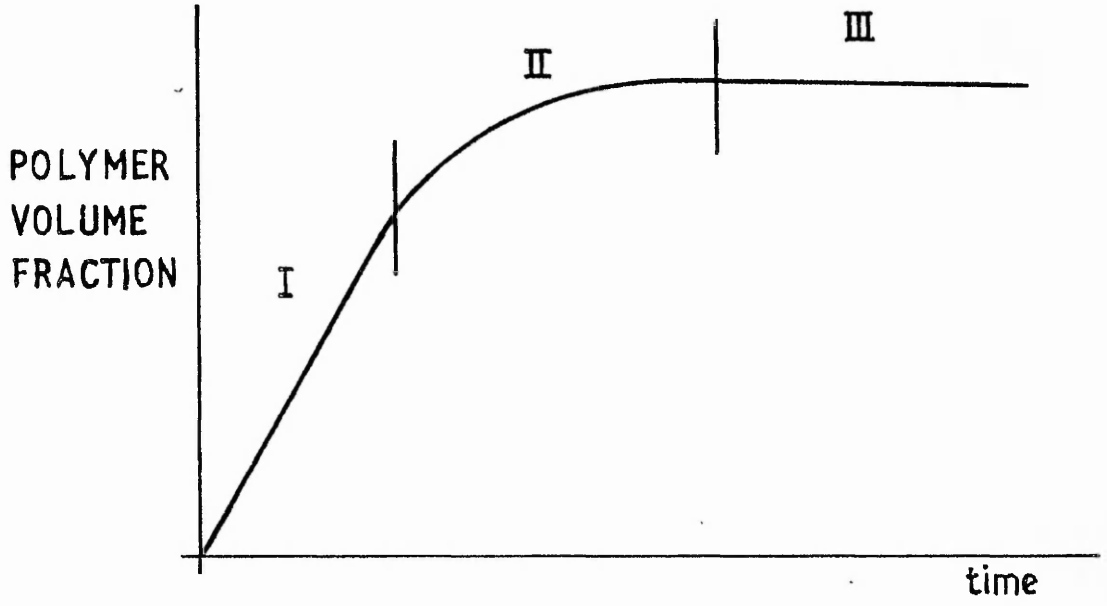

FIG I:3 RATE OF INCREASE IN POLYMER VOLUME FRACTION DURING DRYING OF LATEX FILMS

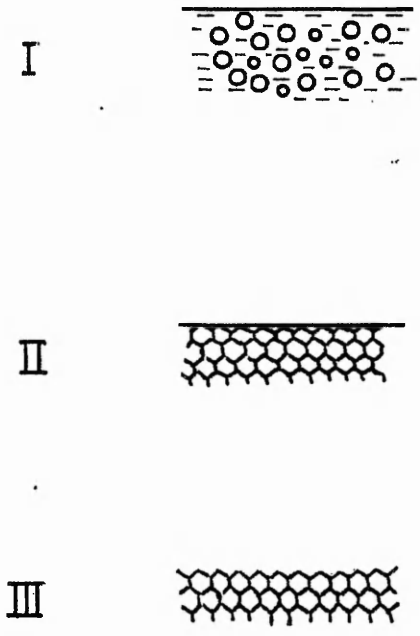

FIG I:4 SCHEMATIC REPRESENTATION OF THE THREE STAGE DRYING PROCESS (FROM VANDERHOFF et al (118))

from a dilute solution of surfactant and electrolyte (i.e. the aqueous phase of the latex). As long as the surface area of liquid latex film does not change e.g. because of disjoining and/or retraction, the rate of evaporation will remain constant. The intermediate stage is the period in which the polymer particles fuse into a continuous film. The rate of evaporation drops off rapidly during this stage due to the reduction in the air/water interfacial area, although the rate per unit area remains the same. The completion of coalescence marks the beginning of the final stage, during which the residual water escapes through capillary channels or by diffusion through the polymer. The small quantity of water remaining in the film and the limited air/water interfacial area result in a very low rate of evaporation.

The borderline between Stages I and II was examined by Hwa[119], who used a specially constructed shallow conical Petri dish to observe a drying latex film. The film dried from the outside inwards, and Hwa was able to record photographically the existence of liquid, flocculated and coalesced regions. The volume fraction at which flocculation occurred was determined and its variation with type of surfactant noted. As expected by analogy with sedimentation, a strongly adsorbed surfactant delayed the onset of flocculation until the particles were well packed. A weakly adsorbed surfactant did not effectively stabilise the particles and a much less densely packed structure resulted.

Although exhibiting similar volume fraction versus time curves, hard, non film-forming latices do not behave in the same way beyond the flocculation point. These rate of drying studies do not, therefore, assist in elucidating the mechanism of coalescence.

1. Initial Stages of Film Formation

The first mechanisms of particle coalescence proposed by Dillon, Matheson and Bradford[120] and later by Brown[121], take as their starting point the premise that, for a film to be formed, the forces tending to cause coalescence must exceed the forces tending to oppose it. Brown considered the possibility of four forces causing coalescence and two opposing it; these were as follows:

(i) F_s, the force produced by the negative curvature of the particle surface: this occurs only after two or more particles have come into contact (i.e. a surface tension force causing a reduction in the surface area).

(ii) F_c, the capillary pressure resulting from the presence of a water surface of negative curvature.

(iii) F_v, the van der Waals attractive forces between the particles.

(iv) F_g, the gravitational force acting on the particles.

(v) F_e, the force of repulsion between the particles. (Brown considered only electrostatic forces, but where surfactant is adsorbed on the particle surface, there may also be a significant steric contribution).

(vi) F_G, the resistance of spherical particles to deformation.

Thus if coalescence is occurring, the sum total of the attractive force must exceed that of the repulsive forces, and this must be true for the whole film formation process if this is to be complete, i.e.:

$$F_s + F_c + F_v + F_g > F_e + F_G \qquad (I:10)$$

Which of these particular forces are most important has been the subject of some debate. Dillon, Matheson and Bradford[120] argued that the large reduction in surface area which occurs when the latex particles coalesce would produce a sufficient shearing stress to cause viscous flow (Fig. I:5). They calculated the pressure exerted on the holes between the packed latex particles using the equation of Laplace[122].

$$P = 2\gamma/r \qquad (I:11)$$

where γ is the surface tension of the latex and r the radius of the hole; they obtained a value of 10^7 Pa for particles of 5 nm and by assuming a surface tension of 25 mN m^{-1}. They concluded that the holes could not maintain this pressure due to the permeability of the polymer to air and water.

An expression for the rate of coalescence by viscous flow was developed by Frenkel[123]

$$\theta^2 = 3\gamma t / 2\pi r \eta \qquad (I:12)$$

where t is the time, η the viscosity of the polymer and θ the half angle of coalescence (see Fig. I:6). Dillon et al applied this relationship to the coalescence of a 75:25 vinyl chloride-vinylidene chloride copolymer latex by measuring r and θ from electron micrographs. Their results plotted as θ^2 against 1/r showed reasonable agreement with the theoretical straight line.

Brown[121] criticised the treatment of Dillon et al on several grounds.

(i) That the film formation occurs concurrently with the evaporation of water, and therefore that the surface tension of polymer could not

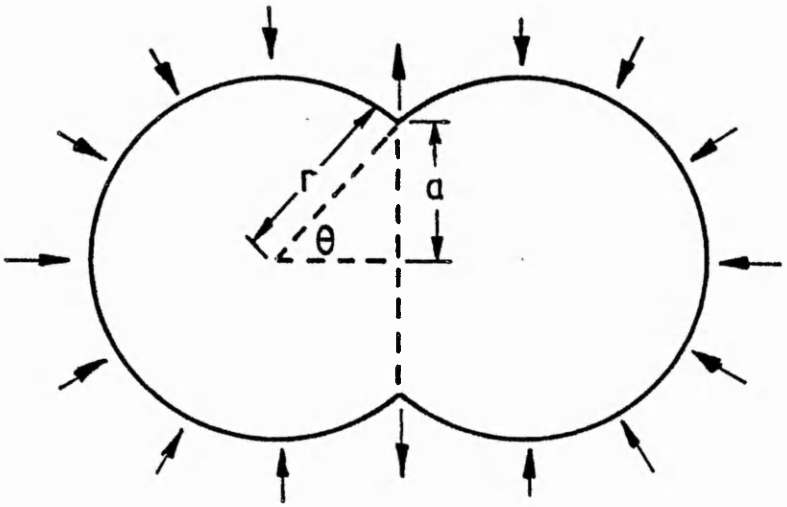

FIG I:5 COALESCENCE OF SPHERES BY VISCOUS FLOW CAUSE BY SURFACE TENSION FORCE (FROM DILLON et al (120))

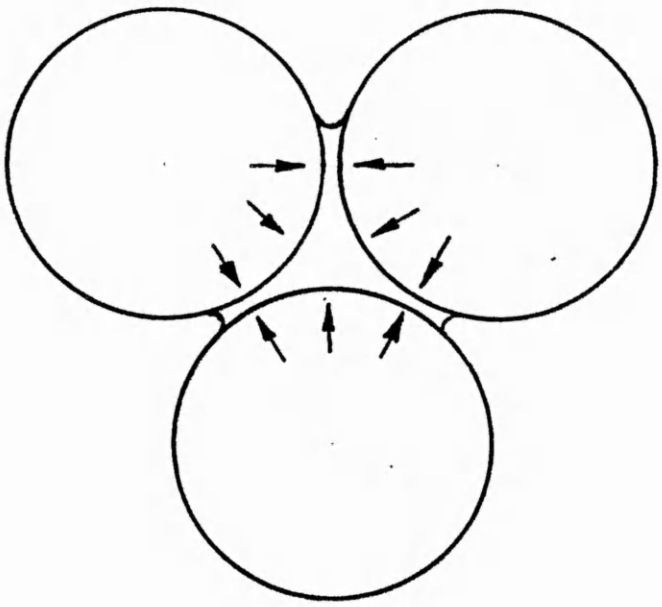

FIG I:6 COALESCENCE OF SPHERES CAUSED BY CAPILLARY FORCES (FROM BROWN (121))

supply the driving force for coalescence. Brown suggested that the polymer surface tension should be replaced by the polymer/water interfacial tension, and that a range of 0 - 10 mN m^{-1} would be realistic for this.

(ii) The observation that the rate of water removal influences the coalescence of borderline film forming latices.

(iii) That porous, incompletely coalesced films were formed by latices below their minimum film formation temperature.

(iv) The ability of lightly cross linked polymer latices (where viscous flow could not occur) to form continuous films, albeit lacking in strength.

Brown then considered the possible forces operating during coalescence (listed above): of these, he eliminated the gravitational force F_g, as being negligible, and assumed that the forces of repulsion, F_e, are greater than the van der Waals forces of attraction, F_v (the condition for a stable dispersion). By implication, the resulting repulsion was not considered to be a significant barrier to coalescence. Brown considered the influence of the surface tension force, F_s, to be small, because this force could only operate when a concave polymer surface existed, and this would only be so in the later stages of coalescence. Moreover, in the presence of surfactant, the surface tension would be low, and this would diminish F_s still further. Having eliminated these forces, the original inequality (Eq. I:10) reduced to:

$$F_c > F_G \qquad \text{(I:13)}$$

for coalescence to occur.

Brown then went on to attempt a semi-quantitative solution. He calculated the capillary pressure, F_c, using the 'throat' which exists in the plane passing through the centres of three contiguous particles, as the capillary (see Fig. I:6). This gave

$$F_c = 12.9\ A / r \qquad \text{(I:14)}$$

where the factor 12.9 arises from geometrical considerations. Brown took the force required to deform the particles to be the product of the shear modulus of

the polymer, G_i, and a geometrical constant, i.e.

$$F_G = 0.37\ G_i\ A \qquad \text{(I:15)}$$

From these results, the condition for film formation becomes

$$G_i < 35\ \gamma / r \qquad \text{(I:16)}$$

since G_i will be dependent on temperature, the minimum film formation temperature is that at which G_i is equal to $35\ \gamma / r$, i.e.

$$G_i\ \gamma / r = 35 \qquad \text{(I:17)}$$

The mechanisms proposed by Dillon et al.[120] and Brown[121] predict that the force tending to cause coalescence varies with particle size. For large particles, of the order of 1 μm, the calculated forces seemed inadequate to cause coalescence. Vanderhoff et al.[124] drew attention to experimental evidence inconsistent with this result. For example, a series of monodisperse styrene-butadiene copolymer latices of particle sizes 0.1 to 1 μm all formed continuous films with essentially equivalent properties, regardless of particle size.

To deal with this problem, Vanderhoff et al extended the model of Dillon et al by arguing that in the incipient stages of coalescence, the radius of curvature between two particles is very small (Fig. I:7). They maintained that, to be valid, any calculation using the equation of Young and Laplace must include these radii as well as the particle radius. According to their analysis, the pressure difference across the particle/water interface is

$$P_2 - P_1 = 2\ \gamma / r \qquad \text{(I:18)}$$

and in the region of coalescence

$$P_3 - P_2 = \gamma\ (1/r_1 - 1/r_2) \qquad \text{(I:19)}$$

γ is the polymer/water interfacial tension and the pressures, P and the radii, r, are shown in Fig. I:7. $1/r_2$ is negative because the polymer surface here is concave. By assuming that $P_1 = P_3$, these equations can be combined to give

$$P = P_2 - P'_2 = \gamma\ (1/r_1 - 1/r_2 + 2/r) \qquad \text{(I:20)}$$

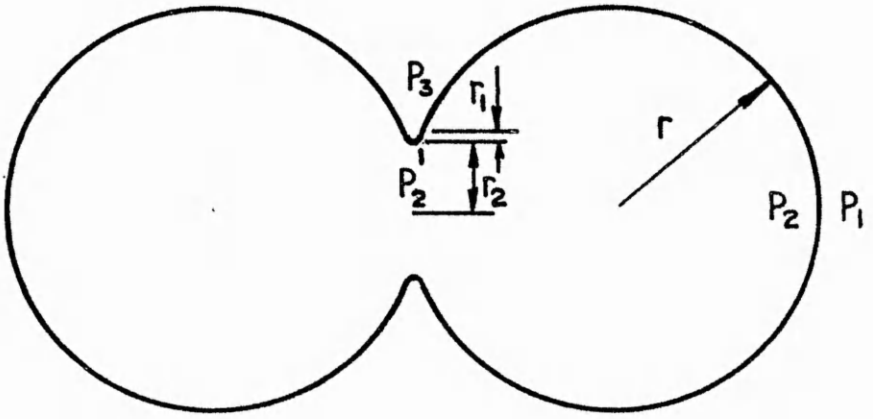

FIG I:7 THE RADII OF CURVATURE INVOLVED IN THE COALESCENCE OF TWO SPHERES FROM VANDERHOFF et al (124))

A sufficiently small value of r_1 would give a pressure large enough to cause coalescence. However, this pressure diminishes as coalescence proceeds, since r_1 will increase.

Mason[125] criticised the models of both Brown[121] and Vanderhoff et al.[124] on the ground that force and pressure were confused, resulting in erroneous calculated values for the pressure forcing two particles together. Brown's calculations were amended to give a revised condition for film formation of

$$G_i < 266 \gamma / r \qquad \text{(I:21)}$$

However, Mason considered the mechanism of Vanderhoff et al. to be completely invalidated because the condition for a large pressure resulted in that pressure acting on a very small area of the stabilising layer. The stabilising layer would be ruptured at the point of contact, but the surface tension force would be insufficient to coalesce the particles.

Mason went on to distinguish four cases:

Mode I — liquid latex particles, having a low elastic limit and shear modulus, will coalesce irrespective of particle size.

Mode II — polymer particles with a low elastic limit and any shear modulus: here coalescence depends on capillary forces exceeding resistance to deformation, and will thus be dependent on particle size.

Mode III — medium elastic limit and medium to high shear modulus. Coalescence will be independent of particle size until the stabilising layer is ruptured, and dependent thereafter. Mason felt that this case was unlikely because it required an improbable combination of physical properties.

Mode IV — high elastic limit and medium to high shear modulus. Here the stabilising layer is easily ruptured, but the polymer will not flow. This is the result expected when drying a non film-forming latex.

Brodnyan and Konen[126] attempted to verify Brown's mechanism by correlating the minimum film formation temperature of a latex with its particle size, surface tension and polymer shear modulus, thereby testing Equation (I:17) which predicts that for a given polymer, the quantity $G_i \gamma/r$ should be constant at the minimum film formation temperature. They found that the ability of a latex to form a film was not strongly dependent on particle size or surface tension. However, the shear modulus of the polymer did fall most rapidly with

increasing temperature in the region of the minimum film formation temperature, as predicted by Brown. Unfortunately, the measurement of minimum film formation temperature was subject to considerable random error. It was not, therefore, possible to prove unequivocally that $G_i \gamma/r$ was constant for one polymer type and a range of surface tensions and particle sizes because of uncertainty in the correct choice of shear modulus.

Although the differences in the value of $G_i \gamma/r$ for different latices of the same polymer were not significant, the differences between different polymer types were much larger, ranging from a value of 0.58 for a non-polar copolymer to 260 for a polar one. These values are to be compared with the values 35 and 266 predicted by Brown and Mason respectively.

Brodnyan and Konen also noted the difference between the minimum film formation temperature and glass transition temperature, T_g, which ranged from $10^{\circ}C$ for non-polar and $-3^{\circ}C$ for polar copolymers. They suggested that this variation with polymer polarity together with that in $G_i \gamma/r$, was partially due to greater plasticisation by water of polymer . However, this factor alone would be insufficient to account for the measured differences.

The most recent theoretical treatment of film formation was given by Lamprecht[127]. The physical model of Brown[121] was accepted, but the calculation was refined, giving a more restricted condition for film formation. The influence of rate of water removal was recognised by treating the polymer physical properties (i.e. shear modulus and creep complience) as being time dependent.

The force opposing deformation F(t), was given as that generated when two viscoelastic bodies are pressed together. This was shown to be

$$F(t) = \frac{8}{3\sqrt{3}}\left(\frac{k}{l}\right)^{3/2} r^2 \int_0^t G\,(t-\tau)\sqrt{\tau}\,d\tau \qquad \text{(I:22)}$$

where k is the (constant) rate of evaporation per unit area, l is the thickness of the film at 74% space filling and t is the relaxation time. For particle coalescence to occur, this force must not exceed the force F_{max} which arises from the maximum external pressure, P_{max}, i.e.

$$F(t) < F_{max} \qquad \text{(I:23)}$$

F_{max} and P_{max} are related by

$$F_{max} = \sqrt{2} \quad (1-a^2/r^2)^2 \; r^2 \quad P_{max} \qquad \text{(I:24)}$$

where a is the contact radius (see Fig. I:5) when coalescence is complete and the once spherical particles are completely deformed into dodecahedra, and the geometric term assumes the value 0.0953. The condition for film formation then becomes

$$1.33 \left(\frac{k}{t}\right)^{3/2} \int_0^{t^*} G(t^*-\tau)\sqrt{\tau}\, d\tau \leq P_{max} \qquad \text{(I:25)}$$

where t^* is the time taken for complete coalescence to occur, and is equal to 0.286 l/k.

Lamprecht commented on the disagreement[127] over the calculation of P_{max} and considered that its practical measurement posed insuperable difficulties, given the length of time required for equilibrium to be attained and the fact that loss of water did not occur uniformly. Instead, he attempted to estimate P_{max} from measured values of G(t), k and l, using Eq. (I:25). This gave an answer of $1.3.10^8$ N m^{-2} ≈ 1280 atmos, which is of the same order of magnitude as that given by Brown [121] and corresponds approximately to the theoretical value for the tensile strength of water[128].

2. Final Stages of Film Formation

According to the models described above, the film formed from a latex dispersion would be comprised of deformed polymer particles held together by physical forces. Voyutskii[129] considered that these forces alone could not account for the mechanical properties of the film. Instead, he postulated the mutual interdiffusion of polymer chain ends, termed autohesion, which tends to make the film more homogeneous. The concept of autohesion, which has been invoked to explain many polymer phenomena, particularly in the field of adhesion, has been examined experimentally (see reviews by Voyutskii[130,131]) and the influence of polymer characteristics qualitatively determined. As might be expected, the rate and extent of autohesion were inversely related to the polymer molecular weight and degree of cross linking: autohesion was greatest for polymer molecules with few, long branches and least for those with many short branches.

In two studies of latex film morphology, Bradford and Vanderhoff[132,133]

demonstrated that freshly formed films behaved in a manner consistent with autohesion theory. Using a poly (vinyl alcohol) replication technique and transmission electron microscopy to examine film surfaces, they found that freshly formed (2½ hours after casting) styrene-butadiene copolymer latex films showed clearly the contours of the coalesced particles, even though the film was continuous and transparent. As the films aged, the contours became less pronounced and blister-like eruptions appeared. After 14 days, the contours had disappeared and the eruptions grown. This exuded material eventually flowed over the surface of the film. It was later shown to be surfactant which had been stabilising the particles prior to drying, and which was incompatible with the polymer.

Further work showed that this process, which was termed further gradual coalescence, could be observed in the interior of the film. The presence of surfactant resulted in films having appreciable porosity, which became greater if the film was washed with water. This porosity appeared to diminish with age. Films cast from latices from which the surfactant had been removed by dialysis were less porous.

The type of substrate on which the film was cast did not affect the course of the further gradual coalescence. However, styrene-butadiene copolymer latices were sensitive to the atmospheric composition. The further gradual coalescence accelerated as the oxygen content increased and stopped completely in a nitrogen atmosphere. This effect was attributed to oxidative softening of the polymer.

Variation in the degree of cross linking and molecular weight produced the expected effect. Thus, adding divinyl benzene to the polymerisation reactants reduced the extent of further gradual coalescence, whilst adding tert-dodecyl mercaptan increased the rate.

Bradford and Vanderhoff[133] also studied other polymer types, including methyl methacrylate/ethyl acrylate and vinylidene chloride/vinyl chloride/ ethyl acrylate copolymers. These films also underwent further gradual coalescence, although the surfactant exudations were not observed. Poly (vinyl acetate) latex films, however, appeared not to age. This was ascribed to surface hydrolysis giving a bound layer of hydrophilic poly (vinyl alcohol), across which the poly (vinyl acetate) chains could not diffuse.

The assertion that latex films become completely homogeneous after the operation of certain coalescence mechanisms is contradicted by the work of Distler and Kanig[134]. These authors reasoned that, although some interdiffusion of polymer chain segments was to be expected, the extent would be restricted by the incompatibility of the hydrophilic surface groups with the

bulk polymer. These surface groups would include surfactant grafted onto the particle surface during the polymerisation reaction[135] as well as the charged endgroups arising from the initiator fragments.

Distler and Kanig[134] produced several pieces of experimental evidence to support their hypothesis. The first indication was given by the turbidity of previously clear films on swelling in water. This effect was ascribed to penetration of water into the interior of the film, along the hydrophilic boundary layers. If the latex from which the film had been prepared was monodisperse with the particle diameters between 200 - 400 nm, and these particles were close packed in the film, then Bragg scattering could be observed in the swollen film. In order to confirm that this effect was not due to deposition of water soluble materials, such as initiator residues and surfactant, a film cast from a latex containing 1% acrylic acid was treated with uranyl acetate. This left uranyl ions bound to the carboxyl groups arising from the acrylic acid as well as to acid residues from initiator fragments and grafted surfactant, most of which were considered to be isolated on the particle surface. The excess uranyl acetate was removed by careful washing in water. A thin section of the treated film examined by transmission electron microscopy showed a point pattern with fine webs between the points. The webs were interpreted as delineating the particle boundaries, with the points being due to water soluble materials in the interstices.

Distler and Kanig[134] also observed particle contours in acrylate latex films by using transmission electron microscopy with the aid of a contrasting technique[136]. This entailed exposure of an acrylate containing polymer films to hydrazine hydrate vapour for several days, washing, sectioning and staining with osmium tetroxide. Films treated in this way had a clearly visible honeycomb structure, showing that the boundaries between deformed latex particles were maintained. This honeycomb pattern was apparent in every latex film examined, including those cast from surfactant-free latices of a single acrylate polymer. The spacing of the honeycomb pattern agreed well with the particle size of the original latex, determined by transmission electron microscopy.

Distler and Kanig[134,137] also examined films cast from solutions of freeze dried polymer in tetrahydrofuran. The solutions were sufficiently dilute (0.1%) for the 'felting' of the polymer chains in the particles to have been overcome, giving a completely homogeneous solution. However, particle boundaries were observed in solvent cast films of poly(ethyl acrylate) and poly(n-butyl acrylate). The particle sizes were roughly the same as the honeycomb spacing in the latex films, showing that the particles had gelled rather than

truely dissolved in the solvent, and that some self-cross-linking must have occurred during the polymerisation. Acrylate monomers contain a labile tertiary hydrogen atom, and are known to undergo chain transfer to polymer side reactions leading to branching and cross-linking[138]. Films cast from a similar solution of poly(n-butyl methacrylate) were featureless, showing that cross linking does not occur in this polymer[137].

3. Conclusions

The various theories of film formations give a reasonable qualitative appreciation of the processes occurring when a latex dispersion is dried. For the first stage (evaporation of water and deformation of the polymer particles) the model of Brown[121], as modified[125,127] is now the most widely accepted mechanism. However, even the latest treatment[127] still only considers capillary forces opposed by the resistance of the particles to deformation. The influence of such factors as flocculation processes during drying, the softening effect of water on many polymers, surface tension forces in the last stages of coalescence and van der Waals forces have yet to be quantified[127].

Studies of the long term behaviour of latex films have shown that changes in morphology do occur[129-133]. Voyutskii's Autohesion theory qualitatively explains these observations. However, in the light of recent work by Distler and Kanig[136-137], it can be seen that the films do not become completely homogeneous. The morphology of a latex film will almost certainly influence its transmission properties. Measurement of these properties may therefore assist in understanding these morphological changes.

C. DIFFUSION AND PERMEATION

The discovery that a rubber membrane is permeable to gases was made by Mitchell in 1831[134]. It was also shown that the rate of permeation varied for different gases and that the gases which penetrated most rapidly were those most easily condensed and most soluble in water and other liquids. These ideas were developed by Graham, who, in a paper published in 1866[140] first described permeation in terms similar to those accepted today. Graham drew attention to the greater similarity of rubber to liquid than to a solid, and postulated that permeation was a three stage process comprising condensation and solution of the gas at one face of the film, diffusion as a liquid to the other face, followed by dissolution and evaporation. The increasing rate of permeation with temperature was attributed to an increase in the softness or liquid nature of the rubber.

The next advance came in 1879, when Wroblewski[141] derived the relationship describing the steady state of permeation by combining the integrated form of Ficks' First Law of Diffusion with Henry's Law.

The advent of airships, in the early 1900's, led to major advances in experimental methods of permeability determination. These were applied to measurements of hydrogen and helium permeability through the rubber coated fabrics used in the construction of airship balloons. The determination of diffusion coefficients from permeation experiments was made possible in 1920, when Daynes[142] gave a solution of Fick's Second Law, which related it to the so-called time lag. However, it was not until 1939 that Barrer[143] fully developed the experimental techniques necessary to use it. Since that time, this approach has accounted for much of the diffusion, solubility and permeation data determined so far.

1. Determination of the Diffusion and Permeability Coefficients

Diffusion may be defined as the process by which matter is transported from one part of the system to another by random molecular motions. In the context of this work, matter refers to gases and vapours and the system is the polymer film through which they must diffuse. Permeation of a gas or vapour through a polymer film, under the influence of a (partial) pressure difference, is a three stage process, comprising solution (condensation followed by mixing) at one face of the film, diffusion to the other face, followed by dissolution.

Suppose that the film is initally free from penetrant. When one face is exposed to the penetrant, there will be an accumulation within the film and the

rate of dissolution from the opposite face will rise from zero to a constant value. This is known as the transient state of permeation. When the constant rate of dissolution is attained, a steady state of permeation prevails.

The starting points for the mathematical treatment of permeation are Fick's laws of diffusion, which were formulated in 1855 by direct analogy with heat conduction. Fick's First Law states[144]:

$$J = -D \frac{\partial c}{\partial x} \qquad \text{(I:26)}$$

where J is the diffusion flow or flux through unit area of film

D is the diffusion coefficient

c is the concentration of penetrant in the film

x is the distance through the film

Consider two planes, parallel to the faces of the film, at distances x and x + dx from the high concentration face (see Fig. I:8). If diffusion is considered through the x-direction only (x normal to the faces of the film), there is an accumulation of permeant, with time, within the volume element bounded by these planes, i.e.

$$J_x - J_{x+dx} = \frac{\partial c}{\partial t} = -D \frac{\partial c}{\partial x} + D \frac{\partial}{\partial x} \left[c + \frac{\partial c}{\partial x} dx \right] \qquad \text{(I:27)}$$

Where dc/dt is the accumulation of permeation as a function of time. As dx → 0, this becomes

$$\frac{\partial c}{\partial t} \quad \frac{\partial}{\partial x} \left[D \frac{\partial c}{\partial x} \right] \qquad \text{(I:28)}$$

If the diffusion coefficient is independent of concentration, this reduces to

$$\frac{\partial c}{\partial t} = D \frac{\partial^2 c}{\partial x^2} \qquad \text{(I:29)}$$

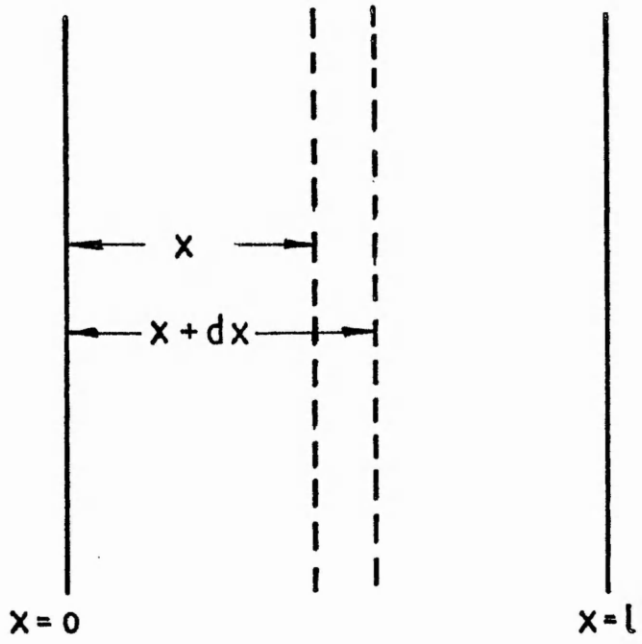

FIG I:8 DIFFUSION THROUGH SECTION OF FILM. PENETRANT ACCUMULATES IN VOLUME ELEMENT BOUNDED BY PLANES x AND x + dx

which is the usual form of Fick's Second Law. Where the diffusion coefficient is dependent on concentration only, Eq. I:28 may be transformed to give

$$\frac{\partial c}{\partial t} = D(c) \frac{\partial^2 c}{\partial x^2} + \frac{\partial D(c)}{\partial c} \left[\frac{\partial c}{\partial x}\right]^2 \qquad \text{(I:30)}$$

If the concentration difference across the film is small, then the term d D(c)/dc will be negligible by comparison with the absolute magnitude of D(c), the concentration dependent diffusion coefficient. The value obtained by this method will be a mean diffusion coefficient $\bar{D}$, which is defined by

$$\bar{D} = \frac{1}{c_1 - c_o} \int_{c_o}^{c_1} D(c)\, dc \qquad \text{(I:31)}$$

Where c_1 and c_o are the concentrations of diffusant at the high and low concentration sides of the film respectively. Thus, in principle, it is possible to estimate the dependence of D (c) on c.

In practice, most permeation experiments are carried out such that $c_o = 0$.

Eq. (I:31) then reduces to

$$\bar{D} = \frac{1}{c_1} \int_{o}^{c_1} D(c)\, dc \qquad \text{(I:32)}$$

In the steady state, the diffusion flow, J, is constant. Eq. (I:33) may be integrated to give

$$J_s = -\frac{1}{l} \int_{c_o}^{c_1} D\, dc = \frac{D(c_1 - c_o)}{l} \qquad \text{(I:33)}$$

where the diffusion coefficient is independent of concentration. Where this is not the case, D must be replaced by $\bar{D}$, as defined by Eqs. (I:31) or (I:32)

a) Calculation of the Diffusion Coefficient from Transient State Permeation Measurements

The calculation of diffusion coefficients from transient state permeation measurements requires the solution of Eq. I:26. The system under consideration here is a flat film of finite thickness l; t is the time from the start of the experiment and the concentrations at the faces of the film x = 0 and x = l are c_l and c_o respectively, the appropriate boundary conditions are

$$c(x,0) = c_o$$

$$c(0,t) = c_l$$

$$c(l,t) = c_o$$

and the solution is[142,144]

$$c(x) = c_1 + \frac{(c_1-c_o)x}{l} + \frac{2(c_o-c_1)}{\pi} \sum_{n=1}^{\infty} \frac{1}{n} \sin\left(\frac{n\pi x}{l}\right) \exp\left(\frac{-n^2\pi^2 Dt}{l^2}\right) \qquad \text{(I:34)}$$

Solutions for different geometrics and boundary conditions have been presented by Crank[144], and for the mathematically analogous process of thermal conductivity, by Carslaw and Jaegar[145].

The rate at which penetrant emerges from unit area of the face x = l of the film can be obtained by differentiating Eq. I:34.

$$\left[\frac{\partial c}{\partial x}\right]_{x=l} = \frac{c_o-c_1}{l} \left[1 + 2\sum_{n=1}^{\infty}(-1)^n \exp\left(\frac{-n^2\,2Dt}{l^2}\right)\right] \qquad \text{(I:35)}$$

Integrating this relationship with respect to time gives Q_t, the amount of penetrant which has permeated through unit area of the film in time t

$$Q_t = \int_0^t D \left[\frac{\partial c}{\partial x}\right]_{x=1} dt$$

$$= \frac{D(c_o - c_1)}{1} \left[1 + 2\sum_{n=1}^{\infty} (-1)^n \frac{-1^2}{n^2\pi^2 D} \exp\left(\frac{-n^2\pi^2 Dt}{1^2}\right) - 2\sum_{n=1}^{\infty} (-1)^n \frac{-1^2}{n^2\pi^2 D} \right] \qquad \text{(I:36)}$$

The steady state is reached when t becomes large and the exponential term approaches zero: Eq. I:36 reduces to

$$Q_t = \frac{D(c_o - c_1)t}{1} - \frac{(c_o - c_1)1}{6} \qquad \text{(I:37)}$$

If Q_t is plotted as a function of t (the so-called 'Barrer' plot) the result is a curve at small values of t, becoming a straight line at far larger t (see Fig. I:9). If the straight line portion is extrapolated back to the t axis, the intercept is termed the time lag, τ. Eq. I:37 becomes

$$\tau = \frac{1^2}{6D} \qquad \text{(I:38)}$$

Eq. (I:3)[38] is the basis of the original Barrer permeation experiment[143], in which Q_t is measured directly as a function of time, and τ is determined graphically. However, the apparatus used in this work measures the instantaneous rate of permeation, J_t, rather than the cumulative quantity Q_t.

One method[146] of calculating the diffusion coefficient directly from this is to define a time, $t_{\frac{1}{2}}$, at which J_t is equal to half the steady state value, J_s. This is related to the diffusion coefficient by

$$t_{\frac{1}{2}} = \frac{1^2}{7.199D} \qquad \text{(I:39)}$$

To make use of this equation requires an accurate knowledge of t = O, i.e. the time at which the change in penetrant concentration above the film occurs. This change in concentration is achieved by operating a switching value, which is necessarily some distance upstream of the film, thereby introducing an uncertain

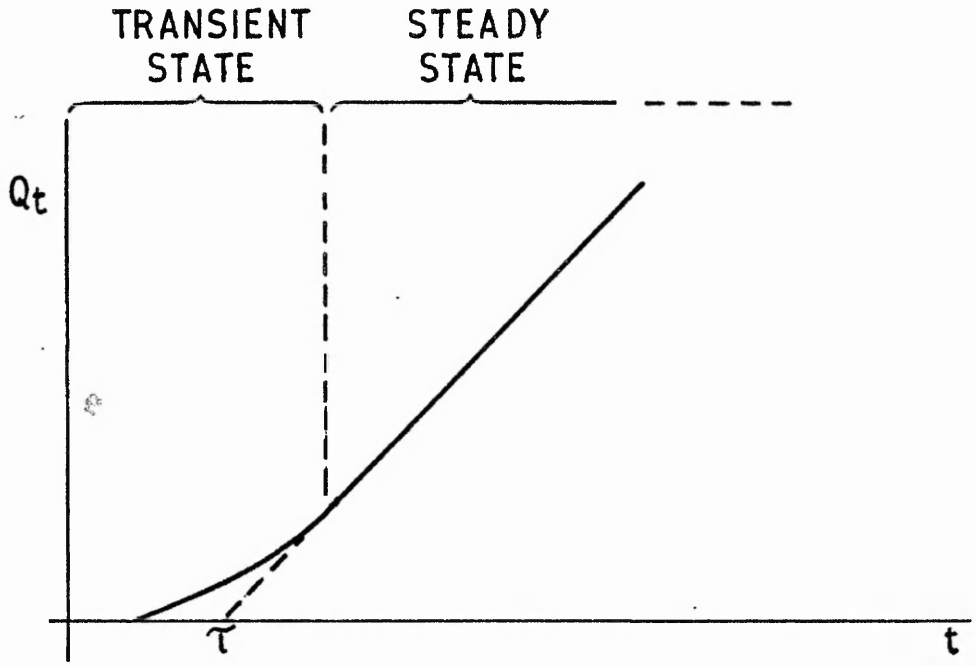

FIG I:9 BARRER PLOT OBTAINED FROM PRESSURE CHANGE PERMEATION EXPERIMENT

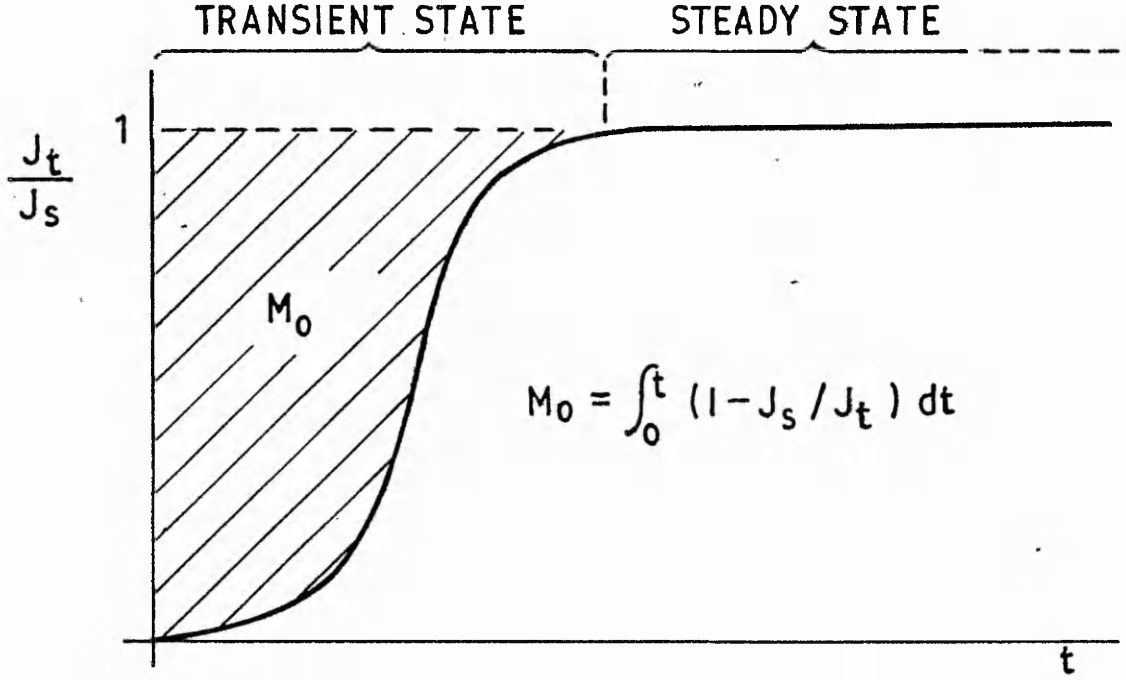

FIG I:10 NORMALISED RESPONSE CURVE OBTAINED FROM CONCENTRATION CHANGE PERMEATION EXPERIMENT

'plumbing' lag. Another disadvantage is that only a single point on the permeation curve is used.

Another approach[147] is to plot the normalised permeation rate J_t/J_s against time (Fig. I:10). The shaded area, which can be evaluated graphically or numerically is defined as M_o. Thus

$$M_o = \int_o^\infty (1-J_t/J_s)\, dt \qquad \text{(I:40)}$$

Now, recalling that

$$J_t = -D \frac{\partial c}{\partial x} \qquad \text{(I:26)}$$

and

$$J_s = \frac{D\,(c_1 - c_o)}{l} \qquad \text{(I:33)}$$

Eq. I:35 may be rewritten

$$1 - \frac{J_t}{J_s} = -2 \sum_{n=1}^{\infty} (-1)^n \exp\left(\frac{-n^2 \pi^2 Dt}{l^2}\right) \qquad \text{(I:41)}$$

Hence,

$$M_o = \int_o^\infty \left[-2 \sum_{n=o}^{\infty} (-1)^n \exp\left(\frac{-n^2 \pi^2 Dt}{l^2}\right)\right] dt \qquad \text{(I:42)}$$

After integration and rearrangement, this becomes

$$M_o = \frac{l^2}{6D} \qquad \text{(I:43)}$$

Although this method uses the whole permeation curve, it still requires an accurate knowledge of t = O.

A more satisfactory method of calculating diffusion coefficients, devised by Pasternak et al.[148] employs an alternative solution of the diffusion equation, derived by using Laplace transforms[144]. The expression for the rate at which penetrant emerges from unit area of the face x = l becomes

$$J_t = 2(c_1 - c_o)\left(\frac{D}{\pi t}\right)^{\frac{1}{2}} \sum_{n=o}^{\infty} \exp\left(\frac{-l^2(2n+1)^2}{4Dt}\right) \qquad \text{(I:44)}$$

Where J_t/J_s is the normalised permeation rate. This approximation is valid for $J_t/J_s < 0.97$, i.e. over most of the transient state.
Substituting $y = J_t/J_s$ and $x^2 = l^2/4Dt$ gives

$$y = \frac{4}{\pi^{\frac{1}{2}}} x \exp(-x^2) \qquad \text{(I:45)}$$

the right hand side of which is the second derivative of the error function.

Numerical values of this function, taken from ref. 148, are given in Table I:1; if plotted, a theoretical permeation curve is obtained. To determine the diffusion coefficient, the experimental curve is analysed to give the times at which J_t/J_s takes the values given in Table I:1. If the corresponding values of $(4Dt/l^2)$ are plotted against these times, a straight line of slope $4D/l^2$ results.

This method has the advantages of using all the experimental data and not relying on precise definition of t = 0. Moreover, by obtaining a straight line graph, the validity of Fick's Second Law is confirmed.

b) Calculation of Permeability Coefficients from Steady State Permeation Measurements

The diffusion coefficient is related to the steady state diffusion flow by

$$J_s = \frac{D(c_1 - c_o)}{l} \qquad \text{(I:33)}$$

In the practical situation, it is the pressures, p, above the faces of the film rather than the surface concentrations, c, which are known. These quantities are related by Henry's Law[144], which states that

$$c = Sp \qquad \text{(I:46)}$$

where S is the solubility coefficient. This relationship is obeyed only at low penetrant concentrations. It is often found that for systems in which the diffusion coefficient is concentration dependent, i.e. those in which the penetrant is a vapour rather than a gas, the solubility coefficient also exhibits a concentration or pressure dependence.

TABLE I:1

NUMERICAL VALUES FOR NORMALISED THEORETICAL PERMEATION CURVE OF RELATIVE FLUX, $y = J_t/J_s$ AGAINST NORMALISED TIME $1/x^2 = 4Dt/l^2$.

$y = J_t/J_s$	$1/x^2 = 4Dt/l^2$	$y = J_t/J_s$	$1/x^2 = 4Dt/l^2$
0.05	0.220	0.55	0.600
0.10	0.265	0.60	0.650
0.15	0.300	0.65	0.705
0.20	0.335	0.70	0.770
0.25	0.370	0.75	0.845
0.30	0.405	0.80	0.940
0.35	0.440	0.85	1.045
0.40	0.475	0.90	1.210
0.45	0.510	0.95	1.570
0.50	0.555		

Combination of Eqs. I:33 and I:46 gives the well known permeation equation

$$J_s = \frac{DS\ (p_1 - p_o)}{l} \qquad \text{(I:47)}$$

The product DS is termed the permeability coefficent, P, so that

$$P = DS \qquad \text{(I:48)}$$

and

$$J_s = \frac{P(p_1 - p_o)}{l} \qquad \text{(I:49)}$$

Peterlin[149] considered that the true definition of the permeability coefficient is Eq. I:49 and that Eq. I:48 is an empirical relationship which is only obeyed by certain ideal systems.

Since J_s is the amount of penetrant, Q, which has passed through the film in time t,

$$J_s = Q/t \qquad \text{(I:50)}$$

For practical purposes, it is convenient to remove the area from the definition of J_s and Q, so that these quantities become respectively the flow, and the amount of penetrant passing, through a sample of film of area A. Thus

$$Q = \frac{PA\ t\ (p_1 - p_o)}{l} \qquad \text{(I:51)}$$

or, after rearrangement,

$$P = \frac{Ql}{A\ t\ (p_1 - p_o)} \qquad \text{(I:52)}$$

so that the permeability coefficient of a film of known surface area and thickness can be calculated from permeation rate data.

Concentration dependence of the diffusion, solubility and permeability coefficients has been dealt with theoretically in the following manner (150). The measured permeability coefficient is a mean value for the pressure gradient p_1 to p_o, corresponding to the equilibrium surface concentrations c_1 and c_o defining the mean diffusion coefficient (Eq. I:31), i.e.

$$J_s = \bar{P}\ \frac{(p_1 - p_o)}{l} \qquad \text{(I:53)}$$

Thus

$$J_s = \left[\frac{1}{c_1 - c_o} \int_{c_o}^{c_1} D(c)\, dc \right] \left[\frac{c_1 - c_o}{p_1 - p_o} \right] \left[\frac{p_1 - p_o}{1} \right] \qquad \text{(I:54)}$$

The mean solubility coefficient is given by

$$\bar{S} = \frac{c_1 - c_o}{p_1 - p_o} \qquad \text{(I:55)}$$

so that

$$\bar{P} = \bar{D}\,\bar{S} \qquad \text{(I:56)}$$

2. Factors affecting the permeability of polymer films

Permeation was previously described as a three stage process of solution, diffusion and dissolution. The penetrant is considered to be in a condensed state during the diffusion process. Where the polymer is amorphous, and above its glass transition temperature, the movement of penetrant molecules is similar to the motions of molecules in a liquid. For a polymer below its glass transition temperature or one having a significant crystalline content, the process is more complex. It has, however, been pointed out[150] that the differences in diffusion behaviour between mobile liquids, amorphous elastomers and crystalline solids are ones of degree rather than kind. Thus, generalised models need not be restricted to one particular state.

An amorphous polymer can be visualised as a tangled mass of polymer chains with spaces or holes between them. The diffusion of a penetrant molecule through a film of such a polymer can then be considered as a series of jumps between holes. There may also be defects within the film, such as cracks, voids, capillaries or grain boundaries, and these will also contribute to the permeation process.

a. Effect of Temperature

Over moderate ranges, the temperature dependence of diffusion, solubility and permeability coefficients are described by Arrhenius relationships (150,151)

$$D = D_o \exp(-E_D/RT) \qquad (I:57)$$

$$S = S_o \exp(-\Delta H_s/RT) \qquad (I:58)$$

$$P = P_o \exp(-E_p/RT) \qquad (I:59)$$

E_D and E_P are the activation energies of diffusion, and permeation respectively, while ΔH_s is the heat of solution. D_o, S_o and P_o are constants.

The most frequently reported departure from these relationships occurs in the region of the glass transition temperature of the polymer concerned. In log coefficient vs. reciprocal temperature plots, a change in slope between two straight lines is often observed. The calculated activation energies are normally greater above the glass transition temperature than below it. A typical example is the data of Mears[152] for poly (vinyl acetate). The diffusion, solubility and permeability coefficients for hydrogen, helium, oxygen, neon and argon through this polymer were found to behave in this way.

There are some polymers, however, where this change in slope of the

Arrhenius plot at the glass transition temperature does not occur, or only occurs for certain gases. Stannett and Williams[115] determined the transport properties of gases ranging from helium to krypton and carbon dioxide through poly (ethyl methacrylate). The Arrhenius plots constructed from their data showed no changes in slope at the glass transition temperature. Kumins and Roteman[153] obtained the same result for a vinyl chloride - vinyl acetate copolymer for several gases, but with the exception of carbon dioxide where the slope did change.

Over extended ranges of temperature, it is often observed that Arrhenius plots are curved. Van Amerongen[154] and Barrer and Skirrow[165] observed deviations from linearity in log D and log P against 1/T plots, with the activation energy decreasing with increasing temperature.

These effects can be discussed in terms of the free volume picture of diffusion, as discussed in below.

b. Nature of the Penetrant

The size and shape of a penetrant molecule will influence its rate of diffusion within a polymer film, whilst the solubility will be affected by its polarity and ease of condensation. The overall effect on permeability will depend on the interplay of these factors.

The non condensable gases have very low solubilities in polymers, and therefore there is little polymer/penetrant interaction. The predominant influence is molecular size, and the reduction in diffusion or permeability coefficient with increasing size is well documented. For example, the permeabilities of cellulose acetate, polystyrene and poly (vinyl chloride) to helium, neon and krypton were shown[155] to decrease rapidly with increasing penetrant diameter. Molecular weight can also be used as a measure of size. One study[156] has demonstrated a good correlation between log D and molecular weight.

As the penetrant size increases and it becomes condensable, its interaction with the polymer becomes more pronounced. This has consequences for both solution and diffusion behaviour. Organic vapours are appreciably soluble in polymers and their effect is to make both the solubility and diffusion coefficients highly concentration dependent. This effect can be qualitatively explained on the basis of sorbed penetrant molecules plasticising the polymer, enhancing the solution and diffusion of further penetrant.

In extreme cases, involving the sorption of organic penetrants by glassy polymers, a boundary is observed between unswollen and highly swollen regions[150]. A dual or two stage mechanism has been proposed to account for this[157], which envisages sorption in the unswollen state to be diffusion

controlled, whilst sorption in the swollen state is controlled both by diffusion and polymer relaxation. Diffusion in the latter is often referred to as anomalous or non-Fickian, since diffusion coefficients are time as well as concentration dependent.

The effect of molecular size appears only to be important for smaller organic molecules. Studies of hydrocarbon diffusion through natural rubber[158] indicated that for the homologous series of n-alkanes above n-butane, the diffusion coefficient was barely affected by increasing carbon chain length. Molecular shape is a more important consideration, and this was demonstrated by the observation that branched alkanes diffuse more slowly than n-alkanes containing the same number of carbons[158].

c. Nature of the Polymer

Polymers are complex materials which can be characterised in many different ways, e.g. in terms of physical properties, such as density and glass transition temperature, or in terms of structure (degree of branching and cross linking). It is virtually impossible to study systematically the influence of these characteristics, because changes in one feature will almost certainly lead to changes in others.

In terms of the hole concept of diffusion, it can be seen that the rate of diffusion will depend on the number and size of existing holes, and the ease with which new holes can be formed. The former will depend on the packing of the chains and is related to the free volume and the density. The latter will depend on the segmental chain mobility and the cohesive energy of the polymer.

In general, polymer properties may change considerably with molecular weight, although most vary in a similar fashion. Mechanical strength does not develop until molecular weights of 5 - 10,000 are reached. Above this figure, mechanical strength increases rapidly and then levels off.

The effect of polymer molecular weight on permeability is variable, depending on the polymer/penetrant systems under consideration. A reduction in permeability coefficient with increasing molecular weight is expected, since both the diffusion and solubility coefficients are likely to fall[150]. This trend has been observed by Furuya[159] and Ito[160] for the permeabilities of polyethylene, poly(vinyl chloride), ethyl cellulose and polyisobutylene to nitrogen, carbon dioxide and water vapour. A more detailed study by Kaminska[110] found that the air permeability of polystyrene films cast from benzene solution depended not only on molecular weight, but dispersity. The polystyrene samples were prepared by fractionation and the films subsequently cast from dilute benzene solution. The permeability coefficient dropped by a

factor of 13 as the molecular weight (calculated from Kaminska's viscosity data, and literature values[85] of k and α via the Mark-Houwink[138] equation) increased from $3.5.10^5$ to $12.7.10^5$. However, several other experimental studies[8,167] have concluded that diffusion and permeability coefficients are not strongly dependent on polymer molecular weight. The activation energies were found to be similarly unaffected.

3. Diffusion Mechanisms and Empirical Relationships

Several theories have been proposed to explain the diffusion of gases through polymers, and in particular, to account for the temperature dependence of diffusion. Diffusion in an amorphous polymer can be visualised in terms of the movement of penetrant molecules through a tangled mass of polymer chains and holes. In a polymer above its glass transition temperature, as in simple liquids, the holes are constantly disappearing and reforming as a result of thermal fluctuations.

The overall diffusion process results from the movement of penetrant molecules from hole to hole under the influence of a concentration gradient. Each jump will require the disruption of polymer-polymer and polymer-penetrant interactions in order that the surrounding polymer chains can rearrange themselves to allow the passage of the diffusing molecule. The extent of the rearrangement, and hence the amount of energy required to produce it, will increase as the size of the hole increases. According to the Boltzmann relationship, the number of holes should decrease exponentially with increasing size.

This simple picture predicts that the diffusion coefficient decreases and the activation energy of diffusion increases for increasing penetrant size, and this is in accord with the experimental evidence discussed above.

The more detailed treatments of diffusion start with the basic premise that the penetrant molecule makes a successful jump between equilibrium positions of distance λ in a random direction with a frequency ν. The diffusion coefficient is related to the jump length and frequency by[161]:

$$D = \frac{\nu\lambda}{6} \qquad \text{(I:60)}$$

It has been argued[161] that the distance which a penetrant molecule travels in jumping between equilibrium positions is unlikely to differ too greatly from polymer to polymer and that the variation in diffusion coefficients, which is several orders of magnitude, must therefore be due to variations in jump

frequency.

Application of the transition state theory of rate processes leads to the following expression for the diffusion coefficient

$$D = \kappa \nu d^2 \exp(-\Delta G^{\dagger}/RT) \qquad \text{(I:61)}$$

where κ is the transmission coefficient, ν is the vibration frequency of the diffusing molecule and $\Delta G^{\dagger}$ is the free energy of activation. $\Delta G\dagger$ is possessed only by the penetrant molecules.

When the diffusant has surmounted the energy barrier, it is assumed that a successful jump will occur, i.e. $\kappa = 1$. It is also assumed that the degree of freedom involved in the diffusion step is a translational one, with the frequency taken to be kT/h, where k and h are the Boltzmann and Plank constants respectively. Since $\Delta G^{\dagger} = \Delta H^{\dagger} - T\Delta S^{\dagger}$
and diffusion is accompanied by a negligible volume change, Eq. I:61 becomes

$$D = e\lambda \frac{kt}{h} \exp(\Delta S^{\dagger}/R) \exp(-E_D/RT) \qquad \text{(I:62)}$$

Comparison of this expression with equation (I:57) leads to relationships linking the experimentally determined variables E_D and D_o with ΔH, ΔS and λ;

$$E_D = \Delta H^{\dagger} + RT \qquad \text{(I:63)}$$

$$D_o = e\lambda^2 \frac{kt}{h} \exp(\Delta S^{\dagger}/R) \qquad \text{(I:64)}$$

The activated zone theory of diffusion, developed by Barrer[164], assumes that the activation energy is acquired by the chain segments involved in the diffusion step as well as the diffusant molecule. These segments and the diffusent molecule comprise a zone of activation of f degrees of freedom, which must acquire a certain energy, E, before a diffusion step can occur. According to this theory, the diffusion coefficient is given by

$$D = \frac{\nu\lambda}{2} \sum_{f=1}^{f_{max}} \rho_f \left[\frac{(E/RT)^{f-1}}{(f-1)!}\right] \exp(-E/RT) \qquad \text{(I:65)}$$

where f_{max} is the value of f for which $(E/RT)^{f-1} / (f-1)!$ is a maximum: ρ_f is the probability that the f degrees of freedom will permit a diffusion jump and ν is the thermal vibration frequency of the diffusing molecule.

Over moderate temperature ranges above the glass transition temperature of the polymer concerned, the activation energy of diffusion E_D is essentially constant. Barrer assumed that one of the terms in the summation, corresponding to an optimum number of degrees of freedom f', would be sufficiently large that the remainder could be neglected. This is rigorously true if $E >> (f-1)\,RT$[163]. With this approximation,

$$E_D = E - (f-1)\,RT \qquad \text{(I:66)}$$

and the resulting equation for D becomes

$$D \simeq \frac{\nu\lambda^2 \rho_f \,(E/RT)^{f-1}}{2(f'-1)\,!} \exp\,(E/RT) \qquad \text{(I:67)}$$

f' can then be calculated, given reasonable values of D, E and ν. ρ_f is assumed equal to 1/6 by analogy with the movement of Schottky defects in a cubic lattice[165]. For the diffusion of simple penetrants in rubber, a jump length of molecular dimensions requires about 13 or 14 degrees of freedom.

Barrer's simplification has been criticised by Eley[166] and Brandt[167]. The latter's calculations show that for some systems, several terms in the summation are of comparable magnitude. However, the approximation appears to be justified, since the accuracy of most experimental data does not warrant the more involved calculations required by the inclusion of more terms in the summation[150]. The result of the Barrer zone theory provides support for the hypothesis that diffusion results from the cooperative movement of several polymer segments.

The temperature dependence of the activation energies of diffusion and permeation can be accounted for by the transition state[162] and zone[163,164] theories. Van Amerongen[154] showed that the temperature dependence could be formally interpreted by transition state theory by considering the variations in enthalpy and entropy of activation with temperature. This treatment predicts

$$\frac{dE_D}{dT} = \alpha + R \qquad \text{(I:68)}$$

where R is the gas constant and α is a constant arising from a series expansion in

the derivation. Barrer and Skirrow[165] discussed the changes on the basis of the zone theory and derived the following equation:

$$\frac{dE_d}{dT} = -(f-1)R \qquad \text{(I:69)}$$

The reduction in activation energy with increasing temperature is interpreted as resulting from an increasing zone of activation.

The question of whether or not a change of slope in Arrhenius plots occurs at the glass transition temperature of the polymer concerned has been discussed by Yasuda and Hirotsu[168]. After examining the available data, they tentatively proposed that if the value of the diffusion coefficient exceeded a critical value (ca. 5.10^{-12} m^2 s^{-1}) at the glass transition temperature, then no change of slope would be observed, regardless of penetrant size. Although no theoretical significance could be attached to this critical value, a qualitative interpretation was proposed. At temperatures above the glass transition temperature, the polymer segmental mobility is greater and it is easier to increase the free volume. The activation energy increases as a result, since more energy is required to cause the necessary perturbation of the polymer chain configuration. However, if the value of the diffusion coefficient is sufficiently large at the glass transition temperature there will be enough free volume within the polymer resulting from normal thermal fluctuations for the additional activation energy not to be required.

Several more sophisticated theories of penetrant diffusions through polymers have been proposed. These involve defining models for the movement of polymer segments during the passage of penetrant molecules and detailed considerations of the energetics of diffusion. Correlations with other polymer properties, particularly viscosity, are attempted. These theories have been reviewed by inter alia, Kumins and Kwei[161] and Fujita[169]. They are, however, outside the scope of this thesis, since many of the parameters necessary to apply them are unknown for latex films.

Several empirical relationships for permeation through polymer films have been devised[170-175]. Although they have little theoretical significance, they are useful in getting a 'feel' for the amount of penetrant likely to be transmitted by a polymer film. This is helpful when designing apparatus for measurement of transmission properties when deciding, for example, the cell dimensions.

The most useful of these relationships for gas permeability is that of Stannett and Szwarc [170]. They found that the permeability coefficient for a particular polymer/penetrant combinations, P_{ij}, could be expressed as the product of two factors determined by the nature of the polymer (F_i) and of the penetrant (G_j), together with an interaction factor, $\gamma_{ij} \cong 1$, i.e.

$$P_{ij} = F_i G_j \gamma_{ij} \qquad \text{(I:70)}$$

This relationship was shown to hold for a wide range of polymers with simple gases at one temperature (303K).

The 'Permachor' relationship[171-173] was derived for the transmission of a wide range of organic penetrants through polyethylene and unplasticised poly(vinyl chloride).

$$\ln P = a + \frac{b}{T} + c\pi \qquad \text{(I:71)}$$

a, b and c are constants for a particular polymer, π is a factor which is characteristic of the penetrant and T is the absolute temperature. π can be evaluated for any common organic penetrant by summing contributions (tabulated in Refs: 171-173) made by its functional groups.

Comparison of Eq. (I:71) with the log forms of the Arrhenius equation (Eq. (I:57)) and the Stannett and Szwarc relationship (Eq. (I:7)), i.e.

$$\ln P = \ln P_o - E_p/RT \qquad \text{(I:72)}$$

$$\ln P_{ij} = \ln F_i + \ln G_j + \ln \gamma_{ij} \qquad \text{(I:73)}$$

shows them to be of the same type. However, the polymer/penetrant combinations for which the various constants have been evaluated do not overlap, and the constants cannot be correlated.

3. Heterogenous Media

In most practical situations, polymer films are not simple materials, but complex mixtures of two or more components. Thus, paint films contain pigments and many packaging materials are laminates. A common example of the latter is the use of poly(vinylidene chloride) as a laminate on other, cheaper plastics. Its low permeability to water vapour makes it ideal for food packaging applications.

Even pure polymers can be two phase materials, if they have crystalline regions. The transmission properties of amorphous and crystalline polymer are widely different and the crystalline content and distribution must, therefore, be taken into account.

Heterogenous media have been classified into three types[176], namely:

(i) disperse phase (or phases) in a continuum

(ii) two (or more) interpenetrating continuous phases

(iii) laminates

These can be further divided into sub-groups which are distinguished mainly by the size, shape, orientation and distribution of the components.

Of the three main classes, laminates are the easiest to study, since the equations derived for these systems are capable of exact solution. The corresponding general treatment for a material comprising a dispersed phase in a continuum is mathematically intractable. Most of the work in this area has concentrated on dilute suspensions and regular distributions of disperse phase, for which approximate solutions can be obtained. Much of the theoretical work has been done in the mathematically analogous field of dielectric permittivity[176], even when the results are intended for application to diffusion or thermal conductivity problems.

a. Solution, Diffusion and Permeation in Crystalline Polymers

Several experimental studies of polymers having crystalline regions (e.g. polyethylene, poly(ethylene terephthalate), poly(hexamethylene sebacamide)) have demonstrated that solution in and diffusion through these regions does not occur. The degree of crystallinity is easily modified by thermal treatments, such as annealing. (It is, however, implicit in all these studies that such thermal treatments leave other characteristics of the polymers, which might affect their transmission properties, unchanged). The density is almost always used as a measure of the degree of crystallinity: the latter can be calculated when the specific volumes of the crystalline and amorphous polymer are known.

The reduction in diffusion, solubility and permeability coefficients with increasing crystalline content was first noted by Van Amerongen[177] with gutta percha. Subsequently, several workers attempted to quantify the influence of crystallinity on transmission properties. Lasoski and Cobbs[178] reasoned that if solution and diffusion occurred only in the amorphous regions, then the solubility and diffusion coefficients might be proportional to the volume fraction of amorphous polymer, α, i.e.

$$D = \alpha D^* \qquad (I:74)$$

and $$S = \alpha S^* \qquad (I:75)$$

where D^* and S^* are respectively the diffusion and solubility coefficients for a

completely amorphous polymer. Since

$$P = DS \qquad \text{(I:48)}$$

then

$$P = \alpha^2 P^* \qquad \text{(I:76)}$$

where P^* is the permeability coefficient of a completely amorphous polymer. This relationship was applied to the permeation of water vapour through polyethylene, poly (ethylene terephthalate) and poly (hexamethylene sebacamide). A reasonable correlation between P and α^2 was obtained.

Michaels and Parker[11] studied the transmission properties of oxygen and nitrogen through polyethylenes from various sources. They obtained the same result as Lasoski and Cobbs for the variation in solubility coefficients with volume fraction of amorphous polymer. The diffusion coefficient also varied with volume fraction of amorphous phase, but in a fashion different from that predicted by Eq. (I:74). A common instance was that of film samples having similar amorphous phase contents, but displaying different diffusing coefficients. It was postulated, by analogy with flow through porous media, that the path which had to be followed by penetrant molecules to avoid crystalline regions would influence the diffusion coefficient, and that this could be accounted for by the introduction of a tortuosity factor, τ. It was also necessary to introduce a chain immobilisation factor, β, to account for the reduction in polymer segment mobility in the region of the crystalline regions. The relationship between D and D^* is then

$$D = D^*/ \tau\beta \qquad \text{(I:77)}$$

and thus for P

$$P = \alpha D^* S^*/ \tau\beta \qquad \text{(I:78)}$$

At constant α, τ should be temperature independent, since it depends only on the geometrical arrangement of the crystalline regions. However, β would be expected to vary exponentially with temperature, because it is affected by the segmental mobility.

It is not, unfortunately, possible to calculate the parameters τ and β from any characteristics of polyethylene. However, from an examination of the values obtained from their experimental data, Michaels and Parker[11] concluded that the crystalline regions were likely to be anisometric. Subsequently, Michaels and co-workers[12,13] confirmed the validity of these relationships for

a wide range of gases through hydrogenated polybutadiene, rubber and poly(ethylene terephthalate).

An alternative treatment developed by Klute[179,180] allows for the possibility that not all the amorphous polymer is utilised by the penetrant molecules in their passage through the film. His relationship between the permeability of a semi crystalline polymer and that of a completely amorphous polymer is

$$P = \Psi P^* \qquad \text{(I:79)}$$

where the function $(1 > \Psi > 0)$ accounts for the reduction in the permeability of the semicrystalline film below αP^*. This function, termed the transmission function, can be separated into a transport volume function, ψ_1, and a detour ratio, ψ_2. The former allows for the proportion of amorphous polymer either inaccessible to penetrant molecules or forming a 'blind alley' and being ineffective in the diffusion process. The latter takes account of the tortuous path which must be followed by the penetrant molecules. Its reciprocal is therefore equivalent to the tortuosity factor of Michaels and Parker[11].

Klute tested his equations with the water vapour permeability data of Lasoski and Cobbs[178] and claimed reasonable agreement between theory and experiment.

b. Filled Polymers

The transmission properties of filled polymer films cannot be treated in the same fashion as partially crystalline polymers. Although the size and shape of the filler particles may be better defined than polymer crystallites, they may be more or less permeable than the surrounding polymer phase, or highly adsorbent. Furthermore, filled polymers may contain an additional disperse phase in the form of vacuoles. These are to be expected in any system where the polymer does not wet the filler particles; and have been detected, for example, in zinc oxide filled natural rubber by density measurements[181,182].

For the general case of a polymer containing vacuoles and non-adsorbent filler in which the penetrant is soluble, the overall solubility coefficient is given by[177]

$$S = V_f S_f + V_v + V_o S^* \qquad \text{(I:80)}$$

where V_f and V_v are the volume fractions of filler and vacuoles and S_f and S^*

are the solubility coefficients in the filler and unfilled polymer respectively. The volume fraction of vacuoles can be calculated if the densities of the filler polymer and filled film are known. Adsorbent fillers are less easily dealt with, since they adsorb less when incorporated as a filler than the adsorption isotherm of the pure material might suggest. For highly adsorbent fillers, the polymer medium can only interfere to a limited extent, and so the adsorptive capacity of the filler is only slightly affected[182]. Moreover, the amount of penetrant sorbed by the polymer is negligible by comparison.

For an impermeable filler, and in the absence of vacuoles, the solubility coefficient is simply

$$S = V_o S^* \qquad (I:81)$$

The effect of fillers on diffusion is complicated by the ambiguity in defining the true diffusion coefficient of the composite film, since transient and steady state data often yield different results. This effect has been ascribed to the dead volume of polymer which is not available for steady state flow, but which does participate in the transient state process[182].

The effect of an impermeable filler is to reduce the diffusion coefficient and hence increase the time lag. As with crystalline polymers, this is because the penetrant molecules have a more tortuous path to negotiate. However, in this case, the reduction in diffusion coefficient cannot be simply correlated with volume fraction of filler, but must take into account shape and orientation of filler particles. Lameller fillers are considerably more effective barriers to flow, especially if the lamellae are aligned normal to the direction of flow.

The dependence of diffusion on filler shape, orientation and distribution can be rationalised by use of structure factors, which are functions of volume fraction. The exact form of the function varies with shape orientation and distribution, and, like the relationships to be discussed in the next section, are derived from electrostatic principles.

c. Dispersion of One Polymer in a Continuum of Another

The theoretical treatment for this system has been derived in terms of dielectric permittivity. The film is considered as the dielectric between the plates of a large plane capacitor. The electric field, E, produces a dielectric displacement D: these are related by

$$D = \varepsilon E \qquad (I:82)$$

where ε is the permittivity of the film. The displacement of charge under the

influence of an applied elecric field is analogous to the displacement of penetrant molecules under the influence of a potential gradient (cf. Fick's First Law).

$$J = - D \frac{dc}{dx} \qquad \text{(I:26)}$$

Given the permittivities of the dispersed and continuous phases, e_1 and e_o respectively, the problem is to calculate the permittivity of the composite, e_m. Many of the theoretical treatments have been reviewed by de Vris[183] and Barrer[176]. Only the results will be summarised here, together with those of an alternative treatment derived by Higuchi[184] and an empirical relationship devised by Pearce[185]. These equations relate the permeability of the composite, P_m, to the volume fractions, v, and permeabilities of the components. The subscripts 1 and 0 refer to the dispersed and continuous phases respectively.

(i) Theory of Maxwell

Maxwell's treatment assumed that the suspensions were so dilute that interactions between the particles could be neglected. The resulting expression

$$P_m = P_o \left[1 + 3v_1 / \left(\frac{P_1 + 2P_o}{P_1 - P_o} - v_1 \right) \right] \qquad \text{(I:83)}$$

would therefore only be expected to apply where the volume fraction of disperse phase was small.

(ii) Development by Rayleigh[176], Runge[176] and de Vris[183]

Rayleigh developed an expression for the special case of identical spheres arranged in a simple cubic lattice.

$$P_m = P_o \left[1 + 3v_1 / \left(\frac{P_1 + 2P_o}{P_1 - P_o} - v_1 + \frac{\alpha (P_1 - P_o) v_1^{10/3}}{P_1 + (4P_o/3)} + \ldots\ldots \right) \right] \qquad \text{(I:84)}$$

α is a constant for the simple cubic lattice. de Vris[183] extended the treatment of Rayleigh to include body centred and face centred cubic arrangements, which gave different values of α.

(iii) Theory of Böttcher[176], and Polder and van Senten[176]

These authors, who considered the dielectric properties of spherical powder particles, assumed that the powder could be represented as a continuous dielectric whose permeability was the same as the bulk solid. Their expression for a two phase material is

$$\frac{P_m - 1}{3P_m} = \frac{v_1 (P_1 - 1)}{P_2 - 2P_m} + \frac{(1 - v_1)(P_o - 1)}{P_o - 2P_m} \qquad \text{(I:85)}$$

(iv) Theory of Bruggeman[176]

Bruggeman used the same model as Böttcher, but used a differential method to calculate the permittivity of the medium. He obtained

$$\frac{P_1 - P_m}{P_1 - P_o}\left(\frac{P_o}{P_m}\right)^{1/3} = 1 - v_1 \qquad \text{(I:86)}$$

(v) Theory of Higuchi[184]

By assuming that the disperse phase particles were point entities with a polarisability proportional to the radius cubed, Higuchi derived an expression for a random dispersion of spheres in a continuum, which took into account particle-particle interactions. In terms of permeabilities, this equation is

$$P_m = \frac{2P_o^2(1-V_1)+P_oP_1(1+2V_1)-KP_o((P_1-P_o)/(2P_o+P_1))^2(2P_o+P_1)(1-V_1)}{P_o(2+V_1)+P_1(1-V_1)-K((P_1-P_o)/(2P_o+P_1))^2(2P_o+P_1)(1-V_1)} \qquad \text{(I:87)}$$

To a first approximation, the factor K is a fraction of v_1 only. Calculation of a precise value of K requires, amongst other factors, details of the radial distribution function for the dispersed spheres as a function of their volume fraction. Higuchi argued, however, that an accurate test was possible, even if K was unknown. An analysis of permittivity data for powders and suspensions demonstrated that with K = 0.78 Eq. I:87 predicted the dielectric properties of binary mixtures satisfactorily over a reasonable range of volume fraction, provided the shape of the disperse phase did not deviate too much from spherical.

(vi) Pearce's Emperical Equation[185]

Pearce derived an empirical equation

$$(P_m - P_o)/(P_1 - P_o) = (1 - c)\, v_1/(1 - cv_1) \qquad \text{(I:88)}$$

which was able to account for all the available literature data. The constant c was envisaged as being dependent, not on composition, but rather the ratio of the relative permeabilities of the components.

Comparison with Experiment

Several authors[183,185,187,188] have sought to reconcile experimental data with results predicted by the foregoing theories. Although there are data for the permeability and thermal conductivity of composites, the comparisons have mainly been made with dielectric permittivity measurements, since these are capable of greater precision.

De Vris[183] examined both dielectric permittivity and thermal conductivity data and concluded that for $P_1/P_0 < 1$, the Maxwell expression (Eq. I:83) gave satisfactory agreement. The computed values were too large, but by less than 10%. For $1 < P_1/P_0 < 200$, the experimental values lay between those predicted by Maxwell and Bruggeman (Eq. I:86), the latter giving the larger value.

Pearce[185] claimed that Bruggeman's expression agreed with some of the available dielectric data, but required an empirical 'form' or 'agglomeration' factor to cope with the rest. The form of this equation was different to Pearce's empirical relationship, which is in good agreement with much of the data.

Higuchi calimed that his relationship was in satisfactory agreement with the available dielectric permittivity data[184], and could also be used to explain the barrier properties of ointments[187]. Peterson[188] applied the Higuchi relationship to heterogeneous polymer films containing a random dispersion of one polymer in a continuum of another, and obtained exceptionally good agreement between theory and experiment.

D. AIM AND SCOPE OF THE PROJECT

The aim of this investigation was to study the transmission properties of polymer latex films with a view to improving their utility as charcoal binders. A soft, film forming ethyl acrylate/methyl methacrylate copolymer latex is currently employed in the manufacture of protective clothing. An aqueous slurry containing the latex and adsorbent charcoal granules is sprayed onto a non-woven fabric, which is then heated to evaporate the water. The latex forms a film over the charcoal, binding it to the fabric. The degree of protection afforded by this material is critically dependent on the rate of adsorption of toxic materials by the charcoal. This rate is reduced by the presence of the latex film although the adsorptive capacity of the charcoal is not measurably affected. The performance of the material diminishes further on long term storage, and this is thought to be due to migration of polymer into the macroporous structure of the charcoal. An additional problem is the occlusion of small latex particles (less than 100 nm in diameter) in the pores of the charcoal during preparation of the slurry, which provide a further barrier to adsorption. This investigation entailed work in three different areas, namely preparation of polymer latices by emulsion polymerisation, preparation of films from these latices and determination of the film permeabilities.

The surfactant free method of preparation was preferred for the first of these objectives because it was known to produce monodisperse latices of controllable particle size (48) which would be comparitively easy to characterise [28]. A wide range of homopolymer, copolymer and core-shell latices can be prepared using this general technique. A consequence of carrying out the emulsion polymerisation in the absence rather than in the presence of surfactant is the much greater (ca. 10 times) particle size produced. This is desirable for the intended application, since the extent of particle occlusion by the charcoal, alluded to above, will be reduced.

Film forming core-shell latices having rigid, undeformable cores were also prepared, since it was anticipated that the migration of polymer into the macroporous structure of the charcoal, referred to above, could not occur. It was hoped that films cast from these latices would constitute a model heterogeneous system, having a regular close packed arrangement of core particles in a continuous medium of film forming polymer. Such films provide a means of testing the various theoretical treatments of the properties of composite materials [176,183,184].

The usual method for the preparation of core-shell latices is the seeded growth process [80-82,100] in which a seed latex, which has been previously

prepared and sometimes cleaned beforehand, is reacted with further monomer. Extra surfactant is often added to assure the stability of the larger particles. Unfortunately, this frequently leads to the formation of a second crop of particles, so that the final product contains the desired core-shell particles, together with smaller particles of the coating polymer. Secondary growth particles are also obtained in surfactant-free systems if the total surface area of the seed particles is less than a certain critical value [30].

Sakota and Okaya [112] have attempted to prepare polystyrene latices having a thin coat of functional group containing polymer by adding the appropriate monomer towards the end of a styrene emulsion polymerisation. This technique appeared to have advantages over the usual seeded growth method, and was evaluated as a means of preparing the required core-shell latices.

A freshly prepared latex will contain unreacted monomer and reaction byproducts, such as electrolyte, products of oxidation side reactions such as benzaldehyde, oligmeric material etc. The traditional methods available for cleaning polymer latices, namely dialysis and ion exchange, are inefficient in removing some of these impurities, and can lead to further contamination [47]. A microfiltration technique was devised and evaluated in the course of this work and this proved to be superior to other methods of cleaning. Surfactant free polymer latices cleaned using using this technique contain only charge stabilised polymer particles dispersed in water.

Surfactant free latices are good starting materials from which to cast films because, where surfactant is present prior to film casting, its fate after particle coalescence is uncertain. Exudations containing surfactant have been observed on styrene-butadiene copolymer latex films [132] their occurrence being attributed to expulsion of material incompatable with the polymer. In other polymer films where the exudations do not occur [133], the surfactant must remain within the interior of the film, either dissolved in the polymer, accumulated in the interstices or present as a separate interpenetrating network [128]. It is known that during emulsion polymerisation reactions, some surfactant is grafted on to the particles [135], and this must remain within the film, whether or not it is compatible with the polymer.

Several techniques for preparing films from polymer solutions or latex dispersions have been reported in the literature [113,189-193] and these were evaluated in the course of this study. In addition, a flash casting technique was devised. This was adapted from a method of tablet coating used extensively by the pharmaceutical industry [194,195].

The transmission properties of polymer films have been widely studied, and

many different techniques for their measurement have been devised. Most fall into two categories namely sorption and permeation methods [189]. Sorption methods measure the rate of penetrant uptake as a function of time, from which data the diffusion coefficient can be calculated. The solubility coefficient is obtained from the equilibrium uptake. This method is useful for vapour penetrants. However, with gases, the equilibrium uptake is too small, and occurs too rapidly for accurate measurements to be made. Permeation methods measure the rate of penetrant transmission through the film. The diffusion and permeability coefficients are obtained from the transient and steady states of permeation respectively. It was anticipated that the latex films would be fragile, and therefore those permeation methods which exposed the films to a pressure difference were not considered. 'Dynamic' permeation techniques, which have been reported by several authors [146-148,196-198], avoid this problem. An apparatus similar to that devised by Pasternak et al. [148] was constructed and used to determine the transmission properties of latex films.

E. REFERENCES

1. B.J. Hennesey, J.A. Mead and T.C. Stenning, "The Permeability of Plastics Films", The Plastics Institute, London (1966)

2. R.E. Kesting. "Synthetic Polymeric Membranes", Mc.Graw-Hill (1971)

3. N. Yi-Yan, R.M. Felder and W.J. Koros, J. Appl. Polym. Sci., 25, 1755 (1980)

4. L.A. Luzzi, M.A. Zoglio and H.V. Maudling, J. Pharm. Sci., 59, 338 (1970)

5. T.M.S. Chang, in "Sorbents and their Clinical Applications", C. Gordano (ed), Academic Press, Chapter 9, p. 195 (1980)

6. D.C. Blackley, "Emulsion Polymerisation", Applied Science Publishers (1975)

7. H. Warson, "The Application of Synthetic Resin Emulsions", Ernest Benn Ltd. (1972)

8. D.W. Brubaker and K. Kammermeyer, Ind. Engng. Chem., 45, 1149 (1953)

9. W.W. Brandt, J. Polym. Sci., 14, 403 (1959)

10. A. Kaminska, Polymary (Warsaw), 25, 47 (1980)

11. A.S. Michaels and R.B. Parker, J. Polym. Sci., 41, 53 (1959)

12. A.S. Michaels and H.J. Bixter, ibid, 50, 393, 413 (1961)

13. A.S. Michaels, W.R. Wieth and J.A. Barrie, J. Appl. Phys., 34, 1, 13 (1963)

14. F. Hofmann and K. Delbruk, German Patent 250 690 (1909)

15. Idem, German Patent 254 672 (1912)

16. Idem, German Patent 255 129 (1912)

17. R.P Dinsmore, U.S. Patent 1 732 795 (1927)

18. M. Luther and C. Henck, German Patent 558 890 (1927)

19. W.D. Harkins, J. Amer. Chem. Soc., 69, 1428 (1947)

20. W.D. Smith and R.H. Ewart, J. Chem. Phys., 16, 592 (1948)

21. J.W. Vanderhoff, in "Vinyl Polymerisation", Vol.1, Part II, G.E. Ham (ed), Marcel Dekker, p1 (1969)

22. J.W. Vanderhoff, in "Characterisation of Metal and Polymer Surfaces", Leing-Huang Lee (ed), Academic Press (1977)

23. W.P. Hohenstein and H. Mark, J. Polym. Sci., 1, 127, 549 (1946)

24. T. Matsumoto and A. Ochi, Kobunshi Kagaku, 22, 481 (1965)

25. M.E. Woods, J.S. Dodge, I.M. Krieger and P.E. Pearce, J. Paint Technol., 40, 541 (1968)

26. A. Kotera, K. Furusawa and Y. Takeda, Kolloid-Z. u. Z. Polymere, 239, 677 (1970)

27. A. Kotera, K. Furusawa and K. Kudo., ibid, 240, 837 (1970)

28. J.W. Goodwin, J. Hearn, C.C. Ho and R.H. Ottewill, Brit. Polym. J., 5, 347 (1973)

29. Idem. Colloid Polym. Sci., 252, 464 (1974)

30. J. Hearn, Ph.D thesis, University of Bristol (1971)

31. K. Furusawa, W. Norde and J. Lyklema, Kolloid-Z. u. Z. Polymere, 250, 908 (1972)

32. J. Laaksonen, J.C. La Bell and P. Stenius, J. Electroanal. Chem., 64, 207 (1975)

33. A.R. Goodall, M.C. Wilkinson and J. Hearn. J. Colloid Interface Sci., 53, 327 (1975)

34. A.R. Goodall, Ph.D thesis, Trent Polytechnic (1976)

35. A.R. Goodall, M.C. Wilkinson and J. Hearn. J. Polym. Sci., Polym. Chem. Ed., 15, 2193 (1977)

36. R.A. Cox, M.C. Wilkinson, J.M. Creasy, A.R. Goodall and J. Hearn. ibid, 15, 2311 (1977)

37. A.R. Goodall, J. Hearn and M.C. Wilkinson. Brit. Polym. J., 10, 141 (1978)

38. M.C. Wilkinson, J. Hearn, A.R. Goodall and P. Cope. ibid, 10, 205 (1978)

39. A.R. Goodall, J. Hearn and M.C. Wilkinson. J. Polym. Sci., Polym. Chem. Ed., 17, 1019 (1979)

40. D. Munro, A.R. Goodall, M.C. Wilkinson, K.J. Randle and J. Hearn. J. Colloid Interface Sci., 68, 1 (1979)

41. A.R. Goodall, K.J. Randle and M.C. Wilkinson, ibid, 75, 493 (1980).

42. D.H. Everett, M.E. Gulteppe and M.C. Wilkinson, ibid, 71, 336 (1979).

43. M.C. Wilkinson, J. Hearn, P. Cope and A.R. Goodall, ibid, 77, 566 (1980).

44. J. Hearn, M.C. Wilkinson, A.R. Goodall and P. Cope, in "Polymer Colloids II", R.M. Fitch (ed.), Plenum Press, p. 379 (1980).

45. A.R. Goodall, M.C. Wilkinson and J. Hearn, ibid, p. 629.

46. M.C. Wilkinson, in "Treatise on Surface Characterisation", K. Mittal (ed.), Plenum Press (1984).

47. J. Hearn, M.C. Wilkinson and A.R. Goodall, Adv. Colloid. Interface Sci., 14, 173 (1981).

48. J.W. Goodwin, R.H. Ottewill, R. Pelton, G. Vianello and D.E. Yates, Brit. Polym. J., 10, 173 (1978).

49. A.F. Miller and F.R. Mayo, J. Amer. Chem. Soc., 78, 1017 (1956)

50. M.C. Wilkinson, R. Sherwood, J. Hearn and A.R. Goodall, Brit. Polym. J., 11, 1 (1979).

51. P. Kasargod and R.M. Fitch in "Polymer Colloids II", R.M. Fitch (ed.), Plenum Press, p. 487 (1980).

52. Li-Jen Liu and I.M. Krieger, in "Emulsions, Latices and Dispersions", P. Beecher and M.N. Yudenfreund (eds.), Marcel Dekker p. 41 (1978).

53. R.A. Cox, J.M. Creasey and M.C. Wilkinson, Nature, 252, 468 (1974).

54. E. Dickenson and A. Patel, Colloid. Polym. Sci., 257, 431 (1979).

55. T.G.M. van de Ven, T. Dabros and J. Czarnecki, J. Colloid Interface Sci., 93, 580 (1983).

56. J.L. Gardon, J. Polym. Sci., Part A1, 6, 623, 643, 665, 687, 2853, 2859 (1968).

57. J.L. Gardon, Brit. Polym. J., 2, 1 (1970).

58. A.E. Alexander and D.H. Napper, in "Progress in Polymer Science", A.D. Jenkins (ed.), Pergamon Press, p. 145 (1971).

59. J. Ugelstad and F.K. Hansen. Rubber Chem. Technol. 49, 536 (1976).

60. J.W. Vanderhoff, in "Science and Technology of Polymer Colloids", G.W. Poehlein, R.H. Ottewill and J.W. Goodwin (eds.), Martinus Nijhoff NATO ASI, p 1 (1983).

61. S.S. Medvedev, in "International Symposium on Macromolecular Chemistry", Pergamon Press, p. 174 (1959).

62. R.M. Fitch and C.H. Tsai, in "Polymer Colloids", R.M. Fitch (ed.) Plenum Press p. 73 (1971).

63. G. Odian, "Principles of Polymerisation", second edition, Wiley Interscience (1981).

64. W.H. Stockmayer, J. Polym. Sci., 24, 314 (1957).

65. J.T. O'Toole, J. Appl. Polym. Sci., 9, 1291 (1965).

66. J.W. Vanderhoff, Proc. Water Borne and High Solids Coatings. Symposium, University of Southern Mississippi (1976).

67. M.R. Grancio and D.J. Williams. J. Polym. Sci., Part A1, 8, 2617, 2733 (1970).

68. D.J. Williams, J. Elastoplast, 5, 6 (1973).

69. P. Keusch and D.J. Williams, J. Polym. Sci., Polym. Chem. Ed., 11, 143 (1973).

70. D.J. Williams, ibid, 11, 301 (1973).

71. P. Keusch, J. Prince and D.J. Williams, J. Macromol. Sci. - Chem., A7, 623 (1973).

72. D.J. Williams, J. Polym. Sci., Polym. Chem. Ed., 12, 2123 (1974).

73. P. Keusch, R.A. Graff and D.J. Williams, Macromolecules, 7, 304 (1974).

74. J.L. Gardon, J. Polym. Sci., Polym. Chem. Ed., 11, 241 (1973).

75. D.H. Napper, J. Polym. Sci., Part A1, 9, 2089 (1971).

76. G. Lohr and R. Reinecke, Paper presented at NATO Advanced Studies Institute Symposium on Polymer Colloids, Bristol (1982).

77. N. Friis and A.E. Hamielec. J. Polym. Sci., Polym. Chem. Ed., 11, 3321 (1973).

78. B. Vollmert, "Polymer Chemistry", translated by E.H. Immergut, Springer Verlag (1973).

79. D.J. Williams and E.G. Bobalek, J. Polym. Sci., Part A1, 4, 3065 (1966).

80. E.B. Bradford, J.W. Vanderhoff and T. Alfrey, J. Colloid Sci., 11, 135 (1956).

81. J.W. Vanderhoff, J.F. Vitkuski, E.B. Bradford and T. Alfrey, J. Polym. Sci., 20, 225 (1956).

82. Y Chung-Li, J.W. Goodwin and R.H. Ottewill, Progr. Colloid Polym. Sci., 60, 163 (1976).

83. J.W. Goodwin, R.H. Ottewill, N.M. Harris and J. Tabony, J. Colloid Interface Sci., 78, 253 (1980).

84. R.A. Wessling and I.R. Harrison, J. Polym. Sci., Part A1, 9, 3471 (1971).

85. J. Brandrup and E.H. Immergut (eds.) "Polymer Handbook", Second edition, Wiley-Interscience (1975).

86. D.P. Sheetz, U.S. Patent 2914 499 (1959).

87. W.J. Le Fevre and D.P. Sheetz, U.S. Patent 3 108 979 (1963).

88. F.J. Hahn and J.F. Heaps, U.S. Patent 3 256 233 (1966).

89. D.F. Herman, A.L. Resnick and D. Simone, U.S. Patent 3 265 644 (1966).

90. H.L. Pfluger and C.G. Gebelin, U.S. Patent 3 291 768.

91. D. Goodman, I.E. Isgur and D.M. Wacome, U.S. Patent 3 397 165 (1968).

92. P.E. Pearce and R.M. Holsworth, U.S. Patent 3 423 351 (1969).

93. C.F. Ryan and R.J. Crochowski, U.S. Patent 3 426 101 (1969).

94. C.F. Ryan, U.S. Patent 3 562 235 (1971).

95. G.L. Meier, U.S. Patent 3 575 913 (1971).

96. R.E. Gallagher and J.C.H. Hwa, U.S. Patent 3 657 172 (1972).

97. R.A. Dickie and S. Newman, U.S. Patent 3 787 522 (1972).

98. D.R. Bassett and K.L. Hoy, U.S. Patent 3 804 881 (1974).

99. J.R. Erickson and R.J. Seidewand, U.S. Patent 4 226 752 (1980).

100. D.R. Bassett and K.L. Hoy, in "Emulsion Polymers and Emulsion Polymerisation", D.R. Bassett and A.E. Hamielec (eds.), ACS Symposium Series No. 165, Chapter 23, p. 371 (1981).

101. B.W. Greene, J. Colloid Interface Sci., 43, 449-462 (1973).

102. D.I. Lee, in "Emulsion Polymers and Emulsion Polymerisation", D.R. Bassett and A.E. Hamielec (eds.), ACS Symposium Series No. 165, Chapter 25, p. 405 (1981).

103. D.I. Lee and T. Ishikawa, J. Polym. Sci., Polym. Chem. Ed., 21, 147 (1983).

104. T. Matsumoto, M. Okubo and S. Shibao, Kobunshi Roubunshu, Eng. Ed., 5, 784 (1976).

105. T. Matsumoto, M. Okubo and S. Onoe, ibid 5, 771 (1976).

106. M. Okubo, A. Yamada and T. Matsumoto, J. Polym. Sci., Polym. Chem. Ed., 16, 3219 (1980).

107. M. Okubo, Y. Katsuka and T. Matsumoto, J. Polym. Sci., Polym. Lett. Ed., 18, 481 (1980).

108. M. Okubo, M. Ando, A. Yamada, Y. Katsuka and T. Matsumoto, ibid 19, 143 (1981).

109. M. Okubo, Y. Katsuka and T. Matsumoto, ibid, 20, 45 (1980).

110. J.E. Vandegaer, J. Appl. Polym. Sci., 9, 2929 (1965).

111. J.R. Erickson and R.J. Seidewand, in "Emulsion Polymers and Emulsion Polymerisation", D.R. Bassett and A.E. Hamielec (eds.), ACS Symposium Series No. 165 (1981).

112. K. Sakota and T. Okaya, J. Appl. Polym. Sci., 20, 1735, 2583 (1976).

113. V.T. Stannett, U.S. Nat. Technol. Inform. Service, 73, 61 (1973).

114. R.M. Felder, C-C Ma and J.K. Ferrell, A.I. Ch. E.J., 22, 724 (1976).

115. V. Stannett and J.L. Williams, J. Polym. Sci., Part C, 10, 45 (1965).

116. R.R. Myers and R.K. Schultz. J. Appl. Polym. Sci., 8, 755 (1964).

117. D.P. Sheetz, ibid, 9, 3759 (1965).

118. J.W. Vanderhoff, E.B. Bradford and W.K. Carrington, J. Polym. Sci., Symposium No. 41, 155 (1973).

119. J.C.H. Hwa, J. Polym. Sci., Part A, 2, 785 (1964).

120. R.E. Dillon, L.A. Matheson and E.B. Bradford, J. Colloid Sci., 6, 108 (1957).

121. G.L. Brown, J. Polym. Sci., 22, 423 (1956).

122. P.C. Hiemenz, "Principles of Colloid and Surface Chemistry", Marcel Dekker (1971).

123. J. Frenkel, J. Phys. USSR, 9, 385 (1945).

124. J.W. Vanderhoff, H.L. Tarkowski, M.C. Jenkins and E.B. Bradford, J. Macromolec. Chem., 1, 361 (1961).

125. G. Mason, Brit. Polym. J., 5, 101 (1973).

126. J.G. Brodnyan and T. Konen, J. Appl. Polym. Sci., 8, 687 (1964).

127. J. Lamprecht, Colloid Polym. Sci., 258, 960 (1980).

128. J.W. Vanderhoff, Brit. Polym. J. 2, 161 (1970).

129. S.S. Voyutskii, J. Polym. Sci., 32, 528 (1958).

130. S.S. Voyutskii, "Autohesion and Adhesion of High Polymers", Polymer Reviews, Vol. 4, Wiley-Interscience (1963).

131. S.S. Voyutskii and V.L. Vakula, Rubber Chem. Technol., 37, 1153 (1964).

132. E.B. Bradford and J.W. Vanderhoff, J. Macromol. Chem., 1, 335 (1966).

133. E.B. Bradford and J.W. Vanderhoff J. Macromol. Sci. - Phys., B6, 671 (1972).

134. D. Distler and G. Kanig, Colloid Polym. Sci., 256, 1052 (1978).

135. R.M. Fitch and W.T. McCarvill, J. Colloid Interface Sci., 66, 20 (1978).

136. G. Kanig and H. Neff Colloid Polym. Sci., 253, 29 (1975).

137. D. Distler and G. Kanig, Org. Coat. Plast. Chem., 43, 606 (1980).

138. F.W. Billmeyer, "Textbook of Polymer Science", second edition, Wiley-Interscience (1971).

139. J.V. Mitchell, J. Roy. Inst., 2, 101, 307 (1831).

140. T. Graham, Phil. Mag., 32, 401 (1866).

141. S. von Wroblewski, Weid. Annln. Phys., 8, 29 (1879).

142. H.A. Daynes, Proc. Roy. Soc., Ser. A., 97, 286 (1920).

143. R.M. Barrer, Trans. Faraday Soc., 35, 625 (1939).

144. J. Crank, "The Mathematics of Diffusion", second edition, Oxford University Press (1975).

145. H.S. Carslaw and J.C. Jaeger, "Conduction of Heat in Solids". Oxford University Press (1942).

146. D.G. Pye, H.H. Hoehn and M. Panar, J. Appl. Polym. Sci., 20, 282 (1976).

147. R.M. Felder, R.D. Spence and J.K. Ferrell, ibid, 19, 3193 (1975).

148. R.A. Pasternak, J.F. Schimschiemer and J. Heller, J. Polym. Sci., Part A2, 8, 467 (1970).

149. A. Peterlin, in "Permeability of Plastics Films and Coatings", H.B. Hopfenberg (ed.), Plenum Press (1964).

150. C E. Rogers, in "The Physics and Chemistry of the Organic Solid State" Vol. 2, D. Fox, M.M. Labes and A. Weissberger (eds.), Wiley Interscience, Chapter 6, p. 509 (1965).

151. V. Stannett, in "Diffusion in Polymers", J. Crank and G.S. Park (eds.), Academic Press, Chapter 2, p. 41 (1968).

152. P. Mears, J. Amer. Chem. Soc., 76, 3415 (1954).

153. C.A. Kumins and J. Roteman, J. Polym. Sci.. 55, 683 (1961).

154. G.J. van Amerongen, J. Polym. Sci., 5, 307 (1950).

155. F.H. Muller, Kolloid Zt.. 100, 335 (1944).

156. F.J. Norton, J. Appl. Polym. Sci., 7, 1649 (1963).

157. F.A. Long, E. Bagley and J. Wilkins, J. Chem. Phys., 21, 1412 (1953).

158. A. Aitken and R.M. Barrer, Trans. Faraday Soc. 57, 116 (1955).

159. S. Furuya, Chem. High Polymers (Japan) 12, 139 (1955), cited in ref. 1.

160. Y. Ito, ibid, 17, 7 (1960) cited in ref. 1.

161. C.A. Kumins and T.K. Kwei, in "Diffusion in Polymers", J. Crank and G.S. Park (eds.) Academic Press, Chapter 4, p. 107 (1968).

162. S. Glasstone, K.J. Laidler and H. Eyring, "The Theory of Rate Processes", McGraw-Hill (1941).

163. R.M. Barrer, Trans. Faraday Soc., 38, 322 (1942).

164. Idem, ibid, 39, 237 (1943).

165. R.M. Barrer and G. Skirrow, J. Polym. Sci., 3, 549, 564 (1948).

166. D.D. Eley, Trans. Faraday Soc., 39, 168 (1943).

167. W.W. Brandt, J. Polym. Sci., 63, 1080 (1959).

168. H. Yasuda and T. Hirotsu, J. Appl. Polym. Sci., 21, 105 (1977).

169. H. Fujita, in "Diffusion in Polymers", J. Crank and G.S. Park (eds.), Academic Press, Chapter 3, p. 75 (1968).

170. V. Stannett and M. Szwarc, J. Polym. Sci., 16, 89 (1955).

171. M. Salame, SPE Trans., 1, 153 (1961).

172. M. Salame and J. Pinsky, Modern Plastics, 36, 153 (1962).

173. Idem, ibid, 37, 131, 209 (1963).

174. H.L. Frisch, J. Polym. Sci., Part B, 1, 581 (1963).

175. H.L. Frisch and T.K. Kwei, ibid, 7, 789 (1969).

176. R.M. Barrer, in "Diffusion in Polymers", J. Crank and G.S. Park (eds.), Academic Press, Chapter 6, p. 165 (1968).

177. G.J. van Amerongen, Rubber Chem. Technol., 37, 1065 (1964).

178. S.W. Lasoski and W.H. Cobb, J. Polym. Sci., 36, 21 (1959).

179. C.H. Klute, J. Polym. Sci., 41, 307 (1959).

180. Idem, J. Appl. Polym. Sci., 1, 340 (1959).

181. R.M. Barrer, J.A. Barrie and M.G. Rogers, Trans. Faraday Soc., 58, 2437 (1962).

182. Idem, J. Polym. Sci., Part A, 1, 2565 (1963).

183. D.A. de Vris, in "The Thermal Conductivity of Granular Materials", Bull. Inst. Intern. du Froid, Paris (1952).

184. W.I. Higuchi, J. Phys. Chem., 62, 649 (1958).

185. C.A.R. Pearce, Brit. J. Appl. Phys., 6, 113, 358 (1955).

186. C.J.F. Bottcher, "Theory of Electric Polarisation", Elsevier (1952).

187. W.I. Higuchi and T. Higuchi, J. Amer. Pharm. Assn., Scientific ed., 49, 598 (1960).

188. C.M. Peterson, J. Appl. Polym. Sci., 12, 2649 (1968).

189. J. Crank and G.S. Park, in "Diffusion in Polymers", J. Crank and G.S. Park (eds.) Academic Press, Chapter 1, p. 1 (1968).

190. P.E. Pierce and R.M. Holsworth, J. Paint Technol., 38, 584 (1966).

191. J. Harris, Official Digest, Fed. Prant Varnish Clubs, 28, 30 (1956).

192. R.L. Eissler, J. Appl. Polym. Sci., 12, 1983 (1968).

193. Z.J. Lobos, E. Polatakjo-Lobos and V.G. Xanthopoulos, Polym. Latex. Int. Conf. Prepr., paper No. 17 (1978).

194. S.R. Wicks, Ph.D. thesis, University of Bath (1982).

195. D. Simmonite and J. Fennimore, British Patent 1 484 566 (1973).

196. D.W. Davis, Paper Trade J., 123, TS97 (1946).

197. T.L. Caskey, Modern Plastics, 45, 148 (1967).

198. K.D. Ziegel, H.K. Frensdorff and D.E. Blair. J. Polym. Sci., Part A2, 7, 809 (1969).

CHAPTER II

EXPERIMENTAL

A. MATERIALS

1. Monomers

The monomers used were BDH Laboratory reagent grade (BDH Chemicals Limited, Broom Road, Poole, BH12 4NN) containing a small quantity (0.001 - 0.002% w/v) of inhibitor (p-methoxy phenol or tert-butyl catechol). They were purified by double distillation under reduced pressure of nitrogen at 293-313K; the first and last 10% of each distillate being discarded. The distilled monomers were flushed with "white spot" nitrogen (BOC Limited, Millbank Road, Southampton, SO9 1PP) for ten minutes and were stored in sealed Pyrex containers at 253K.

Bifunctional monomers (divinyl benzene and ethylene dimethacrylate) were difficult to distil efficiently. The inhibitor was therefore removed by shaking with a concentrated solution of sodium hydroxide (three times) and water (three times). The monomers, sodium hydroxide solution and water were well flushed with "white spot" nitrogen before washing. The purified monomers were flushed for a further ten minutes and stored in sealed Pyrex containers at 253K. It was necessary to prepare the inhibitor-free divinyl benzene within one day of use, since its colour darkened on longer storage.

2. Water

All the water used was doubly distilled from a Pyrex glass still, and stored in covered Pyrex aspirators or sealed Pyrex flasks. The conductivity was measured routinely before use and was always less than 1.5 $\mu S\ cm^{-1}$. Periodic checks on the surface tension showed this to be in the range 71.9 - 72.0 $mN\ m^{-1}$.

3. Potassium Persulphate

Fisons Analytical reagent grade potassium persulphate (Fisons Scientific Apparatus Ltd., Bishop Meadow Road, Loughborough, Leicestershire) was recrystallised twice from double distilled water. A saturated solution was prepared at room temperature and stored overnight at 276K. The crystals were filtered off and the process repeated. The product was dried and stored in a desiccator, which was kept in a dark cupboard.

4. Surfactants

Sodium dodecyl sulphate was supplied by Fluka (Fluorochem Ltd., Dinting Vale Trading Estate, Peakdale Road, Glossop, Derbyshire SK13 9NV). Its purity was established by the absence of a minimum in the plot of surface tension against log concentration.

Cetyl trimethyl ammonium bromide was BDH Laboratory Reagent Grade and was used as supplied.

5. Biocides

Sodium azide and formaldehyde were BDH analar grade. Kathon 866 MW was supplied by Rohm and Haas Ltd. (Lennig House, 2 Masons Avenue, Croydon, Surrey, CR9 3NB). Thimerosal; phenyl mercuric acetate; 3-methyl 4-chloro hydroxybenzene; 4-chloro m-cresol and chlorohexidene diacetate were supplied by ICI Pharmaceuticals Division, Alderley Edge, Cheshire. All the biocides were used without purification.

6. Solvents

Acetone, toluene and chloroform (BDH Analar grade) and butanone (Fisons laboratory reagent grade) were used without purification.

7. Gases

Hydrogen, nitrogen, oxygen, argon and carbon dioxide were supplied by BOC Ltd., Millbank Road, Southampton SO9 1PP. Helium was supplied by Gas and Equipment Ltd., Unit E12, Heslop, Telford, Shropshire,. Gases were used without purification.

8. Miscellaneous

Sodium chloride was BDH Analar grade and was used as supplied.

B. LATEX PREPARATIONS

1. Basic Polymerisation Procedures

Polymerisations were carried out in 1, 2 or 5 dm^3, three necked round bottomed flasks, depending on the scale of the reaction. The flasks were equipped with a reflux condenser, nitrogen bleed and PTFE paddle stirrer (Fig. II.1). Before use, the flask with stirrer was repeatedly rinsed with double distilled water, until the conductivity of the washings dropped to less than 1.5 μS cm^{-1}. The flask was mounted in a water bath at the appropriate temperature (±0.1K). The stirrer speed was maintained at 360 rpm for all reactions.

Prior to the addition of initiator, the reaction mixture was allowed to attain the temperature of the bath while being flushed with nitrogen via a long bleed tube. A short bleed was substituted when the reaction was initiated. The nitrogen flow rate was reduced to the minimum necessary to maintain a nitrogen blanket over the reaction mixture to avoid loss of monomer. Any materials added during the reaction were well flushed with nitrogen immediately before addition. On completion of the reaction, samples were withdrawn for a gravimetric solids content determination and transmission electron microscope (TEM) examination. Samples for TEM were diluted immediately 100 times with cold water and stored in a cool place.

Several reactions were sampled throughout their course in order to determine the particle size and solids content as a function of reaction time. These multi-sampled reactions were initiated as described above. Two minutes before the sampling time the stirrer was stopped, to allow the monomer to form a separate layer. At the sampling time, the nitrogen inlet was removed, a teat pipette inserted into the centre of the aqueous phase of the reaction mixture, and a sample removed. The nitrogen inlet was replaced and a fast stream of nitrogen was passed into the reaction vessel to expel any air which might have entered. The stirrer was re-started and the nitrogen flow reduced to its previous low rate.

2. Preparation of Homopolymer and Seed Latices

The monomer and most of the water were placed in the flask and flushed with nitrogen. Any sodium chloride required to adjust the ionic strength was dissolved in a small volume of water and added to the flask. The potassium persulphate initiator was dissolved in the remaining water, and flushed with nitrogen. After twenty minutes or so, when the reaction mixture had reached

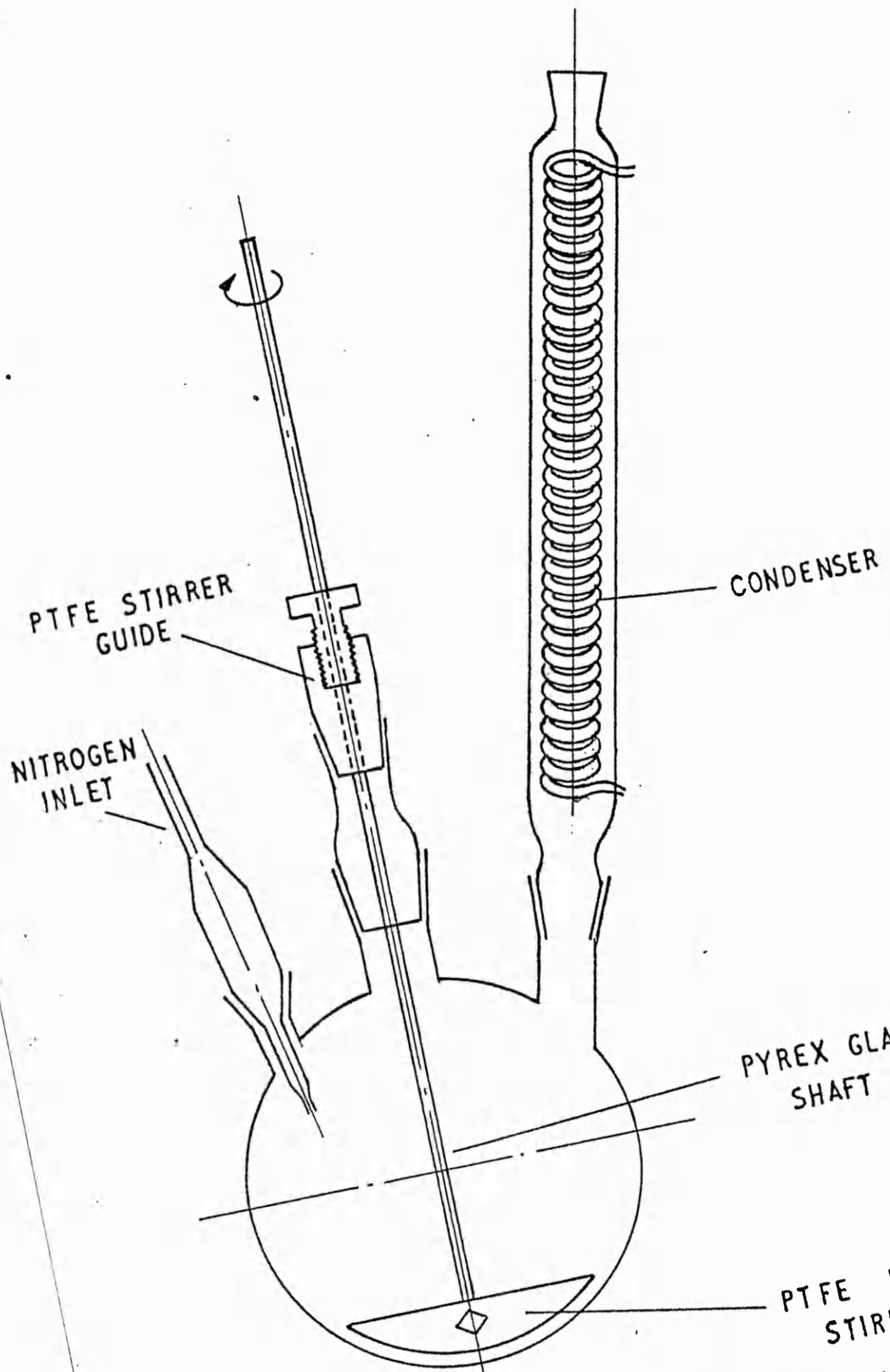

FIG II:1 APPARATUS FOR EMULSION POLYMERISATION REACTIONS

the required temperature, the initiator was added - this marked the beginning of the reaction.

3. Seeded Growth Polymerisation Reactions

The procedure was substantially the same as before, except that the initial reaction mixture contained the second monomer and the seed latex. Again, about twenty minutes was allowed for the mixture to attain the temperature of the bath. It was anticipated that the polymer particles would not be swollen by the monomer to any great extent.

4. Shot Growth Polymerisation Reactions

Styrene was polymerised normally. After the prescribed time, a sample was withdrawn for TEM and solids content analysis, and the second monomer added. The reaction was continued until polymerisation of the second monomer was complete.

5. Copolymerisation

Where a mixture of monomers is being polymerised, it is necessary to add the monomers to the reaction mixture at a rate slower than the propogation rate of the slowest polymerising monomer, i.e. to operate under monomer starved conditions. If this is not done, the resulting latex particles will have a non-uniform copolymer composition, with the cores rich in the faster polymerising component and the shells rich in the slower polymerising component (1).

For the shot growth reactions, the only modification necessary was the use of a metering pump to add the monomer mixture at the requisite rate. In the preparation of homogeneous and seeded growth core-shell copolymer latices, the initiator was included in the initial reaction mixture and the monomers were added using the metering pump.

C. CLEANING OF POLYMER LATICES

1. Introduction

Before a latex can be satisfactorily characterised, any byproducts from the polymerisation reaction must be removed. Methods for cleaning polymer latices have been widely investigated, particularly in connection with the search for a 'model colloid', for use in fundamental studies of colloidal stability.

Dialysis and ion exchange have been the traditional methods of cleaning, but both have disadvantages, many of which have only recently become apparent[2]. Preparation of ion-exchange resins is difficult and time consuming,

and complete removal of leachable polyelectrolytes from some batches has proved impossible. The large volumes of water required for dialysis give ample opportunity for contamination of the latex to occur. Moreover, both methods are slow and inefficient in the removal of residual monomer and oligomeric material.

Different techniques now being developed include microfiltration[3,4], diafiltration[5], ultrafiltration[6], hollow fibre dialysis[7] and treatment with activated charcoal cloth[8]. The filtration methods make use of filters having pore sizes only slightly smaller than the particles being cleaned. Provided pore blockage can be avoided, solute species may pass easily through the filter. This applies even to large species such as polyelectrolyte molecules and surfactant micelles, which are too large to pass through the pores of the semi-permeable membranes used in dialysis. Hollow fibre dialysis resembles conventional dialysis in that it relies on the exchange of materials across a membrane. Activated charcoal cloth is similar in action to ion-exchange, since its effectiveness depends on it being in direct contact with the sol.

Microfiltration, sometimes called serum exchange, is a process in which the aqueous dispersion medium is continuously replaced. This is achieved by pumping double distilled water through a cell containing the latex. The particles are retained by a filter, the latex being stirred to prevent the pores becoming blocked. The eluent water can be collected, and by determining its conductivity and surface tension over the duration of the process, the rate of cleaning may be measured. The latex is considered clean when the conductivity of the eluent is equal to that of the feed water (less than 1.5 $\mu S\ cm^{-1}$).

The effectiveness of microfiltration depends on maintaining the concentration difference between the particles and the aqueous phase, thus ensuring that desorption of impurities is more rapid than is the case, for example, with dialysis. The presence of slowly desorbing species can be monitored by delaying elution and allowing the concentration in the aqueous phase to build up to a detectable level.

Most of the latices prepared during this study were cleaned by microfiltration. Dialysis was used in some instances, for example when complete removal of residual monomer was not desired.

2. Dialysis

Visking 30/32 cellulose tubing (Scientific Instrument Centre Ltd., 1 Luke Street, London WC1) was cleaned by boiling in double distilled water (ca. 3 dm^3) for ten minutes and repeating the process until the smell of sulphur dioxide disappeared. The boiled tubing was kept in distilled water and was normally used

within one week.

A more rigorous cleaning process entailed boiling as before, followed by treatment with sodium sulphide solution (0.3%, ca. 3 dm^3) at 353K for one minute, washing with distilled water at 333K for two minutes, acidification with sulphuric acid (0.2%) and further washing with hot distilled water to remove the acid. This process did not appear to confer any benefits, but made the tubing fragile and liable to disintegrate during use.

Dialysis of latices was carried out against double distilled water in Pyrex glass aspirators. The dialysate was changed daily until no increase in conductivity occured (i.e. remained at less than 1.5 $\mu S\ cm^{-1}$).

3. Ion Exchange

Four ion exchange media were employed:

(i) Dowex 50 X8 and 1X8 (BDH)

(ii) Amberlite XAD12 (BDH)

(iii) Advanced Ion-Exchange Cellulose-AIEC (Whatman Laboratory Sales Ltd., Springfield Mill, Maidstone, Kent. ME1 2LE).

(iv) Bio-Rad AE1X-4 and AG50W-X4 (Bio-Rad Laboratories Ltd., Caxton Way, Holywell Industrial Estate, Watford, Herts. WD1 8RP).

The Dowex resins were purified by the procedure of van den Hul and Vanderhoff (9). The Bio-Rad Analytical grade resins, which are manufactured by purification of the corresponding Dowex resins were used without further treatment. The Amberlite and AIEC materials were cleaned according to the manufacturers recommendations. The latex was mixed with a five-fold excess of resin (based on ion exchange capacity) and mechanically shaken for two hours. The latex was then separated from the resin by filtration through a sintered glass funnel.

4. Microfiltration

Two microfiltration cells were used, depending on the volume of latex to be cleaned, and these are shown schematically in Fig. II.2. Prior to use, the cell was dismantled and the parts boiled in distilled water. It was imperative to ensure that any residue of the previous latex cleaned was removed from the body of the cell. The cell was then assembled and double distilled water passed through until the conductivity of the eluent was the same as that of the feed water. This process was repeated with the filter in position.

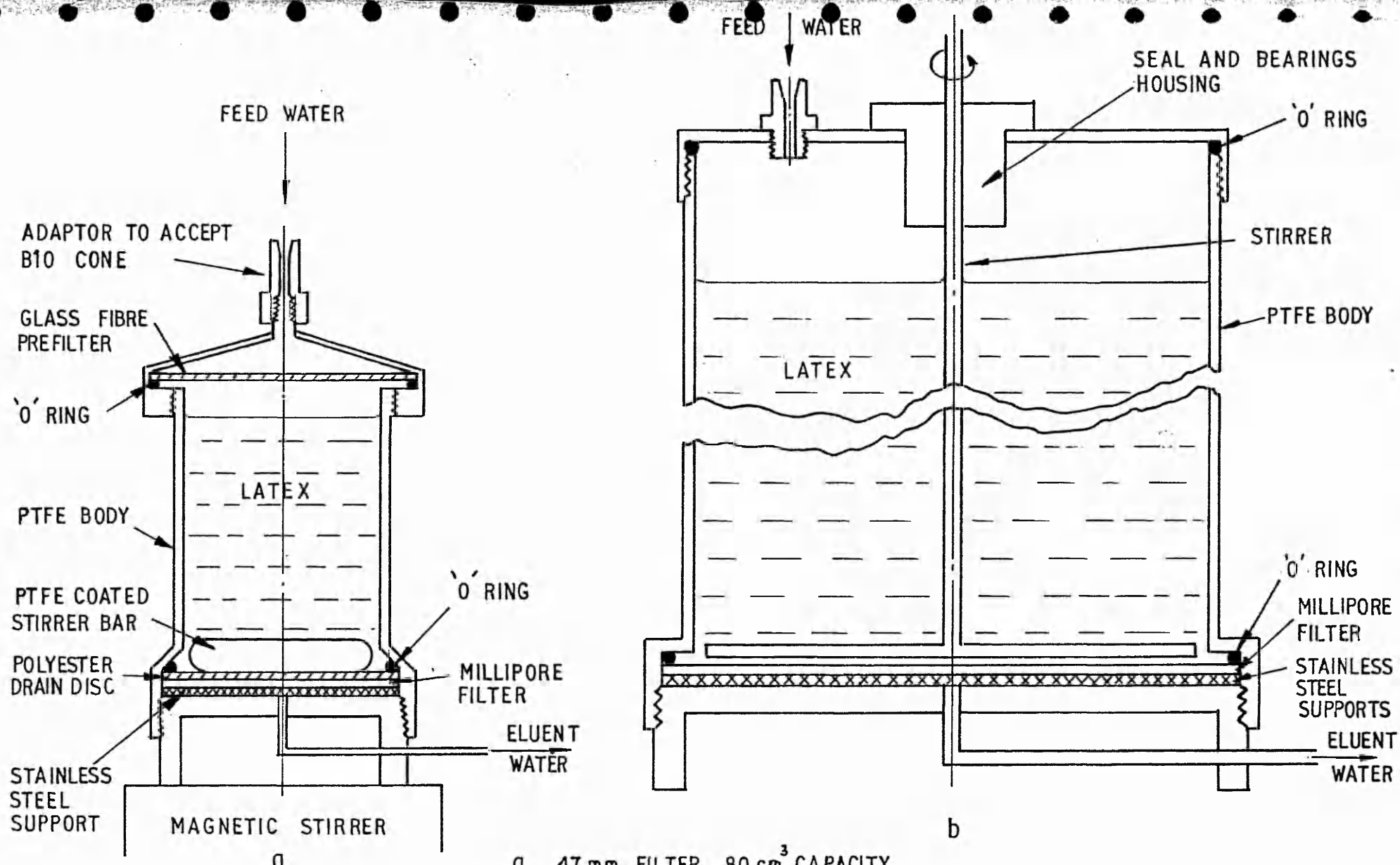

a 47 mm FILTER, 80 cm^3 CAPACITY
b 90 mm FILTER, 1 dm^3 CAPACITY

FIG II: 2 MICROFILTRATION CELLS

The filters used were normally of the cellulosic, tortuous path type (Millipore UK Limited, Millipore House, Abbey Road, London, NW10 7SP). Some initial work was, however, carried out with Nuclepore filters (Sterilin Limited, 43-45 Broad Street, Teddington, Middlesex, TW11 8QZ). These filters are made from thin (ca. 10 μm) polycarbonate sheet. The pores are produced by neutron bombardment followed by etching. A similar filter is marketed by Bio-Rad under the name Uni-pore. The nominal pore size of the filter was chosen to be 50 -75% of the latex particle diameter.

With the filter in position and clean, the latex was introduced into the cell and water pumped through. The stirrer speed was kept to a minimum, typically 100 rpm. This was sufficient to eliminate pore blockage. The applied water pressure was usually 1-2 psi. In most cases, elution was continued for 8 - 10 hours, corresponding to approximately 10 cell changes. This was sufficient to reduce the conductivity of the eluent to that of the feed water. The latex was left in the cell to stand overnight, to allow any slowly desorbing species to enter the aqueous phase. The cell was then briefly eluted, and the conductivity of the first portion of eluent checked. In no case was any change observed.

D. CHARACTERISATION OF POLYMER LATICES

1. Solids Content Determination

Solids contents were determined gravimetrically as follows. An aluminium planchet was washed in acetone, dried and weighed. A small sample of latex (ca 2 cm^3) was added to the planchet, which was reweighed. The latex was dried under partial vacuum (400 mm Hg) at 333 K until dry, and then stored under vacuum until constant weight was attained.

2. Electron microscopy*

a. Transmission Electron Microscopy (TEM)

A Philips EM600 electron microscope was employed. The latex sample was diluted down to about 10 ppm. One drop was spotted onto a 20 μm Formvar film coated grid and allowed to air-dry at room temperature in a dust free box. Normally, three grids were prepared and six micrographs of different regions taken. The operating conditions, chosen to minimise beam damage, were typically 3-4 μA beam current at 80 kV accelerating potential. The electron

*The author is indebted to Mr R A Cox, of CDE Porton Down, for this part of the work.

beam was focussed on one area of the grid and micrographs were taken from different areas in order to reduce the exposure time to a minimum.

The magnification of the prints was determined from the spacings of a carbon replica of a diffraction grating (2160 lines/mm). Micrographs of the replica were taken at the same time as those of the particles to eliminate errors arising from irregularities in the field which alter when the beam is switched off.

The particle size distribution was determined by measuring 100 - 150 particles from different regions of each print. The particles were sized using a magnifying eye-piece fitted with calibrated graticule (Polaron Equipment Ltd., 60/62, Greenhill Crescent, Holywell Industrial Estate, Watford, Herts) measuring to an accuracy of $\pm$ 0.05 mm.

To overcome the problem of particle deformation which occurs when the electron beam impinges on soft polymer particles, a freeze drying/carbon replication technique was employed. A drop of suspension was pipetted onto a Formvar coated grid. Excess liquid was removed with filter paper, to leave a smear of suspension. The grid was immersed in liquid nitrogen to achieve rapid cooling and then freeze dried. The specimen was cooled to approximately 123 K, tilted to 45° and a platinum/carbon mixture evaporated to provide shadows to the particles. Carbon was then evaporated normally. The specimen was allowed to return to room temperature and the grid removed. The Formvar was dissolved in chloroform and the latex in a suitable solvent. The replica was then examined by TEM or SEM.

b. Scanning Election Microscopy (SEM)

A Cambridge Stereoscan model 5150 MkII (resolution 5 nm) was used to examine the morphology of individual latex particles and films cast from them. Latex dispersions of suitable concentration were spotted onto a brass surface, dried in a dust free environment at room temperature and coated with carbon and gold. Film specimens were coated directly. Scans were taken at angles between 0 and 80° to the vertical

3. Conductometric and Potentiometric Titrations

Surface charge densities were calculated from conductometric titration data, which were obtained by the method of Vanderhoff et al.[10]. Potentiometric titration[11], which could conveniently be carried out simultaneously, was used as an aid to interpretation.

The latex samples for titration had been previously cleaned by the microfiltration technique (including acid wash) described in Section C4. A known volume (ca 30 cm^3) of latex, of predetermined solids content, was placed in a 50

cm^3 Pyrex glass beaker. The beaker was covered with a perspex lid having two small holes for the entry of nitrogen and sodium hydroxide solution, and two large holes for the pH and conductance electrodes. The latex was stirred by means of a small PTFE covered magnetic stirrer bar. The beaker and electrodes were housed in a perspex cabinet. The temperature within was maintained at 298K. The apparatus is depicted in Fig. II:3.

The sodium hydroxide standard solution was prepared from BDH 'CVS' ampoules, the concentration being checked periodically. It was added using a Radiometer Autoburette (Model ABU12, V.A. Howe and Co. Ltd., 88 Peterborough Road, London, SW6.) via a fine bore syringe needle. The Autoburette was capable of delivering down to 1×10^{-4} cm^3.

Conductances were measured on a Wayne Kerr Universal Autobalance bridge (model B642, Wayne Kerr Co. Ltd., Durban Road, Bognor Regis, Sussex PO22 9RL) using a dip type cell with blacked platinum electrodes (Pye Unicam Ltd) having a cell constant of 0.72. Sodium hydroxide solution was added in small aliquots, and the conductance and pH noted within 30 s of each addition.

4. Freeze drying

Latices were freeze-dried for molecular weight determination and preparation of solvent cast films. The latex was placed in a flask and cooled to 193K in a solid CO_2/methylated spirits slush bath. The flask was spun rapidly to deposit the frozen latex on its sides. This was then pumped under vacuum for approximately 18 hours, during which time the temperature rose gradually to ambient.

5. Gel Permeation Chromatography (GPC)*

GPC was used to determine polymer molecular weights. This technique is a form of column chromatography, in which the stationary phase is a heteroporous, solvent swollen polymer network (the gel) and the liquid phase is a dilute solution (ca ½% w/v) of the polymer sample. This solution is passed down the column at a known flow rate and the solute polymer molecules diffuse into the porous structure of the gel to an extent dependent on their size and the pore size distribution of the gel. The smaller molecules spend more time in the pores and take longer to pass through the column. Larger molecules are excluded from the smaller pores and pass through more rapidly. The amount of polymer eluting from the column is determined by UV spectroscopy, or more usually differential refractometry.

*The author is indebted to Mr D. Hilman and Mrs C. Heathcoat, of MQAD, Woolwich Arsenal, for this part of the work.

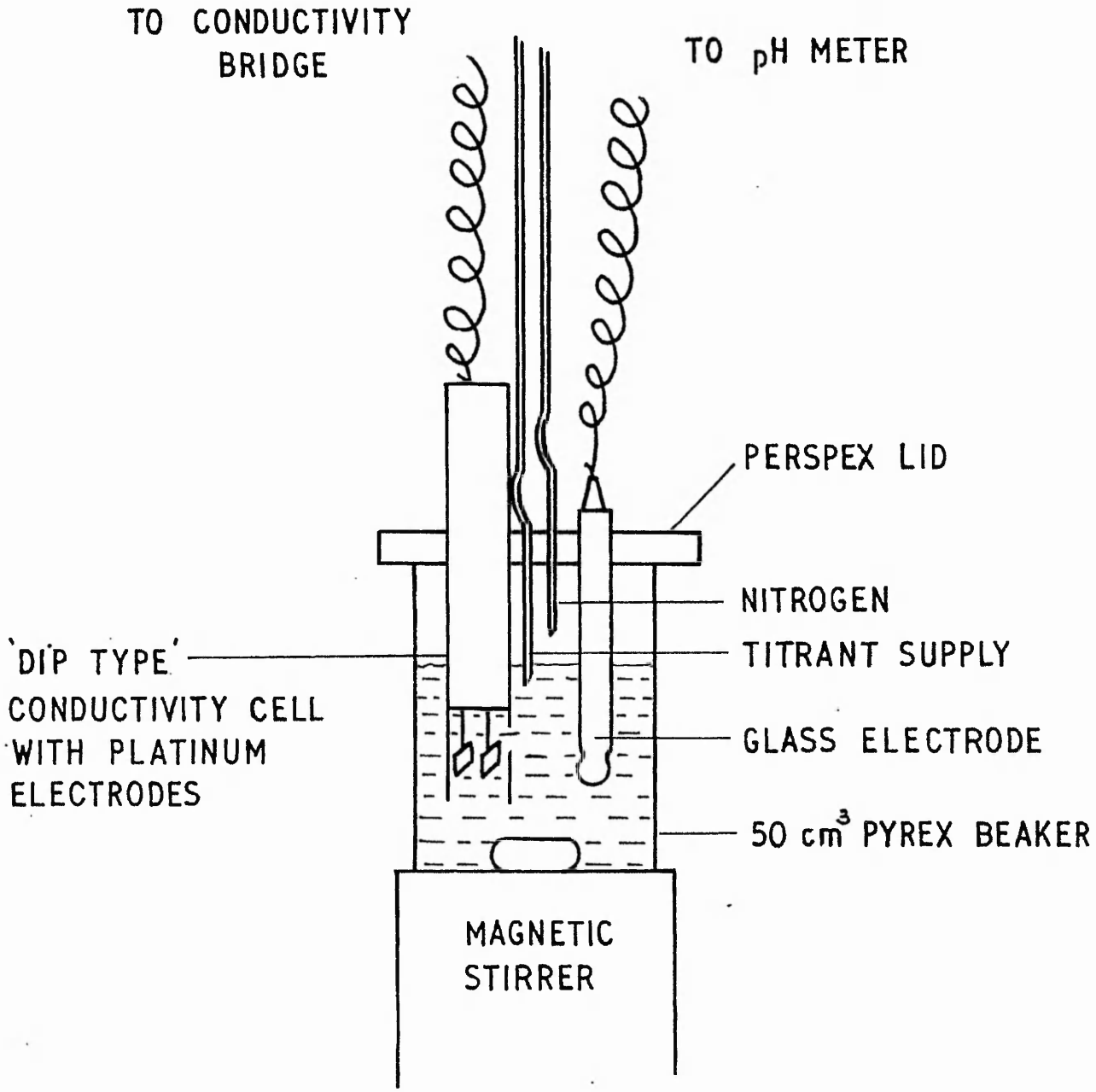

FIG II:3 APPARATUS USED FOR CONDUCTOMETRIC AND POTENTIOMETRIC TITRATION

The chromatograph gives results in the form of a detector response against log (molecular weight) curve, i.e. a molecular weight distribution. From this data are calculated the number and weight average molecular weights, which are respectively defined by

$$\bar{M}_n = \frac{\sum_i n_i M_i}{\sum_i n_i} \qquad \text{(II:1)}$$

$$\bar{M}_w = \frac{\sum_i n_i M_i^2}{\sum_i n_i M_i} \,. \qquad \text{(II:2)}$$

where n_i is the number of moles of molecular weight M_i. The ratio $\bar{M}_w / \bar{M}_n$ is used as a measure of the molecular weight dispersity of the sample, being equal to unity for a perfectly monodisperse sample.

GPC is not an absolute technique, but requires calibration. Commercially produced, narrow distribution polystyrenes, prepared by anionic polymerisation, are available for this purpose[12].

A Waters model 200 gel permeation chromatograph (Waters Associates (Instruments) Ltd., 324, Chester Road, Hartford, Northwich, Cheshire CN8 2BR) was employed for determination of molecular weights. The column was packed with styrene/divinyl benzene copolymer beads of 50 µm diameter, having pore sizes in the range 10^4 -10^7 nm. The polymer samples were dissolved in tetrahydrofuran.

6. Gas-Liquid Chromatography (GLC)

Styrene and benzaldehyde concentrations were determined using a Pye-104 chromatograph. A 1.5 m x 4 mm i.d. column packed with 5% carbowax 20M on chromosorb W (80-100) mesh) was employed. The nitrogen carrier gas flow rate was 50 cm^3 min^{-1} and the oven temperature 373K. Under these conditions, the sensitivity of the instrument to styrene and benzaldehyde was 5.10^{-5} and 1.10^{-5} mol dm^{-3} respectively. Samples for analysis were diluted four-fold with tetrahydrofuran and mechanically shaken for 30 min.

7. Flame Photometry

An EEL flame photometer was used to measure sodium and potassium levels in water and polymer. Sensitivities to sodium and potassium were 1.10^{-3}

ppm (at 589.3 nm) and 5.10^{-2} ppm (at 766.5 nm) respectively.

8. Surfactant titration

Latex samples were titrated with surfactant by the method of Maron et al. (13). Surface tensions were measured by the du-Nouy ring technique.

E. PREPARATION OF LATEX FILMS

1. Introduction

Several techniques for the preparation of films from polymer solutions or latex dispersions have been reported in the literature[14-19]. In general, a liquid film is formed on a substrate, and the solvent or dispersion medium is allowed to evaporate. The substrate is chosen such that the polymer film may be easily removed either by peeling it off the substrate, or by removal of the substrate from the film by chemical means such as solution or amalgamation. Those methods most likely to produce films sufficiently free from contamination and of the required range of thicknesses were evaluated as described below.

In addition, a flash casting technique was devised. This method was based on tablet coating process used by the pharmaceutical industry, in which tablets contained in a heated rotating pan, are sprayed with a solution of polymer[20,21]. To cast a polymer film, a latex aerosol was directed towards a specially constructed PTFE coated hotplate. The aqueous phase was immediately 'flashed off', leaving a thin polymer film behind.

2. Film Casting on a Mercury Surface (14,15)

The mercury was contained in circular glass Petri dishes of 90 mm diameter. The approximate volume of latex required to produce a film of given thickness was calculated from the surface area of mercury covered and the solids content of the latex. This volume was poured carefully onto the mercury to avoid the formation of globules of latex beneath the surface. The liquid film did not spread spontaneously and so a small PTFE spreader was used to cover the surface with latex. A 10-15 mm border between the edge of the film and the side of the Petri dish was maintained to prevent the liquid latex coming into contact with glass, to which the dry film might adhere. The Petri dish was loosely covered and the film allowed to dry overnight. The dry film was lifted off the surface slowly to avoid small droplets of mercury adhering to the surface.

3. Film Casting on Photographic Paper [17]

A sheet of resin backed photographic paper (203 x 254 mm) was held flat on a specially machined vacuum table, which had been previously levelled. The latex film was cast using a brass drawdown bar. When dry, the film was floated off the gelatin surface by placing the paper in warm water. The film was suspended on a brass frame and left to dry. The film thickness could be varied by adjusting the solids content of the latex and/or using a drawdown bar of different gap.

4. Film Casting in PTFE and Silicone Rubber Dishes

The dish was placed on a surface which was level and free from vibration. The volume of latex calculated to give a film of the required thickness was poured into the dish. A PTFE spreader was used to spread the latex over the surface, until the liquid film was in contact with all four walls. The dish was then loosely covered, and the film left to dry.

5. Film Casting on Silanised Glass [18]

A sheet of plate glass (220 x 120 mm) was immersed in chromic acid and then rinsed thoroughly with double distilled water. The cleaned surface was swabbed with a 2% solution of dimethyldichlorosilane in 1,1,1-trichloroethane (Repelcoat; Hopkin and Williams Ltd., Freshwater Road, Dagenham, Essex RM8 1QJ) and then well rinsed with double distilled water. The contact angle of water against this surface was in the range 94 - 96°.

Latex films were cast on the surface with the aid of a PTFE spreader. Disjoining of the liquid film occurred frequently, as with the PTFE and silicone rubber dishes. Application of adhesive tape to the edges of the plate glass, as suggested by Eissler did not prevent this. When a complete film was dry, it was peeled gently from the surface. It was not possible to use the surface a second time without re-treatment, as the film adhered strongly to the glass.

6. Flash Casting

a. Apparatus

The flash casting technique was used to prepare thin polymer films from most of the homopolymer, copolymer and core-shell latices prepared in the course of this study. Some films were also prepared from polymer solutions.

The technique was evaluated using a prototype hotplate, which consisted of a sheet of PTFE, stretched over an aluminium plate (220 x 120 x 6 mm) behind which were mounted two thermostatically controlled heaters. The electrical components were enclosed to prevent latex from coming into contact with them.

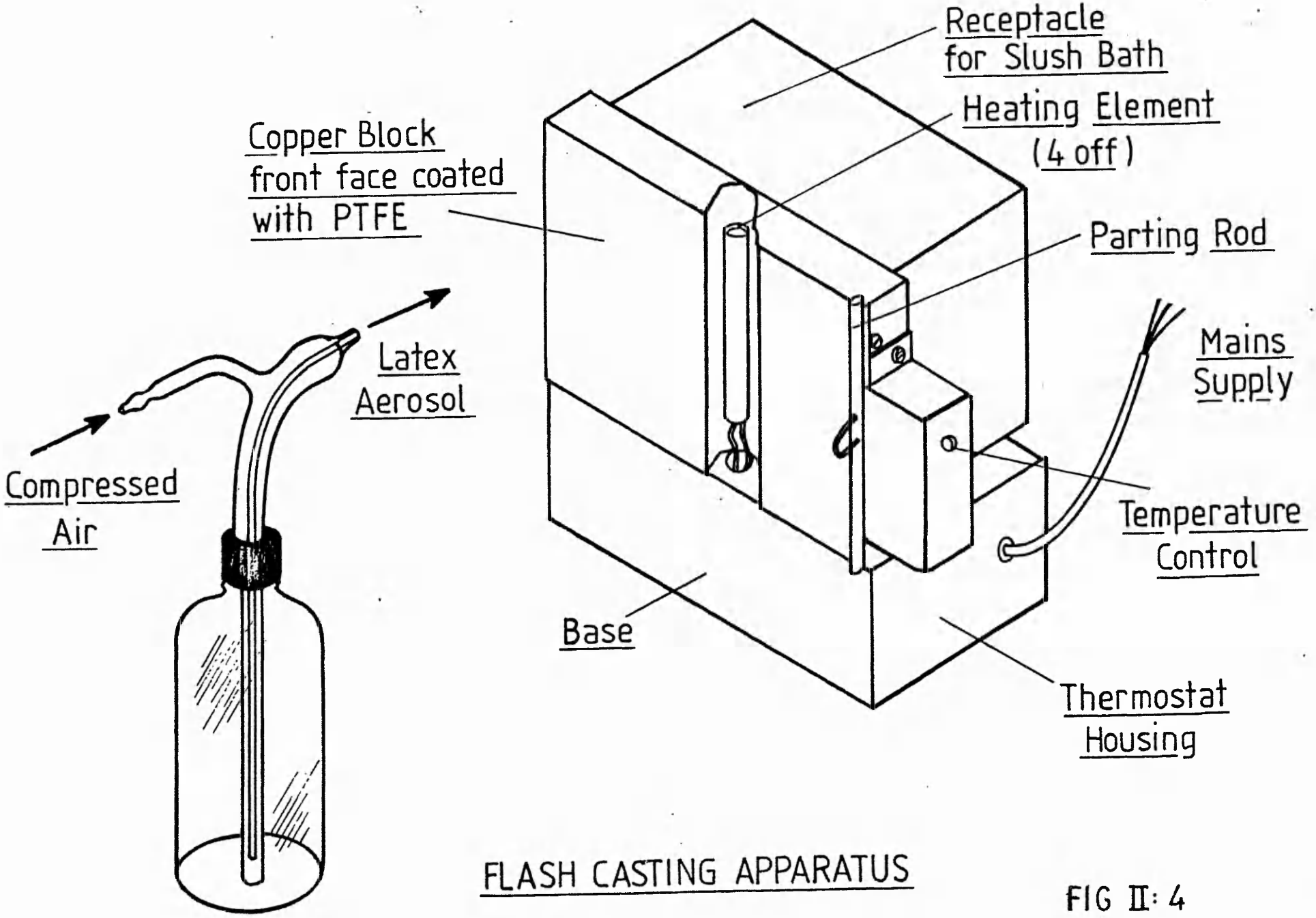

FLASH CASTING APPARATUS

FIG II: 4

TABLE II:1

COOLING MIXTURES

The following liquids were used in admixture with solid carbon dioxide to produce the temperatures shown.

Liquid	Temperature/K
Cyclohexane	279
Methyl salicylate	264
Carbon tetrachloride	250
o-xylene	244
Pyridene	231
Ethyl malonate	223
n-octane	217
Isopropyl ether	213

Small holes to accommodate thermocouples were drilled parallel to the front face and as close to it as possible, permitting easy measurement of the surface temperature.

The second hotplate on which most of the films were cast was similar to the prototype. The PTFE surface was bonded to the front face of a copper block (220 x 120 x 25 mm), which contained four thermostatically controlled heaters. Provision for a slush bath was made so that the block could be cooled below room temperature. The hotplate is depicted in Fig. II:4.

The temperature of the hotplate was measured by placing thermocouples at various depths in the holes provided. The EMF's were measured on a meter (type electronic thermometer; Comark Ltd., Littlehampton, W. Sussex) and could be output to a chart recorder.

Several types of sprayer were evaluated including a chromatography spray powered by an aerosol propellant cannister (Fisons Scientific Apparatus Ltd., Bishop Meadow Road, Loughborough, Leicestershire), an electrically powered airless paint sprayer (model 969; Burgess Power Tools, Sapcote, Leicestershire) and an aerosol generator designed to produce an average droplet size of 2 μm ('Collison' spray[22]). The sprayers were tested to see if they could produce a sufficiently fine aerosol (maximum droplet diameter 20 μm) without blockage by latex polymer. The droplet size produced by the sprayers was estimated by spraying toluene into a vigorously stirred, dilute solution of sodium dodecyl sulphate, and measuring the size distribution of the resulting emulsion on a Coulter Counter. The sprayer selected was a pyrex glass unit (glass spray unit; Sigma Chemicals Ltd., Fancy Road, Poole, Dorset) used with compressed air. The sprayer, which is shown in Fig. II:4, is of the conventional atomiser type. The latex is drawn up a narrow bore glass tube to an orifice, which is surrounded by a larger concentric orifice: a rapid stream of air passes through the latter, atomising the latex.

b. Method

The hotplate was switched on and left until the temperature oscillations settled down. The spray reservoir was filled with latex at the required solids content. The block was then sprayed slowly and evenly, at a distance of approximately 1 m. Depending on the thickness of film required some 20 - 50 passes were necessary taking between one and three minutes. The initial and final bursts of spray tended to contain much coarser droplets, so care was taken to ensure that the sprayer was started and stopped with the jet aimed to one side of the hotplate. Immediately after spraying, the hotplate was switched off and allowed to cool to the temperature at which the film was to be removed. If this

was below room temperature, the appropriate cooling mixture was placed in the bath behind the block (see Table II:1 [23] for a list of slush baths giving temperatures in the range 213 - 279 K).

The film was removed from the surface by means of the parting rod, to which it adhered. With the block at the correct temperature, the grub screw securing the rod was slackened. The parting rod was then pulled away from the block slowly and evenly thereby peeling the film away from the surface. Particular care was necessary to avoid small tears, which generally formed at the edges of the film, from spreading to the centre.

Providing the hotplate was at the optimum temperature for film removal for the polymer concerned, the film could be peeled from the surface without unduly stressing it. In most cases, there was no detectable increase in the length of the film resulting from its removal from the hotplate. Even in the worst cases, the extension was only a few percent of the original length of the film.

Although it is difficult to extrapolate results obtained with polyethylene to the polymers studied in this work, the results of Paulos and Thomas [24], on the effect on gas permeability of postdrawing polyethylene film, are relevant here. They found that to produce a measurable drop in the oxygen permeability, the polyethylene film had to be stretched to beyond twice its original length. It is therefore likely that the amount by which the latex films were stretched during their preparation would not measurably affect their transmission properties.

After the film had been removed, the PTFE surface of the hotplate was cleaned by washing with a solvent mixture containing approximately equal proportions of acetone, butanone and toluene.

F. MEASUREMENT OF TRANSMISSION PROPERTIES

1. Introduction

The most popular methods for the determination of diffusion coefficients have been permeation and sorption methods. Both rely on solutions of Fick's Second Law under the appropriate boundary conditions.

a. Sorption Methods

In this approach, the polymer sample, which is initially devoid of penetrant, is suspended in the penetrant vapour, at constant temperature and pressure. Solution of the penetrant occurs at the surfaces of the film, followed by diffusion towards its centre. The resulting weight increase is measured as function of time. Uptake of vapour continues until equilibrium with the vapour phase is attained. If the vapour concentration is now reduced to zero, penetrant

will desorb from the film, and the weight loss can also be monitored.

The simplest experimental method[25] involves removing the film at intervals and weighing it. More satisfactory techniques utilise a quartz spring or microbalance[26], thus eliminating the errors arising from interruption of the sorption process. The penetrant vapour concentration may be varied by altering the temperature or mixing with an inert diluent of low vapour pressure, e.g. dibutyl phthalate.

If the equilibrium between vapour and surface penetrant concentrations is attained rapidly by comparison with the rate of diffusion, then the surface concentration can be kept effectively constant throughout the experiment. The condition is usually satified by polymers at temperatures well above their glass transition temperature. Under this condition, and where the diffusion coefficient is independent of concentration, the rate of sorption is given by[27]

$$\frac{M_t}{M_\infty} = 4\left[\frac{Dt}{l^2}\right]^{\frac{1}{2}}\left[\frac{1}{\pi^{\frac{1}{2}}} + 2\sum_{n=0}^{\infty}(-1)^n \text{ ierfc } (nl/2(Dt)^{\frac{1}{2}})\right] \qquad \text{(II:3)}$$

where M_t and M_∞ are the masses sorbed at time t and at equilibrium respectively; l is the film thickness and ierfc is the inverse complimentary error function. For short times, this equation simplifies to

$$\frac{M_t}{M_\infty} = \frac{4}{\pi^{\frac{1}{2}}}\left[\frac{Dt}{l^2}\right]^{\frac{1}{2}} \qquad \text{(II:4)}$$

The usual procedure is to plot the relative weight increase, M_t/M_∞, against $\sqrt{t}/l$ and calculate the diffusion coefficient from the initial linear slope. The solubility coefficient may be calculated from the equilibrium amount sorbed. The product of the diffusion and solubility coefficients then gives the permeability coefficient.

In common with most permeation experiments, the film is normally free of penetrant at the start of the experiment. It may, however, be pre-equilibriated at a non-zero vapour pressure. This procedure, which is termed the interval type[28] as opposed to the integral type, allows the calculation of a mean diffusion coefficient between the concentrations of initial and final equilibria, as defined by Eq. II:4. It therefore provides a means of estimating the concentration dependence of the diffusion coefficient.

b) Permeation Methods

In essence, the object of a permeation experiment is to measure the rate of transport of penetrant through a film as a function of time. The division of the permeation process into transient and steady states, and the mathematical

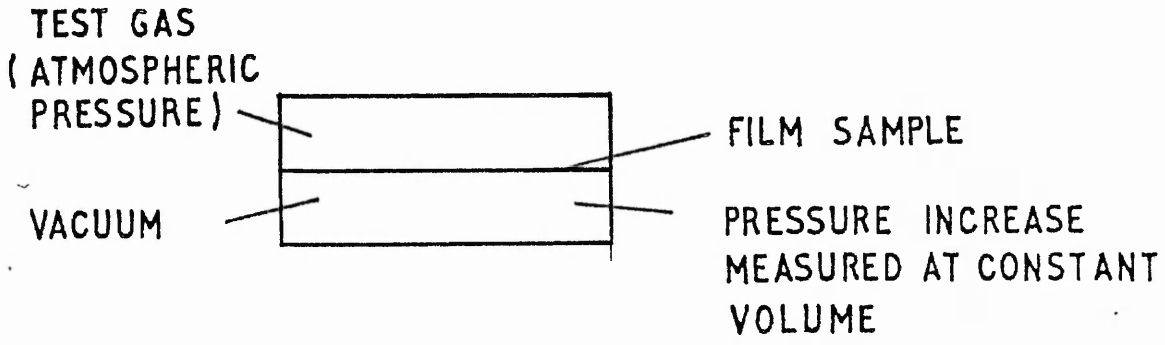

A PRESSURE CHANGE METHOD

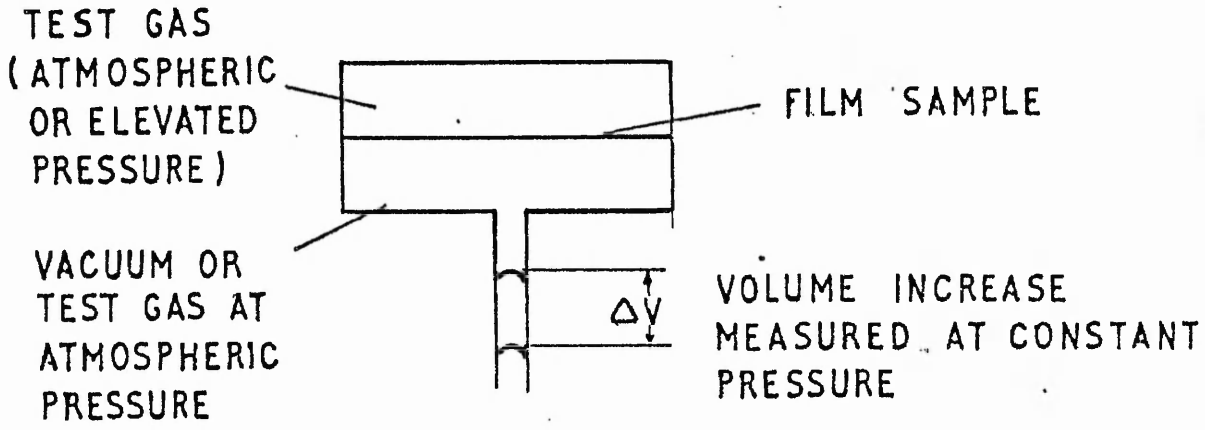

B VOLUME CHANGE METHOD

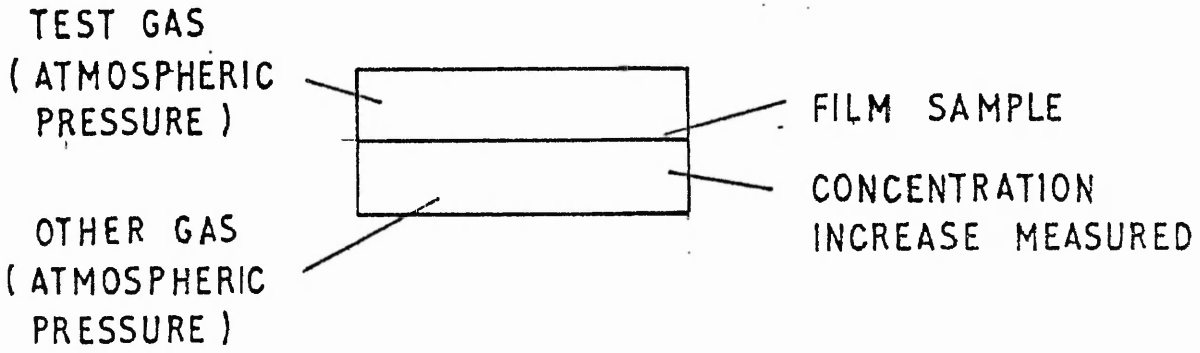

C CONCENTRATION CHANGE METHOD

FIG II:5 SCHEMATIC REPRESENTATION OF PERMEATION METHODS

treatment of these states, have already been discussed (Chapter I) and so only the practical aspects will be dealt with here.

There are three basic methods of measuring penetrant transmission rates, namely pressure, volume and concentration change methods. These are depicted schematically in Fig. II:5. All three methods have been used both in academic studies and for routine industrial testing. Detailed descriptions of the apparatus and procedures for the latter have been given by Stocker[29] and a comparison of the three methods in determining oxygen permeability of commercial polymer films has been made by Taylor et al[30].

The pressure change method was developed by Barrer[31] to determine diffusion and permeability coefficients of gases through polymer films. The technique was refined by Stannett and co-workers[32], who first used it to determine vapour transmission rates. Since that time, it has been extensively used with a large variety of polymers and penetrants. A typical procedure involves placing the film under test in a stainless steel cell, which it divides into two chambers. Both sides are evacuated, and residual vapours frozen out with liquid nitrogen. The penetrant, which can be gas, vapour or liquid, is admitted to one chamber and the increasing pressure in the other measured with a McLeod gauge.

The volume change method was devised by Todd[33], who employed a cell having a chamber of large volume on one side and of small volume on the other. The large chamber was evacuated and the test gas introduced into the small chamber at atmospheric pressure. A horizontal capillary connected to the small chamber contained a mercury plug. As gas permeated into the large chamber, the mercury plug moved in the capillary so as to reduce the volume of the small chamber and maintain the pressure.

The equipment used by Brubaker and Kammermeyer[34] is similar in design. However, the large chamber is filled with test gas at elevated pressure. This permeates into the small chamber, which is maintained at atmospheric pressure by the mercury plug moving in the opposite direction.

Both pressure and volume methods change entail a total pressure difference across the film, which soft polymer films are often unable to withstand. To prevent distortion or destruction of the film, a mechanical support, typically a mesh or sintered material, is required. Although effective, the support may lower the exposed area of film, introducing an uncertainty into the result.

A more serious drawback associated with pressure differential methods is the problem of leaks. These can occur at the edges of the film and through pinholes in the exposed area. The former can be eliminated to some extent by

sophisticated design (e.g. mercury seals), but leaks remain a frequently undetected source of error, and can only be assumed absent when the two lowest results are in good agreement[35].

The concentration change method avoids the necessity for a total pressure difference across the film, and relies instead on a difference in partial pressure of penetrant. This is most easily accomplished by stretching the film under test over a metal cup containing liquid penetrant (PATRA cup[36]), or fabricating pouches or bottles from the test material and filling with penetrant[37,38]. The container is placed in a controlled environment and weighed at intervals. Where the material is highly permeable, it may be necessary to ventilate the chamber to maintain a zero concentration of penetrant outside the container. Alternatively, for impermeable materials where the weight losses are small, the air in the chamber may be sampled and analysed for the penetrant. These techniques are popular in industry, being straightforward and realistic. However, they are inadequate for measurement of time lags, and errors in the measured permeability may arise from stagnant air layers inside the container and an uncertain sample area. Moreover, the method cannot be used for gases and some liquids.

The most popular form of the concentration change method is the 'dynamic' or 'differential' technique. Again, the permeation cell is divided into two chambers by the film under test. The penetrant flows over one side of the film, either as a pure gas, or as a vapour in a carrier gas stream, and is termed the 'span' gas stream. The permeating material is swept away by a second carrier gas stream (the 'sweep' gas stream), which is then analysed. Davis[39], who first used this technique, employed chemical methods to determine the amounts of permeating oxygen and carbon dioxide. Modern instrumental methods, capable of much greater sensitivity, have been used in several studies by Pasternak *et al.*[40,41], and other workers[42-45].

Where the film under test is impermeable and the penetrant difficult to detect at low concentrations, the penetrant may be retained in the second chamber, from which samples are withdrawn at intervals for analysis[46]. Since this method measures the cumulative amount of penetrant rather than the penetrant flux, it is termed the integral technique.

Yasuda and Rosengren[47] have described a somewhat different permeation apparatus. Rather than sweeping the permeating gas to the detector in a carrier gas stream, a thermistor bead is built into the receiving chamber of the cell. The receiving chamber can either be swept by a carrier gas stream, in which case the thermistor measures the instantaneous penetrant flux, or it can be sealed and the accumulation of penetrant measured. These cases correspond to

the differential and integral methods respectively.

The dynamic method can be extended to include permeation of mixtures, in which case samples are taken from the sweep gas stream or the static second chamber. The penetrants may be separated chromatographically, or introduced directly into a mass spectrometer. In the latter case, a suitable peak characteristic of each of the penetrants is selected, and the amount of each can be determined.

The sorption technique has many advantages over permeation methods for obtaining diffusion coefficients of vapours. There is no need for special seals or supports. Sorption kinetics are relatively unaffected by pinholes in the film sample which would have a disastrous effect in a permeation experiment. For low diffusion coefficients, where protracted run times are necessary, the sorption technique is particularly valuable, since errors due to temperature fluctuations are at a minimum. Permeation methods are much more suitable for penetrants with high diffusion coefficients, particularly gases. In these cases, the equilibrium uptake would be too small, and occur too rapidly to be measured accurately by a sorption technique.

2. Apparatus

Permeability and diffusion coefficients were measured by a dynamic technique. As discussed above the penetrant is made to flow over one side of the film, the permeating material being swept away and determined by an instrumental technique.

At the heart of the appartus lies the cell in which the film is mounted: this is shown diagramatically in Fig. II:6. The only theoretical constraint on the cell dimensions is the extent of diffusion through the clamped, unexposed area of the film (the 'edge' effect). Barrer et al. (48) have determined that the error arising from this effect will be negligible if the ratio of film thickness to radius of exposed film is less than 0.2. The maximum film thickness anticipated was 100 μm, and this would impose a lower limit of 1 mm cell diameter. This is well below the minimum diameter necessary to permit the passage of a detectable amount of penetrant.

The sensitivity of the katharometer used to detect gaseous penetrants dictated that the cell diameter should be as large as the availability of uniform film samples allowed. Most of the measurements were made with cells of 35 mm diameter. Where it was impossible to prepare sufficiently uniform films of this size, cells of 25 or 10 mm diameter were used.

It was anticipated that some of the films would be fragile, and incapable of withstanding the transient pressure differences which occur on operating the

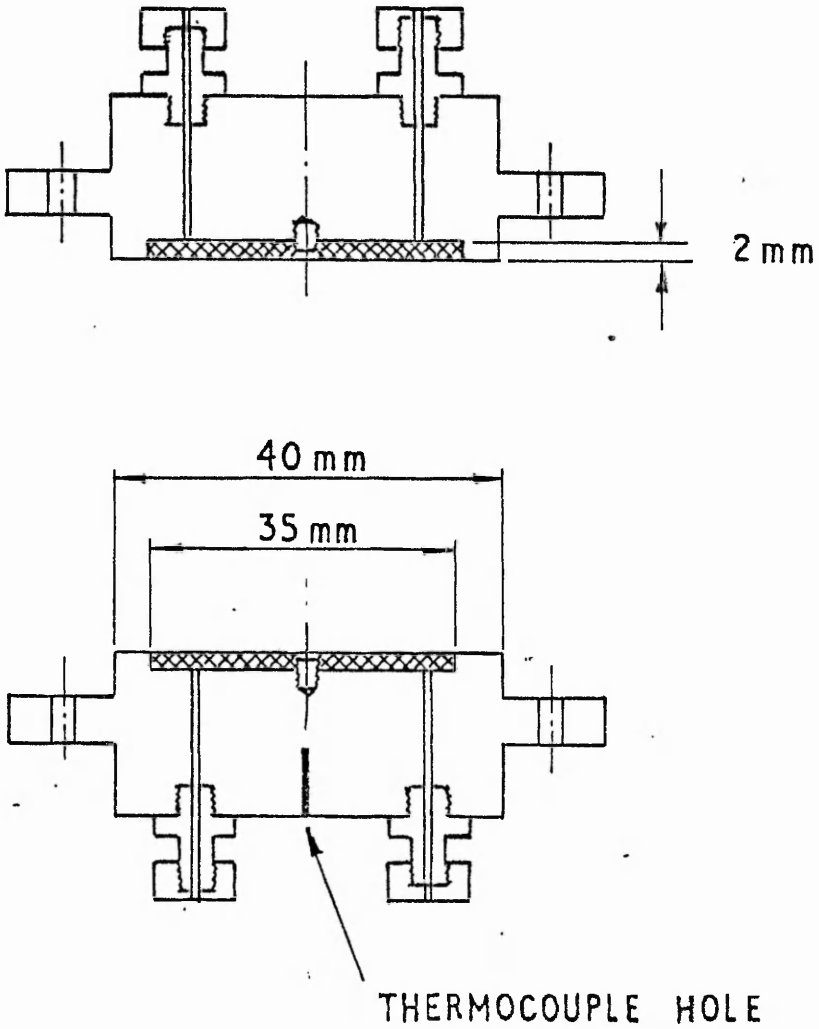

FIG II:6 SECTIONAL VIEW OF PERMEATION CELL

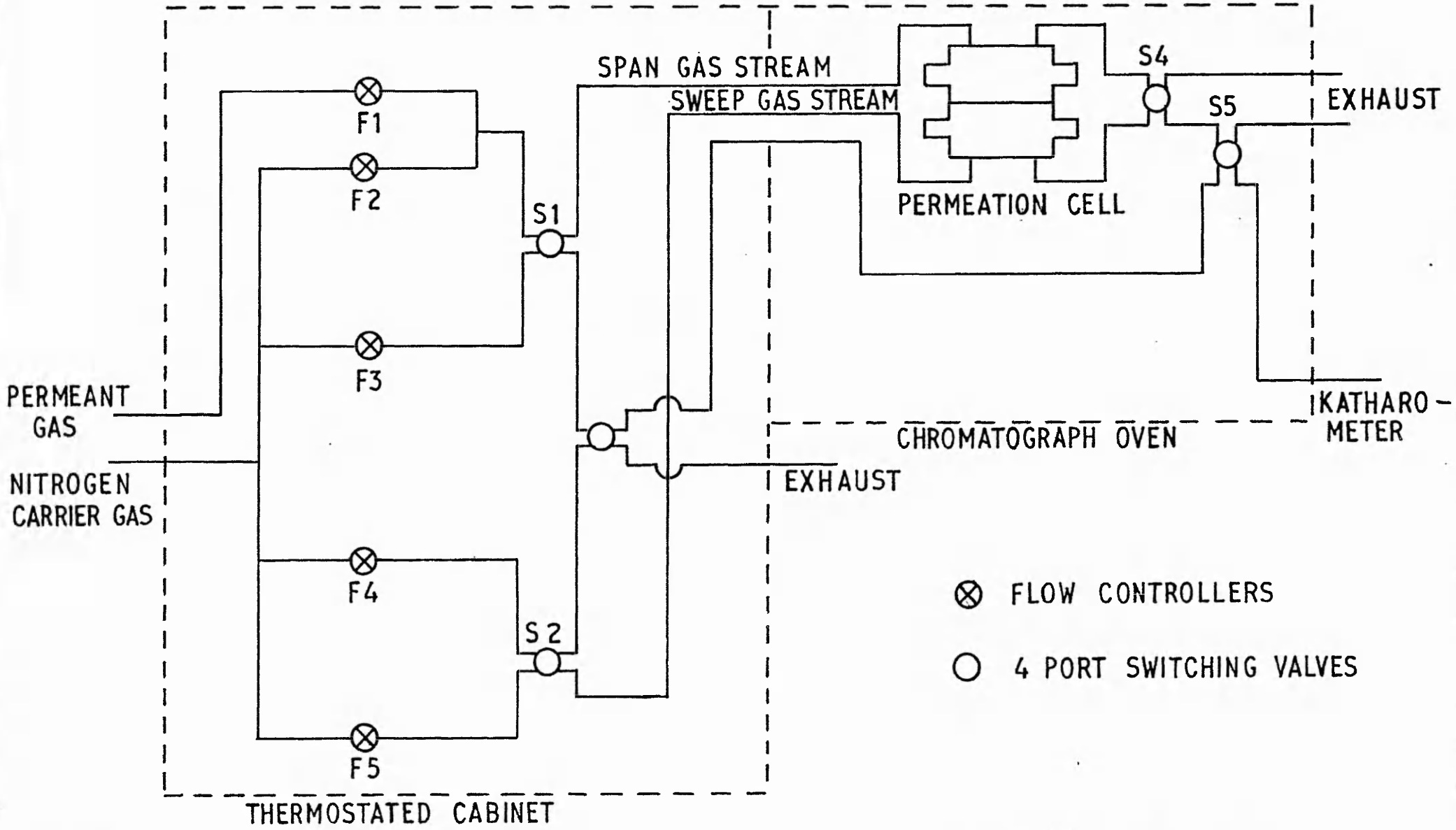

FIG II:7 LAYOUT OF APPARATUS USED TO DETERMINE PERMEABILITIES TO GASES

switching valves. For this reason a support was included in the design of the cell. Sintered bronze was chosen for this purpose because it offered many advantages over the stainless steel mesh normally employed. These included greater mechanical strength and ease of mounting in the cell. The depth of support reduced the cell volume thus reducing the dead space in the system, while the structure ensured turbulent rather than laminar flow over the film surfaces. The support was normally removed for the gas permeation work.

The layout of the apparatus into which the cells were fitted is shown in Fig. II:7. A katharometer detector (Model 158, Servomex Controls Ltd., Crowborough, Sussex) was employed to measure gas concentrations. The flow regulators (model 8744, Brooks Instruments Ltd., Brooksmeter House, Stuart Road, Bredbury, Stockport, Cheshire SK6 2SR) were housed in a perspex cabinet. The temperature within was maintained at 303 $\pm$ 1K by means of two thermostatically controlled 60 W bulbs and a circulating fan. The cell was housed in a chromatographic oven (model LC2F, Phase Separations Ltd., Deeside Industrial Estate, Queensferry, Clwyd, CH5 2LR), from which the injection port, column and detector head had been removed. After modification, the oven temperature could be regulated between 303 and 423 $\pm$ 1K. Gas streams were directed by means of four port switching valves (Carle Instruments model 5511, Techmation Ltd., 58 Edgware Way, Edgware, Middlesex, HA8 8JP).

3. Mounting of Film Samples

A disc, approximately 50 mm in diameter, was cut from sheet of film. To prevent contamination, the film was held between two discs of coated paper (used as separators between 47 mm Millipore filters). The sample disc was then placed on the bottom half of the cell and the other half positioned directly on top, care being taken to avoid lateral movements which might distort the film. The screws which held the two halves of the cell together were then tightened evenly, to avoid unduly stressing the film.

Glassy polymer films were very brittle, and extreme care was necessary when cutting and mounting the discs, as cracking and tearing readily occurred. In many cases, it was necessary to place gaskets between the film and the mating surfaces of the cell in order that the cell could be clamped sufficiently tightly to render it leak proof without distorting the film. Despite these precautions, it was not uncommon to have to replace a glassy film which had ruptured during the process of cutting and mounting.

With the film mounted, the cell could be installed in the chromatography oven. The edges of the mating surfaces of the cell, and the connections between it and rest of the apparatus were painted with a dilute solution of detergent.

Any leakage was immediately detectable by the vigorous frothing which occurred in the region of the leak.

4. Operating Procedure

With the cell installed, the apparatus was operated as follows: The nitrogen carrier and test gases were switched on at the cylinder heads. After ensuring that gas was flowing through both sides of the katharometer, the amplifier was switched on and the supply voltage set to the required value (normally 4.5 V). The heaters and fans in the perspex cabinet and oven were switched on. The apparatus was then left for 30 minutes to attain temperature equilibrium. When this had been achieved, the flow rates were measured, using a bubble flowmeter in conjunction with a stopwatch measuring to 0.1 s. Switching valves S1, S3 and S5 (see Fig. II:7) were positioned such that the flows were measured by bypassing the cell. If necessary, they were adjusted, although day to day stability was generally good. The flow rates were normally 25 cm^3 min^{-1}.

Switching valve S1 was positioned so that the span gas flowing over the top of the film sample was pure nitrogen. The attenuator was set to a value appropriate to the film under test and the recorder pen zeroed. The apparatus was left for several minutes to ensure the absence of baseline drift. Finally, the test gas was directed over the film by reversing the position of switching valve S1, and the permeation trace was recorded.

Diffusion coefficients were determined from the transient state portion of the permeation curves by the method of Pasternak et al.[41], which is described in Chapter I. The nomalised curve (i.e. J_t/J_s against t) was analysed to give the times at which J_t/J_s was equal to simple decimal fractions (0.05, 0.10, 0.15 .... 0.95). The tabulated values of $4Dt/l^2$ corresponding to these fractions (Table I:1) were plotted against these times. Providing the polymer/penetrant system under test obeyed Fick's law, a straight line resulted. The slope was equal to $4D/l^2$, and so the diffusion coefficient could be calculated. It should be noted that this procedure measures the duration of the transient state, and does not require an accurate knowledge of penetrant concentration.

The equation relating the amount of penetrant, Q, passing through a film in time t, to its permeability coefficient, P, was given in Chapter I as

$$P = \frac{Ql}{A\,t\,(p_1 - p_1)} \qquad \text{(II:5)}$$

where l and A are the thickness and area of the film and p, and p_o are the penetrant concentrations on either side of the film. The amount of penetrant

which passed through the film and was carried away by the sweep gas stream was determined from the katharometer response by

$$Q = \frac{f}{60} \; s \; a \; k \qquad \text{(II:6)}$$

where f is the sweep gas flow rate (in $cm^3\ min^{-1}$), s is the katharometer signal in mV obtained at amplifier attenuator setting a. k is the katharometer calibration constant for the penetrant under consideration, and was obtained by use of a suitable calibration gas mixture.

REFERENCES

1. M.S. El-Aasser, T. Makgawinata, J.W. Vanderhoff, C. Pichot and M.F. Llauro, in "Emulsion Polymerisation of Vinyl Acetate", M.S. El-Aasser and J.W. Vanderhoff (eds.), Applied Science Publishers, Chapter 12, p 215 (1980).

2. M.C. Wilkinson, in "Treatise on Surface Characterisation", K. Mittal (ed.) Plenum Press (1984).

3. M.C. Wilkinson, J. Hearn, P. Cope and M. Chainey, Brit. Polym. J., 13, 82 (1981).

4. S.M. Ahmed, M.S. El-Aasser, G.H. Pauli, G.W. Poehlein and J.W. Vanderhoff, J. Colloid Interface Sci., 73, 388 (1980).

5. M.E. Labib and A.A. Robertson, J. Colloid Interface Sci., 67, 543 (1978).

6. J.W. Vanderhoff, Proc. 4th Int. Conf., Org. Coat. Sci. Technol., p. 447 (1978).

7. W.T. McCarvill and R.M. Fitch, J. Colloid Interface Sci., 64, 403 (1978).

8. M.C. Wilkinson and D. Fairhurst, ibid, 79, 272 (1981).

9. H.J. van den Hul and J.W. Vanderhoff, ibid, 28, 336 (1968).

10. J.W. Vanderhoff, H.J. van den Hul, R.M.J. Tausk and J. Th. G. Overbeek, in "Clean Surfaces", G. Goldfinger (ed.), Marcel Dekker, p. 15 (1970).

11. P. Stenius and B. Kronberg in "Science and Technology of Polymer Colloids", G.W. Poehlein, R.H. Ottemill and J.W. Goodwin (eds.), Martinus Nijhoff (NATO ASI, p. 449 (1983).

12. J.V. Dawkins and M. Hemming, Makromol. Chem., 176, 1777, 1795, 1815 (1975).

13. S.H. Maron, M.E. Elder and I.N. Ulevitch, J. Colloid Sci., 9, 89 (1954).

14. J. Crank and G.S. Park in "Diffusion in Polymers", J. Crank and G.S. Park (eds.), Academic Press, Chapter 1, p. 1 (1968).

15. V.T. Stannett, U.S. Nat. Technol. Inform. Service, 23, 61 (1973).

16. P.E. Pearce and R.M. Holsworth, J. Paint Technol., 38, 584 (1966).

17. J. Harris, Official Digest, Fed. Paint Varnish Clubs, 28, 30 (1956).

18. R.L. Eissler, J. Appl. Polym. Sci., 12, 1983 (1968).

19. Z.J. Lobos, E. Polatakjo-Lobos and V.G. Xanthopoulos, Polym. Latex Int. Conf. Prepr., paper No. 17 (1978).

20. S.R. Wicks, Ph.D. thesis, University of Bath (1982).

21. D. Simmonite and J. Fennimore, British Patent 1, 484, 566 (1973).

22. D.W. Henderson, J. Hyg., Camb., 50, 53 (1952).

23. D.D. Perrin, W.L.F. Armarego and D.R. Perrin, "Purification of Laboratory Chemicals". Pergamon Press (1980).

24. J.P. Paulos and E.L. Thomas, J. Appl. Polym. Sci., 25, 15 (1980).

25. J. Crank and G.S. Park, Trans. Faraday Soc., 45, 240 (1949).

26. S. Prager and F.A. Long, J. Amer. Chem. Soc., 73, 4072 (1951).

27. J. Crank, "The Mathematics of Diffusion" Oxford University Press (1975).

28. R.J. Kokes, F.A. Long and J.L. Hoard, J. Chem. Phys., 20, 1711 (1952).

29. J.H.J. Stocker, in "Evaluation of Packaging Performance", Proceedings, PATRAPAK Conf., Oxford (1963).

30. A.A. Taylor, M. Karel and B.E. Proctor, Modern Packaging, 33, 131 (1960).

31. R.M. Barrer, Trans. Faraday Soc., 35, 628 (1939).

32. V. Stannett, M. Szwarc, R.L. Bhargava, J.A. Mayer, R.W. Myers and C.E. Rogers, "Permeability of Plastics Films and Coated Papers to Gases and Vapours", TAPPI monograph No. 23 (1962).

33. H.R. Todd, Modern Packaging, 17, 124 (1944).

34. D.W. Brubaker and K. Kammermeyer, Ind. Engng. Chem., 44, 1465 (1952).

35. B.J. Hennessy, J.A. Mead and T.C. Stenning, "The Permeability of Plastics Films", The Plastics Institute, London (1966).

36. A.C. Newns, J. Text. Inst., 417, 27 (1950).

37. M. Salame and J. Pinskey, Modern Packaging, 36, 153 (1962), 37, 131, 209 (1964).

38. K.D. Jeffs, in "Evaluation of Packaging Performance", Proceedings, PATRAPAK Conf., Oxford (1963).

39. D.W. Davis, Paper Trade J., 123, TS97 (1946).

40. R.A. Pasternak and J.A. McNulty, Modern Packaging, 43, 89 (1970).

41. R.A. Pasternak, J.F. Shimscheimer and J. Heller, J. Polym. Sci., Part A2, 8, 467 (1970).

42. T.L. Caskey, Modern Plastics, 45, 148 (1967).

43. R.M. Felder, K.D. Spence and J.K. Ferrell, J. Appl. Polym. Sci., 19, 3193 (1975).

44. D.G. Pye, H.H. Hoehn and M. Panar, Ibid, 20, 287 (1976).

45. K.D. Ziegel, H.K. Frensdorff and D.E. Blair, J. Polym. Sci., Part A2, 7, 809 (1969).

46 V.V. Kapinin, O.B. Lemanik and S.A. Reitlinger, Polym. Sci. USSR, 16, 1055 (1974).

47. H. Yasuda and Kj. Rosengren, J. Appl. Polym. Sci., 14, 2839 (1970).

48. R.M. Barrer, J.A. Barrie and M.G. Rogers, Trans. Faraday Soc., 58, 2473 (1962).

CHAPTER III

PREPARATION CLEANING AND CHARACTERISATION OF POLYMER LATICES

A PREPARATION AND CHARACTERISTICS OF HOMOPOLYMER AND COPOLYMER LATICES

Single stage reactions, described in Chapter II, were used to prepare latices of polystyrene, poly(methyl acrylate), poly(ethyl acrylate), poly (n-butyl acrylate), poly (methyl methacrylate), poly(ethyl methacrylate) and poly (n-butyl methacrylate). Some copolymers of ethyl acrylate and methyl methacrylate, n-butyl acrylate and n-butyl methacrylate, and ethyl acrylate and n-butyl methacrylate were also prepared. Determinations of solids content and particle size were carried out on samples taken immediately after completion of the reaction. The remaining latex was cleaned by microfiltration and further characterised as described in later sections of this Chapter. The characteristics of latices used in the course of this work are summarised in Tables III-1 and III-2.

It is known that the surface charcteristics of polymer latices alter on long term storage, as a result of chemical [1] and microbial [2] processes. For this reason, the latices were used as soon as possible after preparation and cleaning. Where storage for longer than one week was necessary, the latices were treated with a proprietry inhibitor (Kathon 886 MW, Rohm and Haas (UK) Ltd., Lennig House. 2, Masons Avenue, Croyden, Surrey) to a level of 20 ppm, to prevent microbial contamination. Before use, the latices were cleaned by microfiltration, again usually in small quantities.

TABLE III:1

CHARACTERISTICS OF HOMOPOLYMER LATICES

Latex No.	MC8	MC108	MC119	MC120	MC121	MC141	MC142	MC135	MC139	MC136
Polymer	PS	PS	PS	PS	PS	PMA	PEA	PBA	PMMA	PEMA
Diameter/nm	440	585	588	871	390		230	440	206	161
σ/nm		9.8	11.2	16.4	13.4			-	6.9	6.0
Solids content/%	2.71	9.11	9.20	9.81	3.54	8.67	9.90	9.23	9.56	8.34
Surface* Charge Density/$\mu C\ cm^{-2}$	14.2	9.4	5.0	6.4	11.6					
$10^{-3}\bar{M}_n$			276			1344			464	558
$10^{-3}\ \bar{M}_n$			38			72			90	119
$\bar{M}_n/\bar{M}_n$			18.7			18.7			5.2	4.7

*After microfiltration (including acid washing)

TABLE III:1 (Cont'd)

CHARACTERISTICS OF HOMOPOLYMER LATICES

Latex No.	MC122	MC124	MC125	MC128	MC130
Polymer	PBMA	PBMA	PBMA	PBMA	PBMA
Diameter/nm	462	200	900	480	485
σ/nm	10.9	8.8	15.7		
Solids Content/%	9.27	3.66	938	10.4	8.89
Surface Charge* Density/$\mu C cm^{-2}$	8.5	6.2	6.9		
10^{-3} $\bar{M}w$	877	422	262	365	370
10^{-3} $\bar{M}n$	115	80	86	70	71
$\bar{M}n/\bar{M}n$	7.6	5.3	3.0	5.2	5.2

*After microfiltration (including acid washing)

TABLE III:2

CHARACTERISTICS OF COPOLYMER LATICES

Latex No	MC66	MC144	MC145	MC146	MC147	349/135*	349/130B*	349/133*
Copolymer	EA/MMA	EA/BMA	EA/BMA	EA/BMA	EA/BMA	S/BA	S/BA	S/BA
Ratio of components	67:33	80:20	60:40	40:60	20:80	50:50	67:33	75:25
Diameter/nm	420	465	485	420	455			
Solids Content/%	7.62	8.47	8.88	9.37	9.80	6.24	7.01	6.88

*Supplied by National Adhesives and Resins Ltd, Braunston, Daventry

B. KINETICS OF THE SURFACTANT FREE EMULSION POLYMERISATION OF STYRENE

The preparation of monodisperse polystyrene latices by emulsion polymerisation and their surface characterisation have been widely studied (see Chapter I and also Ref. 3). However, very little information on the kinetics of these reactions has been published, although the uniformity of the particle size from an early stage of the reaction (after the number density has become constant) suggests that mechanistic information could be readily obtained. This Section discusses the results of experiments carried out in pursuit of this information.

The theories most likely to be relevant, and their adaptation, to surfactant free reactions have been discussed in Chapter I. The predictions of these theories were tested by determining the effect of reaction variables (temperature, ionic strength and initiator concentration) on reaction characteristics (reaction rate, particle number density and molecular weight development).

A typical example of the kinetic data obtained from a surfactant-free emulsion polymerisation (taken from Ref. 4) is shown in Table III:3 and the conversion time curve is shown in Fig. III:1.

The decrease in particle number density during the early stages of the reaction is clearly shown, after which it attains a constant value. It can be seen that during the latter period (the analogue of interval II in conventional emulsion polymerisation) the rate of reaction is not constant, but increases continuously with increasing conversion. A distinct interval III, when all the monomer is situated in the polymer phase, is not readily identified here, and interval II can be considered to last until almost complete conversion is achieved. In surfactant-containing systems, Interval III starts at around 55% conversion.

1. Effect of Temperature

Fig. III:2 shows an Arrhenius plot of ln (rate constant) against reciprocal temperature, where the rates were assumed to be proportional to the slopes of linear $C^{2/3}$ against time plots. The data [5,6] were obtained from a series of reactions carried out at temperatures in the range 313 - 371K. The calculated activation energy of 69 $\pm$ 2 kJ mol^{-1} compares with 71 kJ mol^{-1} found for reactions carried out in the presence of surfactant[7] and 105 kJ mol^{-1} for bulk, solution and suspension polymerisation[8].

TABLE III:3

KINETIC CHARACTERISTICS OF REACTION 34B [5]

Sample	Time/ min	Conversion /%	Radius/ nm	σ /%	Particle number density/cm^{-3}
34B2	15	0.33	29	15	2.68×10^{12}
34B3	30	0.55	57	11	0.60×10^{12}
34B4	55	1.77	87	7	0.55×10^{12}
34B5	85	4.43	104	5	0.81×10^{12}
34B6	120	7.75	122	4	0.89×10^{12}
34B7	185	17.61	169	9	0.75×10^{12}
34B8	240	27.46	197	6	0.74×10^{12}
34B9	325	43.63	206	3	1.03×10^{12}
34B10	465	71.50	263	3	0.81×10^{12}
34B11	545	92.14	296	2	0.73×10^{12}
34B12	620	93.80	297	3	0.74×10^{12}
34B13	690	92.25	300	2	0.70×10^{12}
34B14	1440	88.70	298	3	0.69×10^{12}

Styrene concentration: 0.870 mol dm^{-3}.

Potassium persulphate concentration: 3.69×10^{-3} mol dm^{-3}.

Temperature: 343 K.

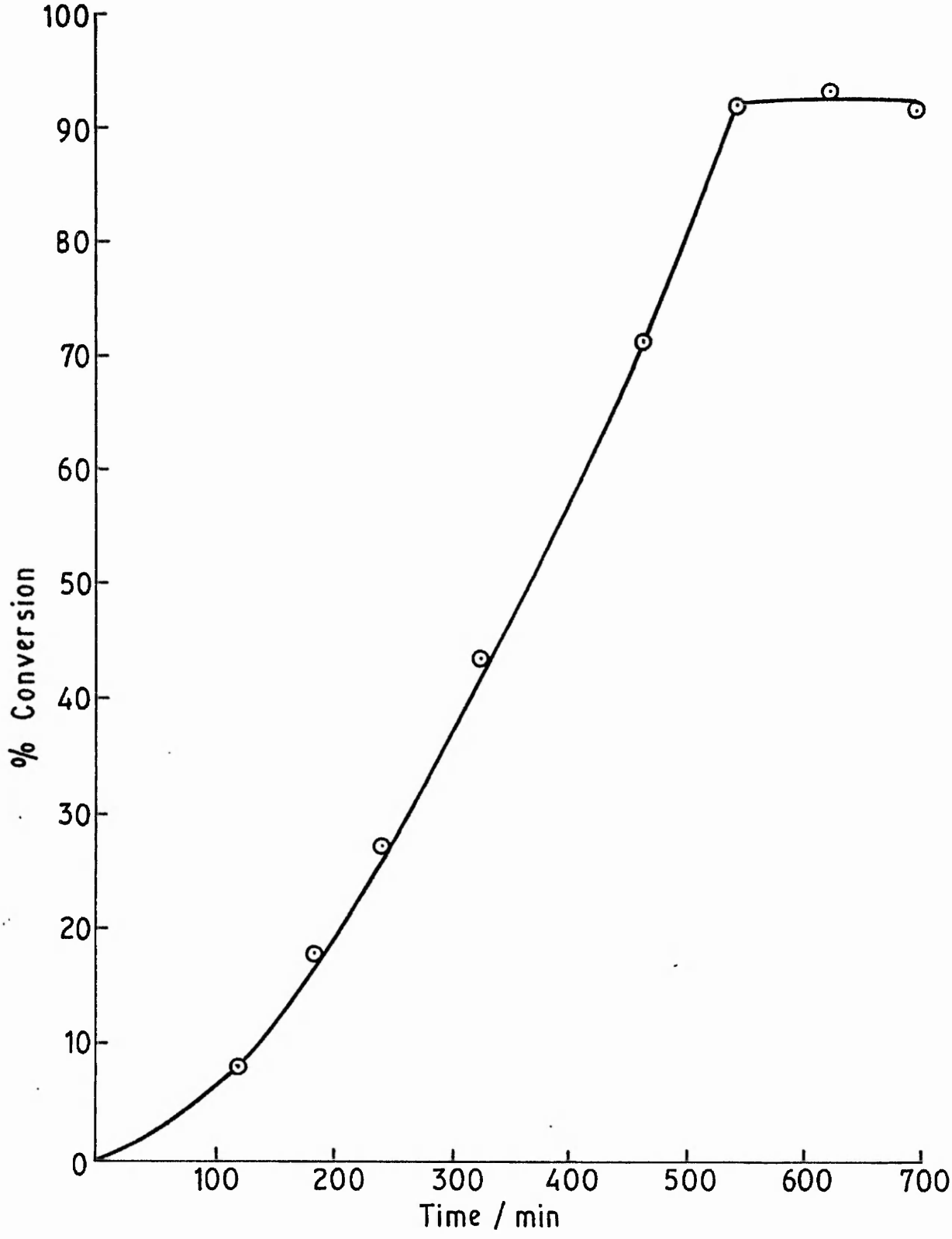

G III:1 % CONVERSION vs TIME CURVE FOR LATEX PS 34 B

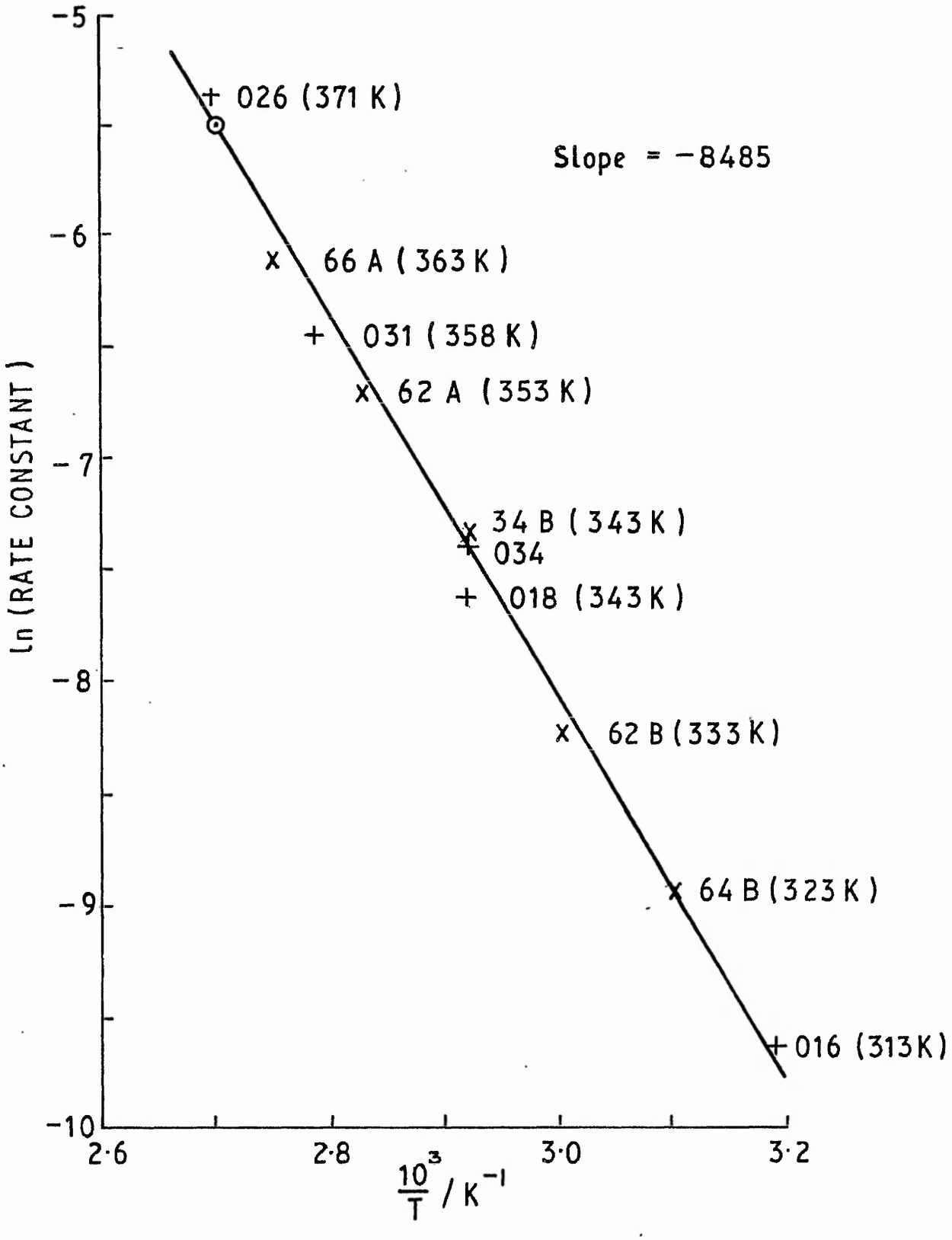

IG III: 2 ARRHENIUS PLOT OF ln (RATE CONSTANT) vs 1/T FOR SEVERAL POLYSTYRENE REATIONS

2. Effect of Initiator Concentration

A series of reactions was carried out in which the initiator concentration, $[P]$, was varied between 5.10^{-4} and 1.10^{-2} mol dm^{-3} and the ionic strength was maintained constant at 3.10^{-2} mol dm^{-3}. The effect of initiator concentration on the rate of the reaction is shown in Table III:4. A plot of log (rate) against log $[P]$ indicates that $R_p \alpha [P]^{0.444}$ (Fig. III:3). This is in reasonable accord with the predictions of the Smith-Ewart Case 3 and surface phase polymerisation treatments of $R_p \alpha [P]^{\frac{1}{2}}$.

TABLE III:4

VARIATION IN RATE WITH INITIATOR CONCENTRATION

Latex	$[P]$/mol dm^{-3}	Rate*
MC49	1×10^{-2}	0.0499
MC55	5×10^{-3}	0.0415
MC69	5×10^{-3}	0.0493
MC70	1×10^{-3}	0.0180
MC68	5×10^{-4}	0.0155

*From slopes of $C^{2/3}$ vs t plots

slope of log Rate vs log $[P]$

$= 0.44 \pm 0.06$

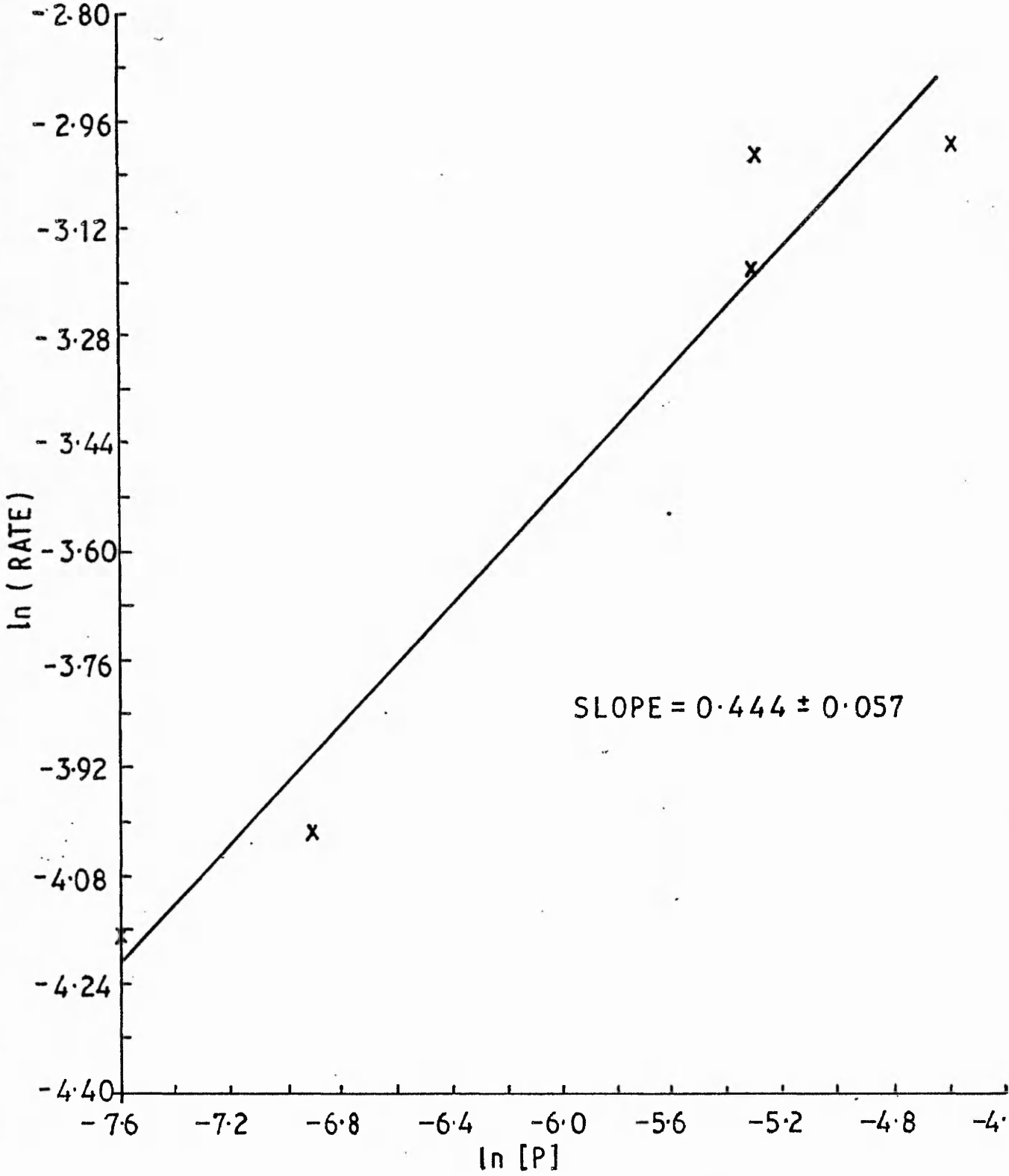

FIG III:3 VARIATION IN RATE WITH INITIATOR CONCENTRATIO

3. Factors affecting Particle Number Density

The mechanisms of surfactant-free emulsion polymerisation discussed in Chapter I suggest that the particle number density, N, finally attained by a reaction depends on the number of nuclei generated, and their stability. The number of nuclei generated is expected to depend on the rate of radical generation, which in turn is dependent on the initiator concentration $[P]$, and the temperature of the reaction. The stability of the nuclei will be dependent on the ionic strength, $[I]$, of the medium, which controls the extent of coagulation required for the nuclei to become colloidally stable. The influence of these factors can be expressed as

$$N \propto [P]^{x} / [I]^{y} \qquad \text{(III:1)}$$

$$\text{and} \quad N \propto T / [I]^{y} \qquad \text{(III:2)}$$

Although they both influence the radical generation rate, $[P]$ and T cannot be combined, since temperature also affects the particle collision efficiency and hence stability.

In order to determine the value of the exponents x, y and z, data from three series of reactions were examined (Table III:5 - III:7 and Figs. III:4 - III:6) and the following results obtained:

(i) At constant initiator concentration and ionic strength, the effect of temperature was found to be (Table III:5 and Fig. III:4:

$$N \propto T^{z}: \; z = 12.24 \pm 0.96 \qquad \text{(III:3)}$$

(ii) At constant ionic strength and temperature, the effect of ionic strength was found to be (Table III:6 and Fig. III:5:

$$N \propto [I]^{-y} : \; y = 0.78 \pm 0.06 \qquad \text{(III:4)}$$

(iii) At constant ionic strength and temperature the effect of initiator concentration was found to be (Table III:7 and Fig. III:6):

$$N \propto [P]^{x} : \; x = 2.36 \pm 0.84 \qquad \text{(III:5)}$$

For comparison, the Smith-Ewart theory applied to surfactant-containing systems gives $N \propto R_i^{0.4} [E]^{0.6}$, where R_i is the radical generation rate and $[E]$ is the surfactant concentration. Thus, stability in these systems is controlled by the surfactant concentration, and the number density is insensitive to ionic strength.

TABLE III:5

VARIATION IN PARTICLE NUMBER DENSITY WITH INITIATOR CONCENTARATION

Latex	$[P]$/mol dm^{-3}	$10^{12} N/cm^{-3}$
MC49	1.10^{-2}	630,000
MC55	5.10^{-3}	50,500
MC70	1.10^{-3}	1,800
MC68	5.10^{-4}	4,200

Slope of log N against log $[P]$ plot $= 2.35 \pm 0.84$.

TABLE III:6

VARIATION IN PARTICLE NUMBER DENSITY WITH TEMPERATURE(5)

Latex	T/K	$10^{12} N/cm^{-3}$
64B	323	0.49
62B	333	0.70
64A	343	1.15
62A	353	1.32
66A	363	2.13

Slope of log N against log T plot = 12.24 $\pm$ 0.96

TABLE III:7

VARIATION IN PARTICLE NUMBER DENSITY WITH IONIC STRENGTH (10)

Latex	$[I]$ /mol dm^{-3}	$10^{12} N/cm^{-3}$
JH A	6.7	219
JH B	10.5	125
JH C	17.6	100
JH D	20.6	90
JH E	24.6	86
JH F	35.0	54
JH G	50.0	42

Slope of log N against log $[I]$ plot = 0.78 $\pm$ 0.06

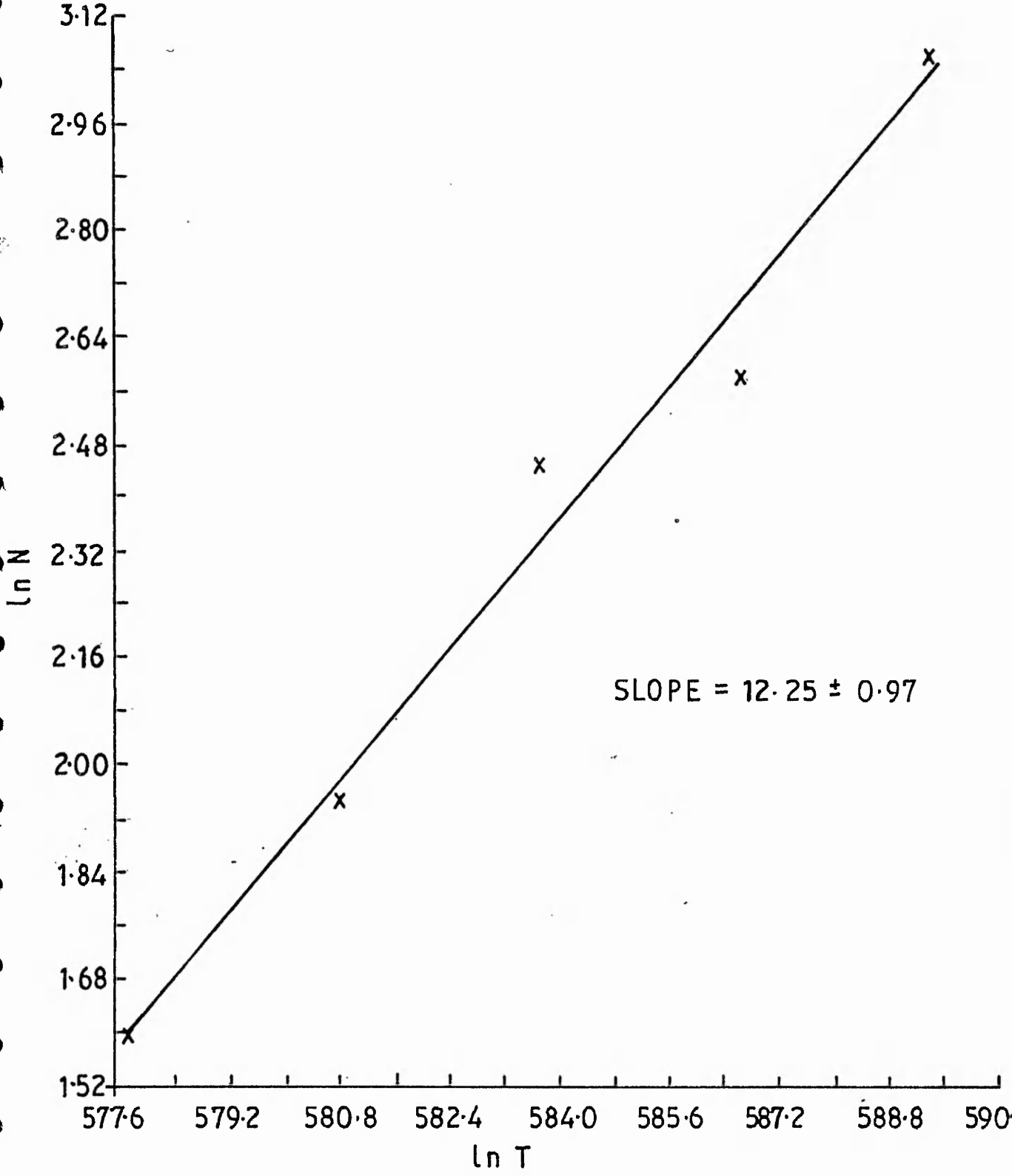

FIG III: 4 VARIATION IN PARTICLE NUMBER DENSITY WITH TEMPERATURE

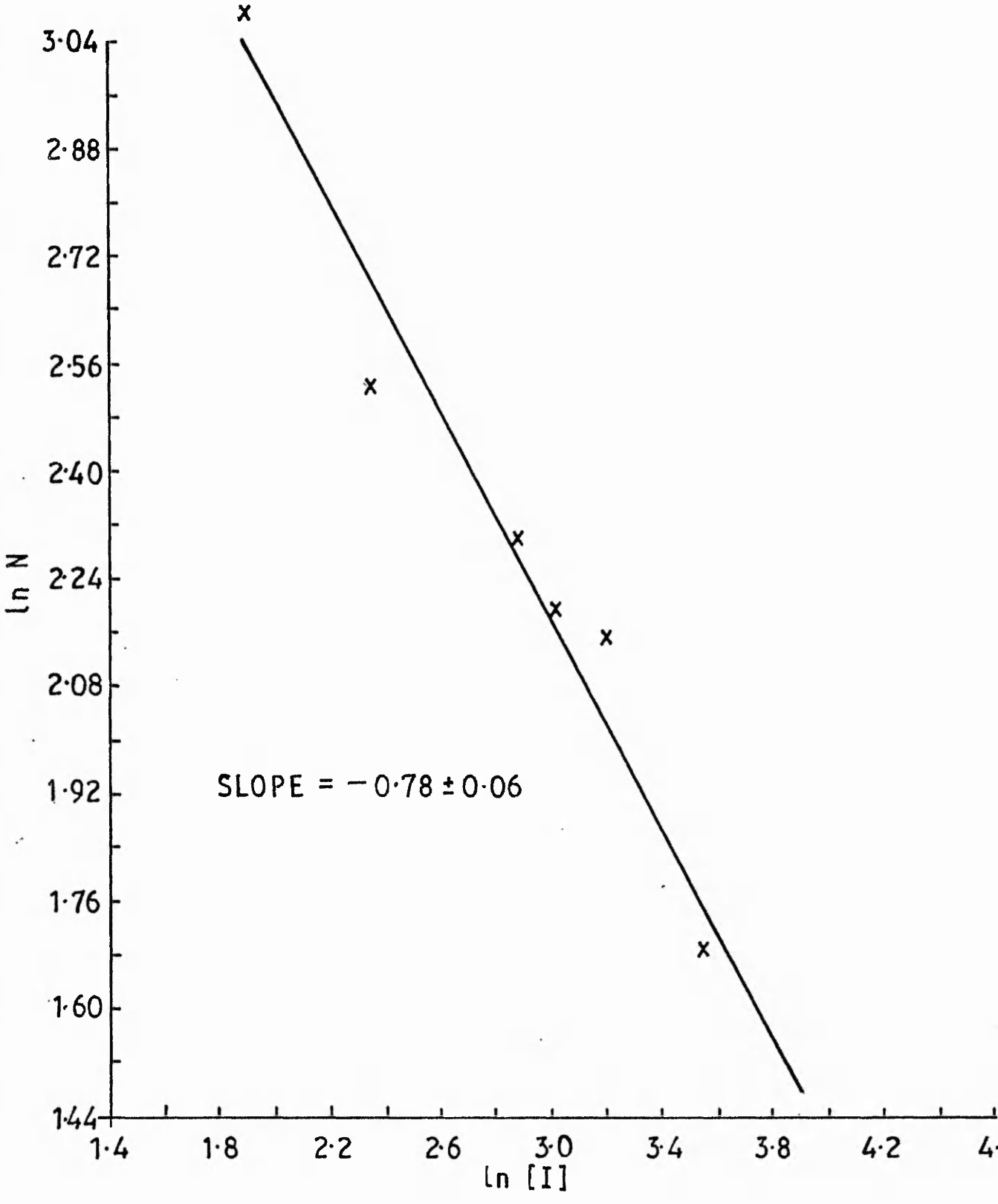

FIG III: 5 VARIATION IN PARTICLE NUMBER DENSITY WITH IONIC STRENGTH

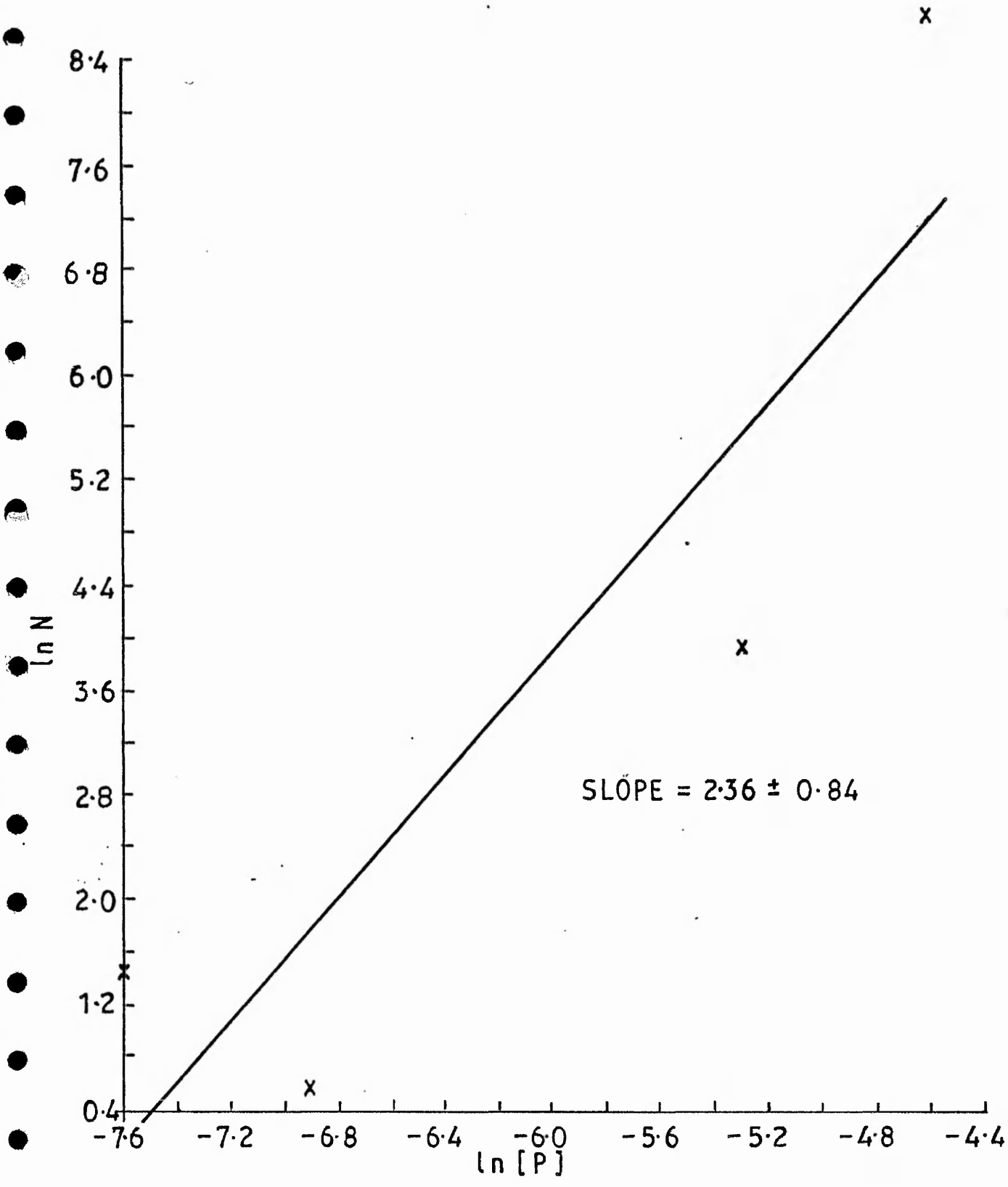

FIG III: 6 VARIATION IN PARTICLE NUMBER DENSITY WITH INITIATOR CONCENTRATION

4. Dependence of Conversion and Particle Radius on Time

Table III:8 lists a series of multi-sampled surfactant-free reactions [5,6] for which the conversion, C, and particle radius, r, had been determined as a function of time t, throughout the course of the polymerisation. For each reaction, log r, log C and log (C/t) were plotted against log t. The slopes of these plots are listed in Table III:8. The results indicate that the exponent, n, in $r^n \alpha t$ is on average 1.80 ± 0.20 while the exponent, in $C^n \alpha t$ is 0.69 ± 0.14. These results suggest that the Smith-Ewart Case 3 treatment applied to a core-shell structure, and the surface phase polymerisation treatment, which predict $r^2 \alpha t$ and $C^{2/3} \alpha t$, are reasonable theoretical treatments of the observed kinetics. The conventional Smith-Ewart Case 3 treatment, which predicts $r^{3/2} \alpha t$ and $C^{\frac{1}{2}} \alpha t$ is not in such good agreement with the experimental data. It is not surprising to find that Smith-Ewart Case 2 kinetics which predict $r^3 \alpha t$ and $R_p \alpha r^0$, are not followed, in view of the greater particle sizes and lower particle number densities which are characteristic of surfactant-free reactions. Furthermore, the Case 2 treatment predicts that the rate of polymerisation is independent of conversion, whereas, experimentally, the rate is observed to increase with increasing conversion. The Gardon treatment of Interval II, predicts C/t vs. t, plots to be linear and of constant slope at a given temperature. The slopes of the C/t vs. t plots (Table III:8) show somewhat greater variations than for the previous treatments, which casts some doubt on the suitability of the Gardon treatment. A direct application of the data to the theoretical treatments is attempted later.

5. Molecular Weight Development

Molecular weight distributions were determined by gel permeation chromatography as a function of conversion for several reactions. The data for surfactant-free emulsion polymerisation show several characteristic features, namely the occurrence of a peak at 1,000 molecular weight in early samples, and bimodal peaks which move in tandem towards higher molecular weight values as the conversion proceeds. These features are clearly apparent in the data for latex MC69 which are shown in Table III:9 and Figs. III:7 and III:8. Approximately 40 times as much lower molecular weight polymer as higher molecular weight polymer is generated. The bimodal peaks were not always so clearly resolved, but were apparent in most samples examined.

It is unlikely that the bimodal molecular weight distribution arises from chain transfer reactions, since these would be expected to cause the broadening

TABLE III:8

RELATIONSHIPS BETWEEN PARATICLE SIZE, PERCENTAGE CONVERSION AND REACTION TIME

Latex	Slopes of Log/log plots		
	r vs t	C vs t	C/t vs t
66A	2.09	0.80	-
18A	1.80	0.62	0.63
37B	1.47	0.61	0.75
64A	1.66	0.72	0.37
18B	1.87	0.59	0.72
34B	1.87	0.57	0.75
62A	1.75	0.60	-
142	1.71	0.54	0.90
016	2.18	0.80	0.90
034	1.67	0.61	0.64
018	1.75	0.76	0.30
Mean $\pm$ standard deviation	1.80 $\pm$ 0.14	0.57 $\pm$ 0.22	0.63 $\pm$ 0.20
% standard deviation	11	20	32

of a single peak, rather than the occurrance of a second peak. In particular, chain transfer to polymer, which is the only mechanism by which polymer of higher molecular weight can be generated, can be discounted. A comparison of the transfer and propagation rate constants for styrene [10] shows that transfer to polymer will only occur at low monomer concentrations. Assuming a maximum monomer concentration in the polymer particles of 5 mol dm^{-3}, i.e. the equilibrium concentration, the stage of the reaction at which the separate monomer phase disappears can be determined. For reaction MC69, this occurs between samples 9 and 10 (i.e. at ca 62% conversion, cf 55% for surfactant containing systems). Reference to Fig. III:7 shows that high molecular weight polymer is observed in sample 2, i.e. in the early stages of the reaction, when there is still a separate monomer phase and the equilibrium solubility of monomer in polymer can reasonably be expected to be attained.

The differential molecular weight curves (Fig. III:8) indicate the molecular weight distribution of polymer formed in a given conversion interval. The absence of generation of 1,000 molecular weight material after the initial sample is evidence that further nucleation followed by heterocoagulation is not an important mechanism in subsequent particle growth. This evidence cannot be regarded as conclusive, however, since the gel permeation chromatograph response is on a $n_i M_i$ basis, making it less sensitive to low molecular weight polymer. Small amounts could therefore be lost in the baseline error.

Fig. III:9 shows a plot of rate vs. molecular weight, for both molecular weight peaks, to test the hypothesis that these quantities are linearly related. In both cases, a reasonable correlation is observed.

It is tentatively suggested that the twin molecular weight peaks arise from reactions in two loci. Possible pairings include particle surface/particle bulk, particle surface/anomalous region and aqueous phase/particle bulk as possible loci in which high and low molecular weight fractions are generated. In an attempt to correlate one of these fractions with polymerisation at the particle surface, a quantity proportional to the number of free radicals per unit surface area of particles was plotted as a function of molecular weight. The parameters $(a-x)/r^2$ and $(a-x)/r$, where $(a-x)$ is the residual initiator concentration at the sampling time, calculated from the first order decomposition of potassium persulphate have been used as a measure of the number of free radicals per unit surface area of particles: r^2 is proportional to the true surface area, whereas r is used as a measure of the effective surface area since by diffusion theory [9], unit area of a large particle is less efficient at radical capture than the same area of a particle of greater curvature. The linear correlations, shown in Figs. III:10 and III:12, are, at best, reasonable. It is not possible to distinguish which of the high or low molecular weight fractions arises

TABLE III:9

MOLECULAR WEIGHT DATA FOR LATEX MC69

Sample	Time/ min	% Conv	Rate	Particle radius/nm	Particle Number density/cm^{-3}	Integral mol. wt. $M1/10^4$	$M_2 10^6$	Differential mol. wt. $M_1/10^4$	$M_2/10^6$	$\frac{a-x}{r^2}$	$\frac{a-x}{r}$
1	100	8.40	4.13	120	10.0	1.6	0.7	1.6	0.7	2.96	3.55
2	130	11.50	5.90	141	8.5	1.8	0.6	1.8	0.6	2.04	2.88
3	160	16.40	6.45	158	8.5	2.4	0.9	3.2	1.0	1.55	2.45
4	190	23.50	8.20	175	9.0	2.8	1.3	4.0	1.3	1.20	2.10
5	220	29.10	9.46	189	8.8	3.1	1.0	4.5	1.1	0.98	1.86
6	250	36.10	10.92	209	8.2	3.4	1.5	5.6	1.8	0.77	1.60
7	280	36.30	10.96	222	6.8	5.0	1.4	8.0	1.8	0.65	1.43
8	310	48.10	13.22	240	7.2	4.9	2.0	7.7	3.4	0.53	1.26
9	340	58.80	15.12	252	8.0	5.8	1.2	7.2	1.0	0.46	1.15
10	370	82.60	18.97	267	9.0	6.0	2.4	8.9	3.3	0.39	1.03

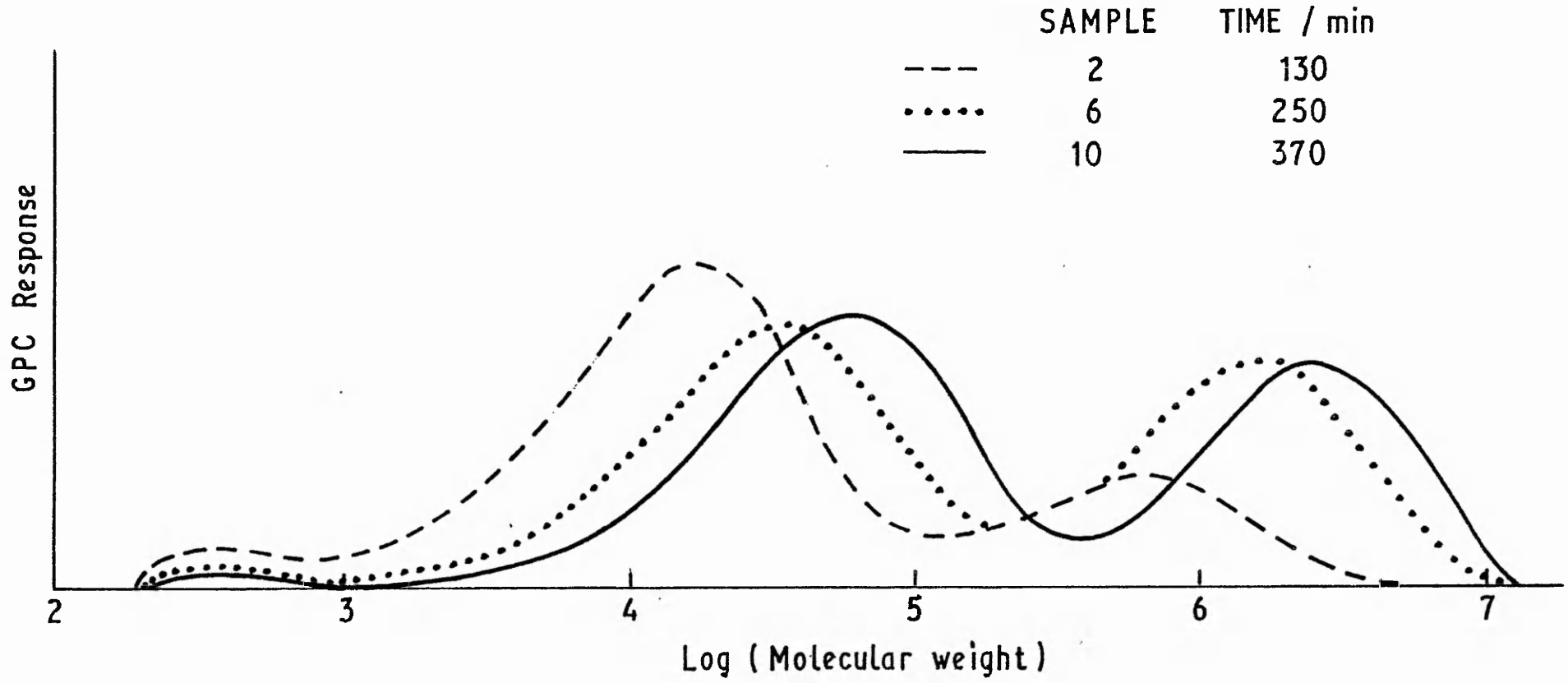

FIG III·7 INTEGRAL GPC CURVES FOR REACTION MC 69

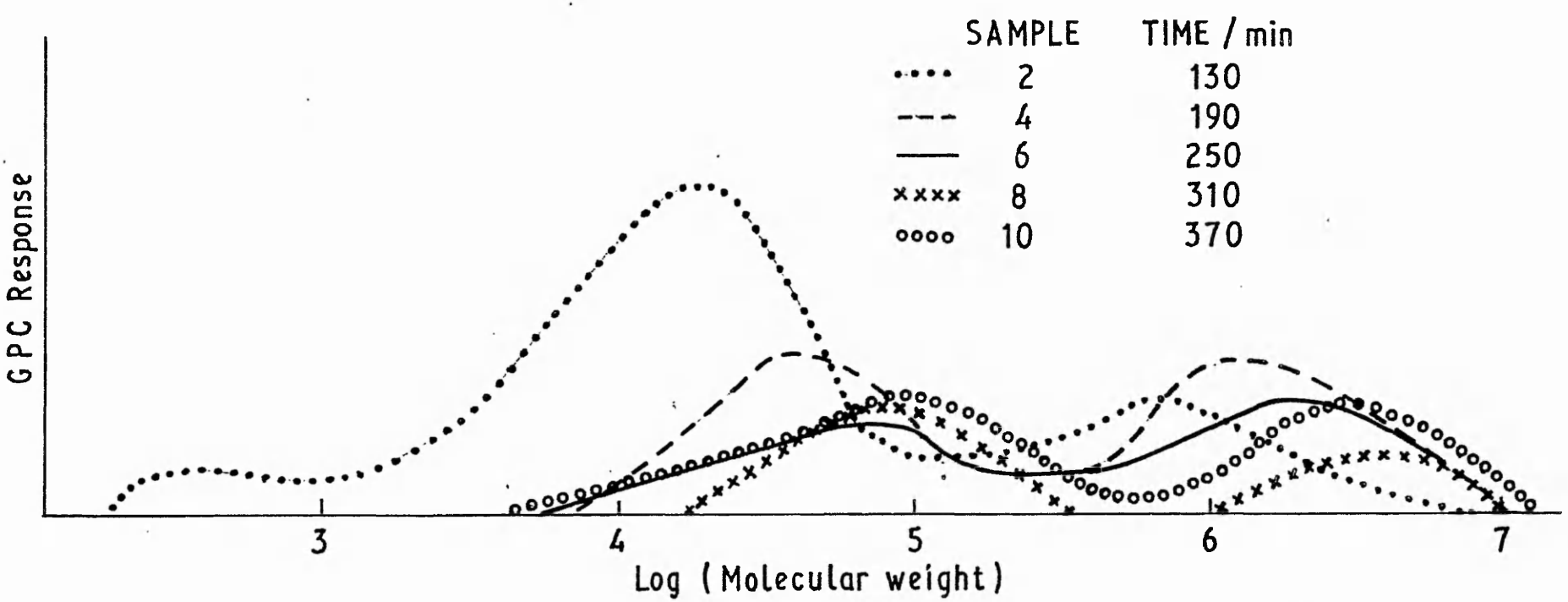

FIG Ⅲ: 8 DIFFERENTIAL GPC CURVES FOR REACTION MC 69

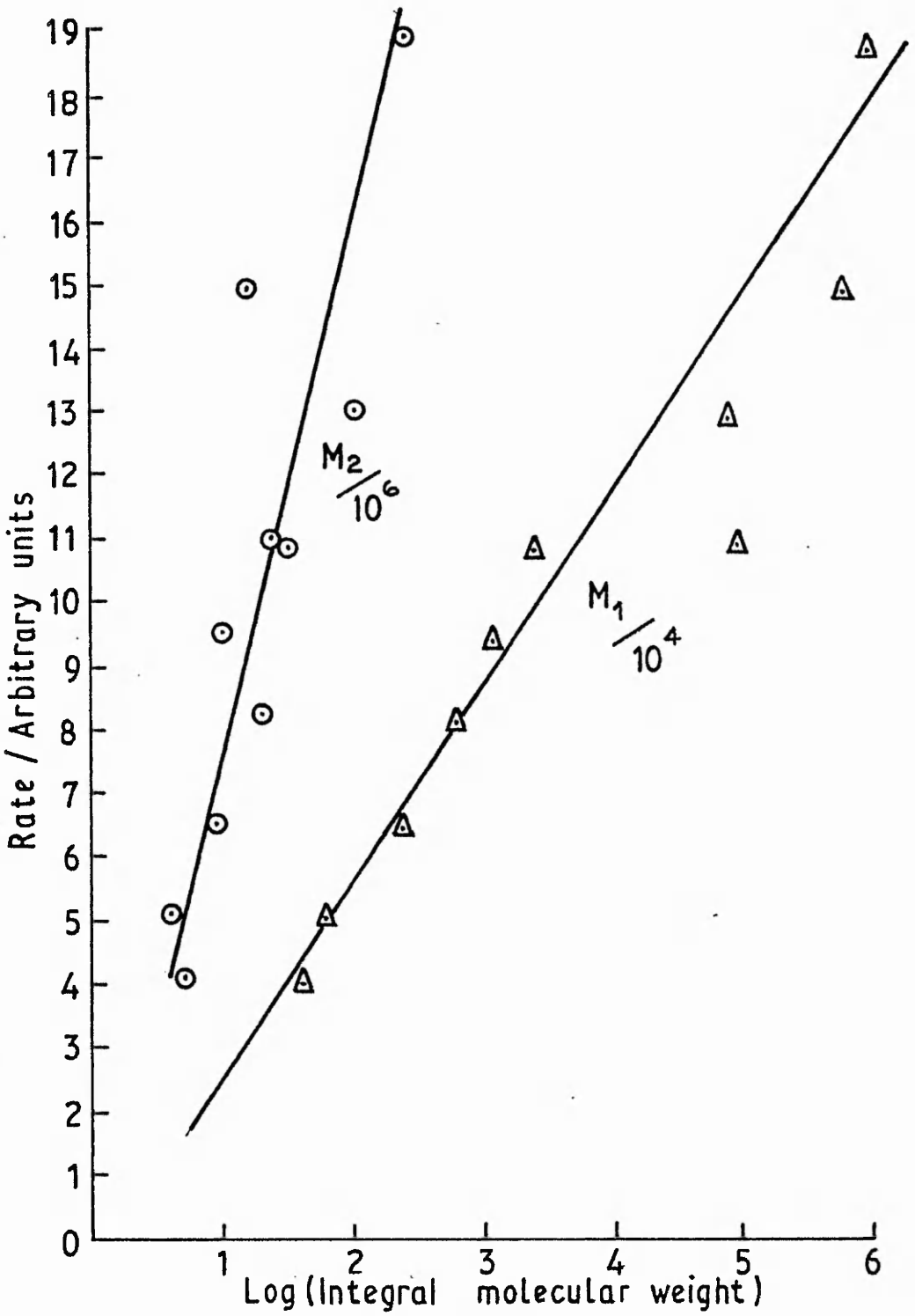

FIG III:9 PLOT OF RATE vs M_1 (LOWER MOLECULAR WEIGHT PEAK) and M_2 (HIGHER MOLECULAR WEIGHT PEAK)

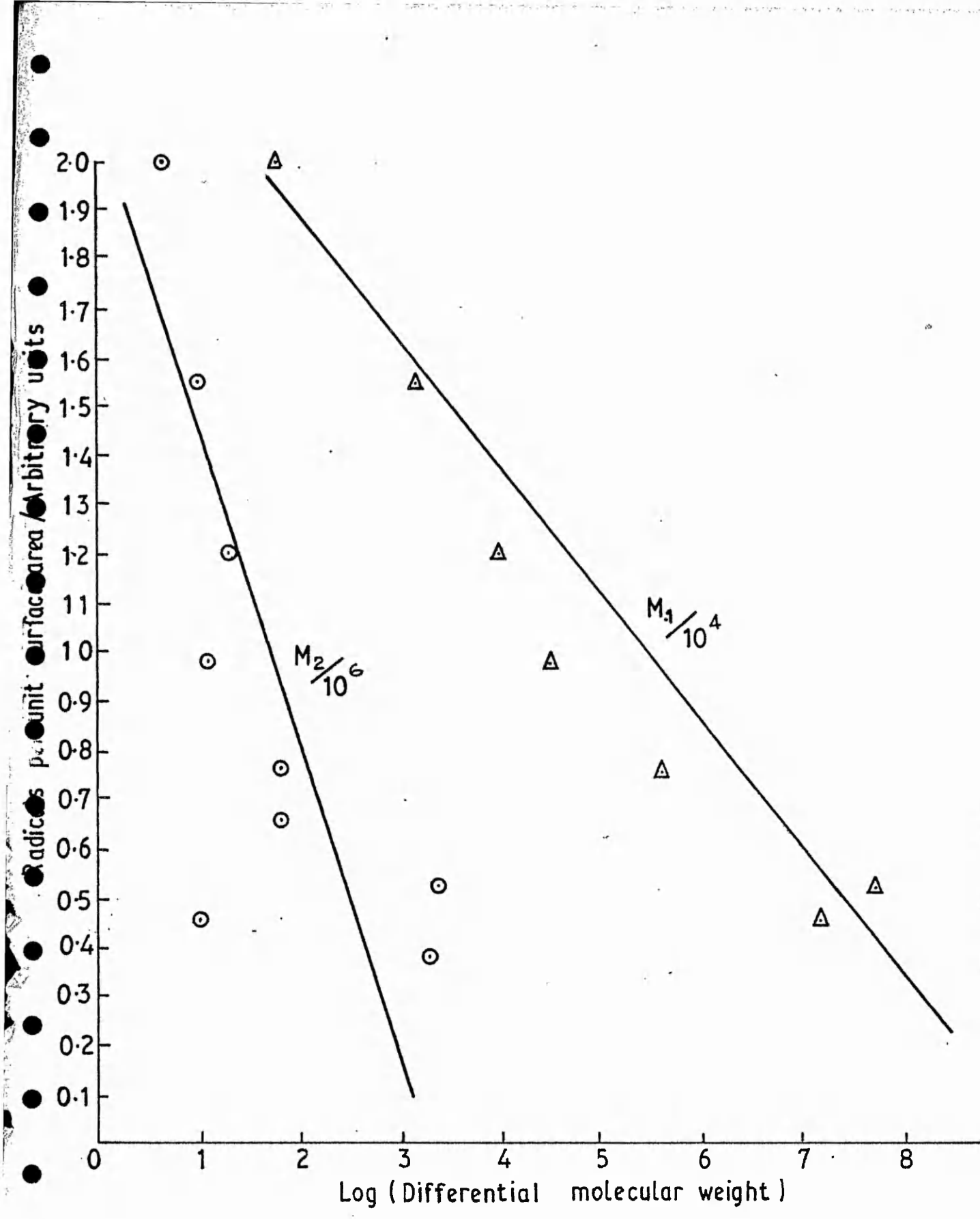

FIG III:10 PLOT OF NUMBER OF RADICALS PER UNIT SURFACE AREAS vs DIFFERENTIAL MOLECULAR WEIGHT

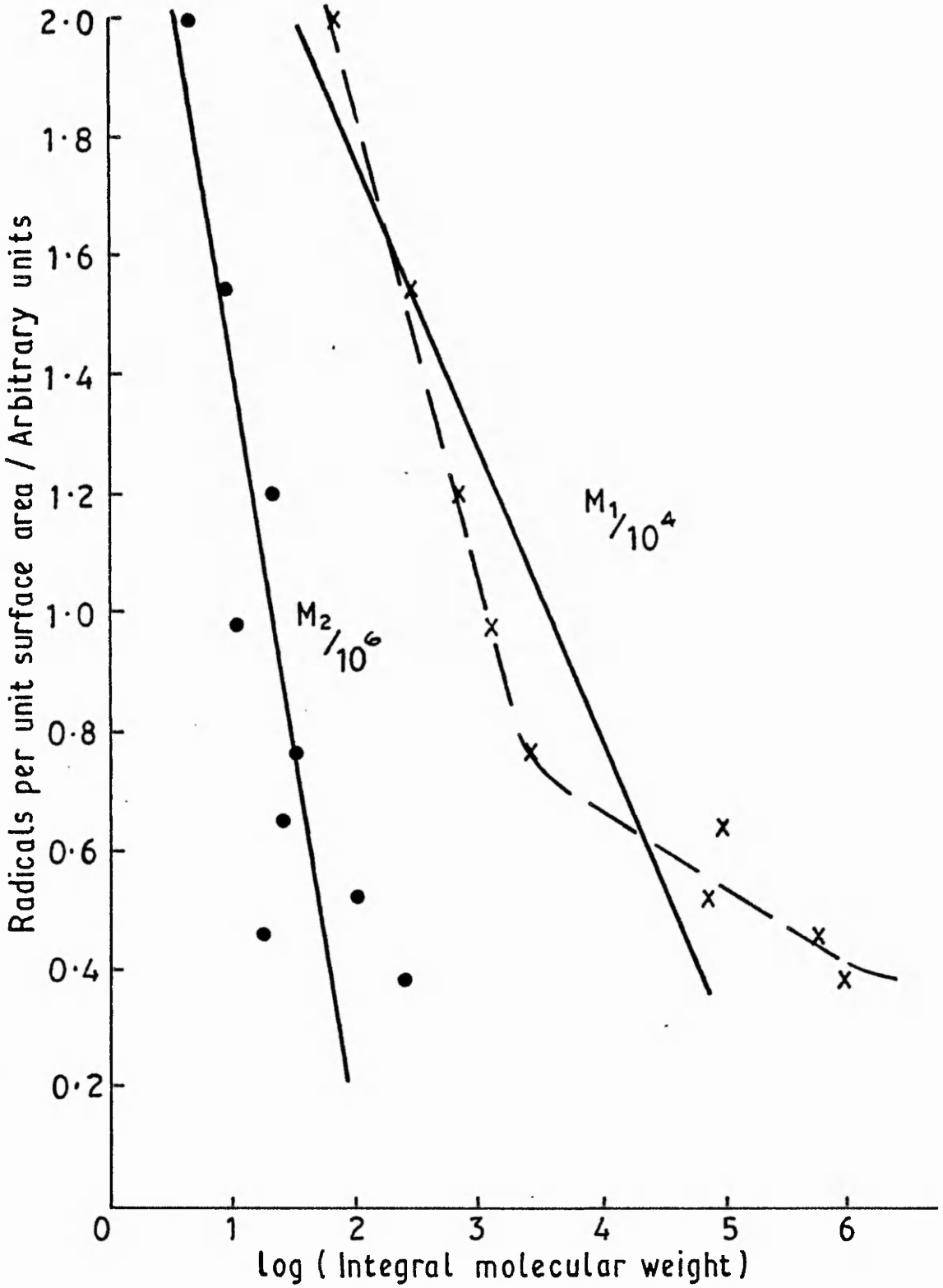

FIG III: 11 PLOT OF NUMBER OF RADICALS PER UNIT SURFAC
AREAS vs INTEGRAL MOLECULAR WEIGHT

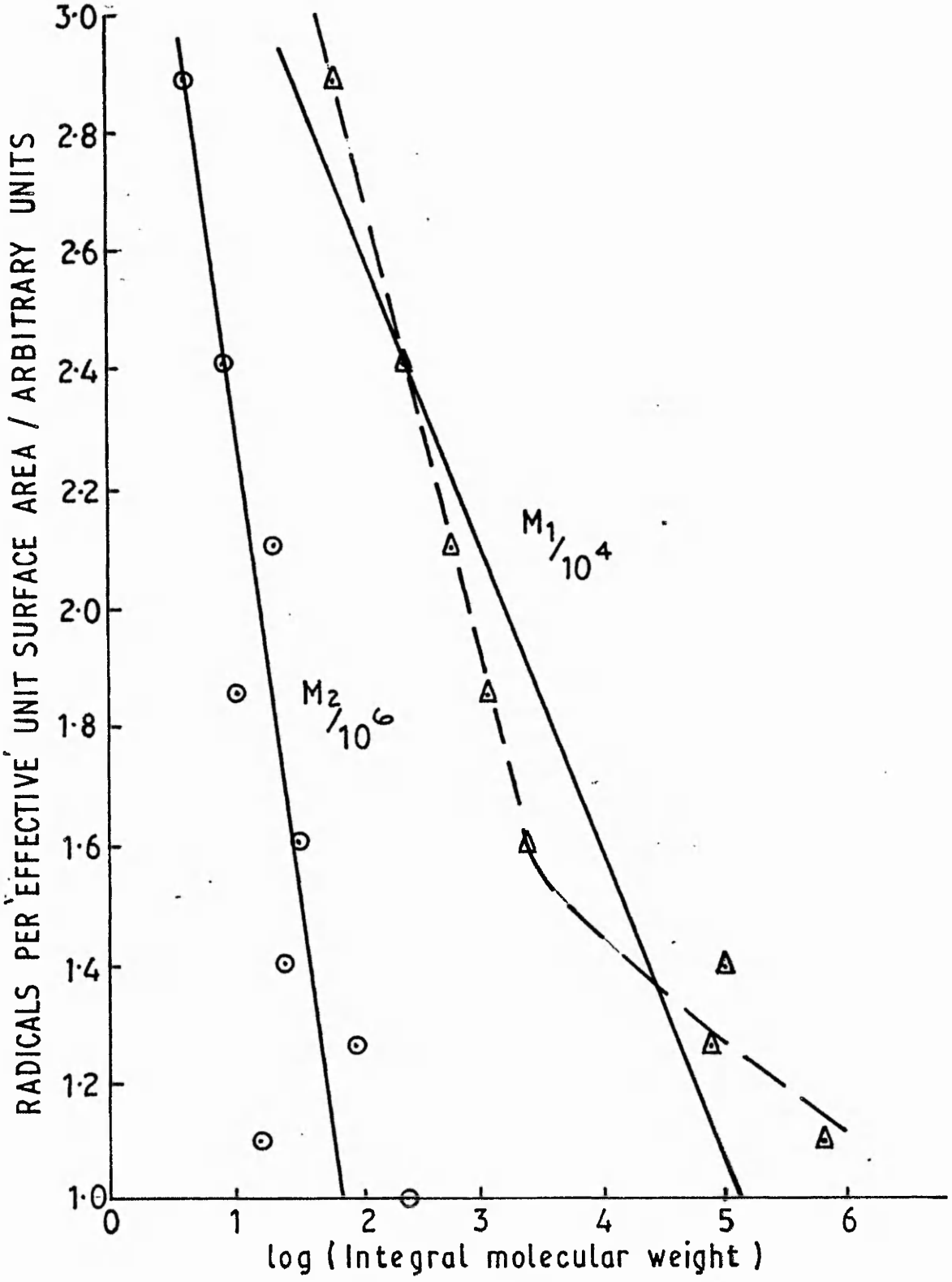

FIG III:12 PLOT OF NUMBER OF RADICALS PER 'EFFECTIVE' UNIT SURFACE AREA vs INTEGRAL MOLECULAR WEIGHT

from reaction at the particle surface.

Although it has not been possible to distinguish between the combinations of reaction loci listed in the previous paragraph, the following observations can be made. The rate of reaction for latex MC69 at low conversions (when the high molecular weight peak is insignificant) of $1.5.10^{-3}$ mol dm^{-3} s^{-1} is too high (by a factor of ca. 10^3) to be explained by polymerisation in the aqueous phase, given published values [10] of the propagation rate constant, the rate of initiator decomposition and the equilibrium monomer concentration in the aqueous phase. Whilst no anomalous regions were observed in the particles of latex MC69, it would be premature to exclude that possibility, since the factors which lead to observable anomalies at lower temperatures may still be present, but to a less observable extent. It has been suggested that the anomalous region, having low molecular weight associated with it absorbs monomer preferentially: the locally high surface charge density in the region protects it from radical entry [11]. Thus different molecular weights, arising from polymerisation in the anomalous region and the particle bulk, may be anticipated.

6. Application of Experimental Data to Quantitative Theories of Emulsion Polymerisation Kinetics

The direct application of the experimental data to the various quantitative theories is difficult, since there is considerable uncertainty concerning the correct values of the necessary parameters. However, in order to compare theory and experiment, these parameters were estimated as follows:

(i) The monomer concentration in the polymer particles, $[M]_p$ was taken to be the equilibrium solubility of styrene in polystyrene, i.e. 5 mol dm^{-3}. This is equivalent to a monomer volume fraction, ϕ_m (the parameter required by the Garden treatment) of 0.58. This choice implies that the polymerisation of styrene is not controlled by the diffusion of monomer to the active sites.

(ii) The propagation rate constant, k_p, for styrene at 343K was evaluated from the data presented in the Polymer Handbook [10]. The data were plotted as log k_p against reciprocal absolute temperature, and the value of k_p at the required temperature calculated from the slope of the least squares straight line. A value of 462 dm^3 mol^{-1} s^{-1} was obtained.

(iii) The termination rate constant, k_t, is known to vary with conversion in bulk polymerisations, as the increasing viscosity of the medium makes encounters between free radicals less frequent. Hui and Hamielec [12] have derived an expression relating k_t and fractional conversion. This expression was adapted to calculate the value of k_t for a given monomer concentration in the polymer particles in emulsion polymerisation by replacing the fractional conversion with $(1 - \phi_m)$, where ϕ_m is the volume fraction of monomer in the particles. The resulting expression is

$$k_t = k_{to} \exp - 2 (B (1 - \phi_m) = C (1 - \phi_m)^2 = D (1 - \phi_m)^3) \qquad \text{(III.6)}$$

where $k_{to} = 1.492.10^7$

$B = 2.57 - 5.05.10^{-3} T$

$C = 9.56 - 1.76.10^{-2} T$

$D = 3.03 + 7.85.10^{-3} T.$

For T = 343K and $\phi_m = 0.58$, this expression gives a value of k_t of 2.2 10^6 dm^3 mol^{-1} s^{-1}. Subsequent calculations require k_t to be in molecular units, i.e. k_t/N_A.

(iv) The rate of radi cal absorption, ρ_A, was assumed equal to the rate of radical production, and is therefore almost certainly an over-estimate. The rate of radical production is given by

$$\rho_A = 2k_d \exp (-k_d t + \ln P). N_A \qquad \text{(III:7)}$$

where k_d is the initiator decomposition rate constant, which for potassium persulphate at 343 K under acid conditions has the value $2.68.10^{-5}$ s^{-1}, and P is the initial concentration of initiator, which, for reaction MC69, was 5.10^{-3} mol dm^{-3}.

(v) The thickness of the shell, L, required for the core-shell treatment was taken as 2.5 nm after Wessling and Gibbs (13).

Substitution of these parameters into the appropriate equations gives the values of reaction rate and number average molecular weight predicted by the Smith-Ewart Case 3, Smith-Ewart Case 3 core-shell/Wessling surface Phase and Gardon treatments. These predictions are compared with the experimental values of rate and molecular weight in Tables

III:10 and III:11 respectively. The rates predicted by the Smith-Ewart Case 3 treatment are higher than those observed at the beginning of the reaction, but the agreement between theory and experiment improves with increasing conversion. Conversely, the Smith-Ewart Case 3 core-shell/Wessling Surface Phase treatments predict a rate which agrees with the observed rate at the beginning of the reaction but which becomes too low at the end. The Gardon treatment predicts rates which are much lower than those observed experimentally.

TABLE III:10

Comparison Between Reaction Rates Predicted by Quantitative Theories and Experimental Data from Reaction MC69

		Calculated		
Sample	Exp	Smith-Ewart	Core Shell	Gardon
MC69/1	1.4	4.5	1.1	0.068
MC69/2	2.0	5.2	1.2	0.077
MC69/3	2.1	6.0	1.3	0.088
MC69/4	2.3	7.0	1.5	0.098
MC69/5	2.8	7.6	1.5	0.11
MC69/6	3.3	8.3	1.6	0.11
MC69/7	3.9	8.1	1.5	0.12
MC69/8	5.0	9.1	1.6	0.12
MC69/9	7.3	9.9	1.7	0.13
MC69/10	27.7	11.4	1.9	0.14

The molecular weights predicted by the Smith-Ewart Case 3 and Smith-Ewart Case 3 Core-Shell/Wessling Surface Phase treatments decrease with increasing conversion, which is the opposite of the trend actually observed. These treatments are not therefore capable of explaining the molecular weight development in surfactant free reactions. The molecular weights predicted by the Gardon treatment increase with increasing conversion, and are in reasonable agreement with the lower of the two molecular weight peaks observed experimentally.

TABLE III:11

Comparison between Molecular Weights Predicted by Quantitative Theories and Experimental Data from Reaction MC69

Sample	$M_1.10^4$	$M_2.10^2$	$\bar{M}_n$ Calculated Smith-Ewart 3.10^6	Core Shell.10^6	Gardon.10^4
MC69/1	1.6	0.7	5.5	22	0.63
MC69/2	1.8	0.6	4.8	21	0.74
MC69/3	2.4	0.9	4.1	19	0.89
MC69/4	2.8	1.3	3.5	17	1.0
MC69/5	3.1	1.0	3.2	16	1.2
MC69/6	3.4	1.5	3.0	16	1.3
MC69/7	5.0	1.4	3.0	17	1.4
MC69/8	4.9	2.0	2.7	15	1.6
MC69/9	5.8	1.2	2.5	15	1.7
MC69/10	6.0	2.4	2.1	13	1.9

A further parameter of importance in emulsion polymerisation kinetics is the average number of free radicals per particle, $\bar{n}$. An expression for this parameter was derived by Stockmayer [14] in an extension of the original Smith-Ewart theory.

$$\bar{n} = (a/4)\, I_o(a)/I_1(a) \qquad \text{(III:8)}$$

where I_o and I_1 are modified Bessel functions of the first kind of order zero and one respectively. a is defined by

$$a^2 = 8\,\alpha \qquad \text{(III:9)}$$

and α by

$$\alpha = \rho_A V_p / N k_t \qquad \text{(III:10)}$$

where V_p is the total volume of polymer and N the particle number density. A simple approximation has been devised by Ugelstad and Mork [15]

$$\bar{n} = (\tfrac{1}{4} + \alpha/2)^{\frac{1}{2}} \qquad \text{(III:11)}$$

and this is claimed to agree to within 4% with the rigorous Stockmayer expression. The Gardon treatment also includes an expression for $\bar{n}$

$$\bar{n} = \tfrac{1}{2}\left[1 + (4A/B^2)\ P_v\right]^{\frac{1}{2}} \qquad \text{(III:12)}$$

where A, B and P_v are as defined in Chapter I. The values of $\bar{n}$ predicted by these expressions are listed in Table III:12, together with experimental values derived from Eq. I:2 using measured values of R_p. The values of $\bar{n}$ obtained from the Stockmayer expression are only available for the early stages of the reaction, since the NAG subroutines used to compute the value of the Bessel functions suffer numerical instability at high values of a. However, where comparison is possible, it can be seen that the values obtained from the Ugelstad approximation are in good agreement with those obtained from the Stockmayer expression. Gardon's treatment gives values which are consistently smaller, by a factor of about four, than the Stockmayer expression. The experimental data are intermediate between the values predicted by the Stockmayer and Ugelstad equations and the Gardon treatment, the agreement being best with the latter at low conversions and the former at high conversions. The unexpectedly high experimental value obtained for the final sample is probably in error, since at this stage of the reaction, the separate monomer phase has disappeared and the monomer concentration in the particles will be lower than the equilibrium solubility used in the calculation.

TABLE III:12

Comparison Between Values of $\bar{n}$ Calculated from Equations of Stockmayer, Ugelstad and Gardon

Sample	Exp	Stockmayer	$\bar{n}$ Ugelstad	Gardon
MC69/1	3.7	11.9	11.8	3.1
MC69/2	6.0	16.1	16.0	4.3
MC69/3	6.5	18.5	18.3	4.9
MC69/4	6.7	20.4	20.3	5.2
MC69/5	8.1	22.7	22.4	5.8
MC69/6	10.6		26.6	6.7
MC69/7	14.7		31.1	8.4
MC69/8	18.2		33.3	8.5
MC69/9	25.1		34.0	8.4
MC69/10	80.8		33.3	7.4

7. Conclusions

Very reproducible data have been obtained for the kinetics of the surfactant-free emulsion polymerisation of styrene. The data have been tested in the region of constant particle number density (Interval II) against theories developed for surfactant-present systems. The dependence of particle radius and conversion on time is best described by treatments based on a surface polymerisation model. However, these treatments predict that the molecular weight should fall with increasing conversion, which is the opposite of the trend actually observed. None of the theoretical treatments predict a bimodal molecular weight distribution.

The quantitative comparison of experimental data with theory is equivocal. The Smith-Ewart Case 3 treatments predict reaction rates which are of the right order of magnitude and molecular weights which are greater than the higher of the two peaks observed experimentally. Furthermore, the theories

predict that the molecular weight should decrease with increasing conversion, whereas both molecular weight peaks are found to increase with increasing conversion. The Gardon treatment predicts molecular weights which are slightly smaller than the lower of the two peaks, and which increase with increasing conversion. However, the predicted reaction rates are much smaller than the experimentally determined rates. The agreement between the values of $\bar{n}$ predicted by the Smith-Ewart Case 3 and Gardon treatments is poor, although the values calculated from the experimental data are intermediate between the two.

The principal reason for the poor agreement between the predictions of the various theoretical treatments and experimental data is the inability of any theory to take account of polymerisation in more than one locus. A contributory factor is the large measure of uncertainty in the values of the necessary parameters which is likely to vitiate further attempts at a fully quantitative understanding of emulsion polymerisation kinetics.

C. PREPARATION OF CORE-SHELL LATICES

1. Results of coating reactions

Both seeded and shot growth methods were used to overcoat polystyrene core particles with poly(methyl acrylate), poly(ethyl acrylate), poly(n-butyl acrylate), poly(methyl methacrylate), poly(ethyl methacrylate) and poly (n-butyl methacrylate). Typical results are summarised in Tables III:13 and III:14. It was possible to prepare monodisperse core-shell latices reproducibly by both methods with any of the above mentioned coating polymers under suitable conditions.

The most common departure from monodispersity was due to the occurrence of small (60 - 150 nm diameter) secondary growth particles, giving the final product a bimodal size distribution. These secondary growth particles were formed when the number density of core particles at the beginning of the coating reaction was below a critical value. For poly (methyl methacrylate) as the coating polymer the critical number densities were approximately 1.10^{12} and 1.10^{11} cm^{-3} for seeded and shot growth methods respectively. Although the critical number density was difficult to measure accurately with the experimental techniques available, it was found to be lower for the shot growth technique for all the coating monomers examined.

Another advantage of the shot growth technique was that the resultant particles were always spherical in shape, whereas the seed grown particles were often rather irregular in shape (compare Plates III:1 and III:2).

TABLE III:13

RESULTS OF SEEDED GROWTH REACTIONS

LATEX	MC4	MC9	MC31	MC11
Seed latex	MC1	MC1	MC26	MC8
Size/nm	480	480	440	440
σ/nm	7.0	7.0	8.3	6.6
Solids content / %	8.0	8.0	6.9	2.7
Volume/cm^3	50	250	425	500
Particle No Density/cm^{-3}	$1.3.10^{11}$	$6.5.10^{11}$	$1.4.10^{12}$	$5.3.10^{11}$
MONOMER	MMA	MMA	MMA	EA
Volume/cm^3	16	11	50	15
Initiator/g	0.16	0.25	0.25	0.25
Water/cm^3	450	250	50	50
Temp/K	353	353	353	353
Total Polymerization Time/Min	180	180	1385	180
PRODUCT				
Particle size/nm	530, 140	500, 65	470	440-450, 10
σ/nm	5.7, 6.3	7.2, 4.1	3.6	-
	Bimodal	Bimodal	Monodisperse	Polydisperse
Solids content / %	3.6	5.6	9.6	7.2
Conversion / %	94	77	25*	92

*Latex had coagulated during reaction.

σ's for large and small particles of bimodal size distribution reported separately.

TABLE III:14

RESULTS OF SHOT GROWTH REACTIONS

Latex	MC19	MC10	MC64	MC78	MC107	MC5	MC45	MC133	MC142
Reaction conditions									
Initiator/g	0.5	0.5	0.5	0.5	0.5	0.5	0.12 + 0.95	0.5	0.5
Temperature/K	353	353	353	353	353	353	353	353	353
Core latex	PS	PS	PS	PS	PS	PS	PS	PS	PS
Diameter/nm	370	460	414	417	418	400	410	425	420
σ/nm	6.1	6.2	10.3	6.8	4.2	7.0	4.3	6.8	6.7
Solids Content/%	4.92	6.74	7.38	6.76	5.61	5.0	0.69	7.57	7.7
10^{12} particle number Density/cm^{-3}	1.9	1.3	1.9	1.7	-	1.7	0.17	-	2.0
Monomer	MA	EA	EA	BA	BA	MMA	MMA	EMA	BMA
Volume/cm^3	14	16	10*	20	40	12	12	20	20
Polymerisation									
Time/min	290	295	315	340	805	250	250	810	180
Product Diameter/nm	530	480-510	471	526	540	490	540	538	562
σ/nm	3.6	3-10	15.4	21.4	8.8	7.7	6.8	8.6	7.4
Solids Content/%	11.34	12.0	11.4	13.7	12.4	11.4	2.7	11.0	15.2
Conversion/%	92	95	117	117	82	55	24		106
10^{12} Particle number Density/cm^{-3}	1.5	-	2.0	1.7	-	1.9	0.31	-	1.8

*Monomer added at constant rate of 0.2 cm^3 min^{-1}

TABLE III:14 (Cont'd)

RESULTS OF SHOT GROWTH REACTIONS

Latex	MC62	MC63	MC71	MC92	MC103	MC104	MC65	MC148
Reaction conditions								
Initiator/g	0.5	0.5	0.5	0.5	0.5	0.5	0.5	0.5
Temperature/K	353	353	353	353	353	353	353	353
Core latex	PS	PS	PS	PS	PS	PS	PS	PBMA
Diameter/nm	463	436	436	238	380	500	446	
σ/nm	10.4	9.6	8.3	19.9	6.2	8.4	14.7	
Solids Content/%	7.51	7.29	8.4	1.6	5.19		8.4	8.68
10^{12} particle number Density/cm^{-3}								
Monomer	BMA	BMA	BMA	BMA	BMA	BMA	EA/MMA	EA
Volume/cm^3	25	30	40	10	60	80	30*	33
Polymerisation								
Time/min	445	520	795	230	220	355	270	295
Product Diameter/nm	525	515	512	333	590	860	497	
σ/nm	8.6	9.2	22.0	68.1	14.4	11.3	14.7	
Solids Content/%	13.1	12.0	14.9	14.7	5.16	17.6	15.8	13.5
Conversion/%	96.8	95.1	88.1	85.9	80.0	60.9	91.3	96.7
10^{12} Particle number Density/cm^{-3}	-	-	1.8	2.5	-	-	2.0	-

*Monomer added at constant rate of 0.2 cm^3 min^{-1}

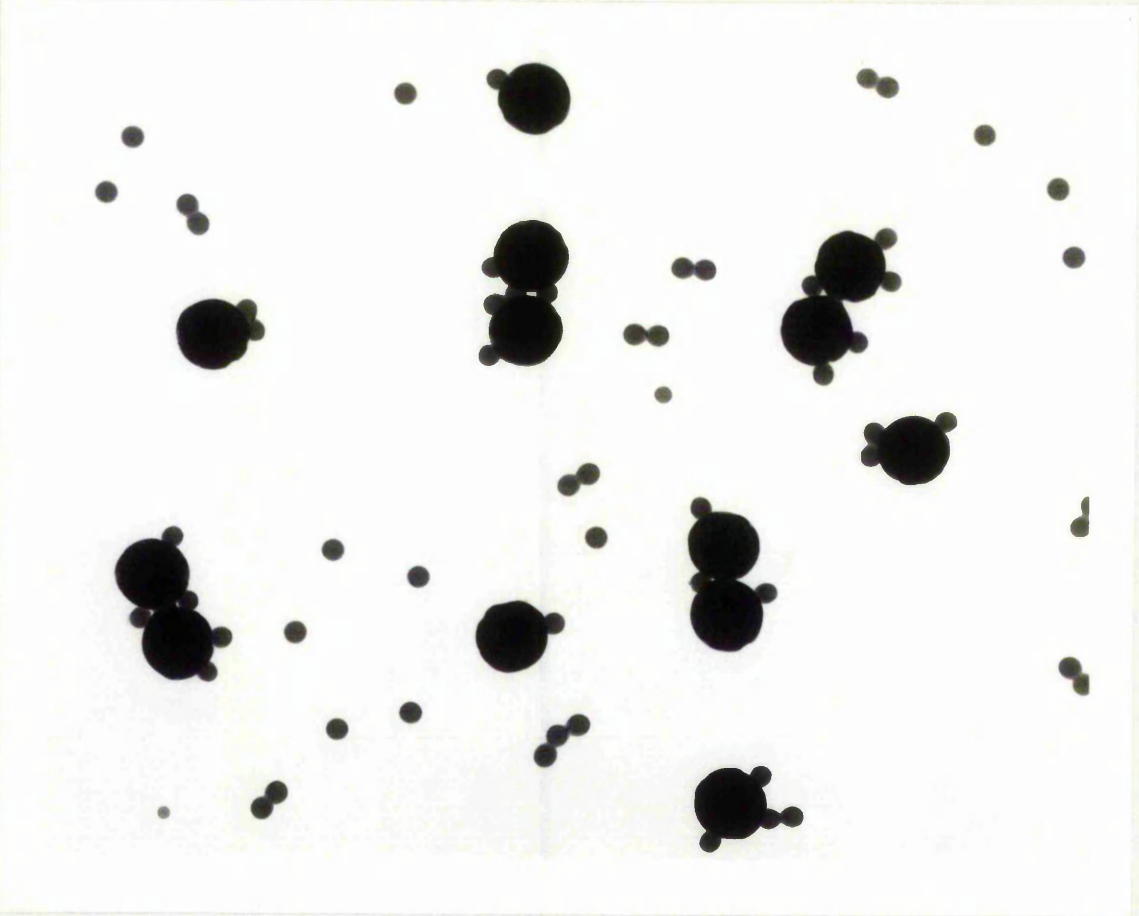

Plate III:1

TEM of latex MC4 (poly(methyl methacrylate) coated polystyrene, prepared by seeded growth technique). Magn. 19,100.

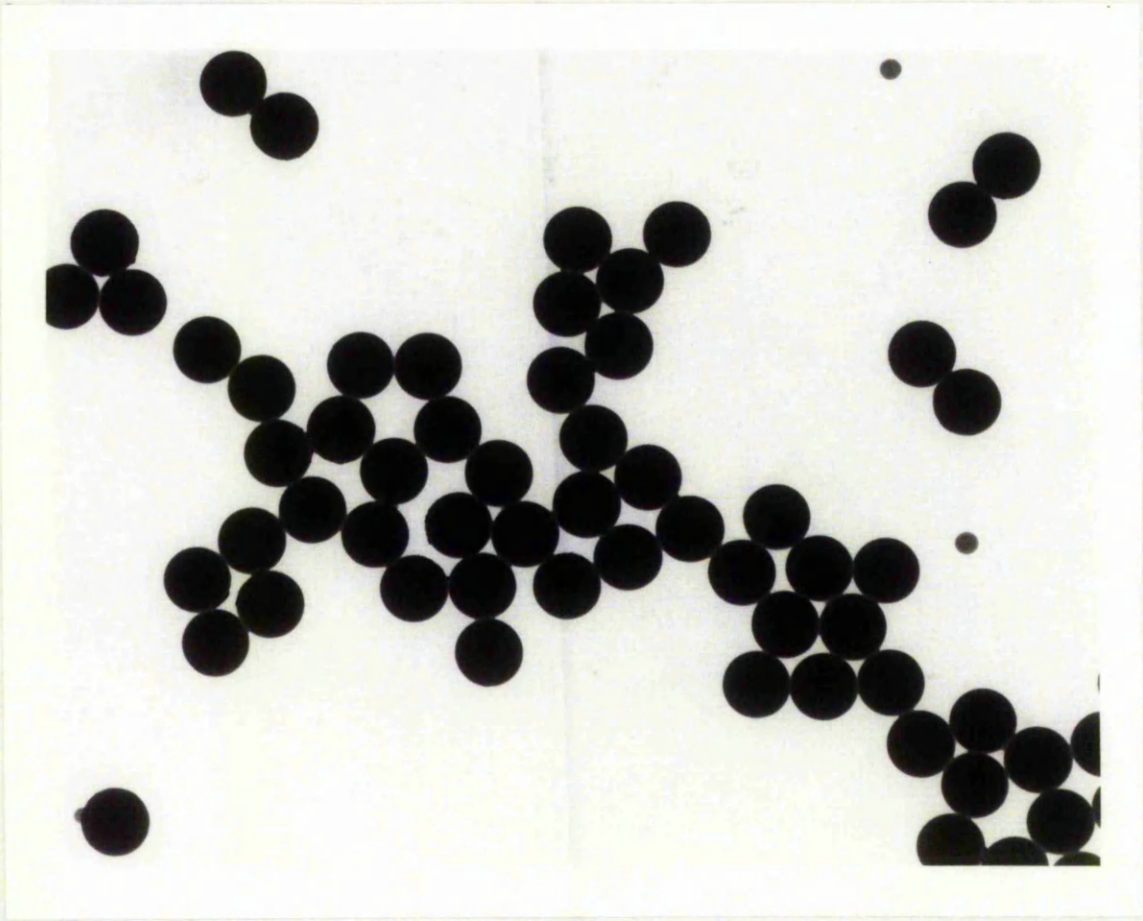

Plate: III:2

TEM of latex MC5 (poly(methyl methacrylate) coated polystyrene, prepared by shot growth technique) Magn. 19,100.

With poly(ethyl acrylate) as the coating polymer, both methods gave a polydisperse product, i.e. one in which there was a variable coating thickness as well as the formation of secondary growth particles. These secondary growth particles were much smaller (usually ca. 10 nm diameter) and more numerous than those formed by other coating polymers (compare Plates III:1 and III:2) although in terms of mass the amounts were similar. Monodisperse poly(ethyl acrylate) coated polystyrene latices were prepared by adding the ethyl acrylate monomer continuously at a rate less than its rate of polymerisation (following the method given for coating with a copolymer).

Secondary growth particles, where obtained in the final product were immediately apparent by their small size (Plate III:3). In the absence of secondary growth, it was possible to prove, by a mass balance calculation, that all the monomer added could be accounted for, within experimental error, by the increase in size of the particles (see Table III:14). By performing this calculation in reverse, it was possible to calculate the amount of monomer required to produce a given coat thickness, and thus to 'tailor-make' core-shell latices.

2. Role of swelling

Although outwardly similar to the seeded growth method, it is apparent from the above results that the shot growth technique operates via a somewhat different mechanism to the heterocoagulation mechanism believed to operate in seeded growth reactions by Chung-Li et al. [16]. The principal difference between the two methods is, of course, the presence or residual monomer in the core particles at the stage at which the coating monomer is added. This residual monomer has been shown to have a profound effect on the rate of swelling (Table III:12).

Different aspects of swelling have been studied by Morton et al. [17], Chung-Li et al. [16], Ugelstad et al. [18] and Goodwin et al. [19]. However, the systems studied varied widely and no clear picture emerges. Morton et al. derived an equation showing that equilibrium uptake varied with particle size. They confirmed the validity of their treatment with swelling experiments on polystyrene latices with a range of particle size 37-173 nm and molecular weights 10^5 - 10^7. They also showed that the equilibrium uptake of toluene was rapid, being attained within 30 min. Ugelstad et al. working with low molecular weight oligomer were able to achieve large uptakes very rapidly. Chung-Li et al. found that the swelling of large particles (greater than 2 μm) took place very slowly (Table III-15), even when the polymer was freshly formed, and contained

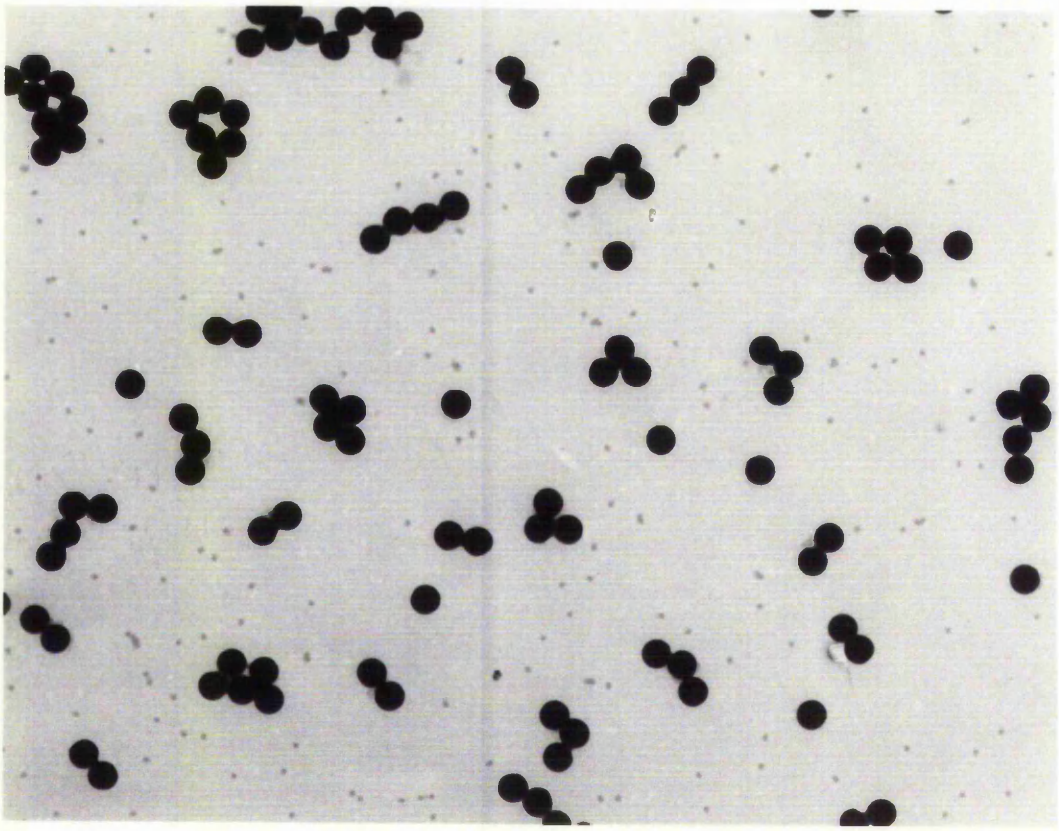

Plate III:3

TEM of latex MC10 (poly(ethyl acrylate) coated polystyrene, prepared by shot growth method) Magn. 9,100.

TABLE III:15

RATES OF SWELLING AND GROWTH
A. STYRENE/POLYSTYRENE

Latex	MC88	MC85	ARG62A	Chung-Li et al. Flask B [16]	Goodwin et al. Steam-stripped [19]
Monomer Content/%	6.6	0	Growth	Not stated	0*
Initial Size/nm	160	572	222	2890	425
Final Size/nm	182	588	290	2930	512
Time/min	10	10	28	60	10
Temperature/K	353	353	353	333	298
10^3 Rate/ $cm^3\ min^{-1}\ cm^{-3}$	47.2	8.63	43.9	0.70	74.8

*assumed, since latex steam-streipped

B. BUTYL METHACRYLATE/POLYSTYRENE

Latex	MC89	MC92
Monomer content/%	6.6	growth
Initial Size/nm	160	259
Final Size/nm	173	282
Time/min	10	10
Temperature/K	353	353
10^3 Rate/ $cm^3\ min^{-1}\ cm^{-3}$	26.4	29.1

residual monomer. Goodwin et al. have recently studied the rate of swelling as a function of the cleaning technique. They found that swelling occurred quite rapidly, irrespective of cleaning technique (dialysis, ion exchange and steam-stripping). Unfortunately, they do not report the monomer contents of the latices prior to swelling, since, for a given particle size, the rate of swelling will vary with monomer content. The rate of swelling of polystyrene by styrene, as determined by photon correlation spectroscopy was greater in the presence of residual monomer (6.6%) than in its absence (Table III-15), as might be expected. However, both results were lower than the rate obtained by Goodwin et al. for a steam-stripped latex, which should contain no monomer. A lower result was observed for the swelling of polystyrene containing residual monomer with n-butyl methacrylate and this is presumbably due to the greater incompatibility of the more polar monomer.

It can be seen from Table III:15 that the rates of swelling and growth are comparable for both styrene in polystyrene and n-butyl methacrylate in polystyrene. Hence, in neither case is there any need to postulate a heterocoagulation mechanism for the shot growth process.

The heterocoagulation mechanism cannot be disproved by transmission electron microscopy or photon correlation spectroscopy since neither technique would be capable of detecting unambiguosly the presence of secondary nuclei prior to heterocoagulation with the core particles. In the former case their size would be below the limit of resolution of the instrument, and in the latter their contribution to the light scattering would be swamped by that of the larger particles. In principle, it should be possible, by assuming a constant particle number density throughout the coating reaction, to deduce the presence or absence of secondary nuclei by calculating whether the increasing solids contents during the reaction could be accounted for by the increasing particle size. Unfortunately, the errors inherent in the size measurement render this test insufficiently sensitive.

3. Mechanism of shot growth reaction

There is considerable experimental evidence to support the idea that conventional emulsion polymerisations is essentially a surface phenomenon [4,20,21]. In seeded growth reactions, it is known that the seed particle number density is a critical parameter (at constant temperature and monomer, initiator and electrolyte concentrations) in determining whether or not secondary growth particles occur [9]. The number density must be high enough to provide a sufficient surface area of hydrophobic interface on which all the freshly formed

polymer can deposit.

The mechanism of the shot growth reaction involving acrylate monomers can be stated in similar terms. The solubilities in water and the rates of polymerisation of these monomers are greater than those of styrene. This combination of properties will promote the formation of oligomeric ion radicals. These would normally be expected to nucleate according to one of the mechanisms discussed in Chapter I, resulting in secondary growth particles, unless the radicals are first captured by the core particles. For similar core particle sizes, and under similar reaction conditions, it was found that the critical number density of core particles, below which secondary growth particles were formed, was lower for the shot growth reaction than the seeded growth reaction. This is presumably due to a higher capture efficiency of the core particles in the shot growth reaction. It is proposed that this high capture efficiency is due to the coating monomer actively polymerising at the particle/water interface, becoming covalently bound to the core particle polymer matrix and unable to transfer back out of the particle.

It is likely that the critical number density of core particles necessary to avoid the formation of secondary growth particles will be influenced by the characteristics of the coating monomer. The higher the water solubility and/or polymerisation rate of the monomer, the more rapidly oligomeric ion radicals will be formed, and the greater will be the number of core particles necessary to capture them before secondary nucleation occurs. The failure of the shot growth process to produce a monodisperse poly (ethyl acrylate) coated polystyrene latex (without recourse to monomer starved conditions) is probably due to the rapid polymerisation rate of ethyl acrylate.

Besides increasing the rate of particle swelling, the residual monomer will also influence the polymerisation of the coating monomer. In this respect, it is interesting to note the results of Mangeraj and Rath [22], in particular, the effect of a small amount of styrene increasing the rate of polymerization of acrylate monomers, in emulsion co-polymerization systems. Thus, the overcoating reaction is very sensitive to the amount of styrene remaining in the particle. In some cases, the reaction had reached completion in a shorter time than was predicted from the rate of pure acrylate emulsion polymerization.

Evidence for the direct combination of acrylate monomer units with free radicals at the core particle surface comes from a comparison of scanning electron micrographs of films cast from core-shell latices. Plate III:4 shows the fractured edge of a film cast from latex MC10 (prepared by the shot growth technique). There is a clear contrast between the polystyrene core particles (dark) and the polyacrylate coat (light) which has presumably been stripped off

the polystyrene core and then has collapsed back on fracture. The small globules adhering to the core particles have been interpreted as polyacrylate chains directly bound to the core particle surface. Clearly, this direct combination cannot occur during a seeded growth reaction, and this is confirmed by Plate III:5 which show fractured edges of a film cast from latex MC11 (prepared by the seeded growth technique). Plate III:5 shows an edge fractured at room temperature, revealing a separation of the acrylate coat from the underlying seed particles, some of which have anomalous regions observed by Cox et al. (11). None of the exposed core particles show the small globules of acrylate polymer.

Plate III:6 shows an edge which was fractured at liquid nitrogen temperature in order to retard the flow of coating polymer as much as possible. Here, some of the coating polymer remains attached to the seed particles. Where this occurs there is only one globule per seed particle (cf Plate III:4, where several small globules are attached to each core particle) and no globules are visible on seed particles displaying anomolous regions. This indicates that at room temperature, extensive coating polymer flow occurs on fracture, and that polymer contained in the anomolous regions is removed. This suggests that direct binding of coating polymer to core particles occurs in the shot growth process, as is demonstrated by the retention of acrylate polymer on the core particles for the "shot-growth" fracture section at room temperature.

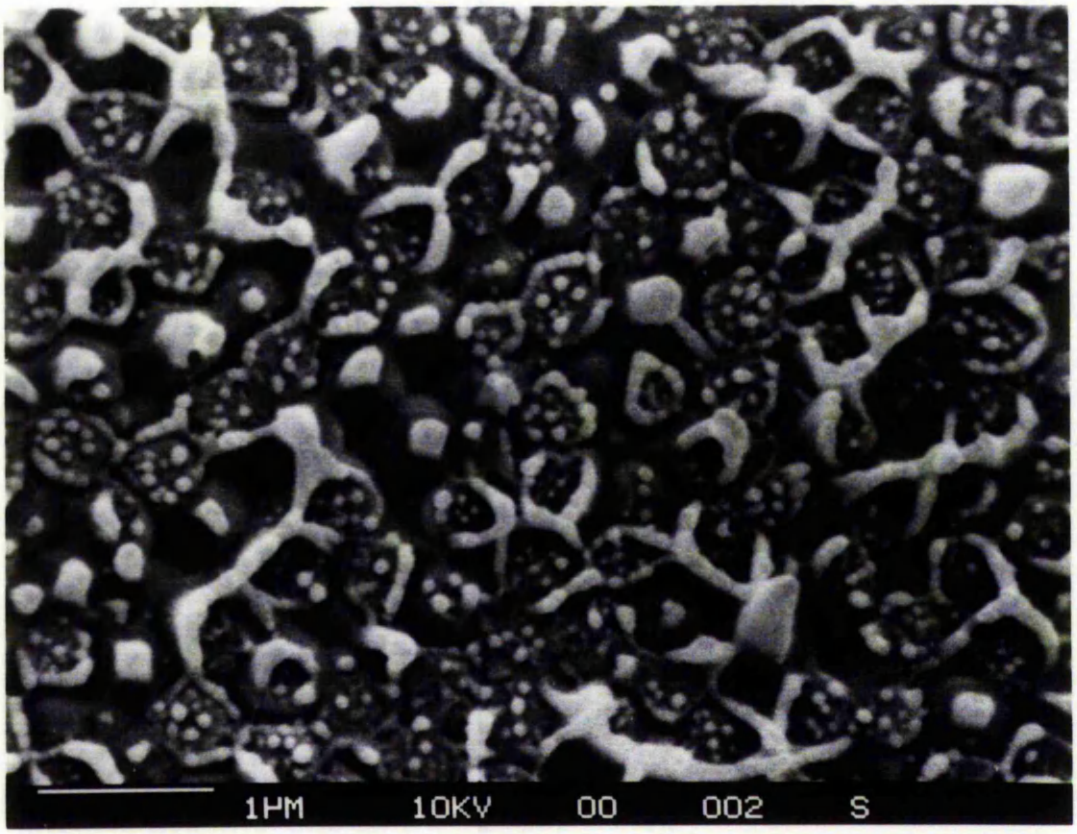

Plate III:4

SEM of film cast form latex MC10 (poly(ethyl acrylate) coated polystyrene, prepared by shot growth method). Cross section fractured at room temperature. Magn. 24,000.

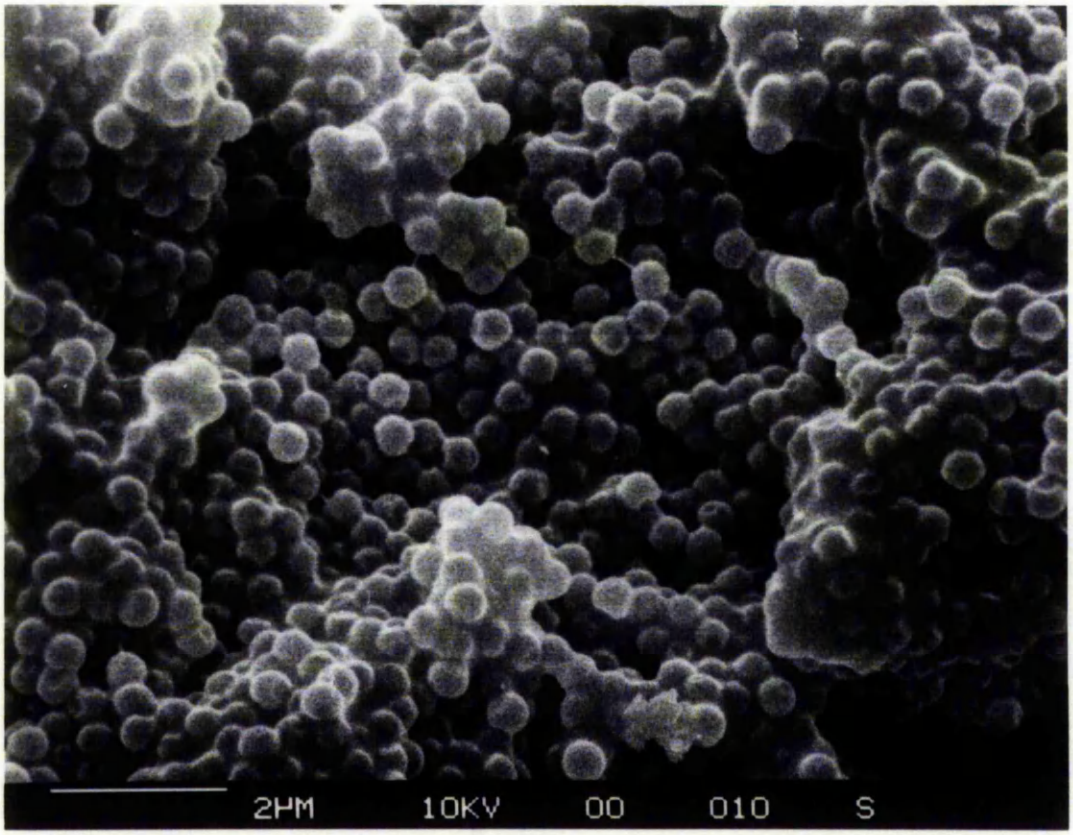

Plate III:5

SEM of film cast from latex MC11 (poly(ethyl acrylate) coated polystyrene, prepared by seeded growth method). Cross section fractured at room temperature Magn. 12,000.

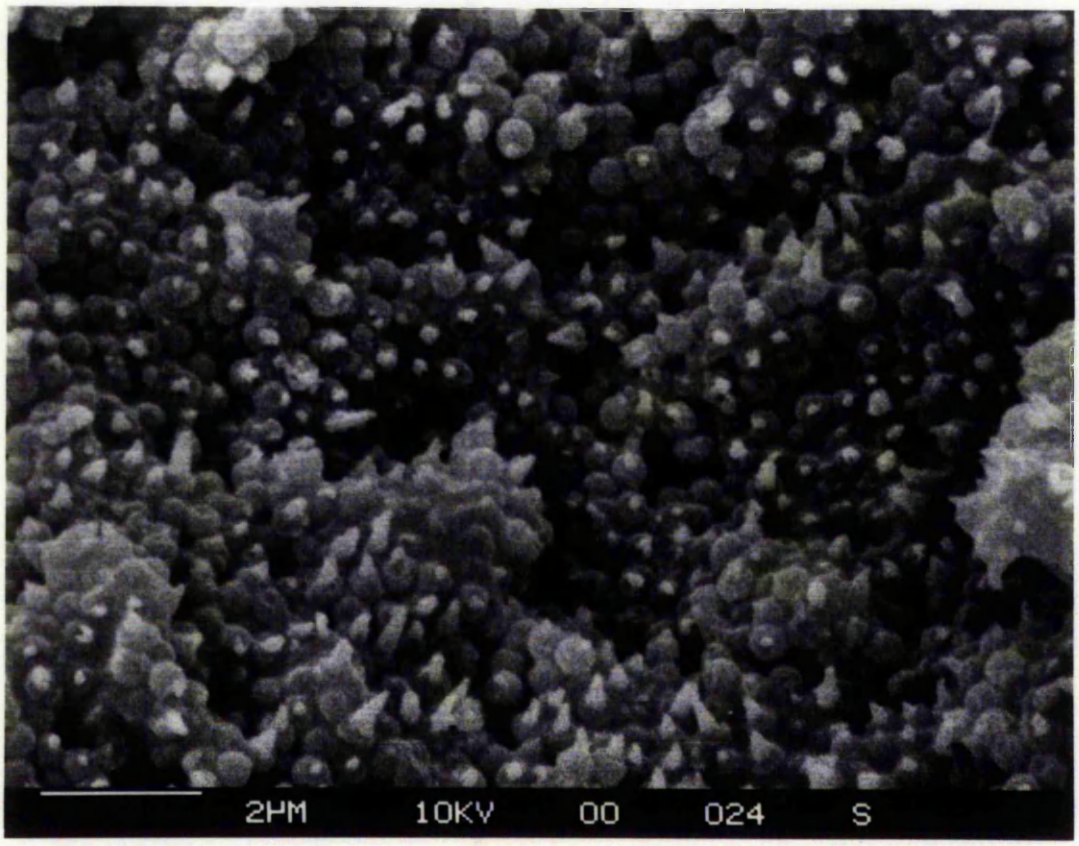

Plate III:6

SEM of film cast from latex MC11 (poly(ethyl acrylate) coated polystyrene, prepared by seeded growth method). Cross section fractured at 77K. Magn. 12,000.

D MICROFILTRATION*

The microfiltration technique, described in Chapter II, was evaluated as a means of cleaning polymer latices. The small microfiltration cell fitted with 47 mm diameter filters was used for this purpose. Ahmed et al. [23] have evaluated a similar cell. They derived equations describing the concentration profile of solute and adsorbate species in a latex undergoing microfiltration and showed that they were obeyed in practice by the model compounds hydrochloric acid and potassium chloride (solute species) and sodium dodecyl sulphate (adsorbate species). This work demonstrated that microfiltration was a convenient means of determining surfactant adsorption isotherms. The purpose of the work described below was to determine the effect of various operational parameters on the efficiency of cleaning and decide whether microfiltration was capable of cleaning a latex to the required degree of purity.

1. Filter type

Both Nuclepore and Millipore filters can be used in the cell. The former are made from thin (ca 10 μm) polycarbonate sheet. The pores are produced by neutron bombardment followed by controlled etching [24]. The manufactures claim that there are no pores larger than the nominal size stated. The filters are very delicate and require careful handling.

Millipore filters are composed of cellulosic fibres. They are much thicker (ca. 150 μm) and consequently more robust. Retention of particles larger than the rated pore size results from random entrapment within the filter. The greater tortuosity of this type of filter results in a lower flow rate (normally of the order of 50% lower) for a given pressure. However, a Nuclepore filter has only about 15% open area (depending on pore size) and it readily becomes blocked by latex particles. Ahmed et al. [23], who worked exclusively with this type of filter, found that latices of 10 - 15% solids filtered at 5 psi clogged the filter and formed enough coagulum to stop the stirrer.

Both types of filter were evaluated initially. However, the Nucleopore filters invariably allowed the passage of latex particles: after about ten cell changes, all the latex had passed through the filter. The most likely explanation for this leakage through the filter, caused either by distortion during mounting or attrition of the surface by the stirrer bar. Special precautions were taken to

*The author is indebted to Mr P. Cope for some of the experimental work described in this Section.

try to prevent this, including an experiment in which a 200 nm Nucleopore filter was sandwiched between two 800 nm Millipore filters.

In addition to mechanical wear of the polycarbonate filter, chemical attack by impurities, especially residual monomer, is possible. Tests showed that styrene did not etch the filters, but that acrylate monomers did. Many other monomers might be expected to attack polycarbonate. It is now possible to obtain Nucleopore filters made from polyester and PTFE, but since they were not available until this study was substantially complete, they have not been evaluated. Because of the problems encountered with Nucleopore filters, most of the work reported here is restricted to Millipore filters.

Although Millipore filters rely on the trapping of larger particles within the filter, no problems with blockage were encountered unless a large amount of residual monomer was present. This could be prevented by the use of a 'drain disc' (polyester, non-woven construction manufactured by Bio-Rad) which was placed above the Millipore filter. In extreme cases, the drain disc became clogged with a monomer/polymer coagulum and had to be replaced. The original Millipore filter was unaffected.

2. Factors affecting Eluent Flow Rate

a. Latex particle diameter/filter pore size

A filter was chosen such that the average pore size was 50 to 75% of the latex particle diameter. Large pore size filters had a greater open area, resulting in higher flow rates. Large particle size latices could, therefore, be cleaned in a shorter time.

b. Stirrer speed

The speed of the magnetic stirrer bar was kept to the minimum necessary to avoid pore blockage, and this was dependent on the particle size and solids content of the latex being cleaned. The minimum speed necessary increased with decreasing particle size and increasing solids content. At high stirrer speeds, some latices, most notably those of poly (ethyl acrylate) and poly(n-butyl acrylate), suffered sheer instability, leading to coagulation and filter blockage.

c. Latex solids content

In general, the eluent flow rate did not decrease with increasing solids content until this reached a value in the region of 20%. This made microfiltration ideal for cleaning surfactant-free latices, since a freshly prepared latex usually had a solids content of around 10%, and did not require dilution prior to cleaning. 'Delicate' latices, i.e. those prone to sheer instability, sometimes required dilution prior to microfiltration to allow the stirrer speed to be reduced (see (b) above). Stable latices having much higher solids contents could be cleaned, but the eluent rate dropped with increasing solids content. Microfiltration could be used to concentrate a latex to as much as 50% solids. This process is particularly useful where the solids content is too low (less than 2%) for a reliable conductometric titration to be carried out [25]. A graph showing the time taken to clean 5 g of polymer as a function of solids content is shown in Fig. III:13. The polystyrene latex had a particle diameter of 440 nm and the time taken includes the three stages of filtration, acid wash and filtration to remove acid.

d. Water pressure

The elution rate could be increased by pressurising the water supply in the aspirator. A 'white-spot' nitrogen cylinder was used for this purpose. The variation in elution rate with applied pressure for two different pore size filters is shown in Fig. III:14.

3. Cleaning of Latex

a. Rate of Removal of Electrolyte

A sample of freshly prepared and untreated latex was centrifuged and the centrifugate and mother liquor analysed by flame photometry. The centrifugate was found to contain 180 μg cm^{-3} sodium. The sodium was derived from the impurity in the potassium persulphate (measured by flame photometry to be 0.002% w/w). The latex was microfiltered using double distilled water and samples of the eluent water analysed after various volumes had been passed. The results in Fig. III:15 show that both potassium and sodium levels in the aqueous phase were reduced to negligible levels after approximately five cell changes. However, this was no indication as to the level of sodium and potassium left associated with the polymer phase (i.e. in the inner part of the electrical double

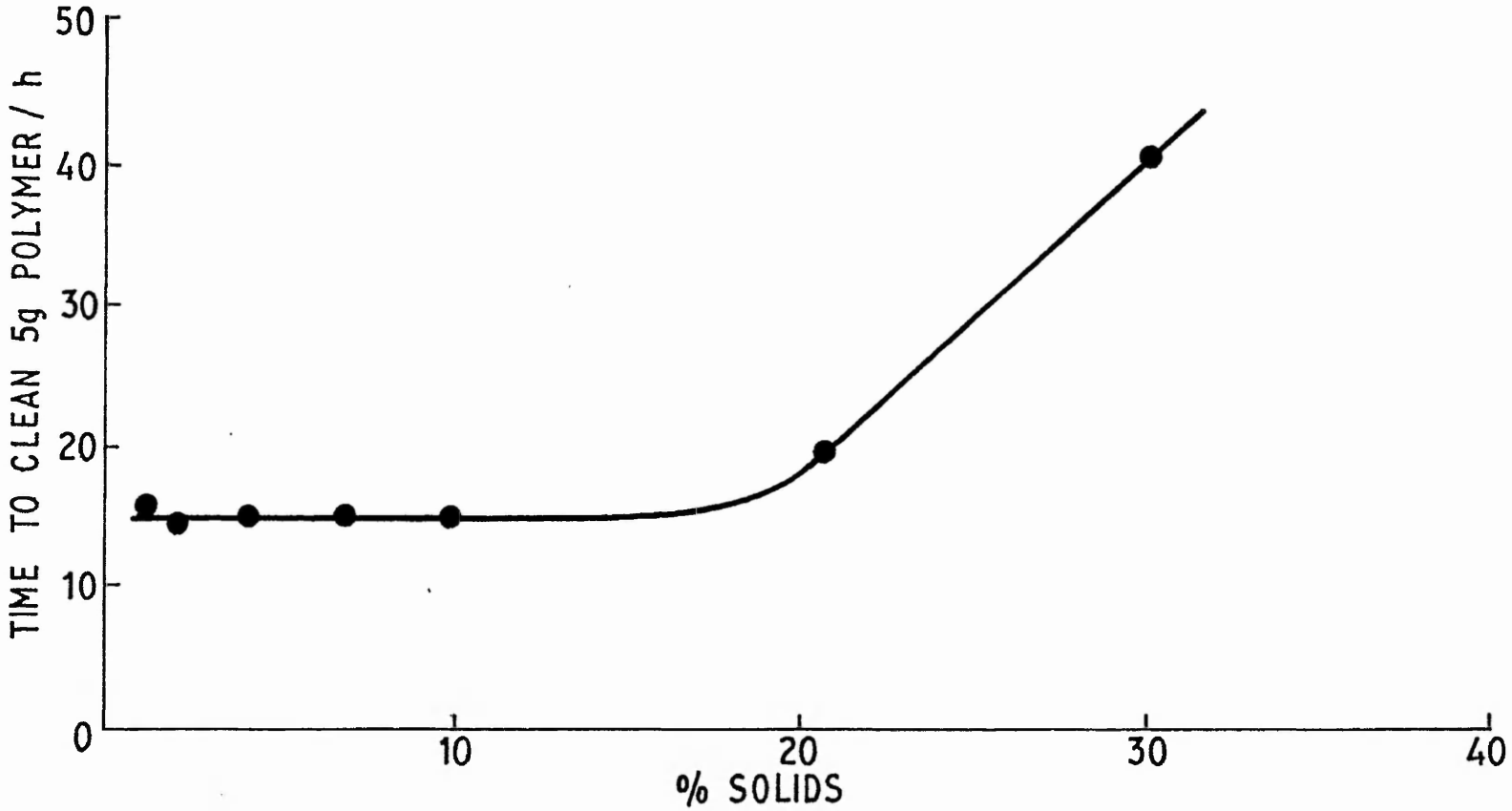

FIG III:13 TIME TAKEN TO CLEAN 5g OF POLYMER AT DIFFERENT SOLIDS CONTENTS (INCLUDES STAGES (i) FILTRATION, (ii) ACID WASH, (iii) FILTRATION TO REMOVE ACID)

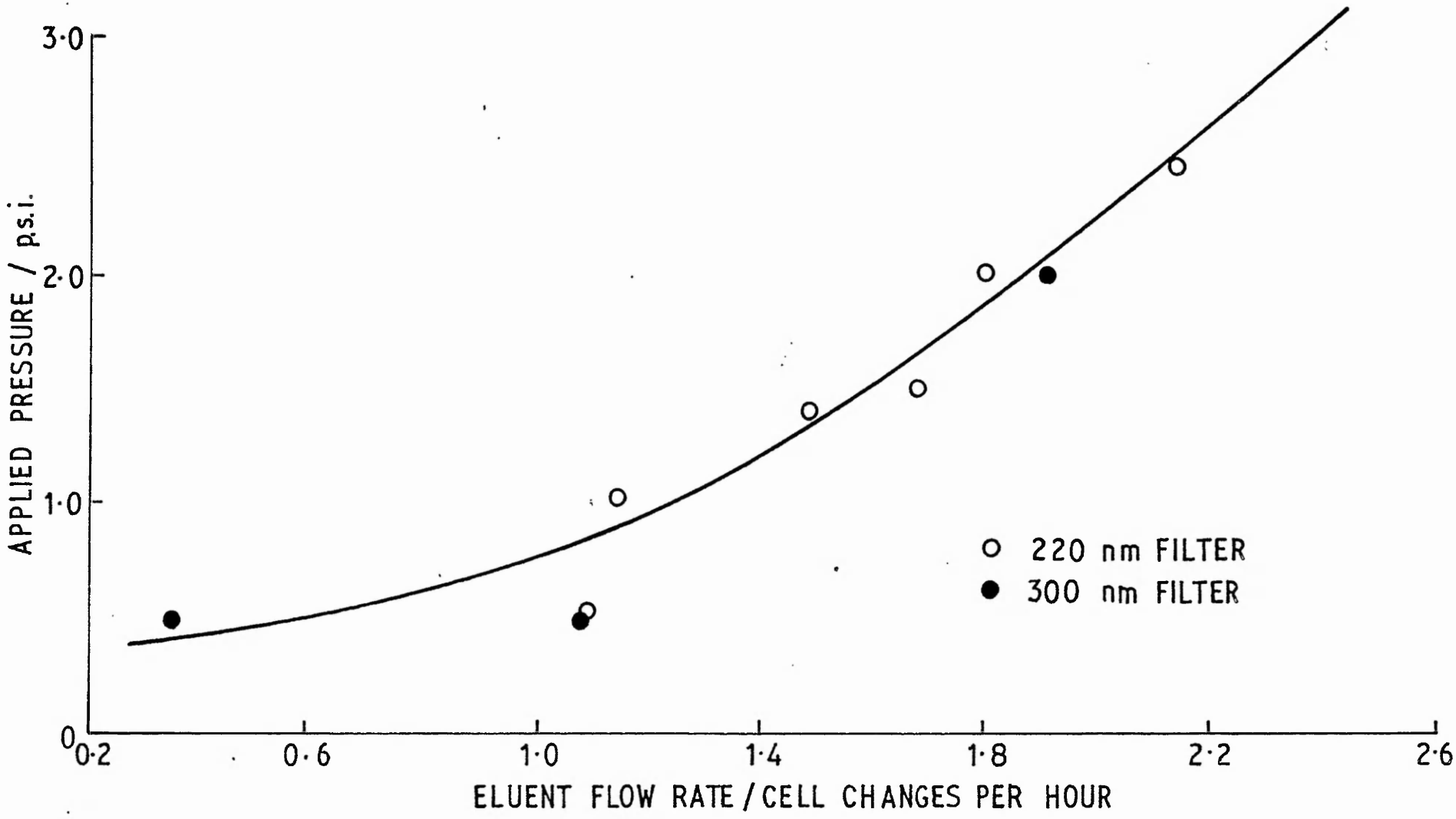

FIG III: 14 VARIATION IN ELUTION RATE WITH APPLIED PRESSURE

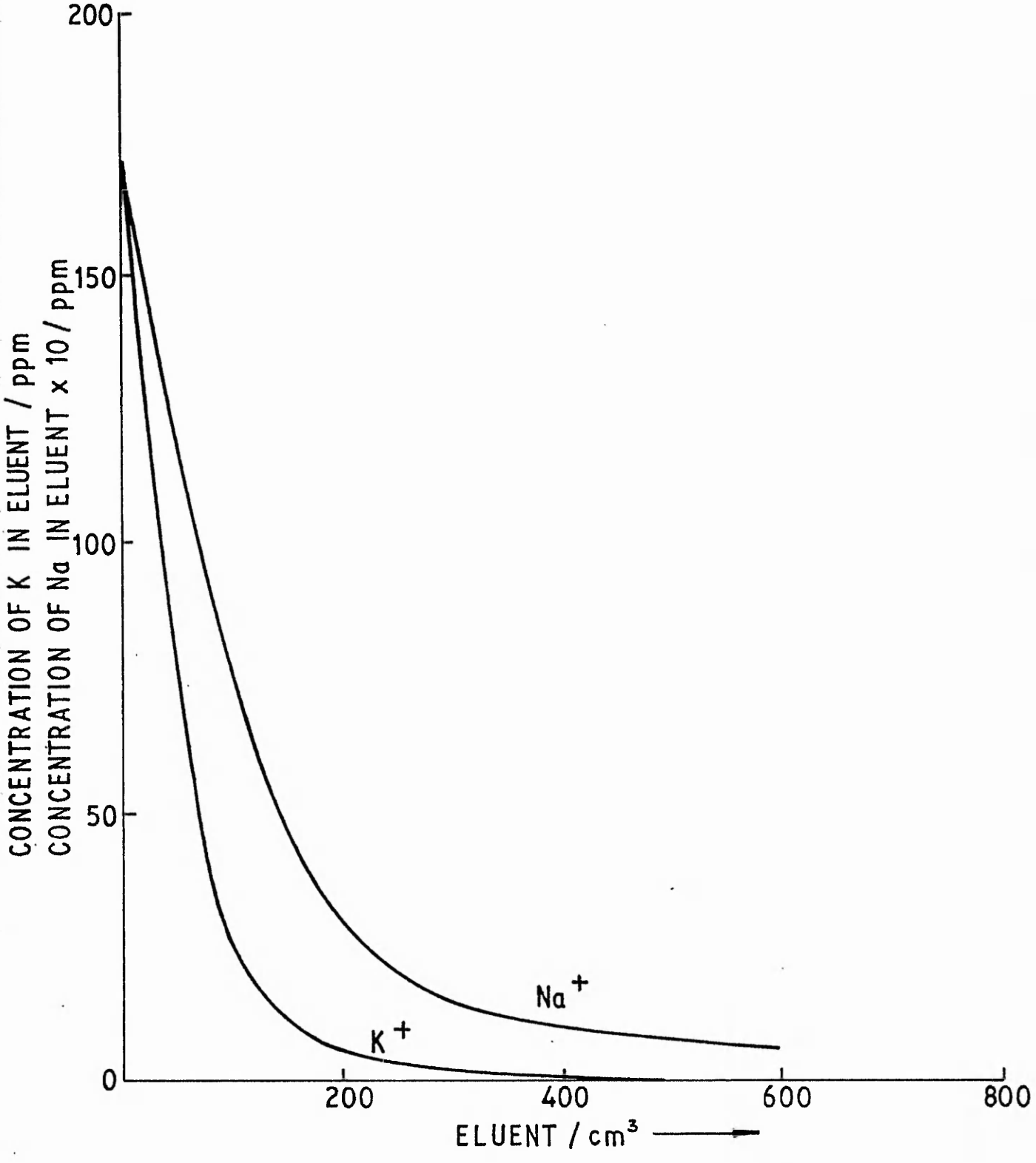

FIG III:15 EFFICIENCY OF REMOVAL OF SODIUM AND POTASSIUM IONS

layer), which as shown by acid washing and ion-exchange techniques can be significant (see (b) below). Thus, this technique, in common with dialysis and similar methods is not capable of ensuring complete removal of electrolytic material associated with the polymer phase.

b. Effect on Surface Charge

Samples of latex were withdrawn during elution and titrated with 1.10^{-2} mol dm^{-3} sodium hydroxide solution. The surface charge fell rapidly such that after 10 cell changes (800 cm^3 of eluent; not acid washed) the surface charge was very similar to that recorded after 28 days dialysis, i.e. 2.31 μeq g^{-1} and 2.20 μeq g^{-1}, respectively. This then varied little with further elution (e.g. after 16 cell changes a value of 2.44 μeq g^{-1} was recorded).

A sample of latex cleaned according to Ahmed et al. [23] with a mixed bed ion-exchange resin gave a significantly higher surface charge of 14.1 μeq g^{-1} (Fig. III.16). It was thought that the low value on dialysis and microfiltration was due to the incomplete exchange of cations for protons [26]. To test this hypothesis the latex was washed in the cell with various concentrations of hydrochloric acid. This was followed by distilled water elution until the conductivity of the eluent was the same as that of distilled water. It was noted that the surface charge changed little until a concentration of ca. 6×10^{-5} mol dm^{-3} acid was reached, whereupon it increased rapidly to ca. 13.5 μeq g^{-1} and remained constant as the acid concentration was increased to 0.1 mol dm^{-3} (Fig. III.16). The value of 13.5 μeq g^{-1} agreed well with the ion-exchanged value of 14.1 μeq g^{-1} and it was assumed that this corresponded to the state where all cations had been replaced by protons.

The sharp increase in surface charge at ca. 5×10^{-5} mol dm^{-3} acid concentration agreed well with the calculated concentration of cations required to be exchanged (i.e. 6×10^{-5} mol dm^{-3}). A 24 h dialysis of the acid washed sample (6 changes of dialysate at 400:1 exchange ratio) did not result in any change of this value (13.6 μeq g^{-1} being recorded). This finding is in agreement with the results of Ahmed et al. [23].

c. Removal of styrene and benzaldehyde

The efficiencies with which styrene and benzaldehyde are removed from polystyrene latex by microfiltration, dialysis and ion exchange are compared in Table III-16. It can be seen that microfiltration is completely effective in removing these contaminants. By comparison dialysis and ion exchange were

TABLE III:16

EFFICIENCY OF REMOVAL OF STYRENE AND BENZALDEHYDE BY VARIOUS TECHNIQUES

	Styrene Removed/%	Benzaldehyde Removed/%
Microfiltration (10 cell changes)	>99	>99
Amberlite XAD-2	58	50
AIEC	8	75
Mixed Dowex	75	85
Dialysis (1 day)	6	-
Dialysis (20 days)	90	-

Notes

Original concentrations: styrene 71 mg/g polymer
benzaldehyde 8 mg/g polymer

Ion-exchange resins present in 5 x excess (based on exchange capacity).
Contact time 5h.
Dialysis carried out at 20:1 ratio.

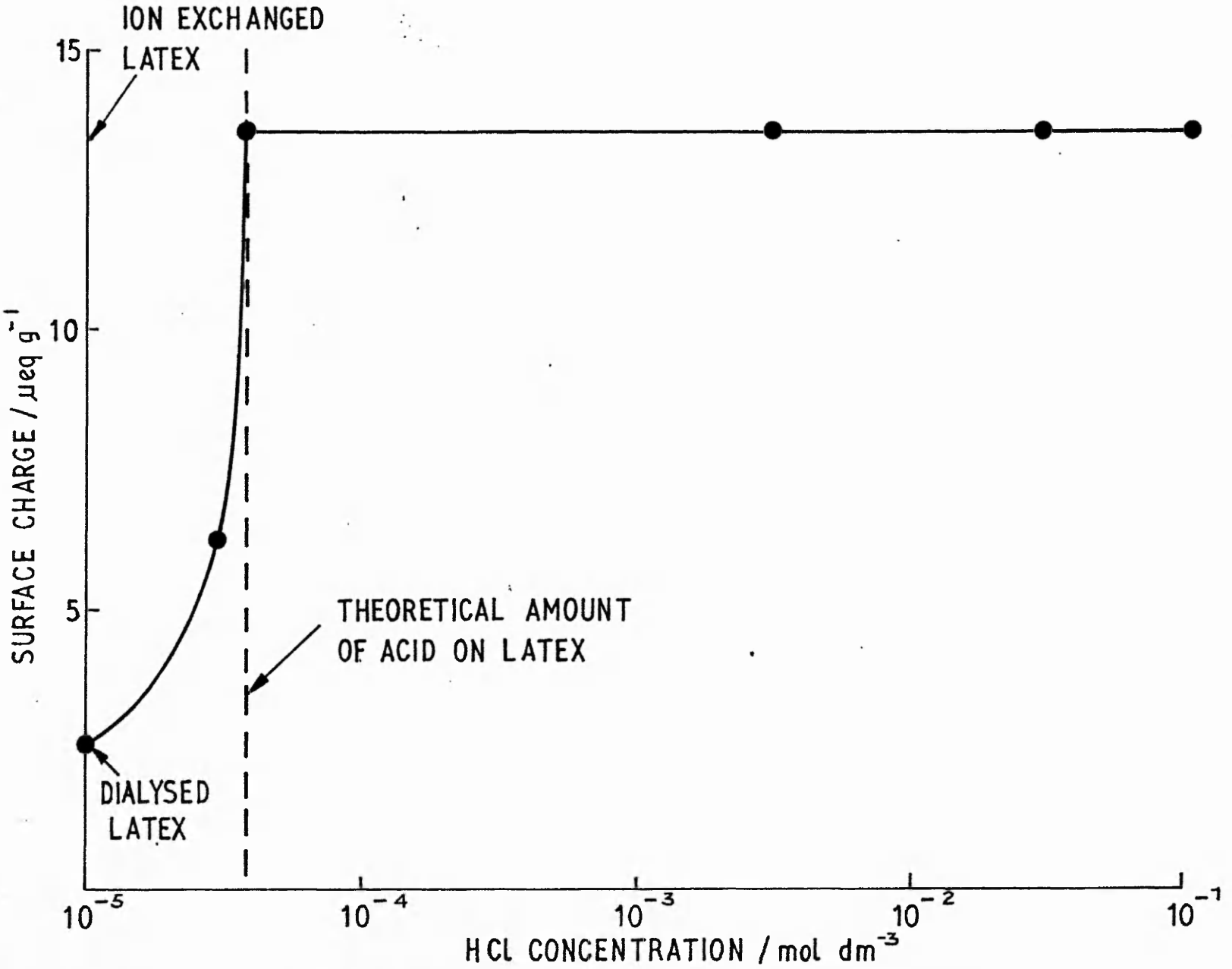

FIG III:16 EFFECT OF ACID WASHING ON SURFACE CHARGE

only partially effective.

The occurrence of 'gel-like' material, in the form of bridges between juxtaposed latex particles when observed by transmission electron microscopy, has been previously reported [27]. Labib and Robertson [28] have found that this material could be removed from polystyrene latices by diafiltration. They did not analyse for this material, but it was almost certainly styrene monomer and low molecular weight oligmer [27]. Microfiltration was equally effective in removal of this gel-like material, as shown by the absence of particle bridges in cleaned latices.

d. Removal of Benzoic acid

Previous work [29] has shown that benzoic acid is formed during the emulsion polymerisation of styrene. This is adsorbed at the polymer/water interface, and is difficult to remove by conventional dialysis. The presence of even small amounts of benzoic acid can have a significant effect on the conductometric titration curve, contributing to an increase in the titratable strong acid at low concentrations (less than 1.10^{-3} mol dm^{-3}) and only appearing as a weak acid species in concentrations above this.

Significant oxidation of styrene can occur during an emulsion polymerisation, even in a nitrogen atmosphere, presumably by oxidation by the persulphate free radical initiator. For example, it was found that benzoic acid was being generated at 1.95 m mol dm^3h^{-1} in 11 m mol dm^{-3} potassium persulphate solution at 343K under nitrogen [29]. Although the levels of benzaldehyde present during a polymerisation will be very much less than this, there is still sufficient to radically affect the nature of the surface charge if converted to benzoic acid.

To determine the efficiency of removal of benzoic acid by the microfiltration technique a clean sample of latex MC8 was dosed with 2% (w/w, polymer) and this was eluted in the usual manner. Samples were withdrawn during elution and titrated conductometrically (Fig. III.17). The surface charge decreased from an initially high value of 68 μeq g^{-1} (an apparent strong acid [29]) to a constant value of ca. 13.9 μeq g^{-1} after 25 changes of cell content. It is of note that almost 3 times as many exchanges were required to remove the benzoic acid (7 m mol dm^{-3}) as the equivalent concentration of hydrochloric acid. This demonstrates the strong adsorption of benzoic acid on the latex particles [29].

The surface charge did not drop to that of the original clean sample (2.4 μeq g^{-1} - not acid washed, refer Fig. III:11), but reached a constant value of 13.9

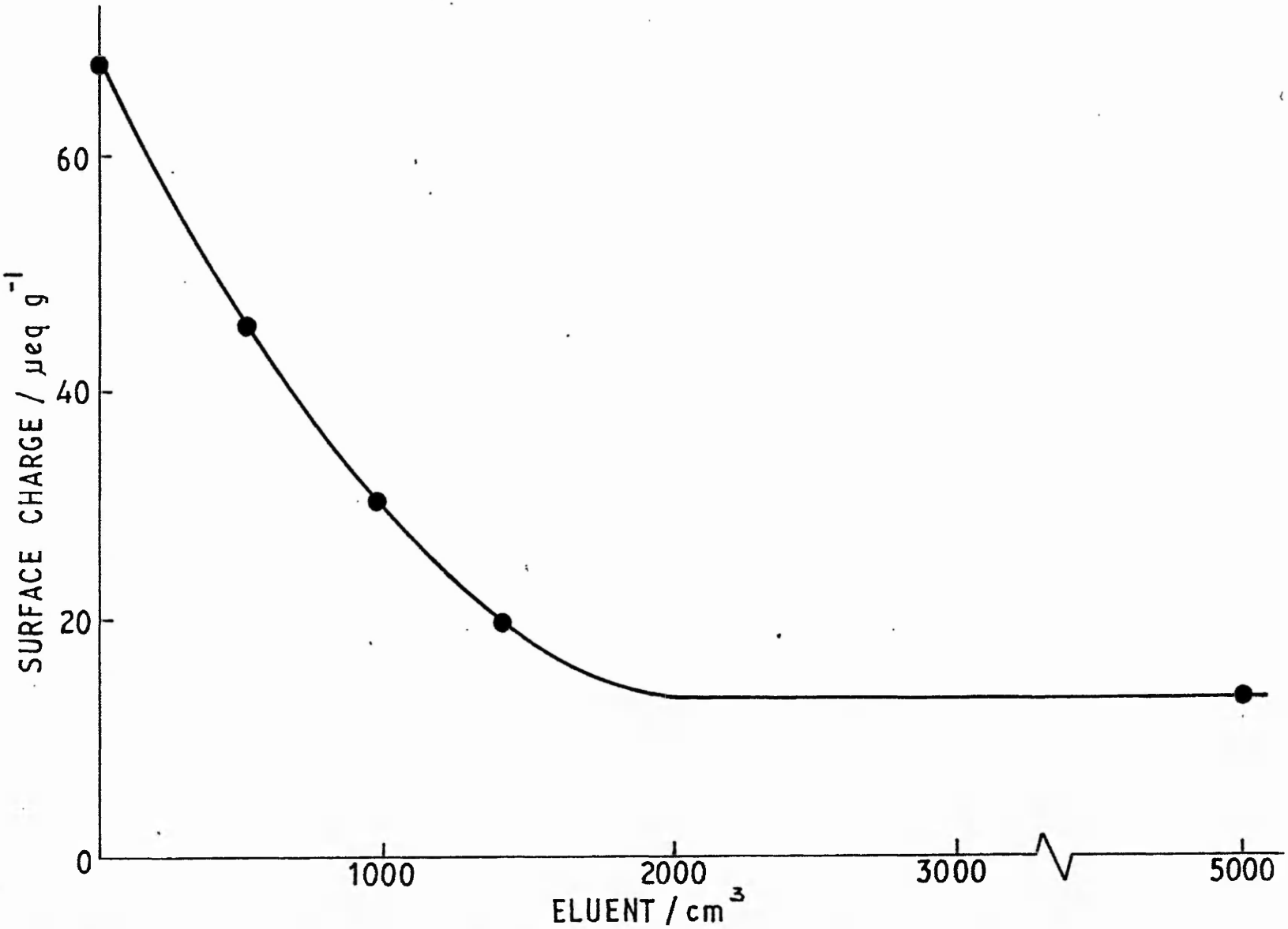

FIG III:17 EFFICIENCY OF REMOVAL OF BENZOIC ACID

$\mu eq\ g^{-1}$. This agrees well with the acid washed sample and is not unexpected since benzoic acid is partially dissociated at room temperature (6.3×10^{-5} mol dm^{-3} in the dissociated form) and could therefore enable complete exchange of cations for protons to be achieved.

e. Removal of surfactant

The large majority of emulsion polymerisations involve the use of a surfactant [8,30] and it is important to evaluate the microfiltration technique in this context. This is particularly pertinent since there are conflicting views on the efficiency of removal of certain surfactants by the dialysis technique [31,32]. Since most of the work in this area has been concerned with sodium dodecyl sulphate this was chosen for study. Relevant details of the polystyrene latices used are given in Table III-17.

TABLE III-17

Details of Polystyrene Latices

Latex	Diameter/nm	Solids content/%	Surface Area in 80 cm^3 Latex/cm^2
MC8	440	7.30	9.6×10^5
271	490	2.29	2.7×10^5

A solution of a pure sample of sodium dodecyl sulphate and a sample of clean latex MC8 were mixed. The concentration of sodium dodecyl sulphate in the latex was 12.5 mmol dm^{-3}: this concentration was chosen because it is above the critical micelle concentration and was capable of reducing the concentration of the latex to a constant low value (38.8 mNm^{-1}). This latex was then eluted continuously in the usual manner until the surface tension and conductivity of the eluent were equal to those of the feed water (Fig. III:18). A sample of the cleaned latex MC8 was titrated with 1.10^{-2} mol dm^{-3} sodium hydroxide solution and this gave an endpoint of 19.4 $\mu eq\ g^{-1}$ (cf. acid washed latex). A second sample of the cleaned latex was back titrated with sodium dodecyl sulphate solution according to the technique of Maron et al. [33] until the surface tension

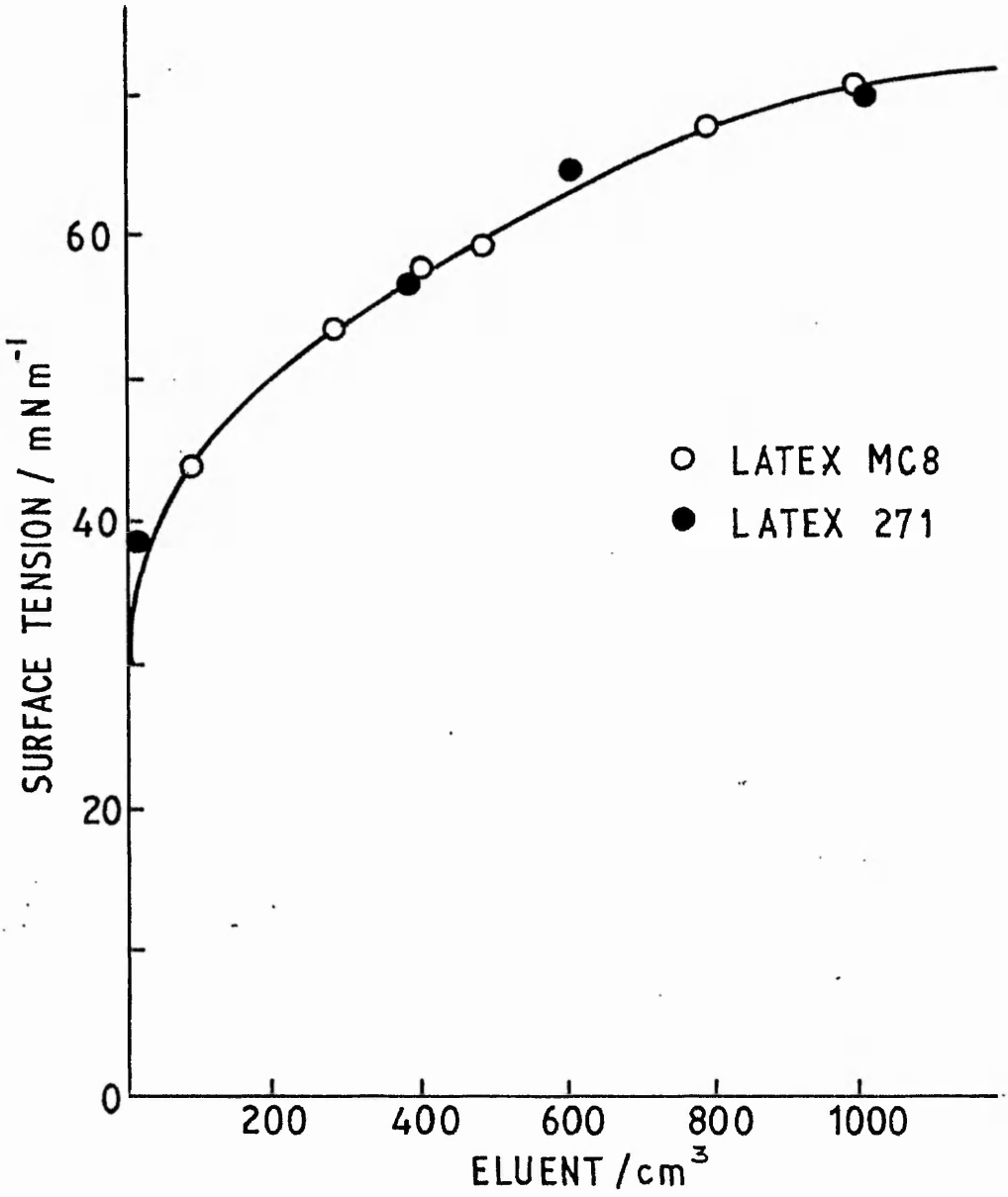

FIG III:18 RATE OF REMOVAL OF SODIUM DODECYL SULPHATE FROM LATEX

decreased to a minimum. The endpoint was used to calculate the critical micelle concentration after allowing for the amount which would be adsorbed on the latex particles. This was 7.9 mmol dm^{-3} compared with the literature value of 8.0 mmol dm^{-3} [34]. If the uncertainty in the critical micelle concentation is 5%, then the minimum detectable surface coverage is ca. 10%.

In order to confirm that all the sodium dodecyl sulphate was recovered by microfiltration when it could no longer be detected by its effect on the conductivity and surface tension of the eluent water, a further experiment was conducted. A fresh mixture of latex 171 and sodium dodecyl sulphate solution was prepared and a portion of this was eluted as before. When the conductivity and surface tension had reached the same values as those of the feed water, elution was halted and the cell left stirring overnight. Elution was continued 13 hours later, and there was no change in the values of conductivity and surface tension of the eluent. This microfiltered latex was then left standing for one week so that equilibrium between sodium dodecyl sulphate molecules in the aqueous phase and those adsorbed on the latex particles was certain to have been attained. The concentration of sodium dodecyl sulphate in the aqueous phase was determined by the method of Barr et al. [35]. A known volume of latex was diluted with 100 cm^3 of distilled water. Five drops of bromophenol blue indicator and 50 cm^3 of chloroform were added. The mixture was then titrated with cetyl trimethyl ammonium bromide solution (10^{-3} mol dm^{-3}) the flask being shaken vigorously after each addition. The endpoint was marked by the appearance of a blue colouration in the lower chloroform layer. The concentration of sodium dodecyl sulphate was below the limit of detection of this method.

Varying concentrations of sodium dodecyl sulphate solution were titrated for calibration: these showed that concentrations as low as 10^{-6} mol dm^{-3} could be detected easily. 1% of the monolayer coverage of the total surface area of 100 cm^3 of latex 271 was equivalent to 9.3 10^{-7} mol of sodium dodecyl sulphate. Thus, it can be seen that this is a sensitive test for this surfactant.

There is a measure of disagreement between the results presented above and those reported by Ahmed et al. [23] with regard to the rate of removal of sodium dodecyl sulphate. The results of the experiments reported here suggest that complete removal of adsorbed anionic surface-active agent is achieved rapidly. For example $12\frac{1}{2}$ cell changes (ca. 6 h at 2.2 cell changes h^{-1}) were required to reduce the concentration of sodium dodecyl sulphate in the eluent from 12.5 10^{-3} mol dm^{-3} to a negligible level: this is to be compared with the 29

h taken to reduce the concentration from 3.35 10^{-4} mol dm^{-3} to 0.17 10^{-4} mol dm^{-3} by Ahmed et al. It seems likely that equilibrium removal of solute and adsorbable species applies at quite rapid elution rates, and it therefore follows that to delay elution to ensure the equilibrium desorption of these species (the technique used by Ahmed et al.) is unnecessary.

4. Separation of Different Particle Sizes

The microfiltration unit was capable of separating two different sized latices, if a Millipore filter was employed where the pore size was greater than the smaller of the two. For example a latex mixture consisting of 1000 nm and 100 nm particles in a ratio of 1:40000 was successfully separated within several hours. This would be useful where it was required to separate the components of a latex having a bimodel size distribution.

5. Comparison of Microfiltration and Dialysis Techniques

The experiments described show that microfiltration will remove all the adsorbed surfactant from a polystyrene latex, in as little as six hours. Dialysis, however, is a slow process and frequently only incomplete removal is achieved. This is principally due to the slow rate of diffusion of large molecules resulting in a rapid increase in concentration just inside the surface of the dialysis membrane. Edelhauser [31] found that the rate of dialysis of surface-active agent solutions was increased by stirring the inside solution, which would minimise this effect. Industrially, dialysis tubes containing latices are rotated or agitated in some way, to achieve the same end. Nevertheless, this slow diffusion will result in latex particles being in a region of high concentration unless they are close to the surface of the dialysis membrane and therefore the extent of desorption of surface-active agent will be small.

Contrast this situation with that inside the microfiltration cell, where the aqueous suspending medium is being changed every 30 - 60 minutes. Here, the latex particles are in a region of low concentration, and the adsorbed surface-active agent will desorb much more quickly.

If, for any reason the concentration of surfactant in the aqueous phase is above the critical micelle concentration, then its removal by dialysis is certain to be incomplete. This has been attributed to materials originally present in the dialysed latex being incorporated in the micelles, thereby stabilising them [31]. Since dialysis relies on diffusion of monomeric species through the dialysis

membrane (the micelle being larger than the pores) removal of surface-active agent from the aqueous phase becomes negligible after a certain point. The pore sizes of the filters used in microfiltration are much larger than the micelles and therefore this problem does not arise. The micelles are simply washed out of the latex, after which the process reverts to the type described earlier.

6. Addition and removal of microbial inhibitors

Microbial ativity in polymer latices occurs very readily, leading to serious contamination [2]. Microorganisms are to be found in all unfiltered atmospheres. Some, particularly those producing spores, can survive the usual processes of materials purification and emulsion polymerisation, and may be present even in a freshly prepared latex. Contamination may also occur during the cleaning of a latex and on subsequent storage. Microbial contamination is only visually apparent at high levels (e.g. 10^5 spores/cm^3 for certain fungi which produce coloured spores) although some techniques of latex characterisation, such as electron microscopy, may detect it at lower levels.

The presence and activity of microorganisms can have serious implications for latex characterisation and stability. Their metabolites include carboxylic acids, which interfere with determinations of charged endgroup type and concentration. The effect of the microorganisms is often to drastically reduce the surface charge density on the particles, ultimately leading to destabilisation and coagulation [2].

Various microbial inhibitors are available commercially. Several were added to samples of polystyrene latex at the manufacturers recommended concentration to determine their ease of removal and effect on the latex surface charge density and stability. The results are summarised in Table III.18. None were entirely without effect, causing either latex instability or irreversible change in surface charcteristics. They could not therefore be used in latices intended for particle interaction studies or other applications where maintenance of surface charge density is important. However, neither sodium azide or Kathon 886 MW destabilised the latex, and the reduction in surface charge density caused by their presence is probably no worse than would be brought about by microbial activity.

7. Conclusions

The microfiltration technique has several advantages over other methods for the cleaning of latices. It avoids the prolonged preparation associated with the purification of ion-exchange resins, and it permits the rapid removal of adsorbed surfactant from the latex, something which may require prolonged periods of dialysis to achieve. The apparatus is simpler and hence cheaper than that required for diafiltration or hollow-fibre dialysis. A further advantage of the microfiltration technique is its versatility: apart from cleaning latices, the solids content may be adjusted easily, and a choice of filters of differing composition and construction may be employed to suit varying circumstances.

Nucleopore filters have the advantage of being a much better substrate for electron microscope analysis. However, as a routine method for cleaning latices for characterisation and other purposes, Millipore filters are more suitable, being more robust and easier to handle, able to cope wth residual monomer, higher solids contents and greater pressures.

TABLE III:18

EFFECT OF MICROBIAL INHIBITORS ON SURFACE CHARGE DENSITY OF POLYSTYRENE LATICES

Latex	Inhibitor Concentration	Surface Charge Density/μC cm^{-2} Before Addition	After Addition	After Microfiltration	Notes
MC8	3-methyl 4-chloro phenol 0.3%	10.0	6.6	4.8	Probably impurity
MC8	Thiomesal[a] 10,000 ppm	14.2	4.0 (5.9)	1.4	Destabilised redispersed ultrasonically
MC8	Phenyl mercuric acetate 1,000 ppm	14.2	-	14.4	Destabilised
MC119	Sodium azide 200 ppm	5.0	3.6	4.6	Strong acid drastically reduced
MC119	Kathon 886 MW[b] 20 ppm	5.0	-	3.3	

[a]Morthiolate: supplied by ICI

[b]Isothiazolene: supplied by Rhom and Haas

TABLE III:18 (Cont'd)

In addition to the above, the following inhibitors were also evaluated:

4-chloro m-cresol
Chlorohexidene diacetate
Sulphur dioxide
Chlorine
Formaldehyde

None were found suitable, due either to irreversible, contamination or destabilisation of the latex.

REFERENCES

1. J.W. Goodwin, J. Hearn, C.C. Ho and R.H. Ottewill, Brit. Polym. J., 5, 347 (1973).

2. M.C. Wilkinson, R. Sherwood, J. Hearn and A.R. Goodall, ibid, 11, 1 (1979).

3. J. Hearn, M.C. Wilkinson and A.R. Goodall, Adv. Colloid Interface Sci., 14, 173 (1981).

4. A.R. Goodall, M.C. Wilkinson and J. Hearn, in "Polymer Colloids II", R.M. Fitch (ed.), Plenum Press, p. 629 (1980).

5. A.R. Goodall, Ph.D. thesis, Trent Polytechnic (1976).

6. P. Cope, unpublished results.

7. W.P. Hohenstein, S. Siggia and H. Mark, India Rubber World, 111, 173 (1944).

8. D.C. Blackley, "Emulsion Polymerisation", Applied Science Publishers (1975).

9. J. Hearn, Ph.D. thesis, University of Bristol (1971).

10. J. Brandrup and E.H. Immergut (eds.), "Polymer Handbook", second edition, Wiley Interscience (1975).

11. R.A. Cox, M.C. Wilkinson, J.M. Creasey, A.R. Goodall and J. Hearn, J. Polym. Sci., Polym. Chem. Ed., 15, 2311 (1977).

12. A.W. Hui and A.E. Hamielec, J. Appl. Polym. Sci., 16, 749 (1972).

13. R.A. Wessling and D.S. Gibbs, J. Macromol. Sci.-Chem., A7, 647 (1973).

14. W.H. Stockmayer, J. Polym. Sci., 24, 314 (1957).

15. J. Ugelstad and P.C. Mork, Brit. Polym. J., 2, 31 (1970).

16. Y. Chung-Li, J.W., Goodwin and R.H. Ottewill, Progr. Colloid Polym. Sci., 60, 163 (1976).

17. S. Morton, S. Kaizerman and M.W. Altier, J. Colloid Sci., 9, 300 (1954).

18. J. Ugelstad, P. Mørk, K.H. Kaggerud, T. Ellengsen and A. Berge, Adv. Colloid Interface Sci., 13, 101 (1980).

19. J.W. Goodwin, R.H. Ottewill, N.M. Harris and J. Tabony, J. Colloid Interface Sci., 78, 253 (1980).

20. D.J. Williams, J. Polym. Sci., Polym. Chem. Ed., 12, 2123 (1974) and references cited therein.

21. J.W. Vanderhoff, Proc. Water Borne and High Solids Coatings Symp. University of Southern Mississippi (1976).

22. D. Mangeraj and S.B. Rath, Polym. Prepr., Amer. Chem. Soc., Div. Polym. Chem., 13, 349 (1972).

23. S.M. Ahmed, M.S. El-Aasser, G.H. Pauli, G.W. Poehlein and J.W. Vanderhoff, J. Colloid Interface Sci., 73, 398 (1980).

24. F.W. Billmeyer, "Textbook of Polymer Science", second edition Wiley Interscience (1971).

25. J. Hearn, M.C. Wilkinson, A.R. Goodall and P. Cope, in "Polymer Colloids II", R.M. Fitch (ed.), Plenum Press (1980).

26. J.W. Vanderhoff, H.J. van den Hul, R.J.M. Tausk and J. Th. G. Overbeek, in "Clean Surfaces", G. Goldfinger (ed.), Marcel Dekker, p. 15 (1970).

27. A.R. Goodall, J. Hearn and M.C. Wilkinson, J. Polym. Sci., Polym. Chem. Ed., 17, 1019 (1979).

28. M.E. Labib and A.A. Robertson, J. Colloid Interface Sci., 67, 543 (1978).

29. A.R. Goodall, M.C. Wilkinson, J. Hearn and P. Cope, Brit. Polym. J., 10, 205 (1978).

30. H. Warson, "The Applications of Synthetic Resin Emulsions", Ernest Benn Ltd. (1972).

31. H.A. Edelhauser, J. Polym. Sci., Part C, 27, 291 (1969).

32. J.N. Shaw, ibid, 27, 237 (1969).

33. S.H. Maron, M.E. Elder and I.N. Ulevitch, J. Colloid Sci., 9, 89 (1954).

34. B.D. Flockhart and A.R. Ubbelhode, ibid, 8, 428 (1953).

35. T. Barr, J. Oliver and W.V. Stubbings, J. Soc. Chem. Ind., 67, 45 (1948).

CHAPTER IV

PREPARATION OF LATEX FILMS

A. EVALUATION OF LITERATURE TECHNIQUES

Polymer latex films were prepared using the techniques described in Chapter II, and were examined according to the following criteria:

(i) Films having a thickness in the range 10 - 100 μm, constant over a circular area of ca. 15 cm^2 were required. This restriction was imposed by the sensitivity of the katharometer detector used in the permeation apparatus (described in Chapter II).

(ii) The surfaces of the films were required to be as smooth as possible, and the interiors free from cracks, voids and fissures.

(iii) It was necessary to avoid techniques which contaminated the films, especially since the latex precursors had been rigorously cleaned beforehand.

1. Mercury Surface

Although apparently simple, this method of film preparation required great care in practice, and suffered several drawbacks. The technique was only suitable for latices having a minimum film formation temperature at least 10K lower than ambient, otherwise strains set in during the drying process. This resulted in distortions in the film, usually in the form of concentrically circular wrinkles. The toxicity of mercury vapour precluded experiments at higher temperatures. The amount of mercury in the film was determined by atomic absorption spectrophotometry and found to be 0.1% (w/w). Washing the film in dilute nitric acid and rinsing several times in water reduced this to 0.03 - 0.04% (w/w). It is therefore likely that a significant amount of this contaminant was contained within the film, and not just on the lower surface. In an attempt to overcome the restriction on minimum film formation temperature, several films were cast on the surface of gallium metal (melting point 310K). However, on removal, these films were almost opaque, indicating gross contamination. Gallium is considerably more reactive than mercury and its surface is readily oxidised. It is probable that this oxide layer remains on the film surface on stripping.

2. Photographic Paper

Liquid films formed by the drawdown bar were unstable. Most of the latex retracted into large globules of substantial thickness (ca. 1 - 2 mm) leaving a

very thin liquid film behind. These regions often produced uniform and very thin (less than 10 μm) film samples. Unfortunately, the films were contaminated by silver salts and gelatin, which were leached from the coating on the paper. The gelatin was held tenaciously within the latex film and could still be detected after exhaustively washing in distilled water. Its presence in the film will probably influence any morphological changes which occur on ageing, since it is likely to adsorb on the particle surface, forming part of the hydrophilic boundary layer.

3. PTFE Dish

PTFE is very difficult to machine and it is doubtful that a specular surface can ever be obtained. Furthermore, it is easily damaged in use. High temperature and pressure moulding techniques are used commercially to fabricate PTFE articles[1], and might have produced better results: unfortunately, this process was not available.

The major disadvantage with PTFE was its extreme hydrophobicity, which restricted the range of film thickness available to greater than 200 μm. This is due to the high equilibrium thickness of a water film on PTFE (0.5 mm[2]), below which the film will disjoin.

4. Silicone Rubber Dish

Silicone rubber dishes were cast in a specially made aluminium alloy mould. It was possible to machine and polish the surface of the mould to a mirror finish, imparting a similarly smooth finish to dishes cast in it. However, the surface was too hydrophobic to permit the preparation of sufficiently thin latex films. Furthermore, it was discovered that the silicone rubber resin contained fillers, from which contaminants were easily leached[3].

5. Silanised Glass

Silanising and mould release agents on glass or metal substrates have been reported as a suitable substrate for the preparation of latex films. Eissler[4] used a dilute solution of fluorosilane or quaternary alkyl ammonium salt on plate glass, giving a fluorocarbon or hydrocarbon surface, respectively. It was claimed that the fluorocarbon surface was stable, even after treatment with chromic acid. However, hydrocarbon surfaces were not so durable, being removed by this treatment.

The fluorosilane compounds used by Eissler were development materials, and were not available in the UK. A hydrocarbon suface was prepared by treating a sheet of plate glass with dimethyl dichlorosilane. The plate glass was

of optical quality, and should therefore have been perfectly smooth. The treated surface was very hydrophobic, and the problem of disjoining and retraction encountered with the PTFE and silicone rubber dishes was experienced here too. Application of adhesive tape to the edges of the plate glass did not prevent this.

The first film cast on this surface could be removed easily, without undue stretching. However, subsequent films adhered strongly, indicating that some of the hydrocarbon surface had been removed by, and remained on, the latex film surface.

As an alternative to the silane, a proprietry mould release agent Cilase 1812 (Compounding Ingredients Ltd., Byrom House, Quay Street, Manchester, M3 3HS) was evaluated. This material was developed for integral skin polyurethane foams, and the treated surface was claimed to be capable of multiple releases. However, subsequent re-use without retreatment did not prove possible.

6. Conclusions

All the conventional techniques of film casting described above had disadvantges which precluded their use with surfactant-free latices. With the exception of PTFE, all the surfaces contaminated the film to some extent. Surface hydrophobicity was another common problem, resulting in the minimum available thickness being several times larger than that required. The only means of overcoming this problem while still using the PTFE dish would be to reduce the surface tension of the latex by adding a surfactant, which would detract from the ideality of the system. Another possible solution lay in forming the polymer film so quickly that the liquid film could not disjoin. This approach was suggested by the flash coating process widely used by the pharmaceutical industry in tablet manufacture. A detailed evaluation of the technique is given below.

B. FLASH CASTING TECHNIQUE FOR THE PREPARATION OF POLYMER LATEX FILMS

1. Evaluation of Technique using Prototype Apparatus

The prototype hotplate and glass spray unit described in Chapter II were tested under a wide range of conditions (e.g. surface temperature, applied air pressure, latex solids content, distance between sprayer and hotplate, etc.) in order to determine the procedure which gave the best film samples. A poly (n-butyl methacrylate) latex was used for the initial work, since this was readily removed at room temperature and amenable to scanning electron microscope examination.

a. Effect of Temperature

The surface temperature could be varied between 373 and 493K. At temperatures below 393K, the first burst of spray cooled the hotplate to below the boiling point of water, giving the aerosol droplets time to coalesce and form spots or runs on the film surface. The upper temperature limit was set by the melting point or decomposition temperature of the polymer concerned[5,6]. However, it was found that poly (n-butyl methacrylate) films left at 493K for about ten minutes became too brittle to remove from the surface. This effect was confirmed by heating a previously prepared film in an oven at 493K and leaving for ten minutes.

b. Effect of Applied Pressure

The average droplet diameter at 20 psi was 12 μm, and the maximum size 17 μm. The droplet size fell slightly with increasing pressure, but below 20 psi, the aerosol was visibly coarser. Any attempt to spray a latex at above 50 psi resulted in blockage of the orifice, presumably due to shear instability. With surfactant-containing latices higher pressures could be employed. The pressure giving the optimum delivery of aerosol was found to be in the range 25 -30 psi.

c. Effect of Solids Content

A film prepared from a latex of greater than 8% solids content usually had a visibly rough top surface. However, if the latex was too dilute, a large number of passes was necessary to obtain the required thickness, and this tended to produce a rougher top surface. Within these limits, there was no apparent difference between two films of similar thickness cast from latices of different solids content.

d. Effect of Latex Particle Size

Films were cast from latices with particle diameters in the range 100 - 900 nm. There was no discernable effect of particle size on the film properties or the ease of preparation.

e. Film Morphology

(i) Film surface cast against PTFE substrate. SEM examination of the bottom surface of a freshly cast poly (n-butyl methacrylate) film showed a pattern of striations (see plate IV:1). Examination of a piece of the PTFE sheet used in the construction of the prototype apparatus showed a similar, but more pronounced pattern (Plate IV:2). The PTFE sheet is manufactured by a process known as skieving, in which the sheet is cut from a rotating

Plate IV:1

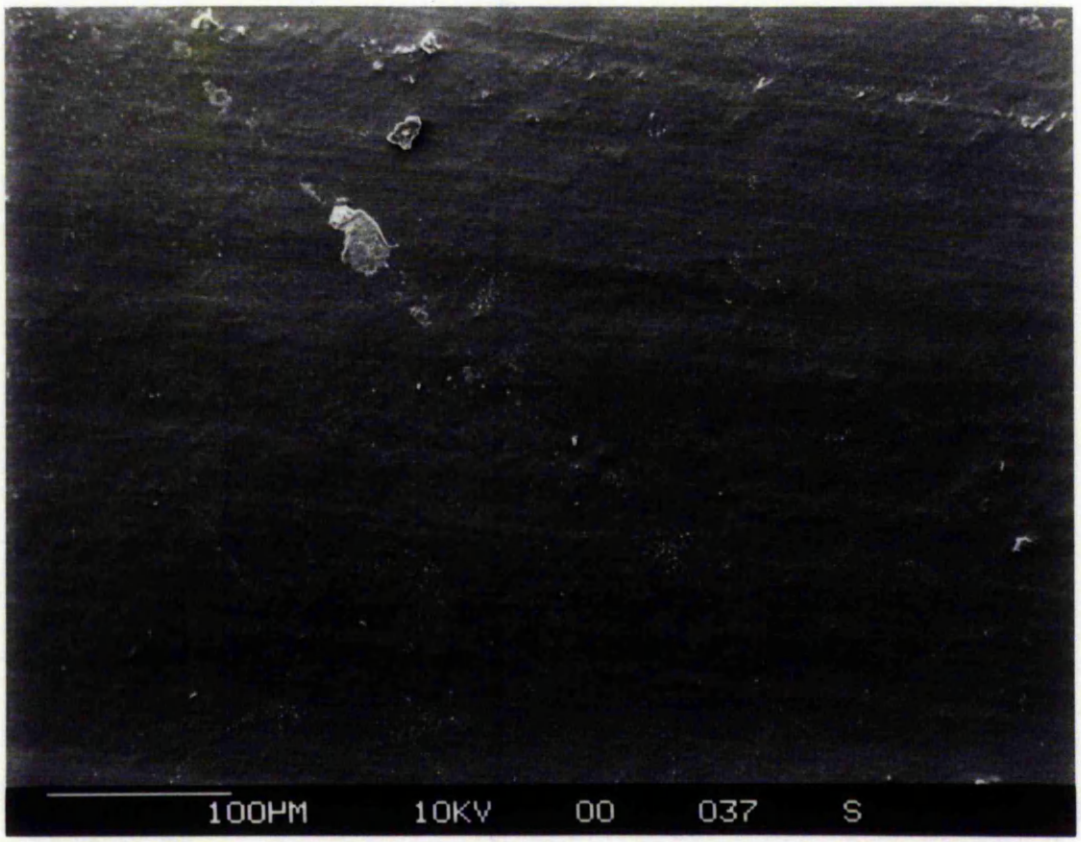

Plate IV:1

SEM of poly (n-butyl methacrylate) latex film. Surface cast against PTFE sheet. Magn. 250 x.

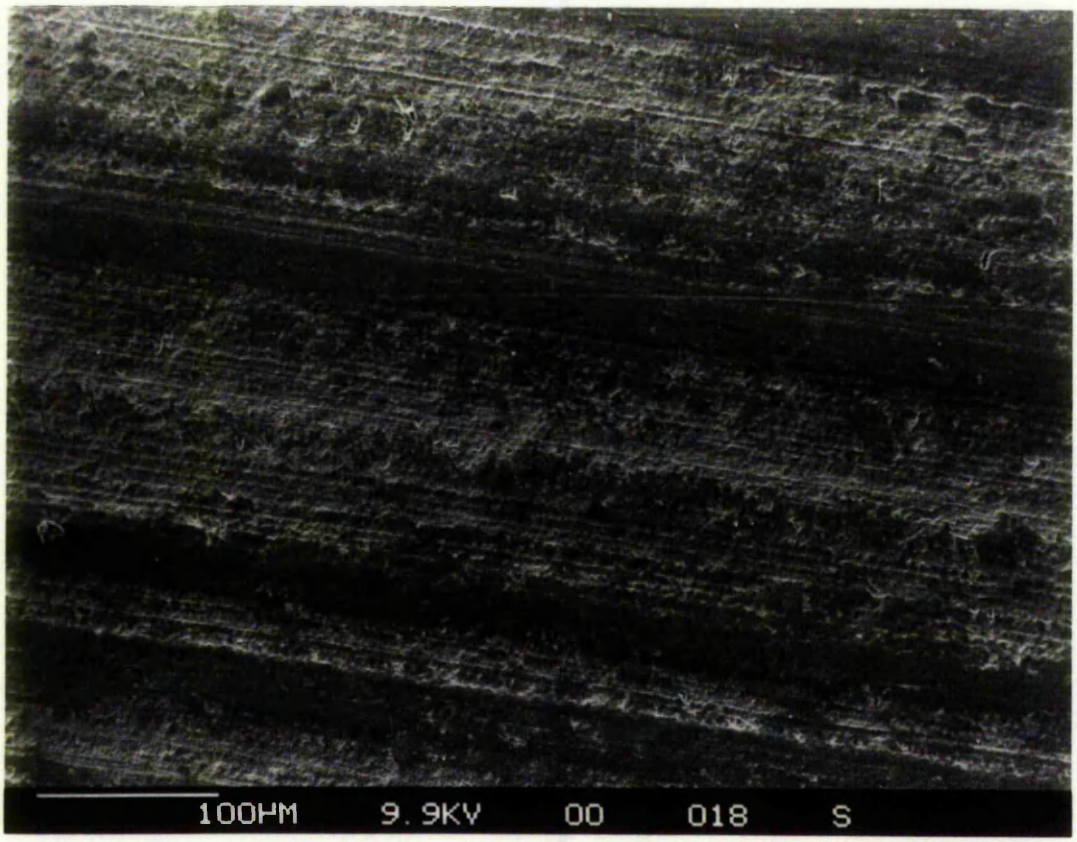

Plate IV:2

SEM of surface of PTFE sheet used in prototype flash casting apparatus Magn. 250 x.

PTFE cylinder by a long knife blade, which results in the observed pattern. The substrate pattern is then reflected on the surface of the film cast against it.

As well as being undesirable per se, the striations make the PTFE surface slightly porous. This is likely to increase the adhesion of the film to the substrate, making removal more difficult.

(ii) Sprayed Film Surface. A freshly cast poly (n-butyl methacrylate) film had a 'lumpy' top surface (see Plate IV:3) presumably arising from the last burst of spray during preparation. The largest of these lumps appeared to comprise 10 - 20 individual particles and extend about five particle diameters above the plateau (Plate IV:4). On fully aged films, these lumps had disappeared, and the surface took on a rippled appearance, with depressions of a few μm deep and hundreds of μm across (Plates IV:5 and IV:6). The debris scattered on the film surface depicted in Plate IV:5 is probably dust which accumulated during the one month storage period. It is possible that some dust is trapped in the interior of the film when the latex is sprayed, although none was ever observed in fracture cross sections. Film thicknesses were measured with a dial gauge having a flat tip. This tip would be expected to bridge several lumps, giving a thickness 2 - 3 μm larger than the plateau thickness. The variation in thickness of any given film sample was around 10%, so it was not possible to determine if the measured thickness altered on ageing.

(iii) Interior Morphology. Several cross-sections of films, prepared by fracturing at liquid nitrogen temperature, were examined by SEM. The fracture cross-section of a freshly cast poly (n-butyl methacrylate) film is shown in Plate IV:7: this is typical of all such films examined, none of which appeared to alter on ageing. It can be seen that approximately equal numbers of small lumps and cavities are scattered around the surface: these are probably due to individual polymer chains having separated from or removed to, the opposite surface, producing the lumps and cavities respectively. If the film was allowed to warm up between fracturing and shadowing, these features disappeared, presumably due to polymer flow. The film shown in Plate IV:7 is approximately 20 μm thick, and its latex precursor had a particle diameter of 480 nm. If it is assumed that one third of the reduction in volume, which accompanies particle coalescence, occurs only along the thickness dimension, then the film will be 45 particles thick. If a particle structure existed and was visible to SEM, then

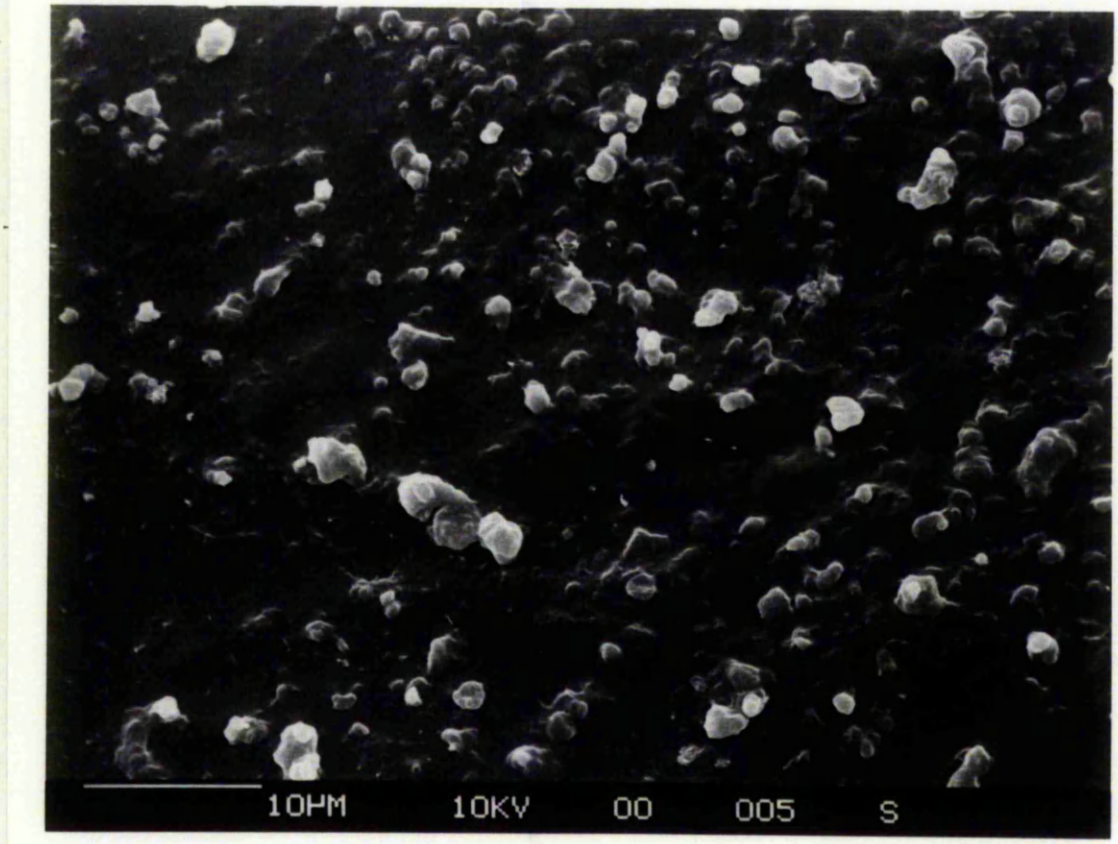

Plate IV:3

SEM of poly (n-butyl methacrylate) latex film. Sprayed surface immediately after casting. Magn. 2,500 x.

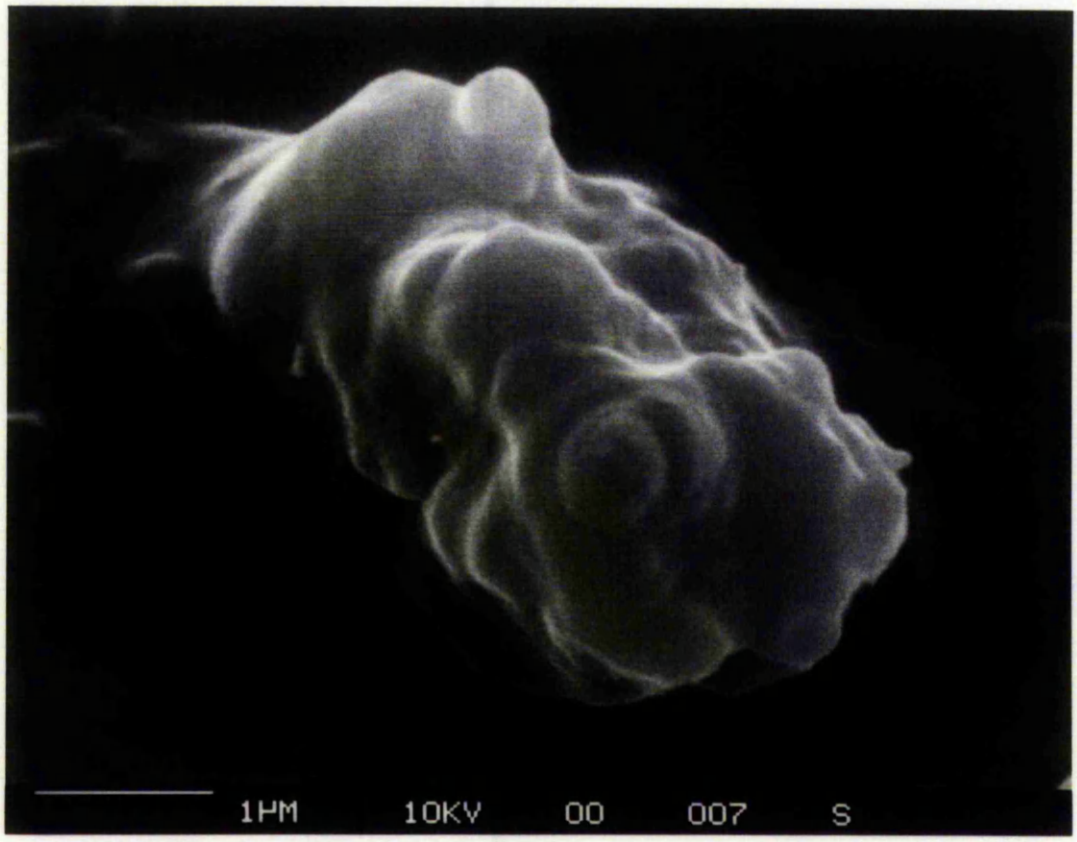

Plate IV:4

SEM of poly (n-butyl methacrylate) latex film. Sprayed surface immediately after casting. Magn. 25,000 x.

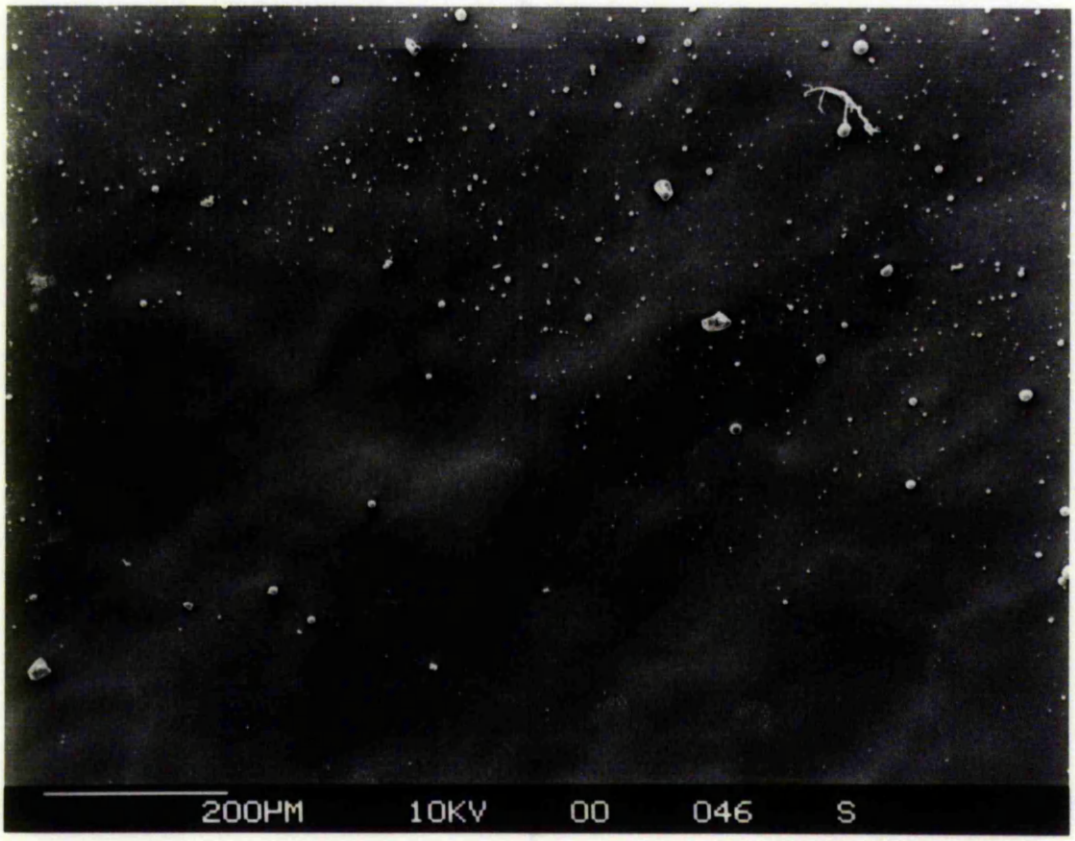

Plate IV:5

SEM of poly (n-butyl methacrylate) latex film. Sprayed surface one month after casting. Magn. 6,250 x.

Plate IV:6

SEM of poly (n-butyl methacrylate) latex film. Sprayed surface one month after casting. Magn. 6,250 x.

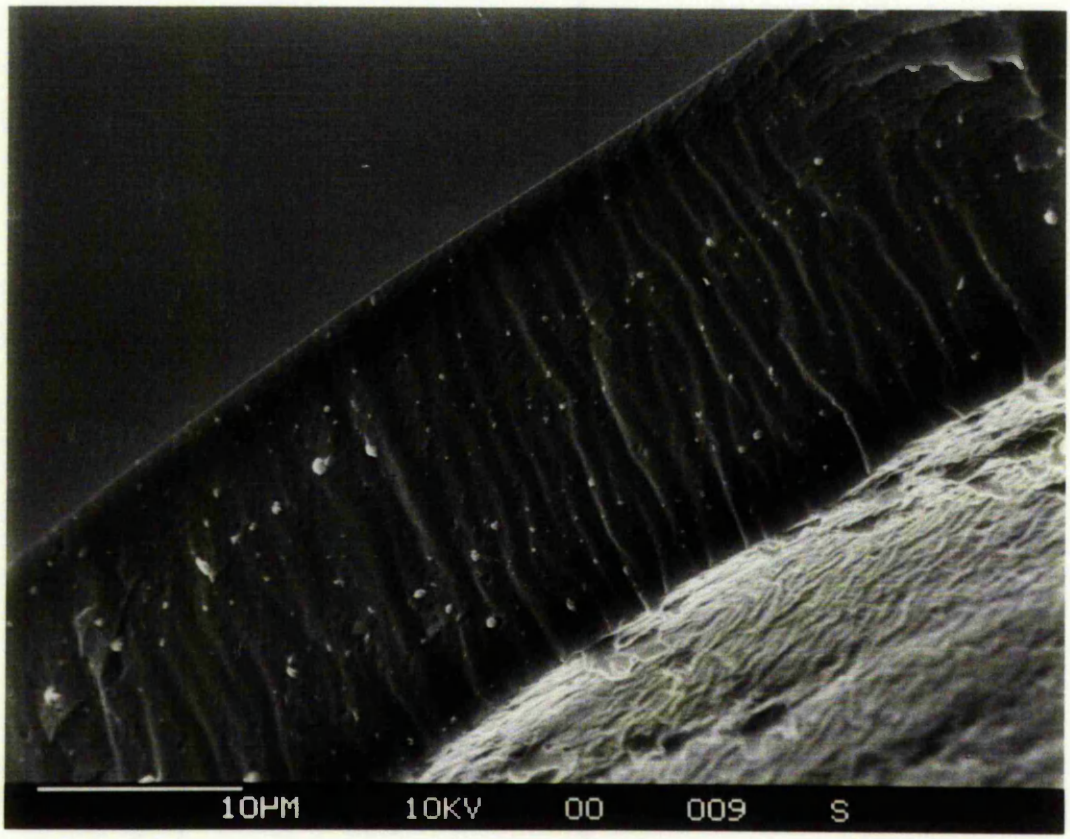

Plate IV:7

SEM of poly (n-butyl methacrylate) latex film. Cross section fractured at 77K. Magn. 2,500 x.

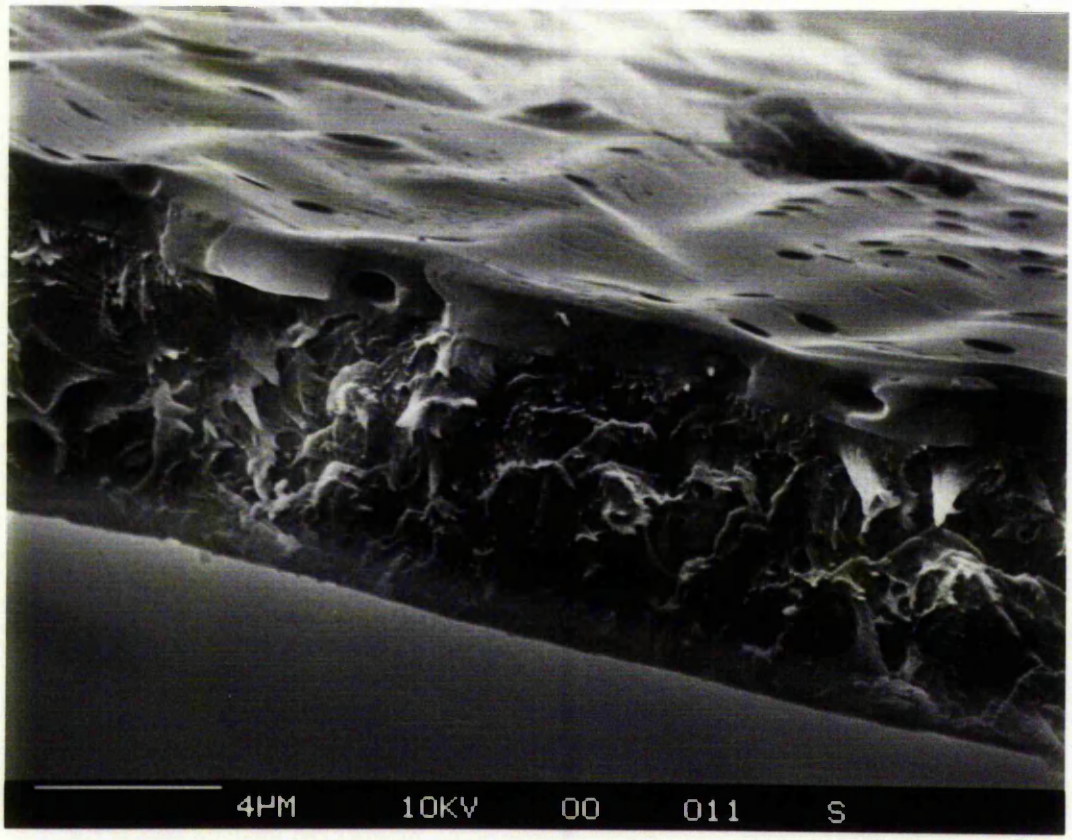

Plate IV:8

SEM of poly (n-butyl methacrylate) film cast from solution in butanone. Cross-section fractured at 77K. Magn. 6,250 x.

it should be visible here. No such structure was ever observed, even at higher magnifications.

It is interesting to compare the apparently featureless fracture cross-section of a flash cast poly (n-butyl methacrylate) latex film (Plate IV:7) with the corresponding solvent-cast polymer films (cast in a dish using butanone as solvent) (Plate IV:8). This film displays the same rippled top surface as the fully-aged flash cast latex films. In addition, there is a separate top layer approximately 1 μm thick, which may be due to a skin forming on the surface of the film during the initial stage of drying. This surface layer contains a number of what appear to be air bubbles. These were found even when the polymer solution was degassed under vacuum prior to casting the film.

A further difference between the fracture cross-sections (which were both done at liquid nitrogen temperature) is that the latex film is much smoother than the solvent cast film. It is tentatively suggested that this is due to the more complete mixing of polymer chains in the soluton prior to casting, causing greater disruption of the structure on fracture. The latex film may simply have cleaved along a line of particle boundaries, presuming these to have been maintained.

The interior morphology of a poly(ethyl acrylate) coated polystyrene film is shown in Plate IV:9. The thickness of coat was only just sufficient (50 nm) to give a coherent film. This was however, very brittle and flaked off rather than peeled from the surface. The film was cast at 393K, ie. 20K above the T_g of polystyrene. It is interesting to note that the polystyrene core particles are easily visible as spheres, and have not deformed into dodecahedra. A polystyrene latex of comparable particle size formed films, under comparable casting conditions, which were usually non-porous (as determined by its low permeability coefficient). Another feature of the film shown in Plate IV:9 is the high degree of order in the packing of the latex particles.

f. Uniformity of Film Thickness

The variation in thickness of sprayed films could usually be kept to less than 10%, and, after practice, variations of as little as 5% could be achieved. As might be expected from the side to side spraying pattern, the variation across this dimension was less than from top to bottom. The optimum thickness for uniformity was in the range 30 - 70 μm. Films thinner than 30 μm were generally less uniform and more prone to pinholes. The thinnest non-porous film prepared was 16 μm. Films thicker than 70 μm could be prepared, but the top surface was often unacceptably rough, due to the high solids content or large

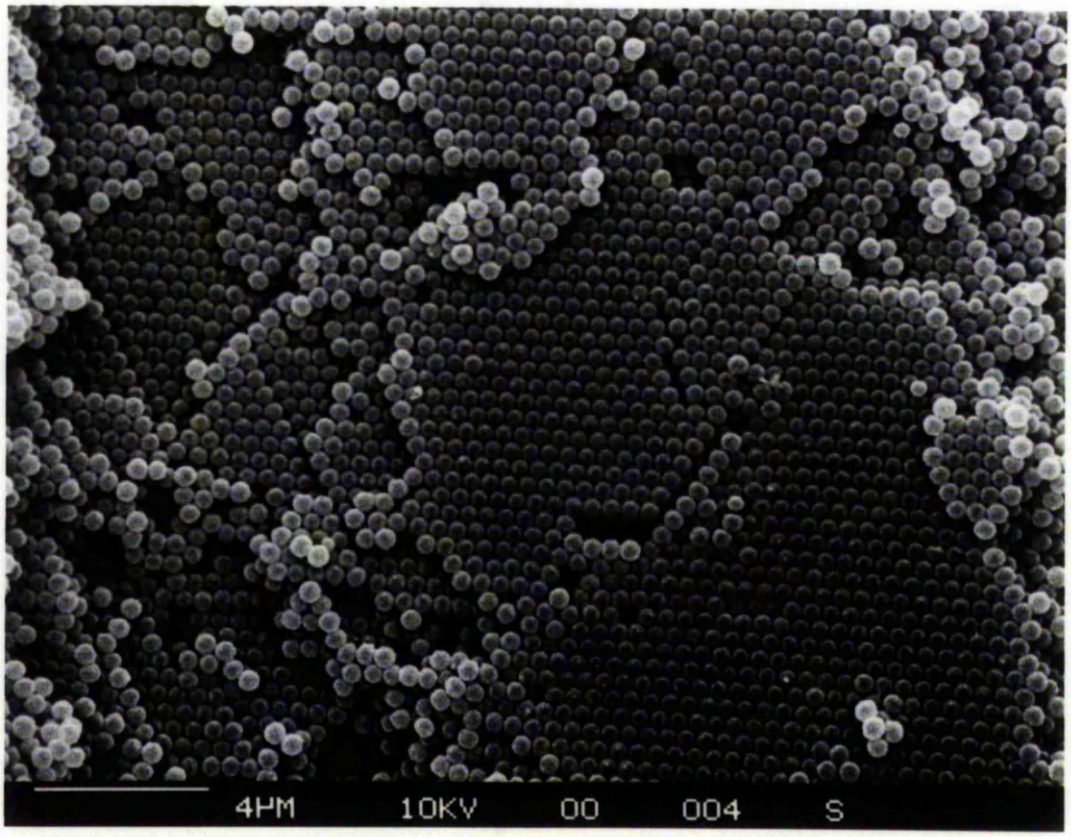

Plate IV:9

SEM of poly (ethyl acrylate) coated polystyrene core-shell latex film cross-section fractured at room temperature. Magn. 6,250 x.

number of passes required. One maladroit pass could ruin a film which had taken upwards of 80 passes already, so thick films were only attempted when strictly necessary.

g. Optimum Temperature for Film Removal

When attempting to cast films other than from poly (n-butyl methacrylate) latices on the prototype hotplate, it became apparent that the optimum temperature range for removal of the films varied according to the polymer type. It was necessary to maintain the block at a temperature within a few degrees of the T_g of the polymer concerned. If the temperature was too high, the film adhered to the surface too strongly and stretched on removal. If too low, the film was quite often brittle and disintegrated. The optimum removal temperature for films cast from core-shell latices was higher than that of the coating polymer. The extent increased with decreasing coating polymer thickness and was greatest (around 40K) where the coating thickness was only just enough to impart adequate strength to the film.

2. Final Design of Hotplate

After some experience had been gained with the prototype a second hotplate was designed which incorporated a number of improvements:

(i) The aluminium plate was replaced by a copper block, 25 mm thick, to give better heat transfer characteristics and ensure a more uniform temperature distribution on the surface.

(ii) The PTFE surface was directly bonded onto the front face of the block, thus obviating the problem of surface roughness encountered with the PTFE sheet.

(iii) A parting rod was included, so that the film could be removed without scraping a corner of the block to lift an edge

(iv) provision for a slush bath was made, so that the block could be cooled below room temperature. This permitted the removal of polymer films having a T_g below ambient.

a. Effect of Operating Parameters on Film Quality

The effects of altering various operating parameters were the same as those observed with the prototype block. The surface cast against the PTFE

substrate was much smoother, as intended (see Plate IV:10). It was not possible to examine the PTFE substrate, since this was bonded to the copper block. However, since films cast against it did not mirror any visible imperfections and it was inferred that the surface was acceptably smooth.

b. Range of Latex Films Available

A wide range of thin homopolymer, copolymer and core-shell latex films were prepared by means of the flash casting technique. The limits of its applicability were set by the temperature at which the film was removed. Where the difference between this temperature and ambient was too great, hard and soft polymer films became respectively too brittle or too elastic, once stripped from the surface, to withstand the remainder of the removal process undamaged. For this reason, no poly(methyl methacrylate) or poly (n-butyl acrylate) films could be prepared. This limitation might possibly be overcome by housing the hotplate in a chamber such that the surroundings could be maintained at a suitable temperature for complete film removal. This solution would, however, preclude manual removal of the film, and hence involves formidable practical difficulties. A few polystyrene films were prepared, with great difficulty, on the prototype hotplate, where the PTFE was stretched over the substrate, rather than directly bonded to it. The surface of the PTFE on this hotplate was slightly plient, and probably stretched slightly during film removal. This would have reduced the tension on the brittle polystyrene film enabling it to be removed.

Copolymer and core-shell latex films were prepared by the flash casting technique. There were no special problems associated with these films (even with polystyrene core contents as high as 68%, which is close to the theoretical maximum). However, films cast from blends (i.e. mixtures of two latices) could not always be successfully prepared. In particular, blends containing more than 20% polystyrene, in combination with any acrylate or methacrylate polymer latex could not be removed from the hotplate, although the films appeared to be continuous. Min et al.[7] found that a film cast from a mixture containing 50% each of polystyrene and poly (n-butyl acrylate) latices, by drying at room temperature, formed an opaque, cracked film. In contrast, core-shell latices of the same composition, prepared by seeded emulsion polymerisation, formed clear, continuous films.

Some workers have, however, reported the preparation of continuous films from blends of hard and soft latices. Hughes and Brown[8] were able to prepare films from a mixture containing equal proportions of polystyrene and poly (methyl acrylate). Peterson[9] prepared films containing 28% polystyrene, poly (vinylidene chloride) or poly (methyl methacrylate) dispersed in poly (vinyl

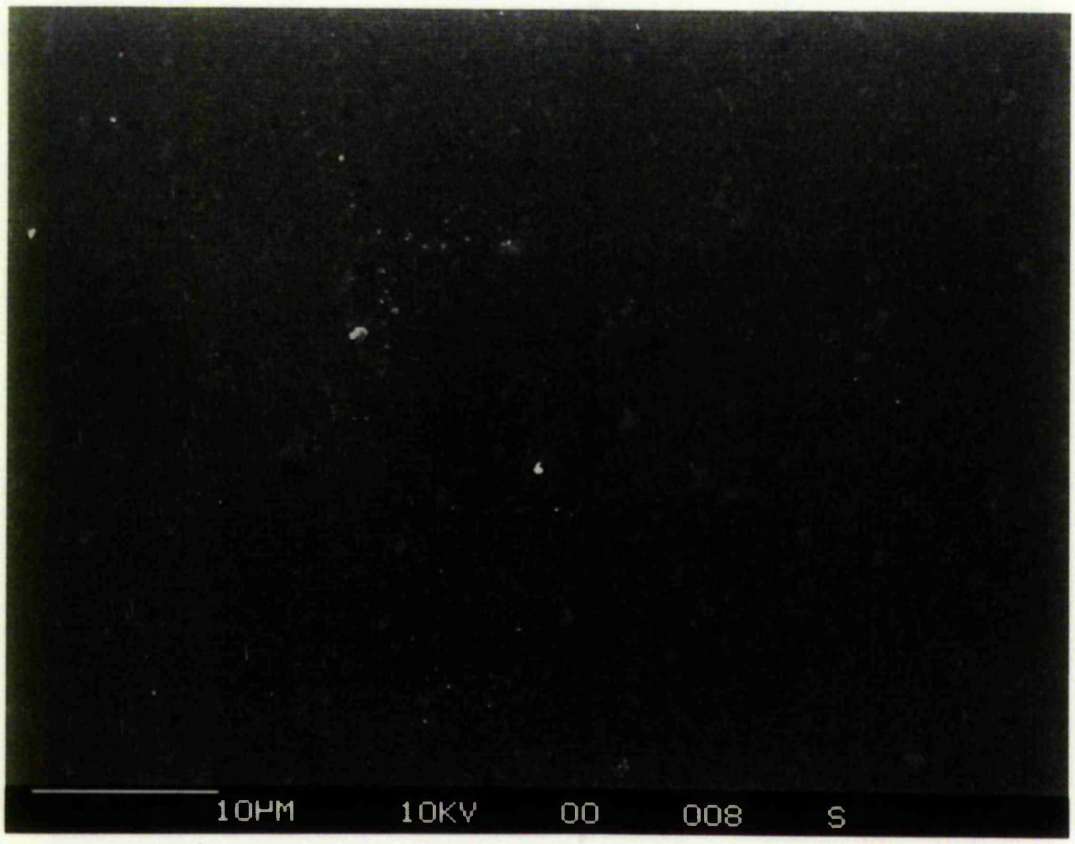

Plate IV:10

SEM of poly (n-butyl methacrylate) latex film. Surface cast against PTFE coated copper. Magn. 2,500 x.

acetate). To prevent agglomeration of the disperse phase latex on mixing, it was necessary to dilute it beforehand. Samples of the films were examined by scanning electron microscopy. This showed that the polystyrene particles were deformed, and this was attributed to powerful compressive forces generated by the continuous phase poly (vinyl acetate) particles on drying. This explanation seems unlikely since spherical polystyrene particles have been observed in fracture cross-sections of core-shell latex films prepared by the flash casting technique (Plate IV:9). It is not certain why these particles remain undeformed. It is possible that the film was not maintained at a sufficiently high temperature for long enough for complete coalescence to occur.

C. APPEARANCE OF LATEX FILMS

This section deals briefly with the visual and mechanical properties of latex films prepared by the flash casting technique. The clarity, flexibility and tackyness of different types of latex film are listed in Table IV:1 and some typical tensions - extension curves are shown in Fig. IV:1. In appearance, the latex films were rarely transparent although films prepared from freeze-dried latex polymer by casting from solution often were. In terms of tackiness and flexibility, the behaviour of latex and solvent cast films usually resembled each other quite closely. The exceptions were films cast from either core-shell latices or blends, which contained a high proportion of a hard core polymer (usually polystyrene). The films were extremely brittle. The corresponding solvent cast films were similar to a copolymer film containing the two components in the same proportions. The brittleness of the core-shell and blend latex films is probably due to the influence of hard, undeformable polystyrene particles which are sufficiently close together as to resist any motion relative to one another. The blend films were more brittle than core-shell films of the same composition, and this may indicate aggregation of the dispersed polystyrene particles, in a manner similar to that observed by Peterson[9]. Solvent cast films prepared from the same precursors behave differently, presumably because the components are more intimately mixed.

The tension-extension curves shown in Fig. IV:1 show the expected rigidity of polystyrene and elasticity of poly (n-butyl acrylate) and poly (n-butyl methacrylate). The core-shell latex films behave in the manner expected of filled polymer films[10], combining the rigidity of the dispersed polystyrene particles with the elasticity of the continuous acrylate polymer phase.

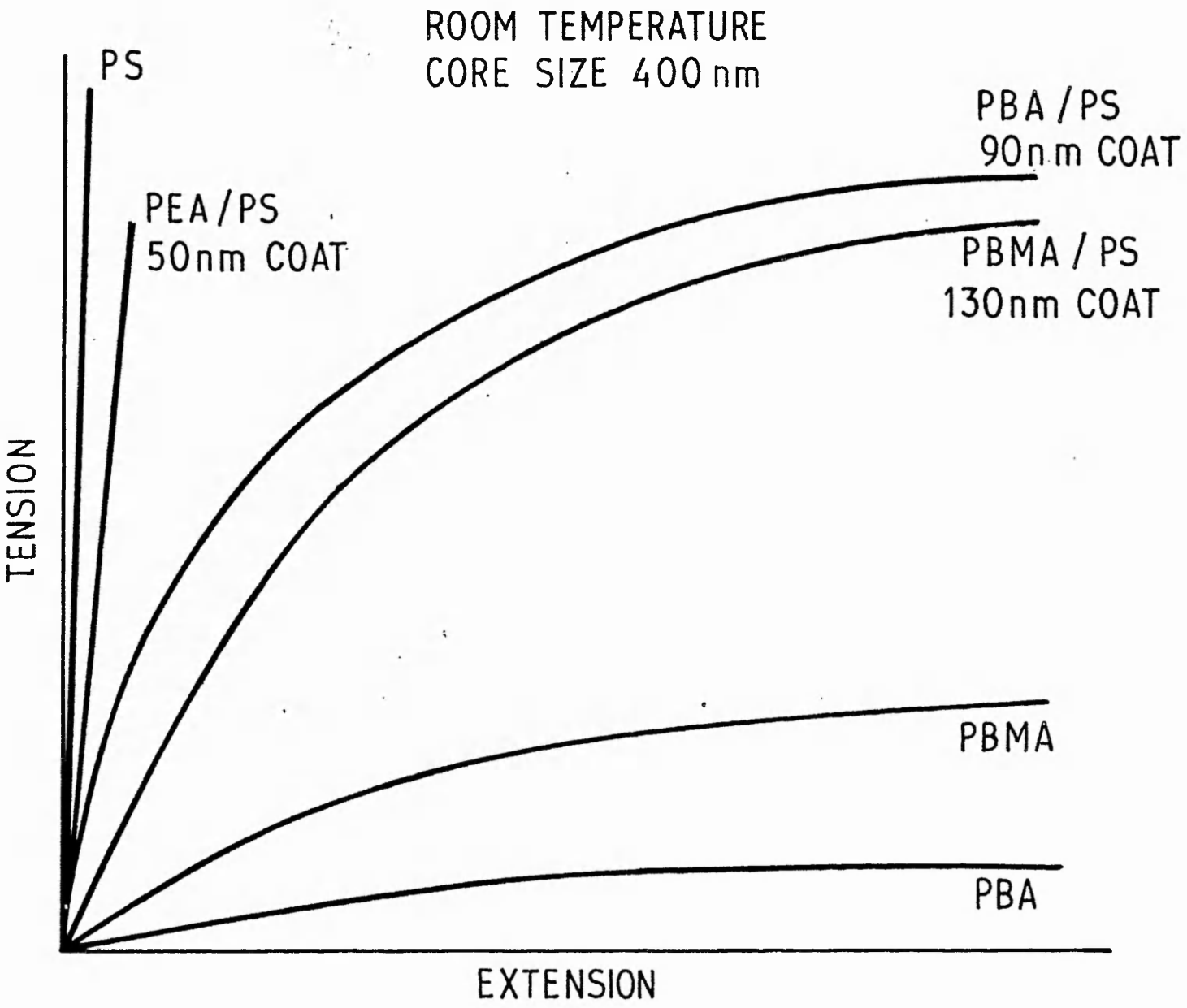

FIG IV:1 GRAPH SHOWING TENSION - EXTENSION CURVES FOR SOME HOMOPOLYMER AND CORE-SHELL LATEX FILMS

TABLE IV:1

VISUAL PROPERTIES OF LATEX FILMS

HOMOPOLYMERS		
Polystyrene		Translucent, brittle, non-tacky
Poly(ethyl methacrylate)		Translucent, brittle, non-tacky
Poly(n-butyl methacrylate)		Translucent, flexible, non-tacky
Poly(methyl acrylate)		Translucent, flexible, non-tacky
Poly(ethyl acrylate)		Transparent, flexible, tacky
COPOLYMERS		
ethyl acrylate-methyl methacrylate	67/33	Transparent, flexible, tacky
	20/80	Translucent, flexible, non-tacky
ethyl acrylate-	40/60	Transparent, flexible, tacky
n-butyl methacrylate	60/40	Transparent, flexible, tacky
	80/20	Transparent, flexible, tacky
BLENDS		
Polystyrene/poly(n-butyl methacrylate)	20/80	Translucent, brittle, non-tacky
Polystyrene/poly(ethyl acrylate)	20/80	Translucent, brittle, non-tacky
	20/80	Translucent, flexible, non-tacky
Poly(ethyl acrylate)	40/60	Transparent, flexible, non-tacky
Poly(n-butyl methacrylate	60/40	Transparent, flexible, tacky
	80/20	Transparent, flexible, tacky
CORE-SHELL		
	19.7/80.3	Translucent, flexible, non-tacky
Polystyrene/poly	26.7/73.3	Translucent, flexible, non-tacky
(n-butyl methacrylate)	42.2/57.8	Translucent, flexible, non-tacky
	60.6/39.4	Translucent, brittle, non-tacky
	68.6/31.4	Translucent, brittle, non-tacky
Polystyrene/poly	20.3/79.7	Translucent, brittle, non-tacky
(n-butyl acrylate	32.8/67.2	Translucent, flexible, non-tacky
Poly(n-butyl methacrylate) poly(ethyl acrylate)	60/40	Translucent, flexible, non-tacky

D. REFERENCES

1. F.W. Billmeyer, "Textbook of Polymer Science, second edition, Wiley Interscience (1971).

2. M.C. Wilkinson, M.P. Aronson, A.C. Zettlemoyer and J.W. Vanderhoff. J. Colloid Interface Sci. 68, 575 (1979).

3. B.J. Meakin, University of Bath, personal communication.

4. R.L. Eissler, J. Appl. Polym. Sci., 12, 1983 (1968).

5. N. Grassie and J.R. MacCallum, J. Polym. Sci., Part A, 2, 983 (1964).

6. J. Brandrup and E.H. Im mergut (eds.), "Polymer Handbook", Second edition, Wiley Interscience (1975).

7. T.I. Min, A. Klein, M.S. El-Aasser and J.W. Vanderhoff, J. Polym. Sci., Polym. Chem. Ed., 21, 2865 (1983).

8. L.J. Hughes and G.L. Brown, J. Appl. Polym. Sci., 5, 580 (1961).

9. C.M. Peterson, Ibid, 12, 2649 (1968).

10. L.E. Nielsen, "Mechanical Properties of Polymers and Composites", Volume 1, Marcel Dekker (1974).

CHAPTER V

TRANSMISSION PROPERTIES OF POLYMER FILMS

A. EVALUATION OF APPARATUS

The apparatus used to determine film transmission properties was equipped with a katharometer to measure the concentration of gaseous penetrants. This type of apparatus has been successfully employed to measure both diffusion and permeability coefficients for certain polymer/penetrant systems[1]. Limitations due to detector sensitivity and response time have also been reported[2]. Since the diffusion coefficient is derived from the approach to the steady state of permeation, it is imperative that the response time is shorter than the time taken to establish this steady state. In borderline cases, the transient state can be extended by increasing film thickness. However, while the increase in the duration of the transient state is proportional to l^2 (where l is the film thickness), the amount of penetrant passing through the film diminishes in proportion to l. Therefore to quadruple the duration of the transient state requires a two-fold increase in film thickness, which entails a two-fold reduction in penetrant concentration. It is often the case that to measure the diffusion coefficient for a particular polymer/penetrant combination requires a film thickness so large that the steady state penetrant concentration is barely detectable.

A further disadvantage of the katharometer as a detector is that its

concentration response is only linear at low concentrations. In the absence of a specially prepared calibration gas mixture, it is difficult to reliably calibrate a katharometer at the low concentrations expected to be present in the sweep gas stream. A suitable calibration mixture was available for helium in nitrogen, and so the helium permeabilities reported here are believed to be accurate. Permeabilities to hydrogen, oxygen, argon and carbon dioxide were also measured for some of the latex films prepared, but as the calibration for these gases is doubtful, these can only be considered order-of-magnitude estimates. The ratios of these permeabilities were, however, in reasonable agreement with those reported by Stannett and Szwarc[3].

As a test of the apparatus the permeability coefficient and activation energy of permeations were determined for the helium/polyethylene system. The polyethylene film, of 12.7 μm thickness, was a sample of a batch specially manufactured for use as a battery separator (Smith and Nephew Plastics Ltd., English Street, Hull). The density of the polymer was 0.920 g cm^{-3} and the crystalline content 35%. The helium permeability was found to be 5.4 10^{-17} s m^3 kg^{-1} and the activation energy of permeation 33.2 kJ mol^{-1}. These values are in satisfactory agreement with literature values [4] for low density polyethylene of 5.1 10^{-17} s m^3 kg^{-1} and 34.7 kJ mol^{-1}.

B. PERMEABILITIES OF SOLVENT CAST FILMS

There is very little published diffusion and permeation data for the polymer/penetrant systems of interest. For example, the Polymer Handbook [4] lists only poly(ethyl methacrylate) out of the six alkyl acrylate and methacrylate polymers studied in this work. Furthermore, it is necessary to treat literature data with some caution, since differences in the method of measurement used, together with a lack of detailed knowledge of the source, history and characteristics of the polymer specimen, results in considerable uncertainty as to their reliability [5]. For these reasons, it was necessary to determine the transmission properties of the polymers of interest by casting samples of freeze-dried latex polymer films from solution in suitable solvents. This then allowed a direct comparison of solvent cast and latex films.

Films of poly(methyl acrylate), poly(ethyl acrylate), poly(n-butyl acrylate), poly(methyl methacrylate), poly(ethyl methacrylate) and poly(n-butyl methacrylate) were cast from solution in butanone. Polystyrene films were cast from solutions in toluene. The permeabilities to helium were determined at various temperatures and the activation energies of permeation calculated. Usually, five films of average thickness in the range 15 - 80 μm were prepared.

The data for each polymer were somewhat scattered, and no correlation with thickness was apparent. The results, together with the T_g's of the polymers are presented in Table V:1.

The permeability coefficients show an increasing trend with decreasing T_g's. Since both these quantities are influenced by chain stiffness and intermolecular forces, this is not unexpected. The differences between individual acrylates and methacrylates are, however, quite small and, in one case, within experimental error. Between acrylates and methacrylates as a class, the difference is much larger. This is presumably due to the relative effect of substituting a hydrogen for a methyl group being greater than, say, a methyl for a n-butyl group. Another possible reason concerns the likely difference in the amounts of branching in acrylate and methacrylate polymers. The former contain a labile tertiary hydrogen, and are therefore susceptible to chain transfer to polymer side reactions [6]. This leads to a more highly branched polymer chain, which in turn results in a more open structure and a higher permeability. A further possibility is that chain transfer reactions occur to such an extent that the polymer becomes significantly cross-linked. Distler and Kanig [7] have observed that freeze-dried poly(ethyl acrylate) and poly(n-butyl acrylate), when dissolved in tetrahydrofuran, give cloudy solutions indicative of gelation rather than true solution. Examination of films cast from these solutions by electron microscopy revealed a honeycomb pattern similar to that previously observed with latex films. The honeycomb patterns were ascribed to particle boundaries. Their appearance in solvent cast films was attributed to sufficient cross-linking in the latex particles that their separate identities were maintained, i.e. the latex particles had swelled extensively in the solvent but had not lost their integrity. This last possibility can, however, be discounted here, since the solutions, from which the films were cast, were invariably clear. Also, the polymers were characterised by gel permeation chromatography. Any significant cross-linking would have resulted in column blockage.

Although the data are more scattered, the activation energies of permeation appear to increase with increasing permeability and decreasing T_g. This is contrary to the trends normally encountered. High diffusion and permeability coefficients are usually associated with low activation energies and, for a related series of polymers, the activation energy of diffusion is expected to increase with increasing glass transition temperature [7]. The explanation for the behaviour observed here is probably connected with the temperature range for which the activation energies were determined - these being in the region of the T_g's of some of the polymers. It is known that some,

TABLE V:1

HELIUM PERMEABILITIES OF SOLVENT CAST POLYMER FILMS AT 303K

Polymer	Tg/K	$10^{16}P/Sm^3kg^{-1}$	$E_p/kJ\ mol^{-1}$
PMMA	378	0.80 ± 0.11	26.6 ± 0.89
PEMA	338	1.0 ± 0.11	28.0 ± 1.4
PEMA[a]	338	0.95 ± 0.14 (0.59)	26.0 ± 0.84 (26.8)
PBMA	293	1.1 ± 0.08	25.7 ± 0.59
PMA	283	1.8 ± 0.10	28.4 ± 0.74
PEA	249	2.0 ± 0.05	32.3 ± 0.28
PBA	219	2.2 ± 0.07	30.8 ± 0.35
PS[b]	373	1.3 ± 0.09 (1.4)	23.8 ± 0.46

Polymer films cast from solution in butanone except (a) chloroform and (b) toluene. Literature values[4] in parentheses.

but not all, polymers have a change in the slope of the Arrhenius plot in the region of the T_g with the calculated activation energy being higher above T_g [9]. No change in slope was observed for polystyrene, poly(methyl methacrylate) or poly(ethyl methacrylate), for which the T_g's could be straddled. This agrees with the findings of Stannett and Williams [10] for poly(ethyl methacrylate). A change of slope has been observed for poly(methyl acrylate) [11]. However, since the T_g is below room temperature, and therefore inaccessible to the apparatus, this could not be confirmed.

In view of the data presented by Kaminska (12) which showed that the air permeability of solvent cast polystyrene films was strongly dependent on molecular weight, it was important to determine the effect of molecular weight on permeability. Three samples of polystyrene and five of poly (n-butyl methacrylate), with molecular weights in the range of interest, were examined. The results, presented in Table V:2, show no significant variation in helium permeability with molecular weight in the range produced by surfactant-free emulsion polymerisation. A more detailed study, involving fractionation of the polymer samples was not thought necessary.

There are very few published results with which to compare the data obtained in the present work and agreement with the little that does exist[4] is not always good. For example, Stannett and Williams' result[10] for the permeability coefficient for helium through poly(ethyl methacrylate) is only some 60% of the value obtained here - a difference which is more than four times the experimental error. The data were obtained, however, by a pressure change method, and the source and previous treatment of the film samples were also different. The poly(ethyl methacrylate) used by Stannett and Williams was either commercially available material of low molecular weight or obtained by slow solution polymerisation thus yielding a higher molecular weight polymer. The intrinsic viscosities in chloroform were respectively 0.10 and 0.32. Unfortunately, the molecular weights cannot be calculated from the relationship $[\eta] = K \bar{M}^{\alpha}$ since there are no published values of K and α for PEMA in chloroform. However, no differences in transmission properties were encountered. The films were compression moulded or cast from solution in chloroform and annealed at 363K for an unspecified duration.

The conditions described above are markedly different to those employed in this study.

The films were prepared from freeze-dried latex polymer, which had an intrinsic viscosity in chloroform of 0.17, by casting from solution in butanone. Once dry, the films were stored under vacuum at 333K for 24 hours, during which time there was no weight loss.

TABLE V:2

VARIATION IN HELIUM PERMEABILITY WITH POLYMER MOLECULAR WEIGHT

A - POLYSTYRENE

Latex Precursor	10^3Mw	10^3Mn	Mw/Mn	10^{16}P/SM^3 kg^{-1}
MC119	276	38	7.3	1.29 ± 0.067
MC120	241	36	6.6	1.31 ± 0.053
MC121	136	17	8.1	1.29 ± 0.047

B - POLY(n-BUTYL METHACRYLATE)

Latex Precursor	10^3Mw	10^3Mn	Mw/Mn	10^{16}P/SM^3 kg^{-1}
M122	877	115	7.6	1.09 ± 0.057
MC124	422	80	5.3	1.09 ± 0.078
MC125	262	86	3.0	1.11 ± 0.062
MC128	365	70	5.2	1.10 ± 0.054
MC130	370	71	5.2	1.11 ± 0.035

The water vapour permeabilities of poly (alkyl methacrylates) have been determined by Morgan[13] using a simple weighted-cell technique. The film samples were prepared by casting from solution in a 70:30 toluene/isopropanol mixture onto a heated chromium plated surface. Their results show the same trend observed here of increasing permeability with decreasing Tg. Recalling the functional relationships of Stannett and Szwarc[3] (see Chapter I), the ratio of the water vapour permeabilities obtained by Morgan may be compared with the ratio of the helium permeabilities determined here. The former gives $P_{PMMA} : P_{PEMA} : P_{PBMA} = 1:1.37 : 1.56$, compared with 1:1.25 : 1.38. (Had the helium permeability of PMMA been 0.7 instead of 0.8, a difference which is within the experimental error of the measurement, the ratio would have been 1: 1.42: 1.57).

C. TRANSMISSION PROPERTIES OF HOMOPOLYMER LATEX FILMS

Having determined the permeabilities of bulk polymer films, similar experiments were performed with latex films so that comparisons between the two could be made. The initial work was carried out with poly(n-butyl methacrylate) films, since these were easiest to prepare and handle. The major influences on latex film permeability were considered to be the characteristics of the latex precursor (namely particle size, polymer molecular weight and surface charge density) and film treatment (preparation and storage conditions). In order to examine the influence of casting and storage temperature, a single latex was used.

A major problem arising from the film casting process was the inherent irreproducibility in initial permeability between different films cast from the same latex. A large variation in initial permeability was also apparent with films flash cast from solution. However, the lowest values recorded were in good agreement with the lowest values obtained from films dish cast from solution. It was therefore concluded that the higher permeabilities were due to imperfections in the film. Therefore, several latex films were prepared for each variable examined, and the three lowest coincident results were taken to be the true result.

1. Variation in Latex Film Permeability with Film Age

The principal feature of poly(n-butyl methacrylate) latex film permeability was that the permeability coefficient was not constant, but decreased over a period of time (Fig. V:1). The initial value varied depending on the temperature

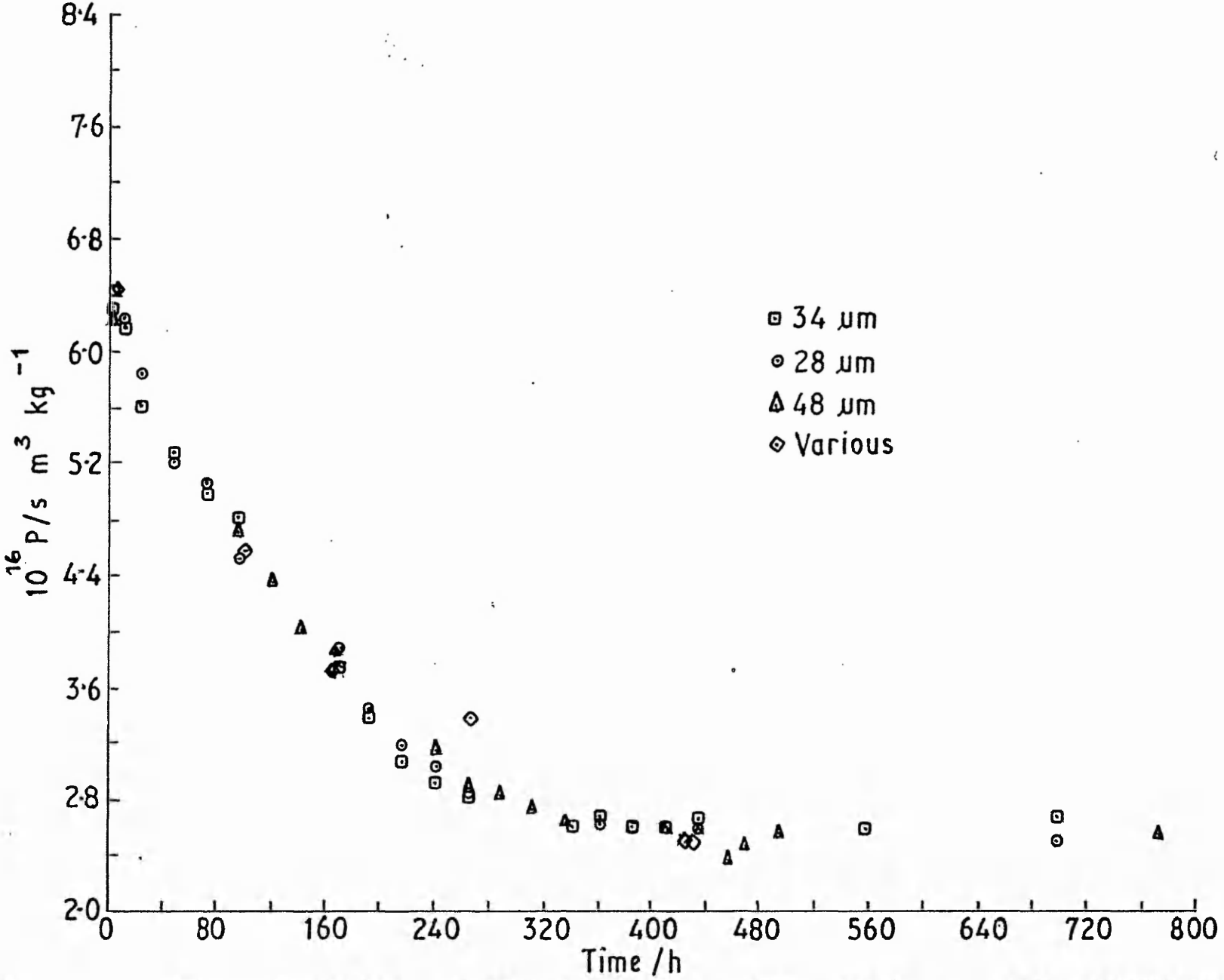

FIG V:1 REDUCTION IN PERMEABILITY WITH TIME OF POLY (n-BUTYL METHACRYLATE) LATEX FILMS CAST AT 438K

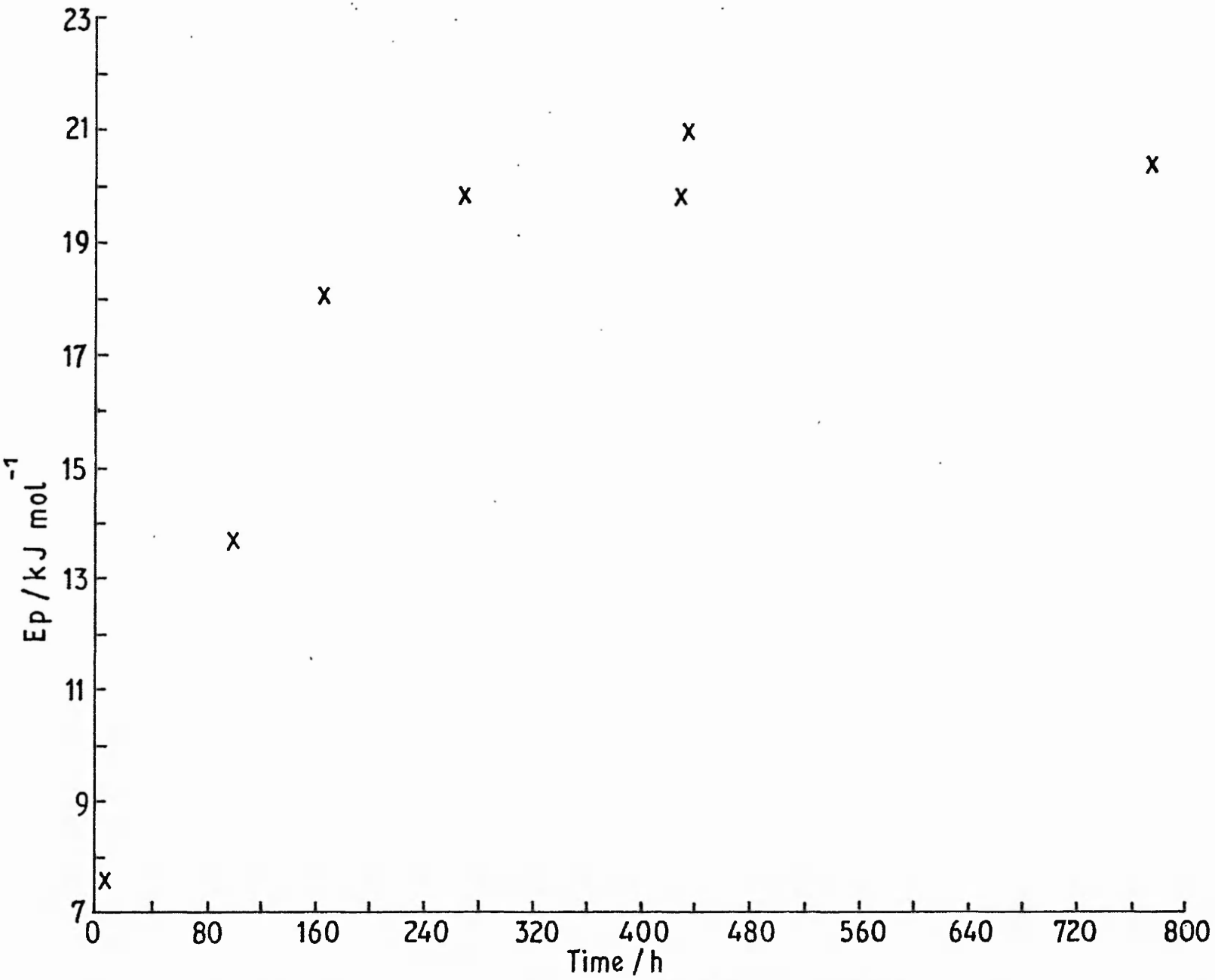

FIG V:2 INCREASE IN ACTIVATION ENERGY OF PERMEATION WITH TIME OF POLY

at which the film was cast, but lay in the range 6 - 8 10^{-16}s m^3 kg^{-1}. Over a period of about 320 hours the permeability coefficient dropped to a constant value of 2.8 10^{-16}s m^3 kg^{-1}, which was independent of the casting temperatures between 393 and 455K. These values can be compared with that for a solvent cast film of 1.1 10^{-16}s m^3 kg^{-1}, which did not vary significantly over a period of several months.

Activation energies of permeation had to be determined on different samples of film, since heating a latex film tended to alter the course of the ageing process. After checking that the initial permeability agreed with the value previously established, the film was stored at 303K for the required period of time. Permeabilities at each temperature were determined as quickly as possible, after ensuring that the permeation cell had attained temperature equilibrium. A study of the temperature dependence of latex film ageing, which is discussed in Section 3, showed that under the conditions used, heating the film to obtain the activation energy of permeation would not cause a significant error. The activation energies of permeation of freshly cast poly(n-butyl methacrylate) latex films lay in the range 7 - 8 kJ mol^{-1}, tending towards the upper limit with increasing casting temperature. The activation energy rose rapidly as the film aged, and levelled off at a value of 20 kJ mol^{-1} after about 320 hours (Fig. V:2). The corresponding figure for solvent cast poly(n-butyl methacrylate) is 25.7 kJ mol^{-1}. The increase in activation energy for latex films parallels the reduction in permeability coefficient, and both are indicative of morphological changes occurring in the film.

The initial activation energy of permeation is considerably lower than literature data for helium permeation through other polymers[4], where values of 15 to 80 kJ mol^{-1} have been reported. It is of note, however, that these data were obtained with penetrants such as carbon dioxide and water vapour through hydrophilic polymers, where penetrant solubility in, and interaction with, the polymer is large - this is not the case with helium.

Two possible hypothesis were considered, to explain the phenomena described above.

(i) A long term ageing process in which the boundaries between individual latex particles becomes less distinct as a result of interdiffusion of polymer chain segments. This mutual interdiffusion, known as autohesion, was first postulated by Voyutskii [14] to explain the mechanical strength of latex films. The concept of autohesion was invoked by Bradford and Vanderhoff [15,16] to explain the disappearance of particle contours on the surface of a variety of copolymer latex films.

(ii) Expulsion of interstitial voids, incorporated in the film by the flash casting method of preparation. This occurs under the influence of surface tension forces, and the reduction in permeability is simply an artifact of the casting technique. The expulsion of voids would parallel the smoothing out of the sprayed surface with time, which was observed by scanning electron microscopy (see Chapter IV).

Hypothesis (ii) was tested by preparing films from polymer solutions by the flash casting technique. These films were examined by scanning electron microscopy and appeared to be free from voids. If the hypothesis was correct, the permeabilities of these films would be expected to start off at a high value and then diminish with time. Although the scatter in the permeability coefficients measured for the solvent cast films was greater than for films cast in dishes, agreement between the lowest results obtained for both sets of films was good. The permeabilities of solvent cast films prepared by the flash casting technique remained constant over a period of several months.

The morphologies of latex and solvent cast films, discussed in Chapter IV, is relevant to this hypothesis. A number of freeze fracture cross sections of latex films were examined by scanning electron microscopy. None showed any evidence of voids within the films. The presence of voids would probably cause a local weakness in the film, through which the fracture would be expected to pass. Comparison of Plates IV:7 and IV:8 shows that the morphology of the latex film is far more uniform than that of the solvent cast film, which displays several voids. Despite the presence of voids, the permeability of the solvent cast film is lower than that of the latex film. On the strength of the foregoing evidence, hypothesis (ii) was discounted.

The reduction in latex film permeability can be discussed in terms of hypothesis (i), although it has not proved possible to observe any morphological changes within the interior of the latex to correspond with it. The time taken for the permeability to drop to a constant value was of the same order of magnitude as the time taken (according to Bradford and Vanderhoff [15,16]) for the particle contours to disappear from the surface of copolymer latex films, eg. nine days for a 67:33 ethyl acrylate-methyl methacrylate copolymer latex film [16].

The fact that the permeability coefficients of fully aged latex films remained higher than those of solvent cast films indicates that the latex films never became completely homogeneous. This agrees with the observations of Distler and Kanig [7,17], who found that particle boundaries were maintained in a variety of acrylate latex films (including those cast from surfactant free

latices). They ascribed this to the presence of hydrophilic boundary layers in the latex film, arising from charged end groups, surfactant and other water soluble materials, across which polymer chain segments could not diffuse. They also considered that the polymer chain ends, which terminated in polar charged species, would be unlikely to penetrate any great distance into the interior of a neighbouring particle because of its hydrophobic nature. This is a similar argument to that used in discussions on the mechanisms of emulsion polymerisation to justify the assertion that charged end groups remain on the particle surface during the reaction [18,19].

The variation in activation energy of permeation with film age is indicative of a change in the mechanism by which penetrant molecules diffuse through a latex film. This can be contrasted with partially crystalline polymer films, where the diffusion and permeability coefficients decrease with increasing crystalline content whereas the activation energies of diffusion and permeation remain constant. This behaviour occurs because the crystallites are impermeable, and the penetrant molecules must diffuse through the amorphous phase. The mechanism of diffusion is the same regardless of the amorphous phase content, and so a constant activation energy is obtained.

The proposed mechanism of ageing is as follows: After the initial stage of film formation, a latex film consists of deformed dodecahedra, delineated by hydrophilic boundary layers. For the systems studied here, these hydrophilic regions will consist of the charged endgroups which previously stabilised the latex particles with perhaps some carboxyl groups arising from hydrolysis of the acrylate or methacrylate ester. Thereafter, a certain amount of polymer segment interdiffusion occurs, as a result of which the hydrophilic boundary layers become more diffuse, and more closely resemble the particle bulk in composition. The extent of this interdiffusion is limited by the incompatibility of the hydrophilic boundary layers and the hydrophobic interior of the particle bulk. Eventually an equilibrium is established in which the particle bulk and boundary layers are still distinguishable. In fact, it is likely that some interdiffusion occurs before the polymer particles are fully deformed. In order for this mechanism to be correlated with the permeability data, it must be assumed that the hydrophilic boundary layers are more permeable than the bulk polymer. The process of diffusion through a latex film is then a two component one of normal diffusion through polymer plus diffusion along the boundary layers. The former component varies little with film age whilst the latter becomes considerably less important. A probable explanation for the higher permeability of the boundary layer is that the polymer segment density is lower in that region. This argument, too, parallels one used in emulsion polymerisation; in this case,

concerning the probable polymer segment density at the particle/water interface[19,20].

If this mechanism is correct, the influences on latex film ageing are likely to be:

(i) particle size, which, for a given film thickness will control the number of boundary layers in the film;

(ii) Surface charge density, which will reflect the amount of hydrophilic material within the film; and

(iii) film treatment, i.e. preparation and storage conditions, which will influence the rate, and perhaps extent of polymer segment interdiffusion.

2. Effect of Casting Temperature

The transmission properties of polymer films are known to be influenced by thermal treatment[20]. It is claimed that a difference as small as 5K in casting temperature (between 292 and 297K) causes a measurable difference in the permeability of solvent cast films[12]. It was therefore important to determine the effect of casting temperature on latex film permeability.

A series of poly(n-butyl methacrylate) latex films were cast at temperatures between 409 and 455 K. Permeabilities were measured within two hours of casting. These initial permeabilities are plotted as a function of casting temperature in Fig. V:3. An approximately linear correlation of decreasing initial permeability with increasing temperature is apparent.

No theoretical significance can be attached to this relationship. However, if extrapolation to higher casting temperatures is valid, it can be shown that an initial permeability of 2.4 10^{-16}s m^3 kg^{-1} (i.e. the permeability of a fully aged film) would be expected from a film cast at about 550K. This is above the decomposition temperature of poly(n-butyl methacrylate). It is notable, however, that poly (ethyl acrylate) films cast at the lowest practicable temperature (393K) did not show the same reduction in permeability as observed with poly(n-butyl methacrylate) films: this was attributed to "instant ageing" during casting (Section 5).

The films were allowed to age at 303K, and the permeabilities measured at intervals. The reductions in permeability as a function of time are shown in Figs. V:1 and V:4 to V:7. Although the initial permeability is lower at higher

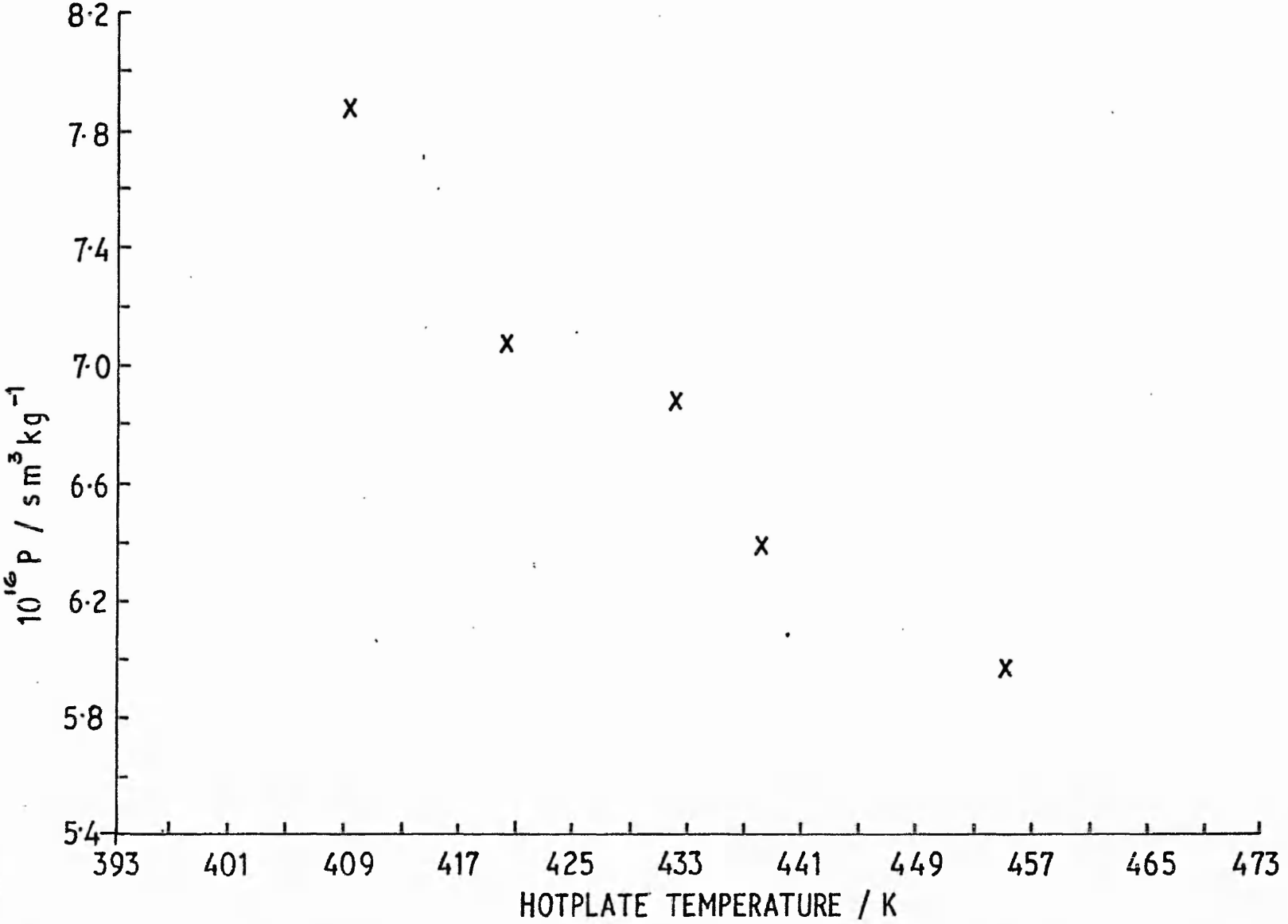

FIG V:3 EFFECT OF TEMPERATURE ON INITIAL PERMEABILITY (2 HOURS AFTER CASTING) OF POLY (n-BUTYL METHACRYLATE) LATEX FILMS

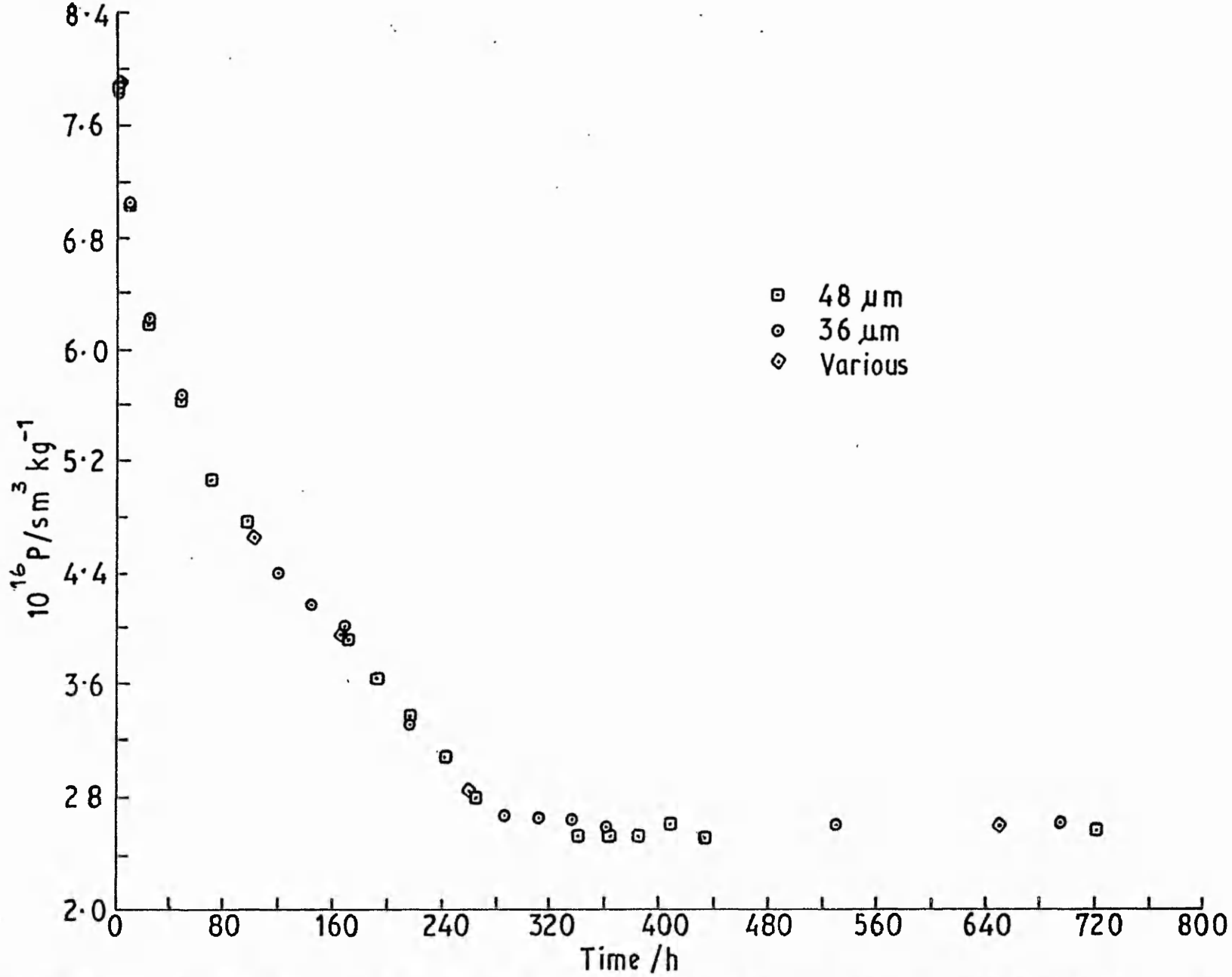

FIG V:4 REDUCTION IN PERMEABILITY WITH TIME OF POLY (n – BUTYL METHACRYLATE)

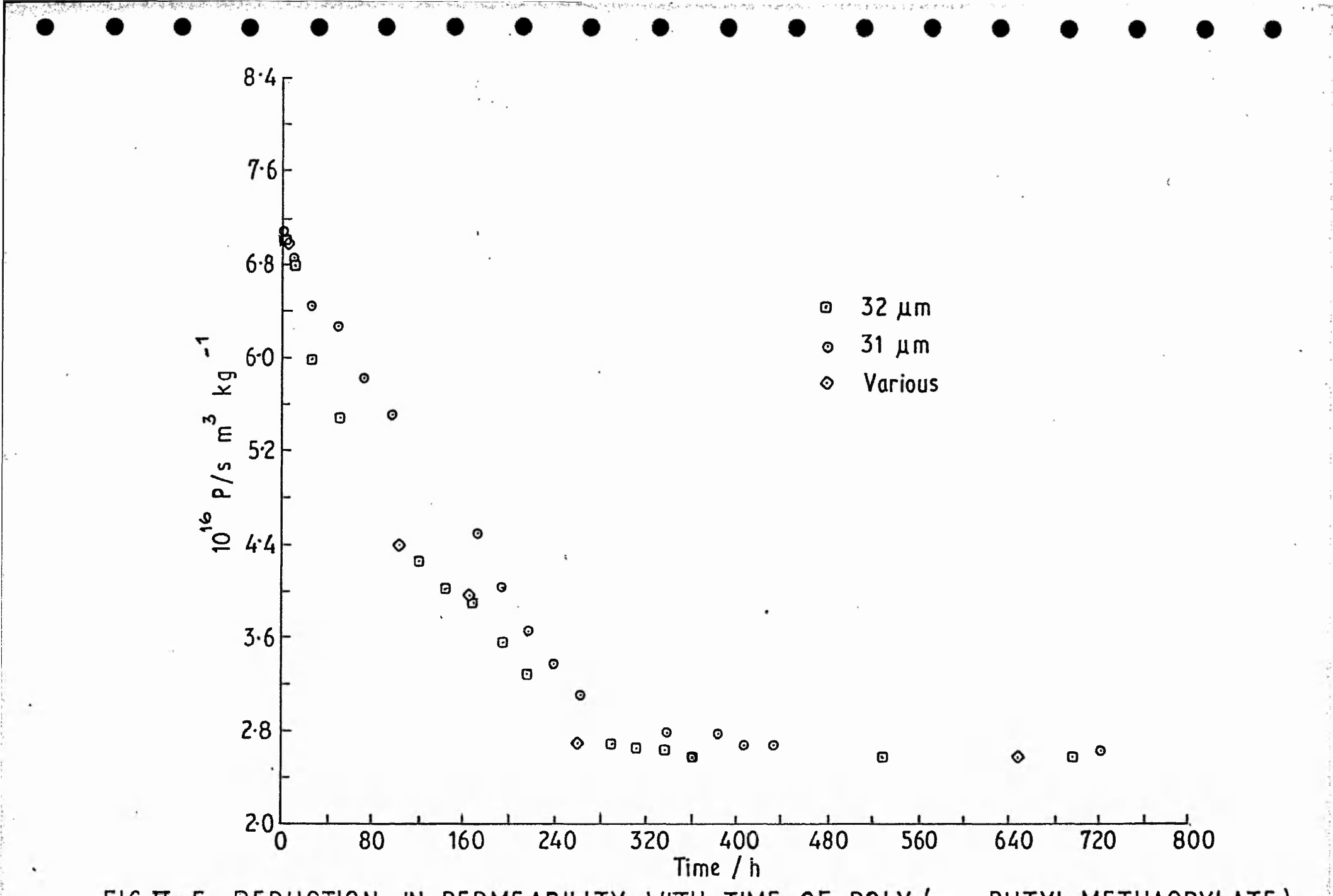

FIG 5 REDUCTION IN PERMEABILITY WITH TIME OF POLY(n-BUTYL METHACRYLATE)

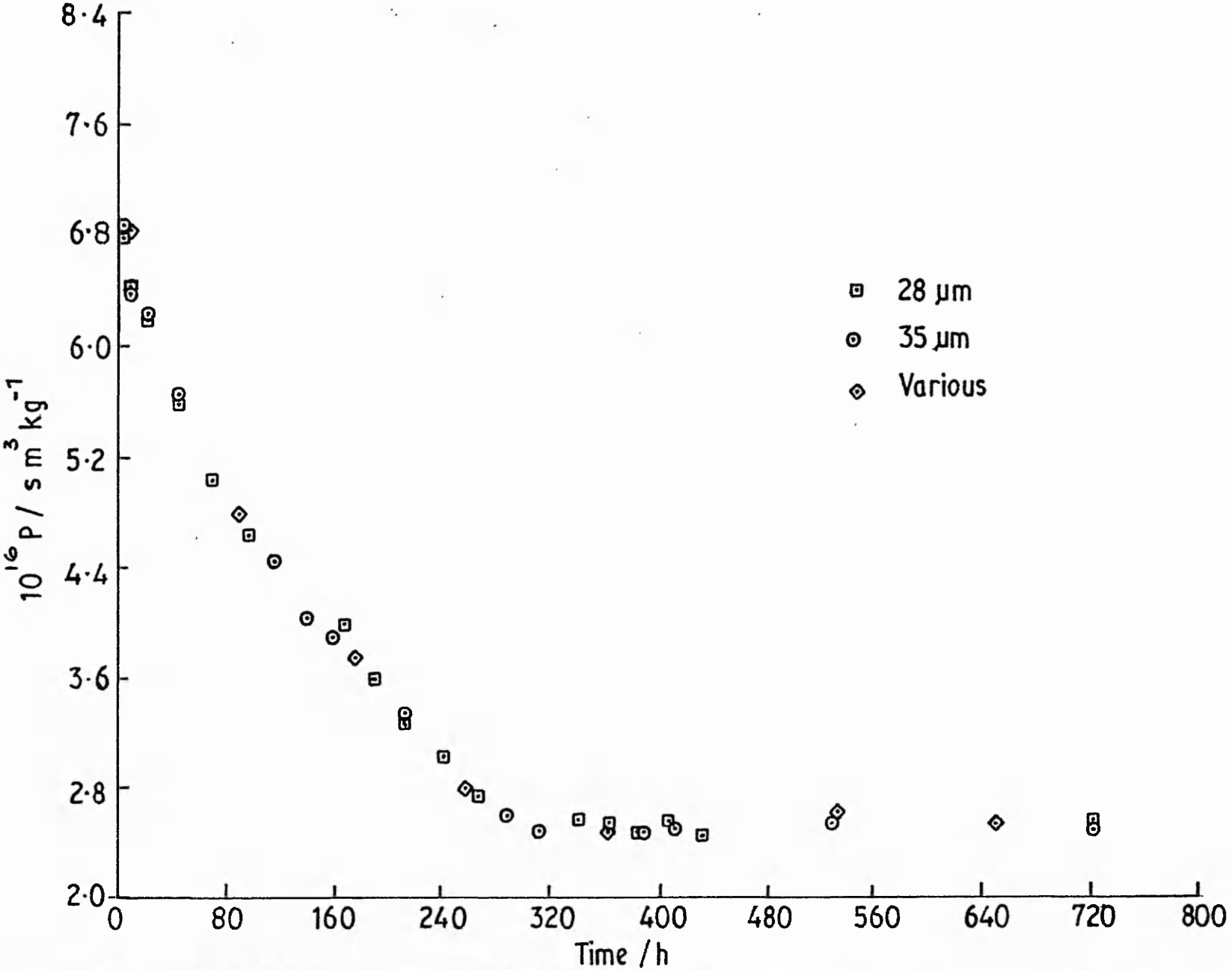

FIG V:6 REDUCTION IN PERMEABILITY WITH TIME OF POLY (n-BUTYL METHACRYLATE)

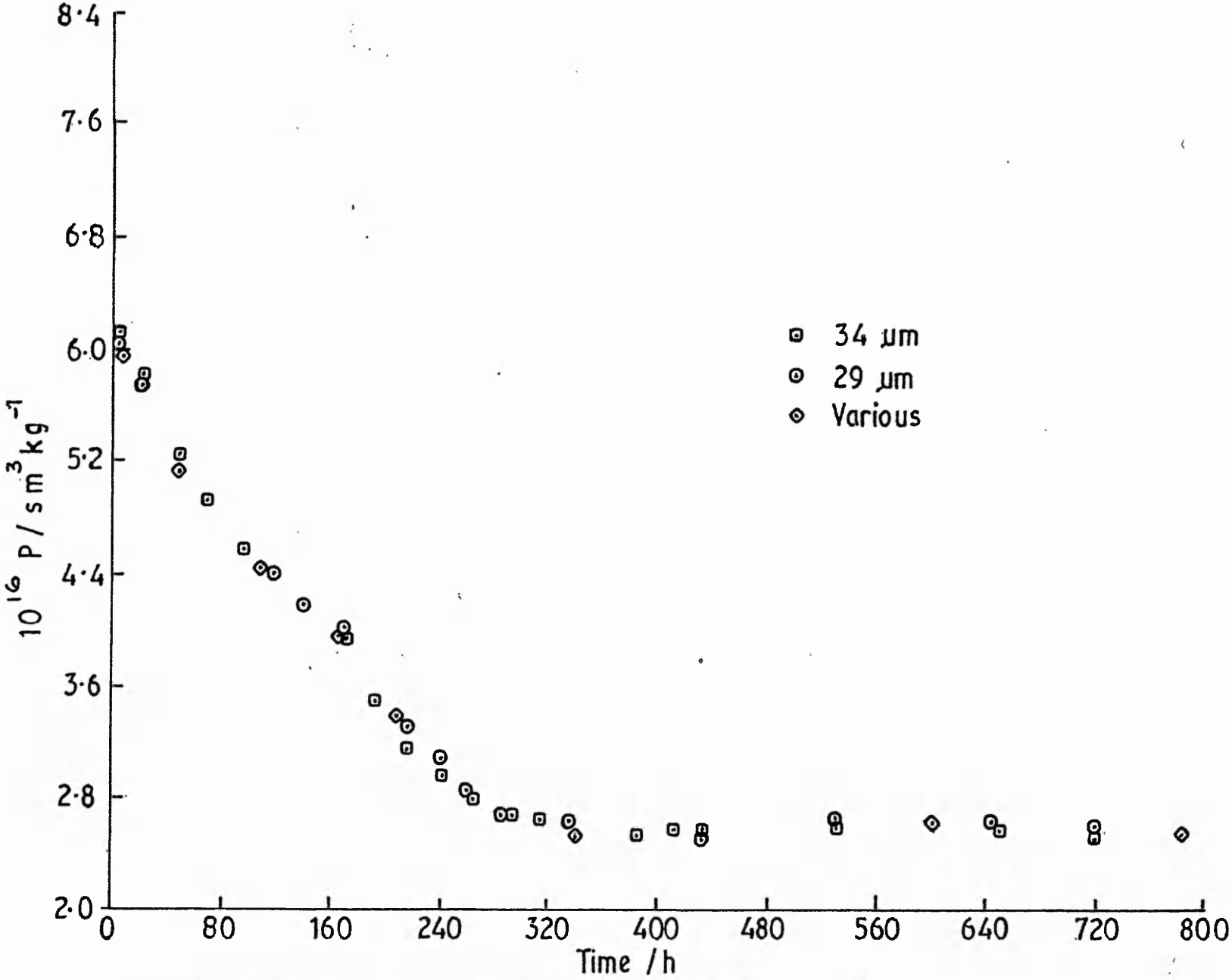

FIG V : 7 REDUCTION IN PERMEABILITY WITH TIME OF POLY (n - BUTYL METHACRYLATE)

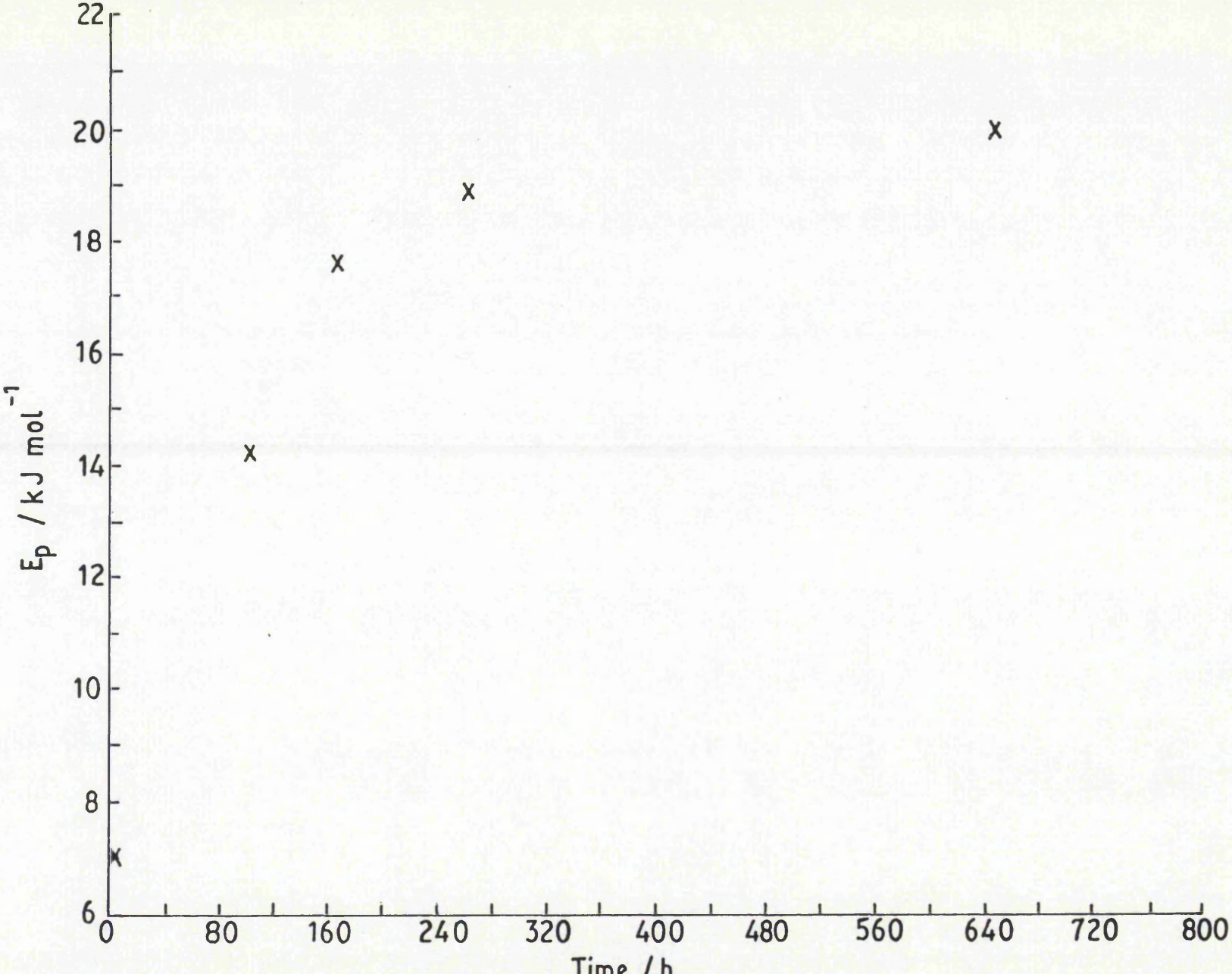
22
20
18
16
14
12
10
8
6
E_p / kJ mol^{-1}
0
80
160
240
320
400
480
560
640
720
800
Time / h

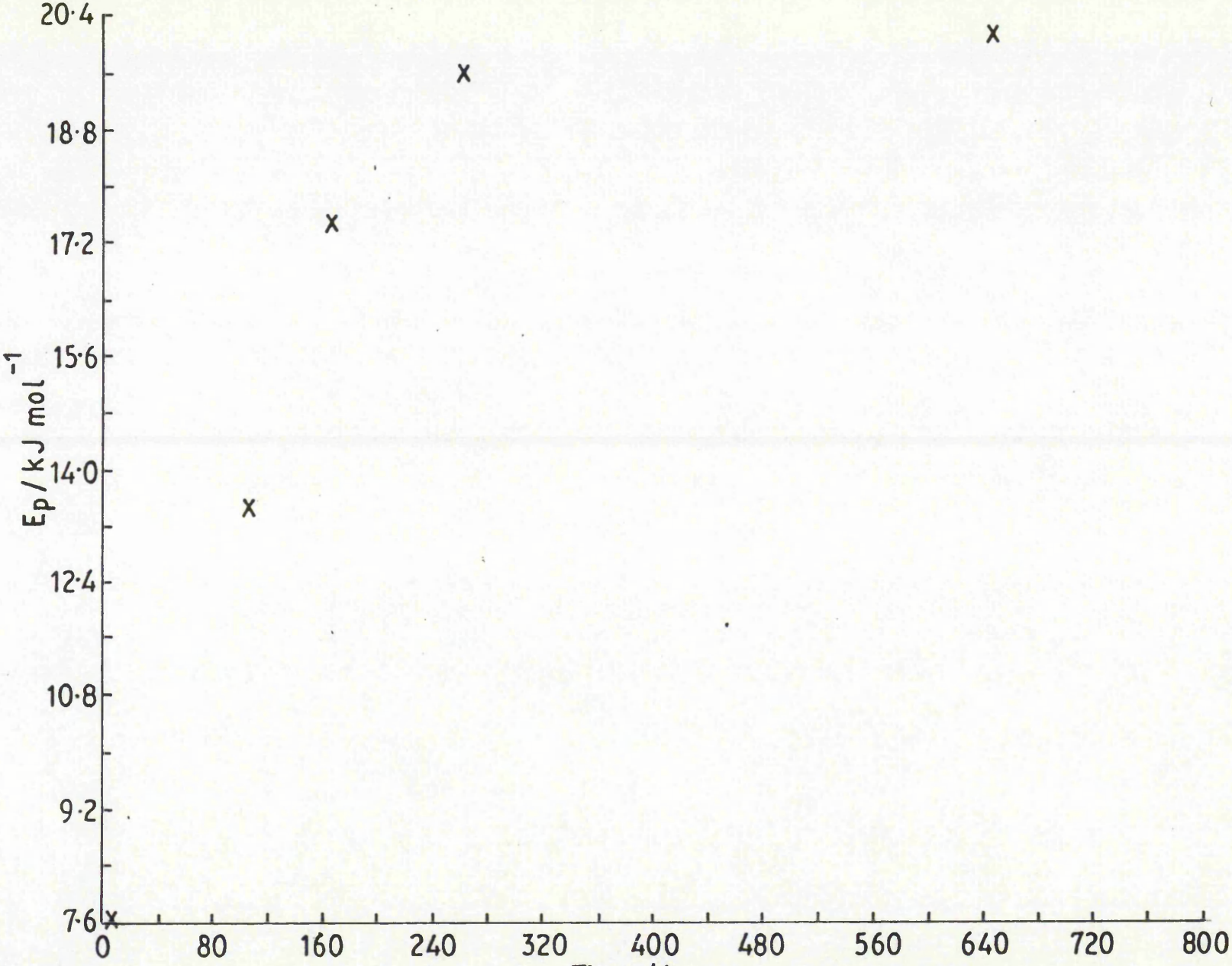
20·4
18·8
17·2
15·6
14·0
12·4
10·8
9·2
7·6
Ep / kJ mol-1
0
80
160
240
320
400
480
560
640
720
800

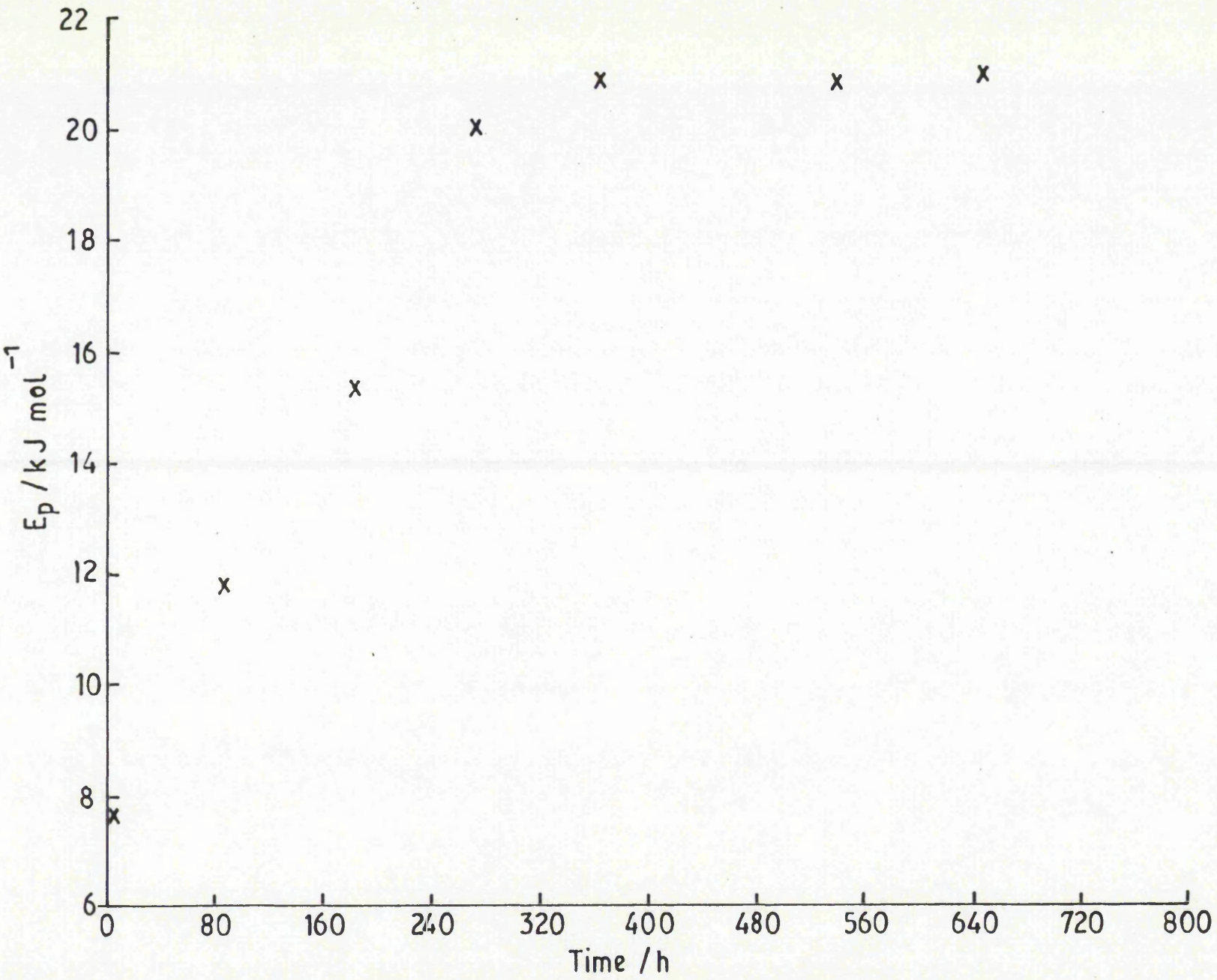
22
20
18
16
14
12
10
8
6
E_p / kJ mol^{-1}
0
80
160
240
320
400
480
560
640
720
800
Time / h

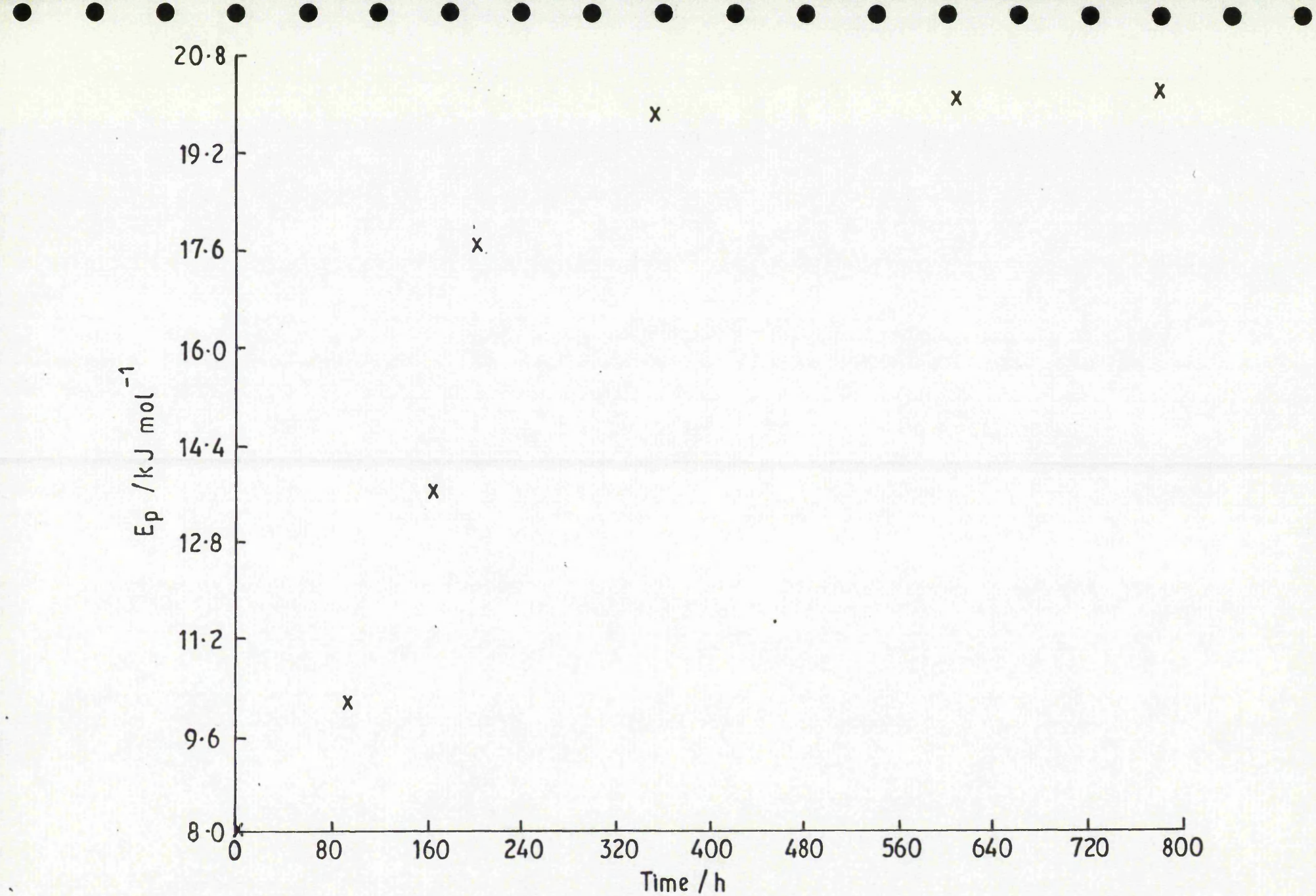

FIG V - 11 - INCREASE IN ACTIVATION ENERGY OF PERMEATION WITH TIME OF POLY

casting temperatures, the rate at which the permeability decreases is also lower, and the films take approximately the same time to level off.

The activation energy of permeation behaves in much the same way (see Figs. V:2 and V:8 - V:11) although the effect is less easily discernable here because there are fewer points, and the initial values at each temperature are more closely grouped.

3. Effect of Storage Temperature

In order to determine the effect of storage temperature latex films cast at three different temperatures (432,438 and 435K) were mounted in permeation cells and all three stored at 323K. A further set of experiments was carried out on films stored at 353K. The reduction in permeabilities observed as a function of time are shown in Figs. V:12 - V:17. It is apparent that the initial slopes are steeper at higher storage temperatures. However, the time taken to reach a constant value did not appear to depend on temperature, and the constant value attained agreed well with the values obtained earlier.

If the rate of ageing is assumed to be proportional to the slope of the permeability-time curve, then it is possible to calculate an "activation energy of ageing". The slopes of various permeability-time curves are listed in Table V:3, and the Arrheneus plot of ln (mean slope) against reciprocal temperature is shown in Fig. V:18. Despite the scatter in the slopes, a surprisingly good straight line is obtained. The activation energy was calculated to be 25 kJ mol^{-1}. Voyutskii[22] quoted a value of 12 kJ mol^{-1} for autohesion in polyisobutylene of molecular weight 150,000, and claimed that this was typical for diffusion processes. The significance of this activation energy of ageing is not certain, although it is of the same order of magnitude as the activation energy of diffusion of small, non-interacting penetrant molecules through polymers of similar composition[4]. The effect of casting and storage temperature on latex film permeability have been examined independently. Comparison of the results shows that an increase in casting temperature produces a greater reduction in permeability than is obtained by heating a previously cast film. For example, increasing the surface temperature from 409 to 438K caused a reduction in initial permeability from 7.9 to 6.4 $10^{-16} sm^3\ kg^{-1}$. Using the activation energy of ageing of 25 kJ mol^{-1}, the reduction in permeability per hour expected at 438 K was calculated to be 0.7 $10^{-16} sm^3\ kg^{-1}$. The extra cooling time from the higher temperature would not amount to more than 5 minutes so that the overall expected reduction is less than 0.2 $10^{-16} sm^3\ kg^{-1}$.

The greater effect of a higher casting temperature is presumably due to the presence of water at the time when the film is being formed. The softening

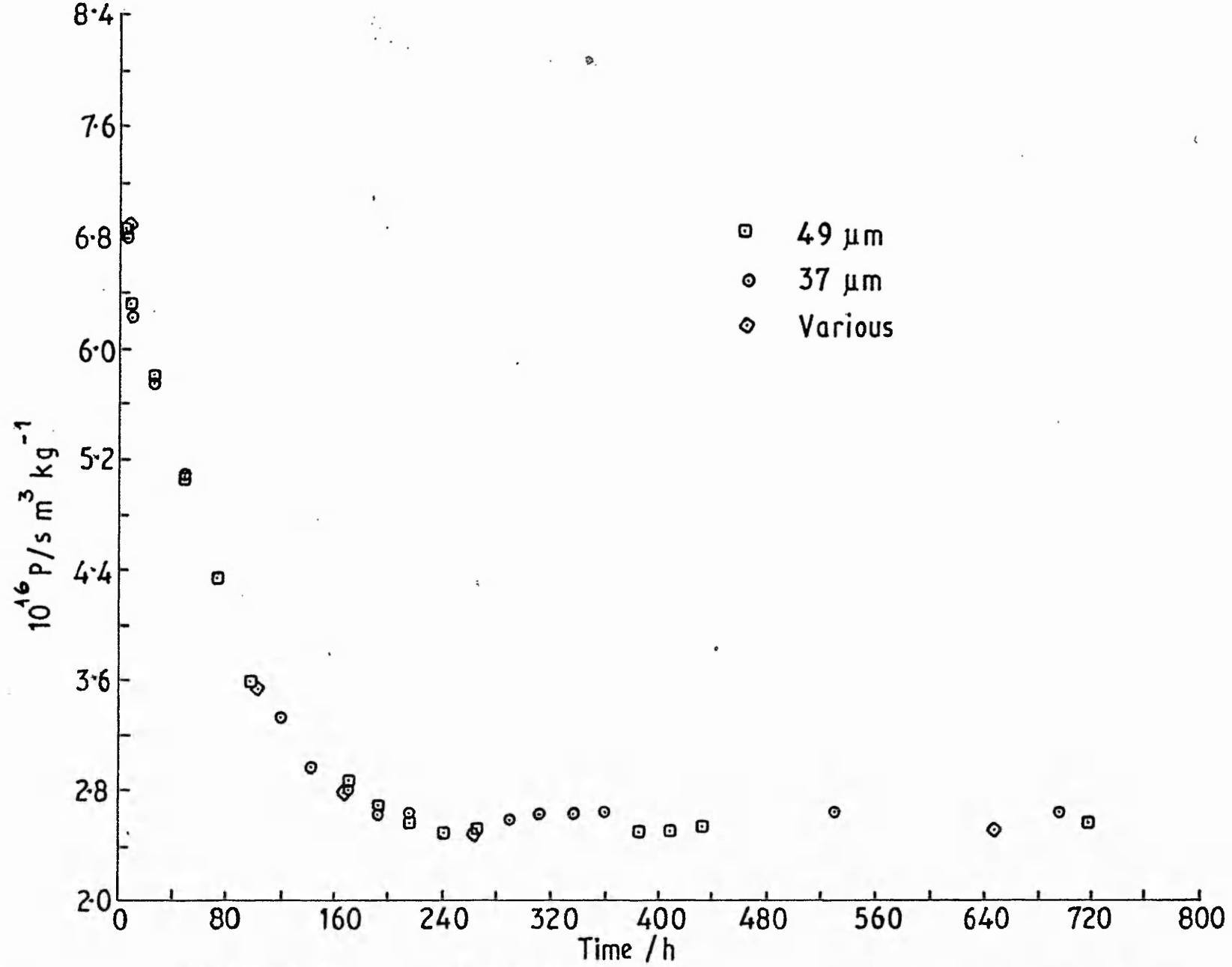

FIG. V·13 REDUCTION IN PERMEABILITY WITH TIME OF POLY (n - BUTYL METHACRYLATE)

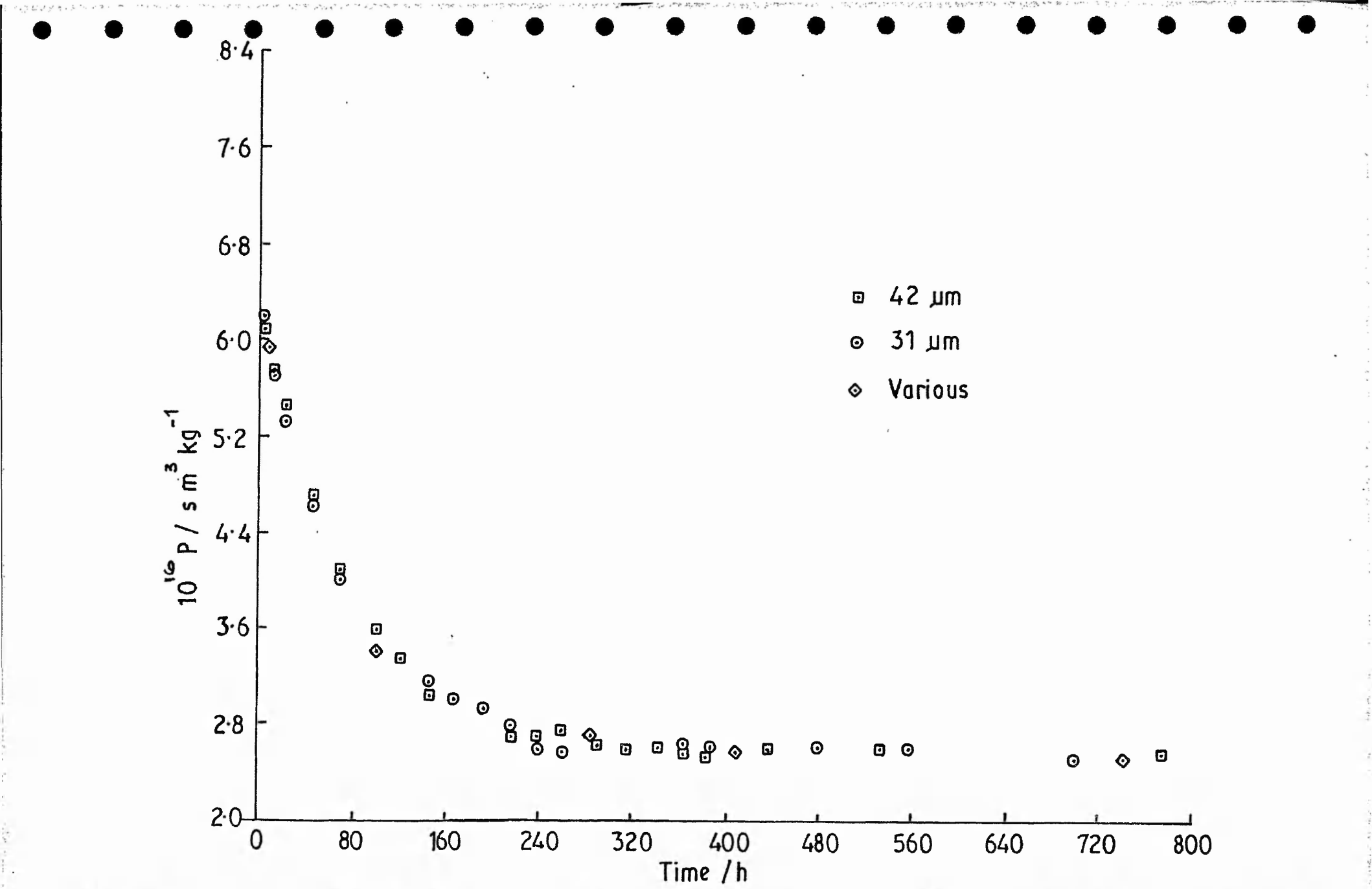

FIG V:13 REDUCTION IN PERMEABILITY WITH TIME OF POLY (n-BUTYL METHACRYLATE)

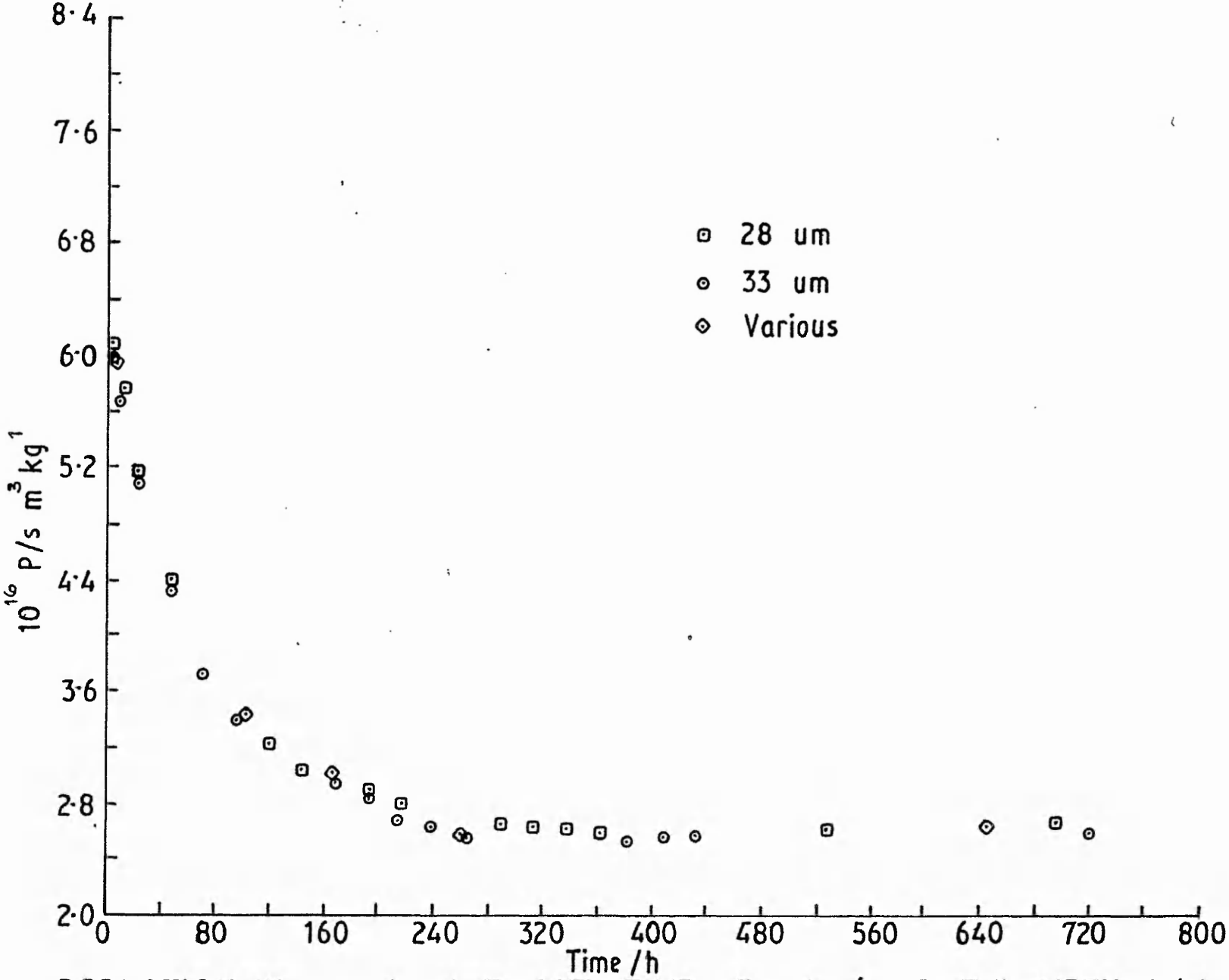
8·4
7·6
6·8
6·0
5·2
4·4
3·6
2·8
2·0
10^{16} P/s m^3 kg^{-1}
0
80
160
240
320
400
480
560
640
720
800
Time /h
28 um
33 um
Various

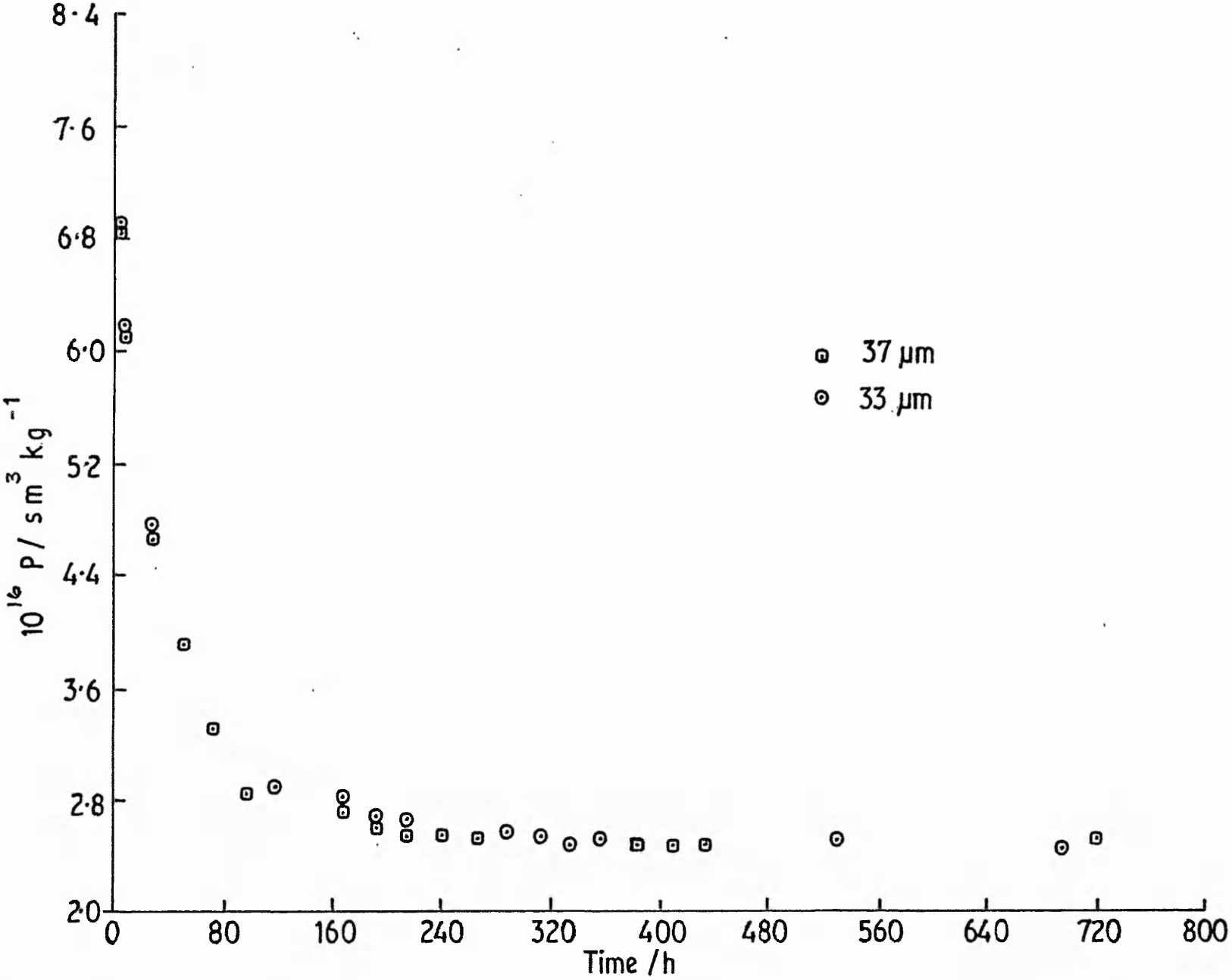

FIG V:15 REDUCTION IN PERMEABILITY WITH TIME OF POLY (n – BUTYL METHACRYLATE)

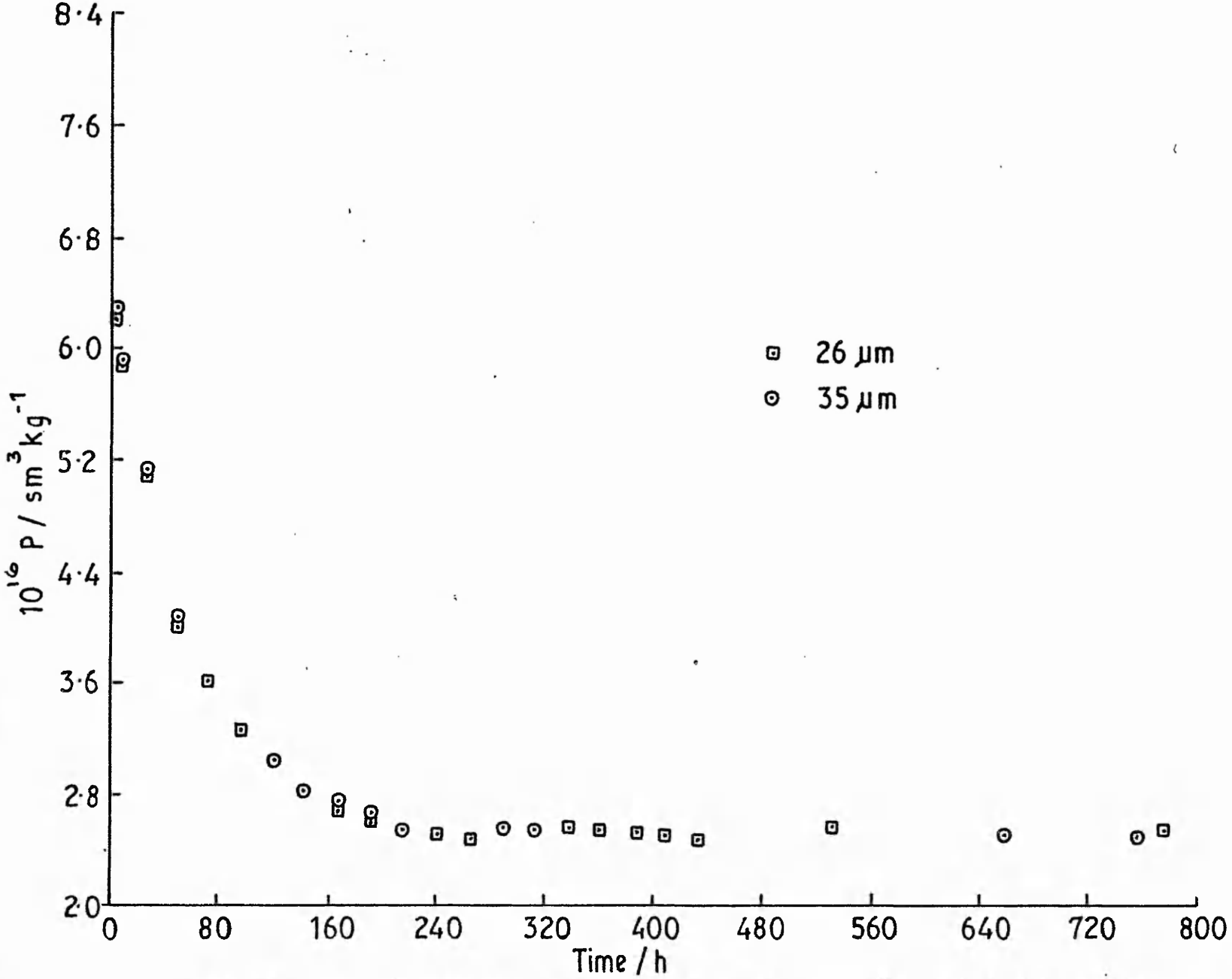

FIG V: 16 REDUCTION IN PERMEABILITY WITH TIME OF POLY (n — BUTYL METHACRYLATE)

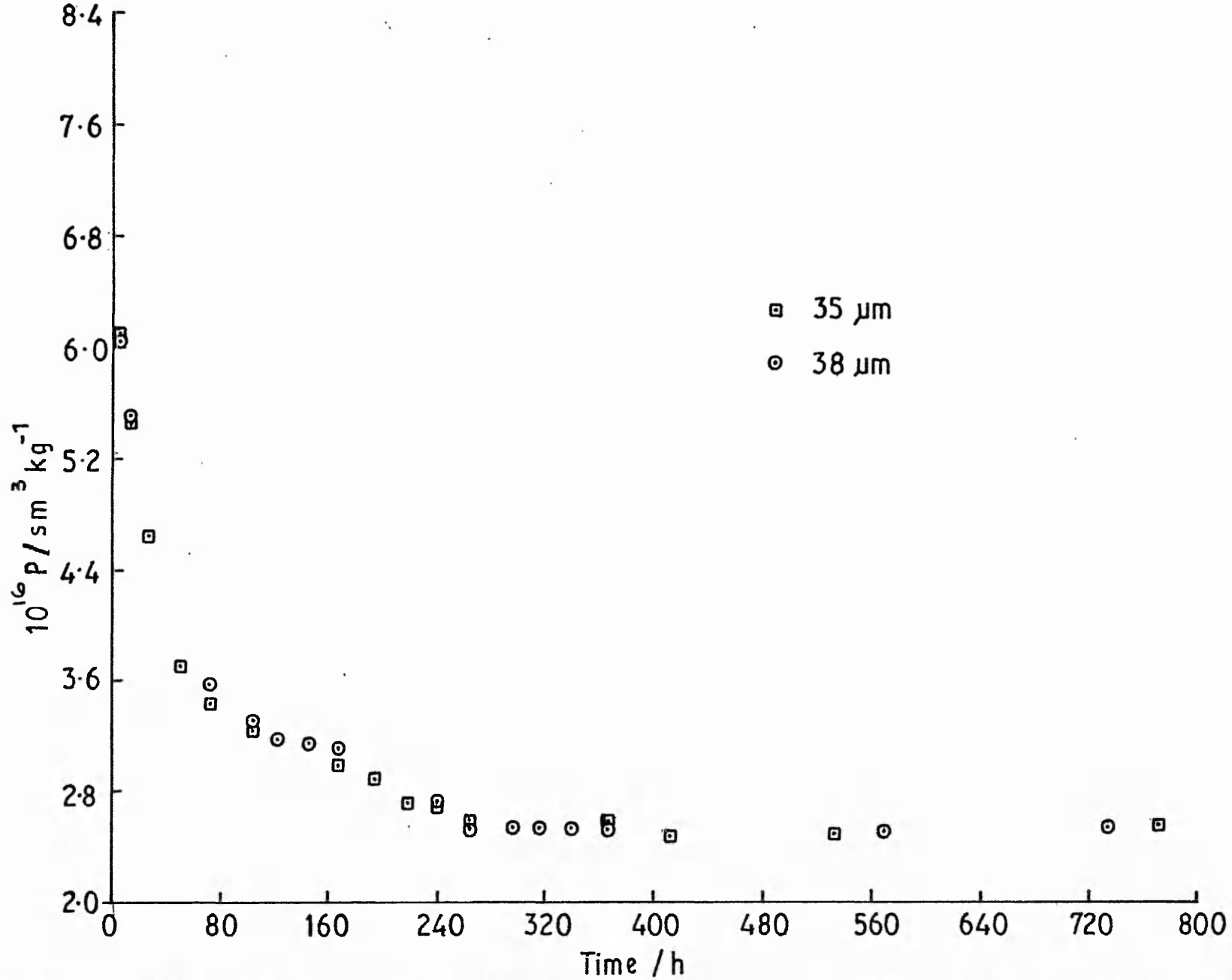

FIG V:17 REDUCTION IN PERMEABILITY WITH TIME OF POLY (n – BUTYL METHACRYLATE)

TABLE V:3

INFLUENCE OF STORAGE TEMPERATURE ON SLOPE OF PERMEABILITY-TIME CURVE

Storage temperature 303K

Casting Temperature/K	Slope	Mean	Std. dev
409	92		
420	113		
432	128	108	14.4
438	111		
435	96		

Storage temperature 323K

Casting Temperature/K	Slope	Mean	Std. dev
432	244		
438	242	258	27.7
455	290		

Storage temperature 353K

Casting Temperature/K	Slope	Mean	Std. dev
432	532		
438	412	461	62.8
455	440		

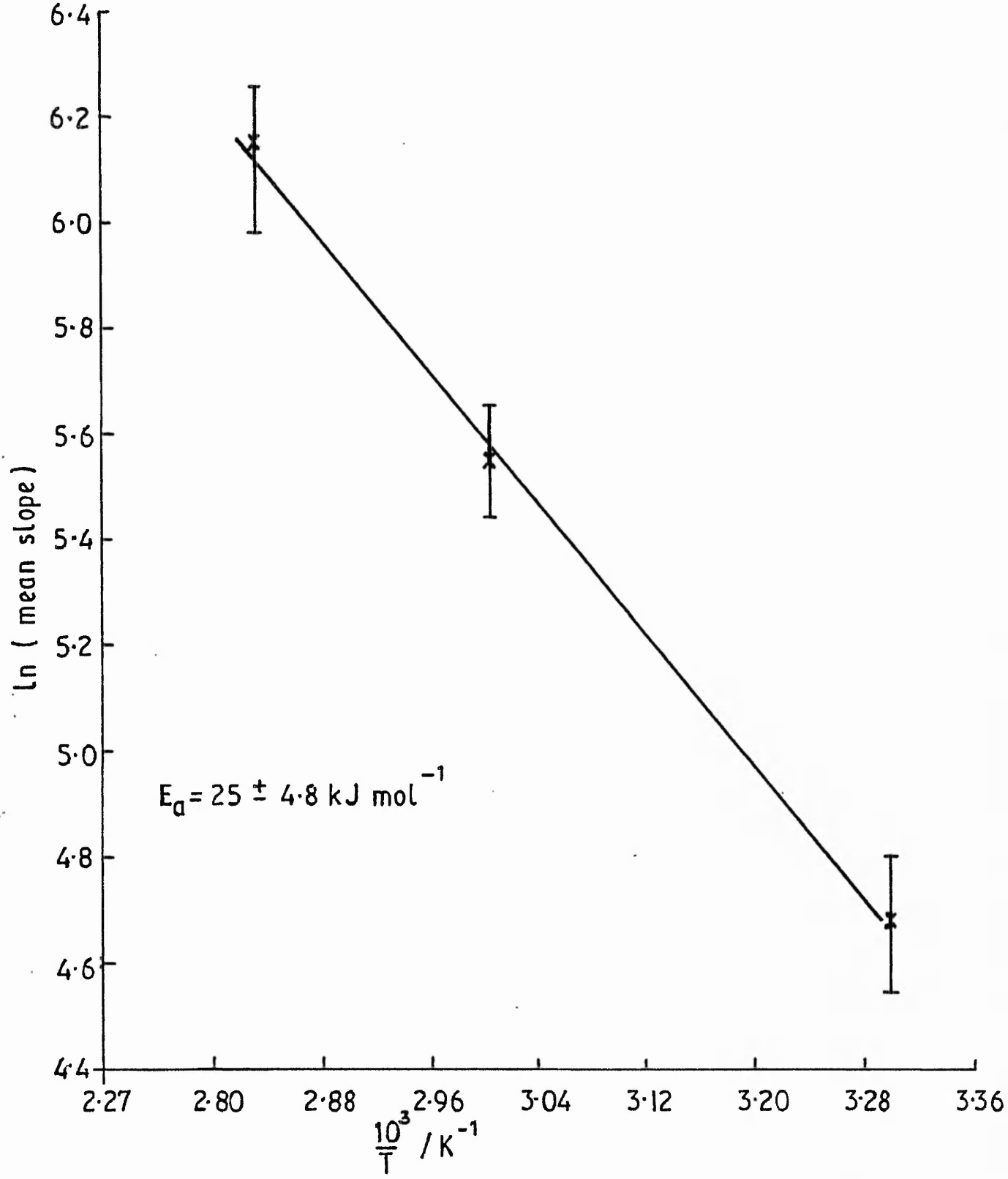

FIG V: 18 ARRHENIUS PLOT SHOWING TEMPERATURE DEPENDENCE OF MEAN SLOPE OF PERMEATION CURVE

effect of water on latex particles has been mentioned by Brodnyan and Konen[23] and Lamprecht[24], and is likely to have a significant effect, given the hydrophilic nature of the polymers in question.

4. Effect of Particle Size

Films were cast from three poly(n-butyl methacrylate) latices with particle diameters in the range 198 to 563 nm. The films were cast at 438K, mounted in the permeation cells and stored at 303K. These conditions were adopted as standard for all subsequent work. The initial and final permeabilities are listed in Table V:4. It is apparent that the difference between the two larger particle size latex films is negligible. The smallest particle size latex film had a larger initial permeability, although the difference between this and those of the other films was within experimental error.

5. Effect of Polymer Type

The permeabilities of films cast from poly(methyl acrylate), poly(ethyl acrylate) and poly(ethyl methacrylate) latices were determined as a function of time. The films were cast at 438K and stored at 303K. Table V:5 lists the initial and final permeabilities, the time taken for the films to attain the final permeability, and the solvent cast film permeabilities for comparison.

a. Poly(methyl acrylate)

The reduction in permeability coefficient and the increase in activation energy of permeation with time for poly(methyl acrylate) films are shown in Figs. V:19 and V:20 respectively. Behaviour observed with poly(n-butyl methacrylate) films is apparent here too. However, the time taken for the permeability coefficient to drop to a constant value was much shorter than the time taken for poly(n-butyl methacrylate) films (approximately 80 compared with 320 hours) and this is presumably due to the lower glass transition temperature (Table V:5). The constant value of the permeability coefficient was not, in fact, truly constant, but dropped slightly (by an average 0.5 $sm^3\ kg^{-1}$) over a period of about two months. It was difficult to study this further fall precisely due to the long observation times required and the fact that not all the films examined behaved in this way. It was not possible to relate this further reduction in permeability to the film thickness, nor did heating the film appear to accelerate it. It was observed with a sufficient number of films for the effect to be considered a real one.

TABLE V:4

EFFECT OF PARTICLE SIZE ON HELIUM PERMEABILITY OF POLY(n BUTYL METHACRYLATE) LATEX

Latex	Particle Diameter/nm	Surface charge density $\mu C\ cm^{-2}$	Permeability 10^{16} (sm^3kg^{-1}) Initial	Final
MC124	200	6.2	6.49	2.86
MC122	462	8.5	6.39	2.82
MC125	900	6.9	6.40	2.80

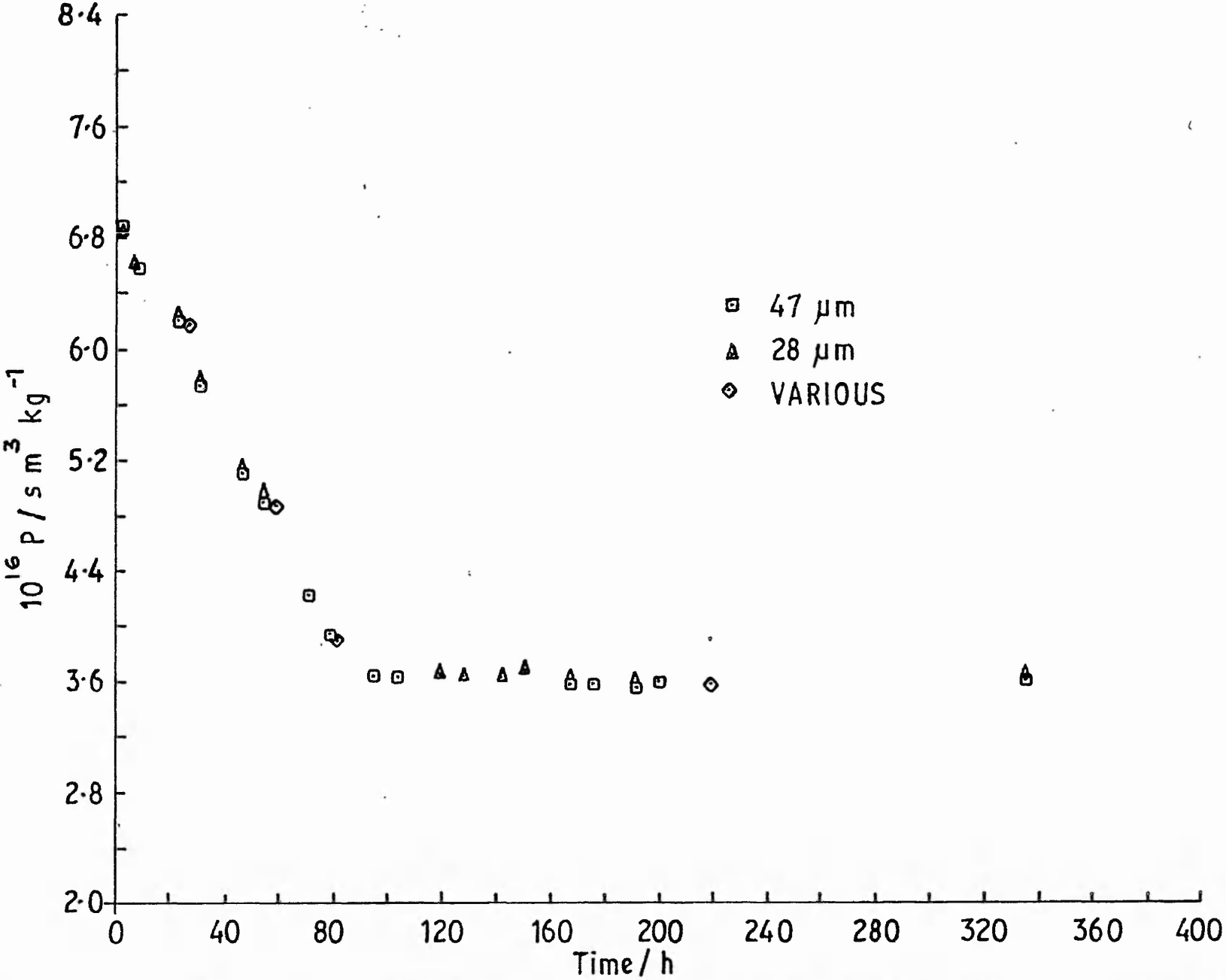

FIG V:19 REDUCTION IN PERMEABILITY WITH TIME OF POLY (METHYL ACRYLATE)

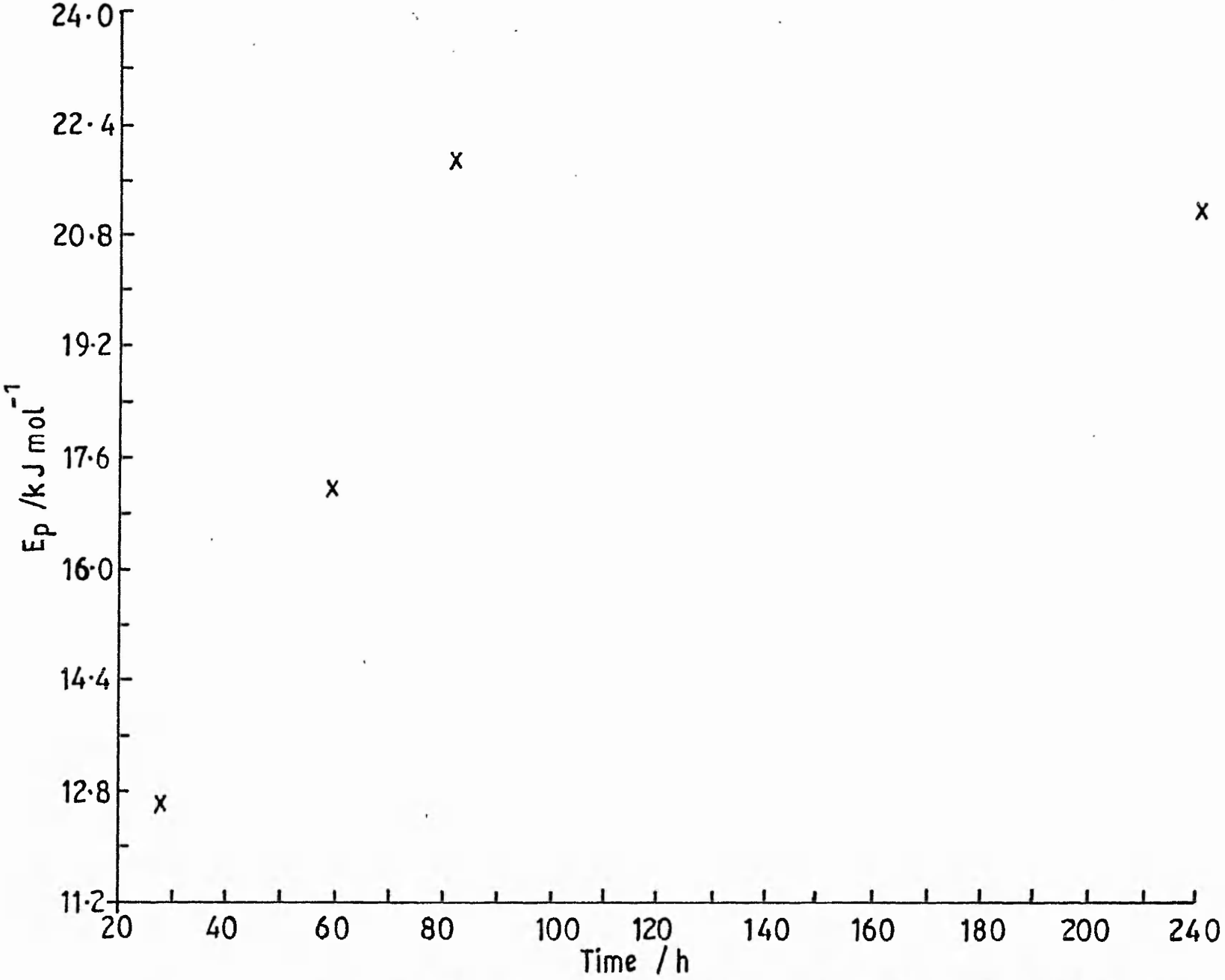

FIG V : 20 INCREASE IN ACTIVATION ENERGY WITH TIME OF POLY (METHYL ACRYLATE) LATEX FILMS

TABLE V:5

HELIUM PERMEABILITY OF LATEX POLYMER FILMS

Latex	Polymer	T_g/K	Permeability 10^{16}/s m^3 kg^{-1}			Time taken for film to age/h[c]
			Latex[a]		Solvent Cast[b]	
			Initial	Final		
MC136	PEMA	338	4.8	4.7 (2.0)[d]	1.0	360[d]
MC122	PBMA	320	6.4	2.8	1.1	320
MC141	PMA	283	6.8	3.6	1.8	80
MC142	PEA	248	2.6	2.6	2.0	0

a. Latex films prepared by flash casting technique at 438K and stored at 303K.

b. Solvent cast films prepared from solution in butanone.

c. Approximate time taken from casting to attainment of constant permeability (excludes slight, long term reduction observed with poly(methyl acrylate) and poly(ethyl acrylate) films).

d. Aged at 343K.

b. Poly(ethyl acrylate) films

The initial rapid fall in permeability observed with poly(n-butyl methacrylate) and poly(methyl acrylate) films did not occur with poly(ethyl acrylate). The permeability coefficient did not appear to alter over a period of two weeks, although a slight, long term (6 - 8 weeks) reduction in permeability was observed for some of the films examined. In view of the small difference between latex and solvent cast film permeability coefficients (Table V:5), it is likely that poly(ethyl acrylate) latex films "age instantly" during the casting process. The same result was obtained with poly(ethyl acrylate) films cast at the lowest practicable casting temperature (393K).

c. Poly (ethyl methacrylate) films

The permeability coefficients of poly (ethyl methacrylate) films aged at temperatures up to 333K diminished only slightly with time. However, on raising the storage tempeature to 343K (above the T_g of 338K) the permeability coefficient dropped more rapidly, reaching a constant value after 360 hours (Fig. V:21). This demonstrates that the molecular motions necessary for the ageing process to take place cease at temperatures below the T_g of the polymer. A similar conclusion was reached by Voyutskii[21] for the variation in the rate of autohesion with temperature.

D. HETEROGENEOUS LATEX FILMS

The various theoretical treatments applicable to permeation through heterogeneous polymer films have been discussed in Chapter I. The only experimental attempt to test these theories with heterogeneous latex films appears to have been by Peterson[25], using an approximate form of the equation derived by Higuchi[26] for a random dispersion of spheres in a continuous medium. The films were cast from blends of hard (poly(methyl methacrylate), poly(vinylidene chloride) or polystyrene) and soft (poly(vinyl acetate)) latices, dried at room temperature. Exact agreement between theory and experiment was claimed, and no variation in latex film permeability with film age was reported.

This section considers the permeabilities of heterogeneous films cast from core-shell latices, which were expected to give a regular dispersion of one polymer in a continuum of another.

Theoretical permeabilities were calculated using the equations derived by Rayleigh[27] for a regular, close packed dispersion of one material in a continuum of another; Bruggeman[27] for spherical powder particles; and Higuchi[26] for a random dispersion of one material in a continuum of another (refer to Chapter I). These equations relate the permeability coefficient of a composite film to those of its components and their volume fractions. Additionally, the equations of Rayleigh and Higuchi contain constants which arise in the course of their derivations. Substitution of appropriate values into these equations gives results which are indistinguishable within experimental error (see Table V:6). This is a consequence of the sizeable experimental error associated with permeation measurements, but more particularly of the comparitively narrow range (two or three orders of magnitude) which encompass most polymer permeability coefficients for a particular penetrant. It is therefore not possible either to confirm the validity of these theories of heterogeneous media to gas permeation systems, or conversely, to assume the validity of these theories and deduce the structure of a heterogeneous film, i.e. whether the dispersed phase is regularly or randomly distributed. However, they should predict the permeability of a composite film, regardless of whether it is prepared from a core-shell latex or a blend of equivalent composition.

TABLE V:6

Comparison of Theoretical Helium Permeabilities Calculated from Expressions Derived by Maxwell, Rayleigh, Bruggeman and Higuchi for the Polystyrene/Poly (n-Butyl Methcrylate) System

Volume Fraction of Polystyrene	Helium Permeability.10^{16}/s m^3 kg^{-1})				
	Maxwell	Rayleigh α = 0.523	Bruggeman	Higuchi K = 0	K = 0.78
0.2	5.1	5.1	5.1	5.1	5.0
0.4	3.8	4.0	3.9	4.0	3.8
0.6	2.8	3.0	2.9	3.0	2.9
0.8	2.1	2.2	2.0	2.1	2.0

Helium permeabilities of homopolymers used for computation.10^{16}/s m^3 kg^{-1}	
Polystyrene	1.3
Poly(n-butyl methacrylate	6.4

Core shell latex films were prepared from five poly(n-butyl methacrylate) coated polystyrene latices of varying composition. The usual conditions of casting at 438K and storage at 303K were employed. The permeability coefficients were found to decrease with film age in the same manner previously observed with homopolymer latex films. The extent of the reduction was less than for poly(n-butyl methacrylate) homopolymer latex films, and decreased with decreasing coating thickness (see Fig. V:22). Where there was a sufficient reduction in permeability for the rate to be measured accurately, this was similar to that found for poly(n-butyl methacrylate) films stored at the same temperature. This suggests that there is an initial stage, the duration of which is dependent on coating thickness, in which the film behaves as if it were composed entirely of homopolymer. Thereafter, the hard, undeformable core particles begin to exert an influence. This may simply be due to their approaching one another so closely as to obstruct further movement by the coating polymer. However, it is more likely that the segmental mobility of the coating polymer chains is impeded by appreciable grafting to the core particles. This grafting has been shown to occur in core-shell latices (see Chapter III), and has also been detected in seeded growth systems[28].

The initial and final permeabilities of the poly(n-butyl methacrylate) coated polystyrene core-shell latex films, together with those calculated from the Higuchi equation are given in Table V:7. The best agreement between theory and experiment was obtained by using the measured latex permeabilities for the shell permeability and the solvent-cast permeability for the core. Even so, the experimental data mostly exceed the calculated values, sometimes by a factor of two. The agreement is best for films having the lowest volume fraction of core particles, which suggests that the poly(n-butyl methacrylate) coating polymer is able to age fully without being hindered by the polystyrene core particles. Films having the highest volume fraction of core particles did not appear to age (Fig. V:22), and agreement between calculated and experimental values was best for the initial permeabilities (Table V:7).

TABLE V:7

CHARACTERISTICS OF POLY (n-BUTYL METHACRYLATE) COATED POLYSTYRENE LATICES AND THEIR HELIUM PERMEABILITIES

Latex	Core Diameter/nm	Final Diameter/nm	ϕ Core	ϕ Shell	Helium permeability 10^{16}/s m^{3}kg^{-1} Initial calc	Initial exp	Final calc	Final exp
MC62	463	525	0.686	0.314	2.6	3.5	1.7	3.5
MC63	436	515	0.606	0.394	3.0	3.7	1.8	3.6
MC42	420	560	0.422	0.578	3.9	4.0	2.1	3.5
MC103	380	590	0.267	0.733	4.7	5.1	2.3	2.6
MC104	500	860	0.197	0.803	5.1	5.4	2.5	2.5

Homopolymer permeabilities 10^{16}/s m^3 kg^{-1}

Polystyrene (cast from solution in toluene) 1.3

Poly(n-butyl methacrylate) Latex (cast by flash casting at 438K Initial 6.4 Final 2.8

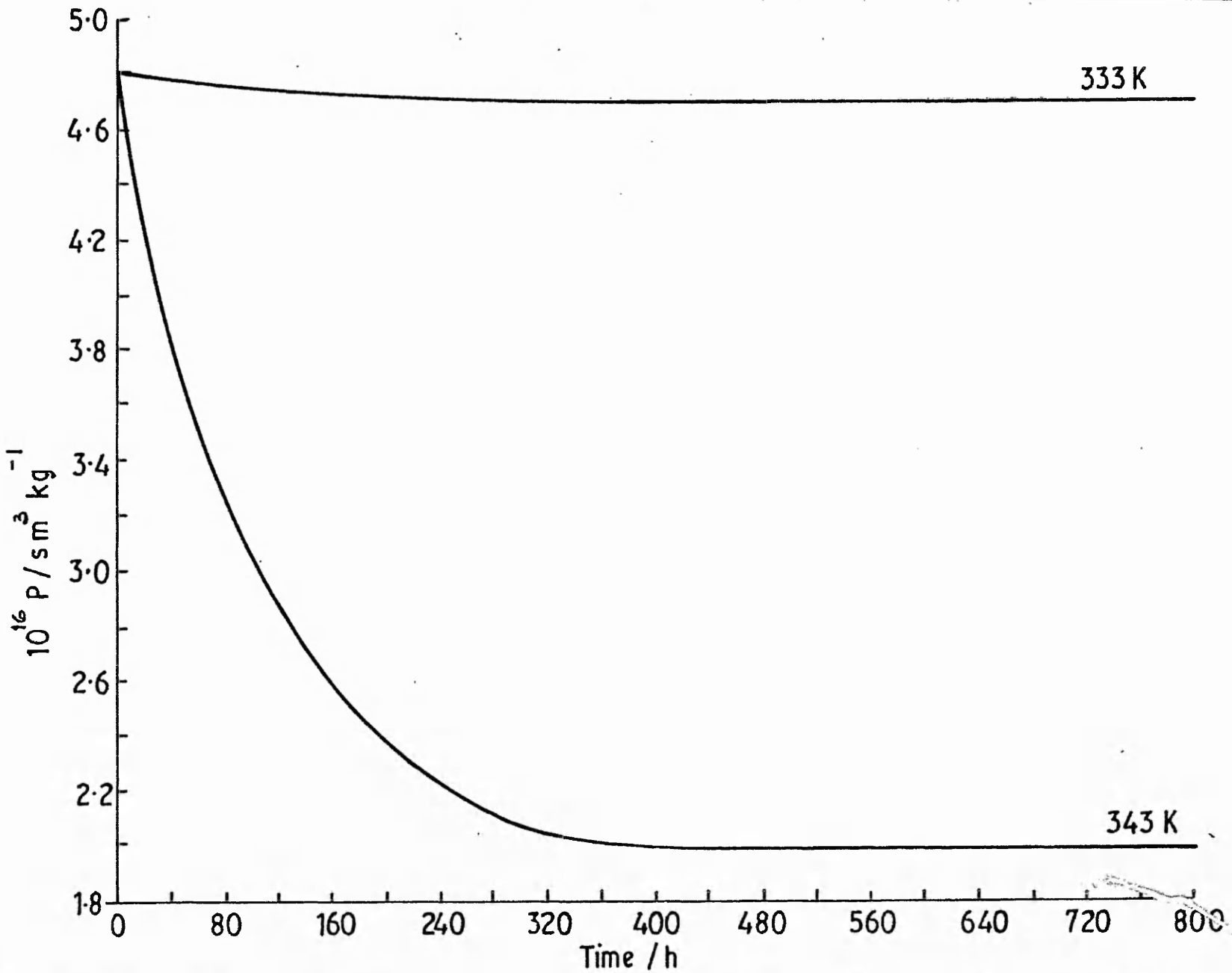

FIG V : 21 REDUCTION IN PERMEABILITY WITH TIME OF POLY (ETHYL METHACRYLATE)

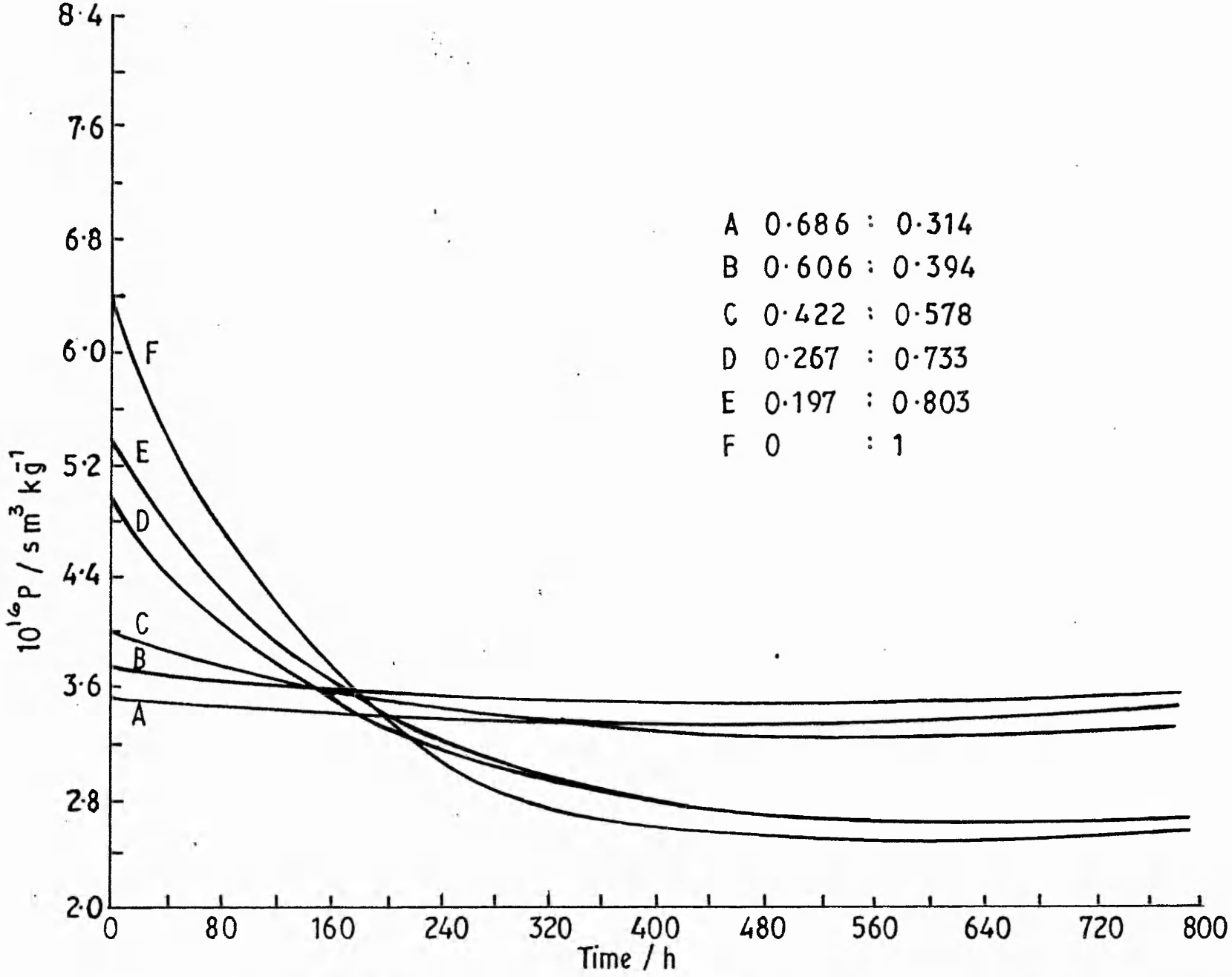

FIG V:22 REDUCTION IN FILM PERMEABILITY WITH AGE FOR POLY (n-BUTYL

REFERENCES

1. H. Yasuda and Kj. Rosengrun, J. Appl. Polym. Sci., 14, 2839 (1970).

2. R.A. Pasternak, J.F. Shimscheimer and J. Heller, J. Polym. Sci., Part A2, 8, 467 (1970).

3. V. Stannett and M. Szwarc, J. Polym. Sci.. 16, 89 (1955).

4. J. Brandrup and E.H. Immergut (eds.), "Polymer Handbook" Second edition, Wiley Interscience, (1975).

5. B.J. Hennessy, J.A. Mead and T.C. Stenning, "The Permeability of Plastics Films", The Plastics Institute, London (1966).

6. F.W. Billmeyer, "Textbook of Polymer Science", second edition, Wiley Interscience (1971).

7. D. Distler and G. Kanig, Colloid Polym. Sci., 256, 1052 (1978).

8. V. Stannett, in "Diffusion in Polymers", J. Crank and G.S. Park (eds.), Academic Press, Chapter 2, p. 41 (1968).

9. P. Mears, J. Amer. Chem. Soc., 76, 3415 (1954).

10. V. Stannett and J.L. Williams, J. Polym. Sci., Part, C., 10, 45 (1965).

11. H. Yasuda and T. Hirotsu, J. Apl. Polym. Sci., 21, 105 (1977).

12. A. Kaminska, Polymery (Warsaw), 25, 47 (1980).

13. P.W. Morgan, Ind. Engng. Chem., 45, 2296 (1953).

14. S.S. Voyutskii, J. Polym. Sci., 32, 528 (1958).

15. E.B. Bradford and J.W. Vanderhoff, J. Macromol. Chem., 1, 335 (1966).

16. Idem, J. Macromol. Sci. - Phys., 36, 671 (1972).

17. D. Distler and G. Kanig, Org. Coat. Plast. Chem., 43, 606 (1980).

18. J.W. Goodwin, J. Hearn, C.C. Ho and R.H. Ottewill, Brit. Polym. J., 5, 347 (1973).

19. J.W. Vanderhoff, Proc. Water Borne and High Solids Coatings Symp, University of Southern Mississippi (1976).

20. D.J. Williams, J. Polym. Sci., Polym. Chem. Ed., 12, 2123 (1974).

21. C.E. Rogers, in "The Physics and Chemistry of the Organic Solid Sate", vol. 2, D. Fox, M.M. Labes and A. Wiessberger (eds.), Wiley Interscience, Chapter 6, p. 509 (1965).

22. S.S. Voyutskii, "Autohesion and Adhesion in High Polymers", Polymer Reviews, vol. 4, Wiley Interscience (1963).

23. J.G. Brodnyan and T. Konen, J. Appl. Polym. Sci., 8, 687 (1964).

24. J. Lamprecht, Colloid Polym. Sci., 258, 960 (1980).

25. C M. Peterson, J. Appl. Polym. Sci., 12, 2649 (1968).

26. W.I. Higuchi, J. Phys. Chem., 62, 649 (1958).

27. R.M. Barrer, in "Diffusion in Polymers", J. Crank and G.S. Park (eds.), Academic Press, Chapter 6, p. 165 (1968).

28. T.I. Min, A. Klein, M.S. El-Aasser and J.W. Vanderhoff, J. Polym. Sci., Polym. Chem. Ed., 21, 2685 (1983).

CHAPTER VI

CONCLUSIONS AND RECOMMENDATIONS FOR FURTHER WORK

Although most of the work described in this thesis was concerned with the preparation and properties of core-shell latices and polymer latex films, some was a continuation of earlier work on the preparation and characterisation of polystyrene latices[1]. Aspects of the surfactant-free emulsion polymerisation of styrene, and problems associated with the use of polystyrene latices as model colloids have been previously studied. The kinetics of the nucleation stage were examined, and a mechanism proposed. This considered that the initial nuclei formed became unstable, flocculated and coalesced to produce a latex with a relatively polydisperse size distribution, which became narrower on subsequent growth[2,3].

This work has been extended and data for the post-nucleation stage of the reaction examined. Several published theories [4-7] derived for emulsion polymerisation in the presence of surfactant have been examined and adapted to surfactant-free systems. The trends in experimental data best agree with the predictions of theories based on a surface phase polymerisation model, although agreement for the full quantitative treatment is less than satisfactory. This is partially due to large uncertainties in the literature values of various constants, but also to the inadequacy of the currently available theoretical treatments. A characteristic feature of surfactant-free reactions is the bimodal molecular weight distribution. The two molecular weight peaks move in tandem towards higher values with increasing conversion. No existing theory predicts this bimodal distribution, which is attributed to polymerisation in two loci. There are four possible loci of polymerisation, namely in the aqueous phase, the polymer/water interface, the anomalous region and the particle bulk. It has not proved possible to assign either molecular weight peak to polymer generated in a particular locus, and further study to resolve this problem would be worthwhile.

The surface characterisation of polymer latices has been complicated for many years by the shortcomings of the available cleaning techniques, namely dialysis and ion-exchange[8]. The microfiltration cell devised in the course of this work proved to be rapid and efficient in the removal of both organic and inorganic impurities. Addition of inhibitor and its subsequent removal by microfiltration is a satisfactory means of preventing microbial contamination in latices whose surface charge is not a prime concern. It is not, unfortunately, satisfactory where maintenance of the latex surface characteristics is

important, for example, in model colloid studies.

The preparation of core-shell latices is an increasingly important means of producing films and coatings with desirable properties. The shot-growth technique devised during this study proved to be a useful method of preparing core-shell latices having a hydrophobic core and a hydrophilic shell. Although latices of this type can be prepared by the more conventional seeded growth method, the shot growth technique produced a monodisperse product with a lower number density of core particles. Swelling and growth experiments carried out in connection with this part of the work suggested that the rate of the polymerisation reactions were limited by transport of monomer to the reaction site. The heterocoagulation mechanism of monomer supply[9] could not be disproved, although it was considered unlikely to operate in the systems studied, since the rates of swelling and particle growth were comparable.

Apart from differences in reaction mechanism, between seeded and shot growth reactions, the products differ in the amount of grafting between core and shell. This is apparent from fracture cross-sections of films cast from latices prepared by the two methods. A thin layer chromatography (flame ionisation detector (TLC/FID) technique has recently been employed to determine the amounts of graft polymer in latices prepared in seeded growth reactions[10]. Application of this technique to latices prepared by the shot growth technique would give a quantitative estimate of the extent of grafting.

It is likely that differences in the amount of grafting will be manifested in the mechanical properties of the films cast from core-shell latices. It was not possible to measure more than basic tension/extension curves for the core-shell latex films. However, these curves were of a form characteristic of filled materials. It would be interesting to know if seeded and shot growth latex films performed differently, and whether any trends with extent of grafting (as determined by TLC/FID) could be discerned.

The preparation of thin polymer films, free of contamination, from surfactant-free polymer latices could not be achieved by means of any previously reported technique. To overcome this hurdle, a flash casting technique was devised and successfully employed to cast films from homopolymer, copolymer and core-shell latices. The main limitation of the technique was that films of polymers having Tg's too far removed from ambient (less than 248 K and greater than 373 K) could not be removed from the PTFE substrate intact. The flash casting technique was mainly used with surfactant-free latices, and no problems with thermal decomposition were encountered. However, due caution should be exercised if using latices containing surfactant or other additives, since these may decompose during film preparation. The resulting film might well have a

more open or porous structure, similar to that produced by chemical blowing agents.

The surfaces of films prepared by flash casting appeared smooth to the naked eye, but the sprayed surfaces of freshly prepared poly(n-butyl methacrylate) films were rough when viewed by scanning electron microscopy. The surfaces smoothed out on ageing, and after one month's storage resembled the surface of a solvent cast film. This would appear to suggest that surface tension forces are operative during the final stages of film formation and act to reduce the film surface area. The current theories of film formation, which only consider capillary forces, need to be extended to take account of this.

No particle structure was visible on the surface of or within homopolymer and copolymer films, when examined by scanning electron microscopy even when freshly cast. The greater resolution of transmission electron microscopy, with appropriate replication techniques, would probably allow this structure to be observed, and any changes in film morphology with age monitored.

The gas permeability of films cast from polymer solutions and latex dispersions have been shown to differ considerably. The permeability coefficients of most latex films started off at a value considerably higher than that of the corresponding solvent cast film, and then dropped at a rate dependent on the type of polymer. The permeability coefficients levelled off at a value which was closer to, but still higher than, that of the solvent cast film. This reduction in the permeability of latex films is attributed to ageing processes occuring in the film after casting. These processes probably involve the interdiffusion of polymer segments across the original particle boundaries[11]. The fact that the permeability coefficients of fully aged latex films remain higher than those of solvent cast films has been interpreted as showing that latex films never become completely homogeneous, in accord with the observations of Distler and Kanig[12] that latex films contain hydrophilic particle boundary layers. For a given polymer, the latex particle size and surface charge density were expected to influence the film permeability.

The effect of particle size over a limited size range showed no difference in permeability. Further work needs to be done on a much wider size range to establish whether these findings of non-reliance of permeability on particle size are valid. It is not easy to prepare latices at the extremes of this range without altering other characteristics. In particular, monodisperse latices of less than 100 nm diameter are difficult to prepare by surfactant-free methods, and latices of greater than 1 μm usually require the addition of stabiliser to prevent irreversible aggregation. These restrictions will hamper any further work aimed at determining the influence of particle size on latex film permeability.

The effect of surface charge density was not studied systematically because of the difficulty in preparing lattices with controlled surface characteristics. Kamel et al.[13] have recently reported a series of methods for producing polystyrene latices with controlled amounts of a single type of charged endgroup. It is unlikely, however, that a sufficiently large range of surface charge densities could be produced by these methods. Higher surface charge densities could be produced by incorporating carboxylic acid co-monomers or a copolymerisable surfactant. Increasing the size or hydrophilic nature of the endgroups or their concentrations would increase the size of the hydrophilic boundary layer. If the proposed mechanism of latex film ageing is correct, the expected effect of a larger boundary layer would be to increase the initial and final permeabilities because of its higher permeability. A larger boundary layer would also be a greater impediment to the interdiffusion of polymer chain segments. This might well have repercussions for the mechanical strengths of the film.

In view of the industrial importance of surfactant-containing latices, it is important to examine the influence of surfactant on the variation of permeability with age of latex films. Several types of behaviour can be imagined, depending on the type of surfactant, the degree of adsorption and its compatibility with the polymer. Bradford and Vanderhoff found that surfactants were expelled from some latex films, but not from others[14,15]. They also found that surfactant containing latices formed more porous films than when the surfactant had been first removed by dialysis. More recently, Padget and Moreland [16] determined that particle coalescence was accelerated by the presence of a block copolymer surfactant, an effect which was attributed to plasticisation of the latex polymer. It would be interesting to know if the permeability of the surfactant containing films, which would be expected to start from a very high permeability because of their porous structure, decreased with time, and if so, to what extent. This information would be particularly valuable where a latex film or coating is intended for barrier applications.

REFERENCES

1. A.R. Goodall, Ph.D thesis, Trent Polytechnic (1976)

2. D. Munro, A.R. Goodall, M.C. Wilkinson, K.J. Randle and J. Hearn, J. Colloid Interface Sci., 68, 1 (1979)

3. A.R. Goodall, K.J. Randle and M.C. Wilkinson, ibid, 75, 493 (1980)

4. W.V. Smith and R.H. Ewart, J. Chem. Phys., 16, 592 (1948)

5. J. Ugelstad and F.K. Hansen, Rubber Chem. Technol., 49, 536 (1976)

6. J.L. Gardon, Brit. Polym. J., 2, 1 (1970)

7. R.A. Wessling and I.R. Harrison, J. Polym. Sci., Part A1, 9, 3471 (1971)

8. M.C. Wilkinson, in "Treatise on Surface Characterisations", K. Mittal (ed.), Plenum Press (1984)

9. Y. Chung-Li, J.W. Goodwin and R.H. Ottewill, Progr. Colloid Polym. Sci., 60, 163 (1976)

10. T.I. Min, A. Klein, M.S. El-Aasser and J.W. Vanderhoff, J. Polym. Sci., Polym. Chem. Ed., 21, 2865 (1983)

11. S.S. Voyutskii, "Autohesion and Adhesion of High Polymers", Polymer Reviews, Vol. 4, Wiley Interscience (1963)

12. D. Distler and G. Kanig, Colloid Polym. Sci., 256, 1052 (1978)

13. A.A. Kamel, M.S. El-Aasser and J.W. Vanderhoff, J. Dispersion Sci. Technol., 2, 183 (1981)

14. E.B. Bradford and J.W. Vanderhoff, J. Macromol. Sci., 1, 335 (1966)

15. Idem, J. Macromol. Sci.-Phys., B6, 671 (1972)

16. J.C. Padget and P.J. Moreland, J. Coatings. Technol., 55, 39 (1983).

TABLE A:1

Kinetic Characteristics of Reaction MC49

Sample	Time/min	Conversion /%	Radius/ nm	σ /%	Particle number density/cm^{-3}
MC49/1	30	4.4	73	2.3	2.3×10^{12}
MC49/2	60	7.8	108	3.6	1.3×10^{12}
MC49/3	90	12.6	138	1.4	0.98×10^{12}
MC49/4	135	20.4	174	1.7	0.80×10^{12}
MC49/5	181	40.0	210	1.4	0.89×10^{12}
MC49/6	225	38.2	241	1.1	0.56×10^{12}
MC49/7	270	53.9	242	1.8	$0.78 \times 10_{12}$
MC49/8	316	77.7	278	2.3	0.75×10^{12}
MC49/9	360	85.2	300	1.8	0.65×10^{12}
MC49/10	411	86.1	304	1.7	0.63×10^{12}
MC49/11	1405	88.5	310	1.7	1.6×10^{12}

Styrene concentration 0.870 mol dm^{-3}. Potassium persulphate concentration 1×10^{-2} mol dm^{-3}. Temperature 343 K.

TABLE A:2

Kinetic Characteristics of Reaction MC55

Sample	Time/min	Conversion /%	Radius/nm	σ/%	Particle number density/cm^{-3}
MC55/1	60	6.93	92	8.0	1.9×10^{12}
MC55/2	120	14.5	133	1.3	1.3×10^{12}
MC55/3	180	25.5	181	0.91	0.88×10^{12}
MC55/4	240	32.9	218	1.3	0.65×10^{12}
MC55/5	300	44.8	259	1.3	0.53×10^{12}
MC55/6	360	61.9	277	0.72	0.60×10^{12}
MC55/7	420	82.5	313	1.8	0.55×10^{12}
MC55/8	485	96.8	361	0.63	0.42×10^{12}
MC55/9	540	98.8	363	0.88	0.43×10^{12}
MC55/10	690	990	364	0.85	0.42×10^{12}
MC55/11	1460	98.6	354	2.1	0.48×10^{12}

Styrene concentration 0.870 mol dm^{-3}. Potassium persulphate concentration 1.5×10^{-2} mol dm^{-3}. Temperature 343 K.

TABLE A:3

Kinetic Characteristics of Reaction MC68

Sample	Time/min	Conversion /%	Radius/nm	σ/%	Particle number density/cm^{-3}
MC68/1	720	14.9	396	1.2	4.9×10^{10}
MC68/2	840	20.5	436	1.4	5.1×10^{10}
MC68/3	960	26.7	480	0.74	5.0×10^{10}
MC68/4	1080	33.3	530	1.0	4.5×10^{10}
MC68/5	1200	44.7	600	1.2	4.3×10^{10}
MC68/6	1320	62.6	685	0.88	4.0×10^{10}
MC68/7	1440	65.3	680	0.81	4.3×10^{10}
MC68/8	2160	65.4	685	0.8	4.2×10^{10}
MC68/9	2640	63.4	675	1.9	4.2×10^{10}

Styrene concentration 0.870 mol dm^{-3}. Potassium persulphate concentration 5×10^{-4} mol dm^{-3}. Temperature 343 K.

TABLE A:4

Kinetic Characteristics of Reaction MC69

Sample	Time/min	Conversion /%	Radius/nm	σ/%	Particle number density/cm^{-3}
MC69/1	100	8.5	120	1.9	1.0×10^{12}
MC69/2	130	11.4	141	2.0	0.85×10^{12}
MC69/3	160	16.4	158	1.7	0.85×10^{12}
MC69/4	190	23.5	175	1.6	0.90×10^{12}
MC69/5	220	29.1	180	2.1	0.88×10^{12}
MC69/6	250	36.1	209	1.2	0.82×10^{12}
MC69/7	280	36.3	222	1.9	0.68×10^{12}
MC69/8	310	48.1	240	0.77	0.72×10^{12}
MC69/9	340	58.8	252	1.3	0.80×10^{12}
MC69/10	370	82.6	267	1.3	0.90×10^{12}
MC69/11	465	98.6	335	1.1	0.54×10^{12}
MC69/12	1350	106	344	0.87	0.53×10^{2}

Styrene concentration 0.870 mol dm^{-3}. Potassium persulphate concentration 5×10^{-3} mol dm^{-3}. Sodium chloride concentration 1.5×10^{-2} mol dm^{-3}. Temperature 343 K.

TABLE A:5

Kinetic Characteristics of Reaction MC70

Sample	Time/min	Conversion /%	Radius/nm	σ/%	Particle number density/cm^{-3}
MC70/1	600	16.1	480	2.1	3.0×10^{10}
MC70/2	720	20.2	531	1.7	2.8×10^{10}
MC70/3	835	28.7	610	1.2	2.6×10^{10}
MC70/4	900	35.4	650	0.54	2.7×10^{10}
MC70/5	1200	56.9	665	1.0	2.6×10^{10}
MC70/6	1020	39.8	679	1.7	2.6×10^{10}
MC70/7	1080	63.9	710	1.1	3.7×10^{10}
MC70/8	1140	50.7	744	7.0	2.5×10^{10}
MC70/9	2380	88.8	10110	11.2	1.8×10^{10}

Styrene concentration 0.870 mol dm^{-3}. Potassium persulphate concentration 1×10^{-3} mol dm^{-3}. Sodium chloride concentration 2.7×10^{-2} mol dm^{-2}. Temperature 343 K.

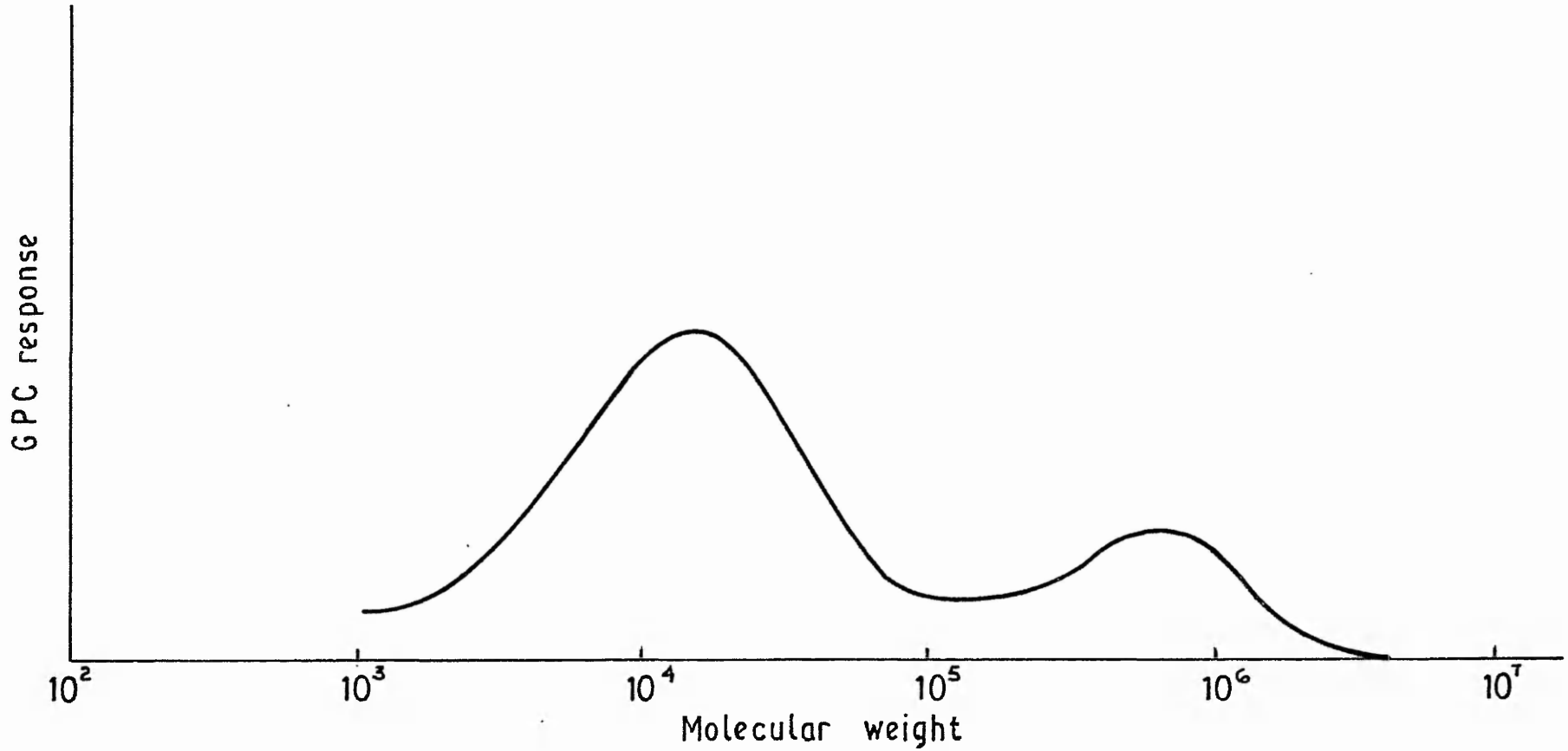

FIG A:1 GEL PERMEATION CHROMATOGRAPH FOR SAMPLE MC 69/1

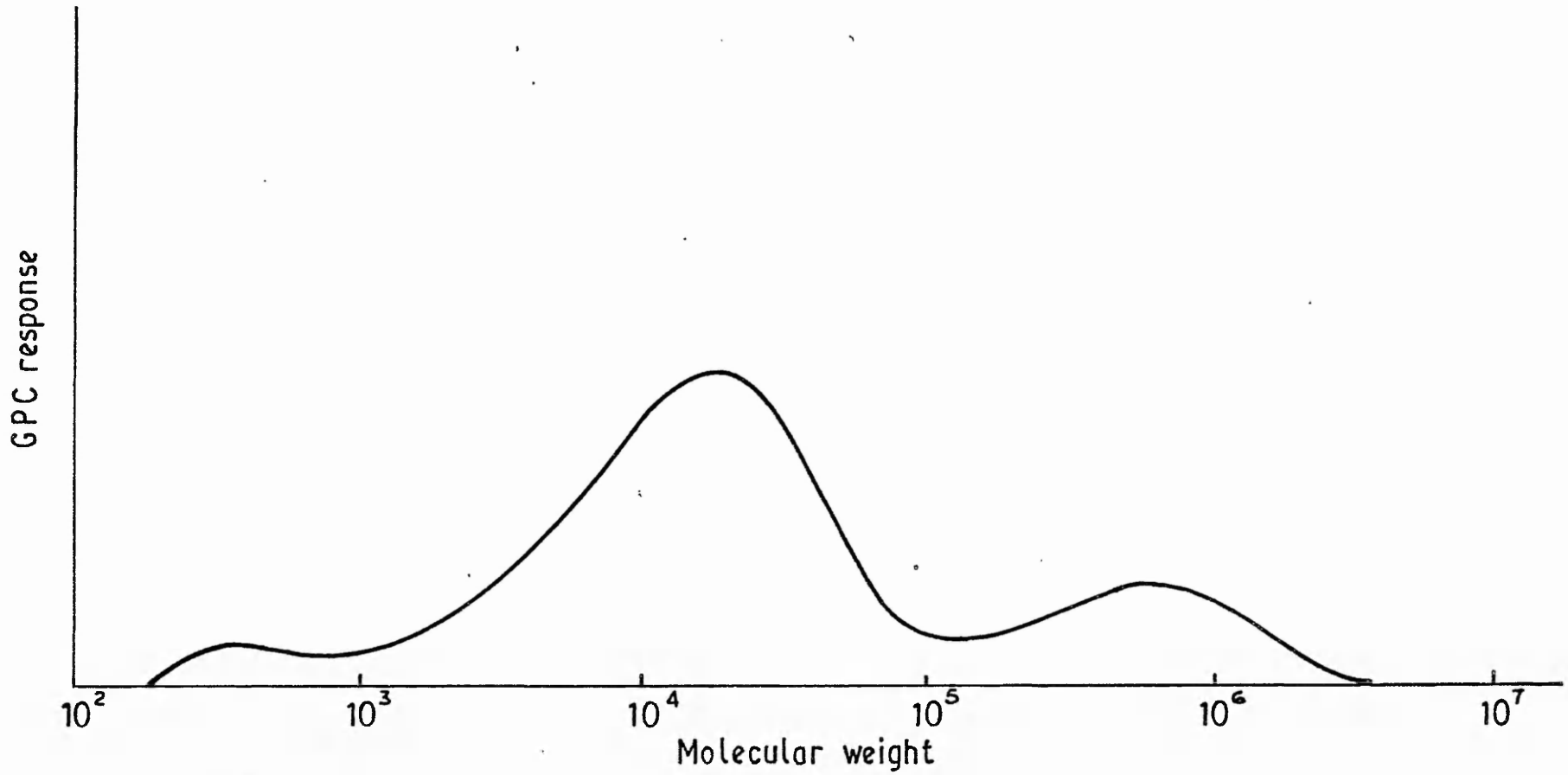

FIG A:2 GEL PERMEATION CHROMATOGRAPH FOR SAMPLE MC 69/2

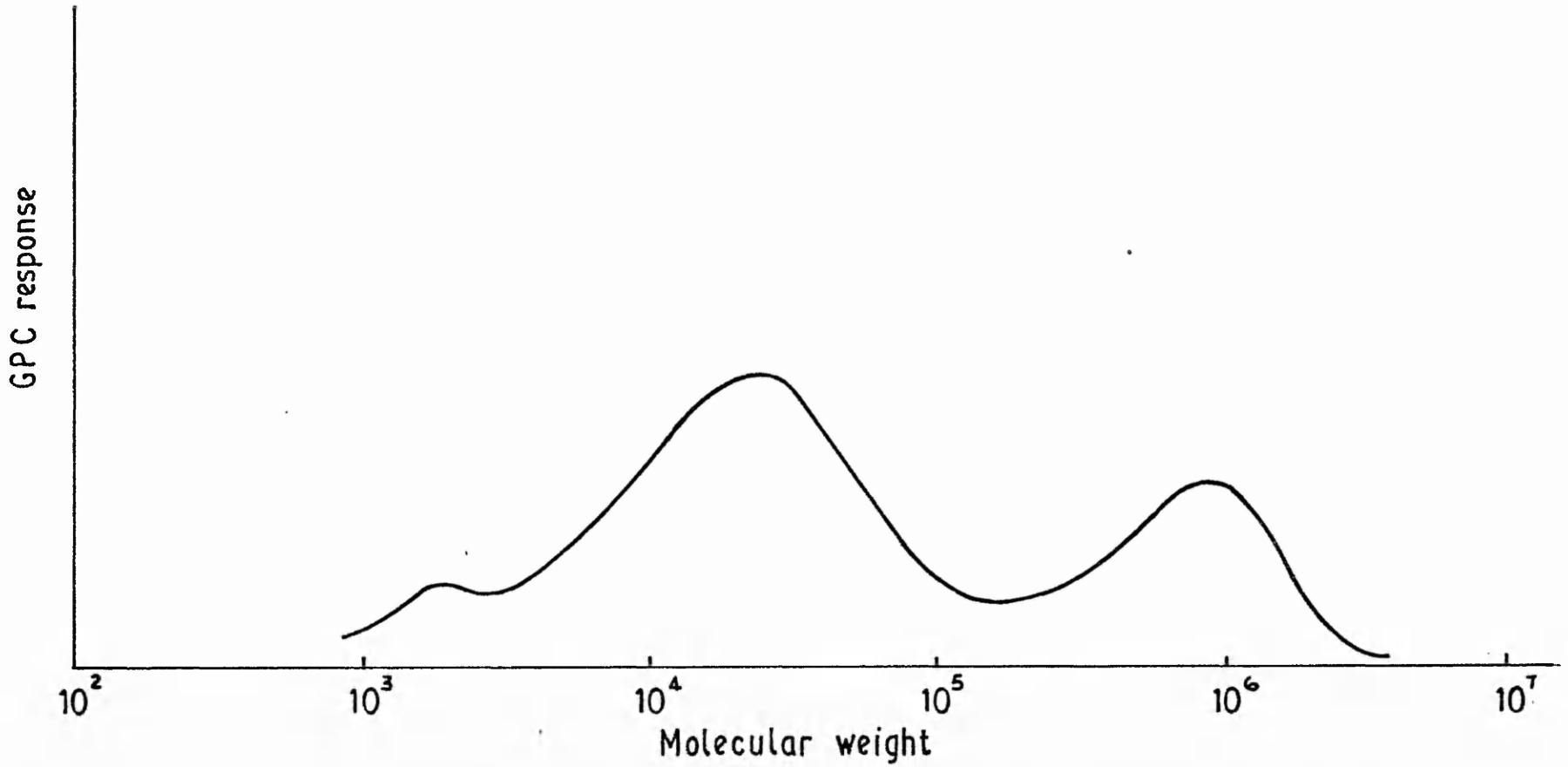

FIG A:3 GEL PERMEATION CHROMATOGRAPH FOR SAMPLE MC 69/3

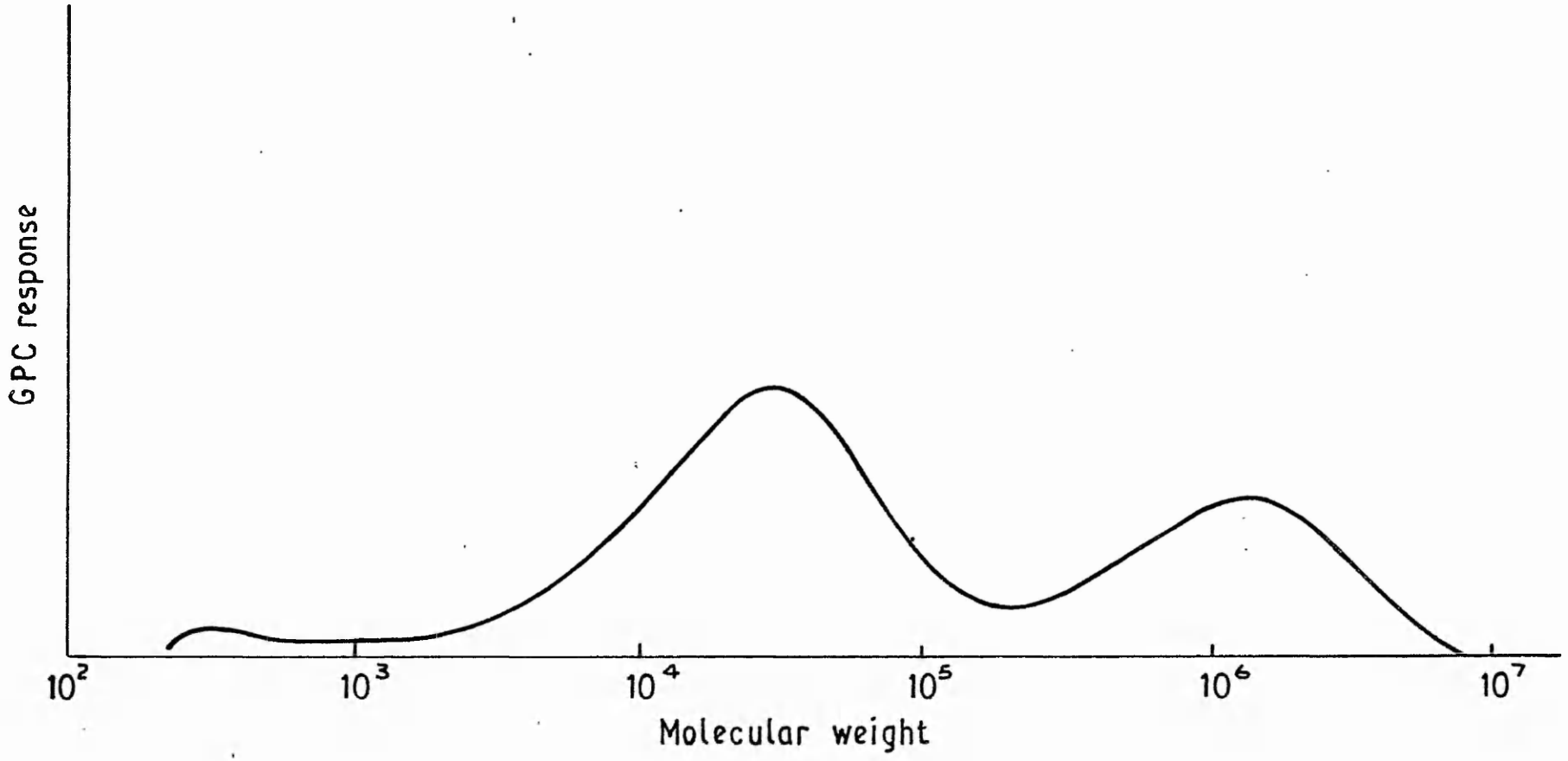

FIG A:4 GEL PERMEATION CHROMATOGRAPH FOR SAMPLE MC 69/4

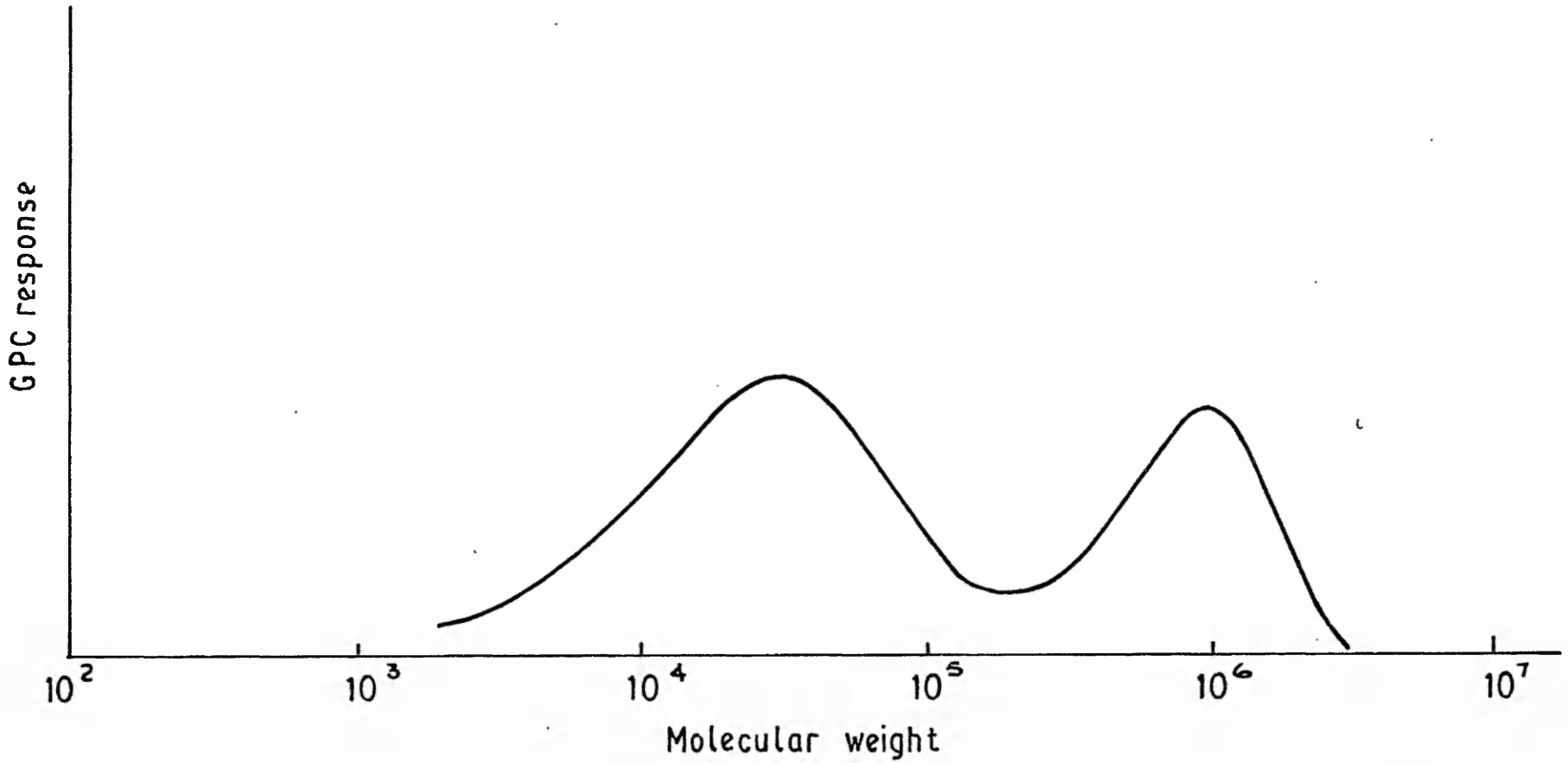

FIG A:5 GEL PERMEATION CHROMATOGRAPH FOR SAMPLE MC 69/5

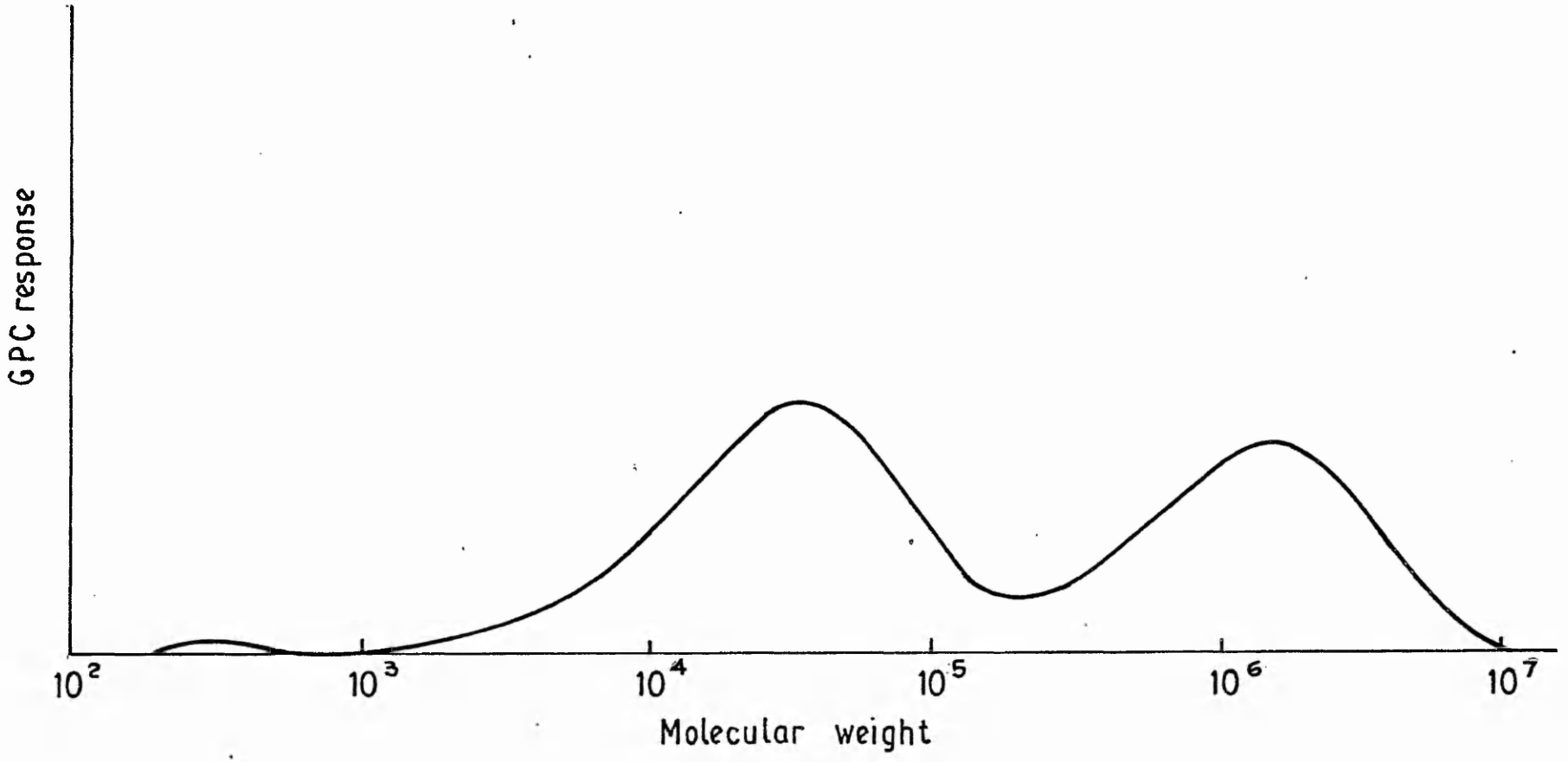

FIG A:6 GEL PERMEATION CHROMATOGRAPH FOR SAMPLE MC 69/6

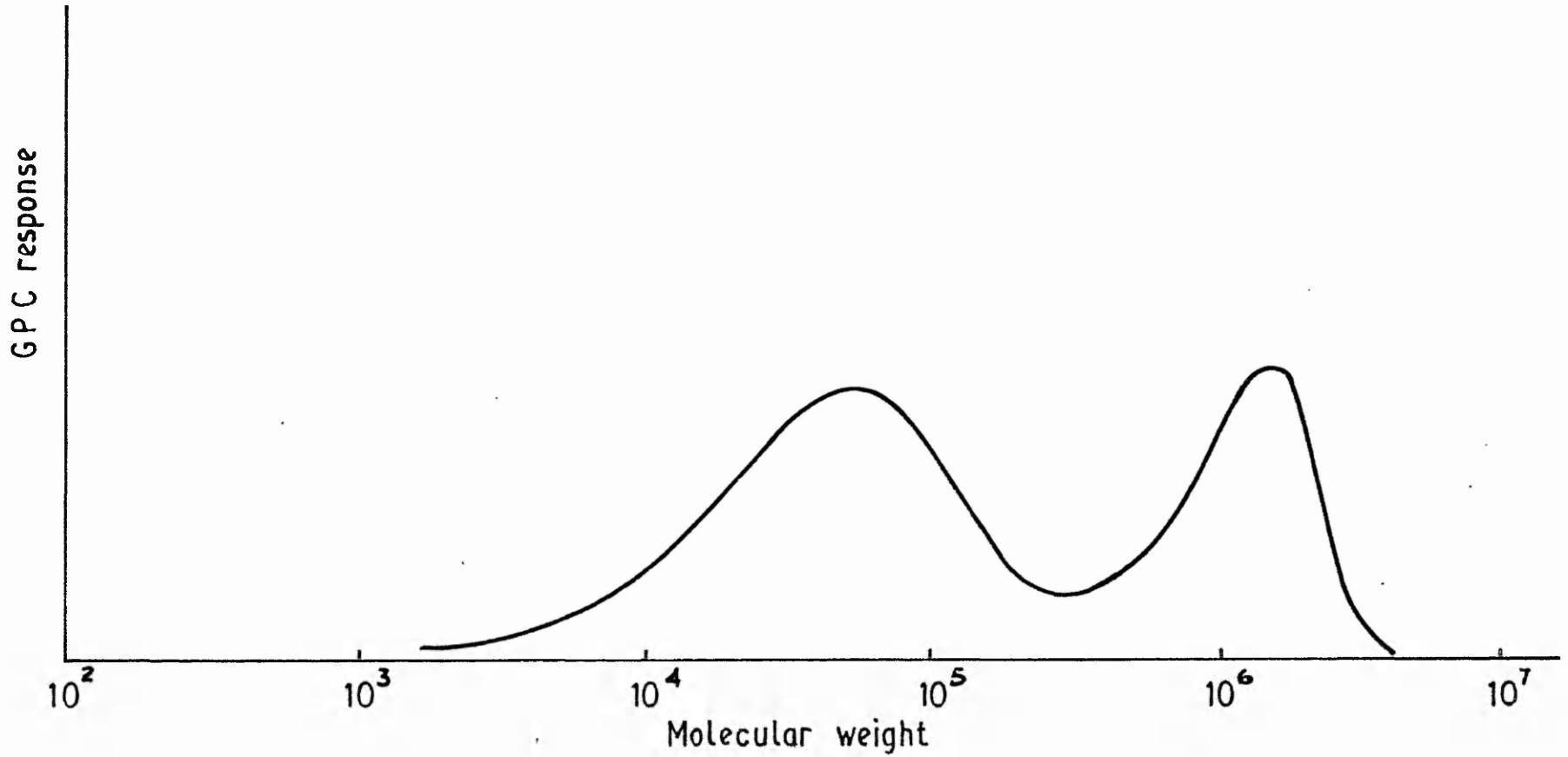

FIG A:7 GEL PERMEATION CHROMATOGRAPH FOR SAMPLE MC 69/7

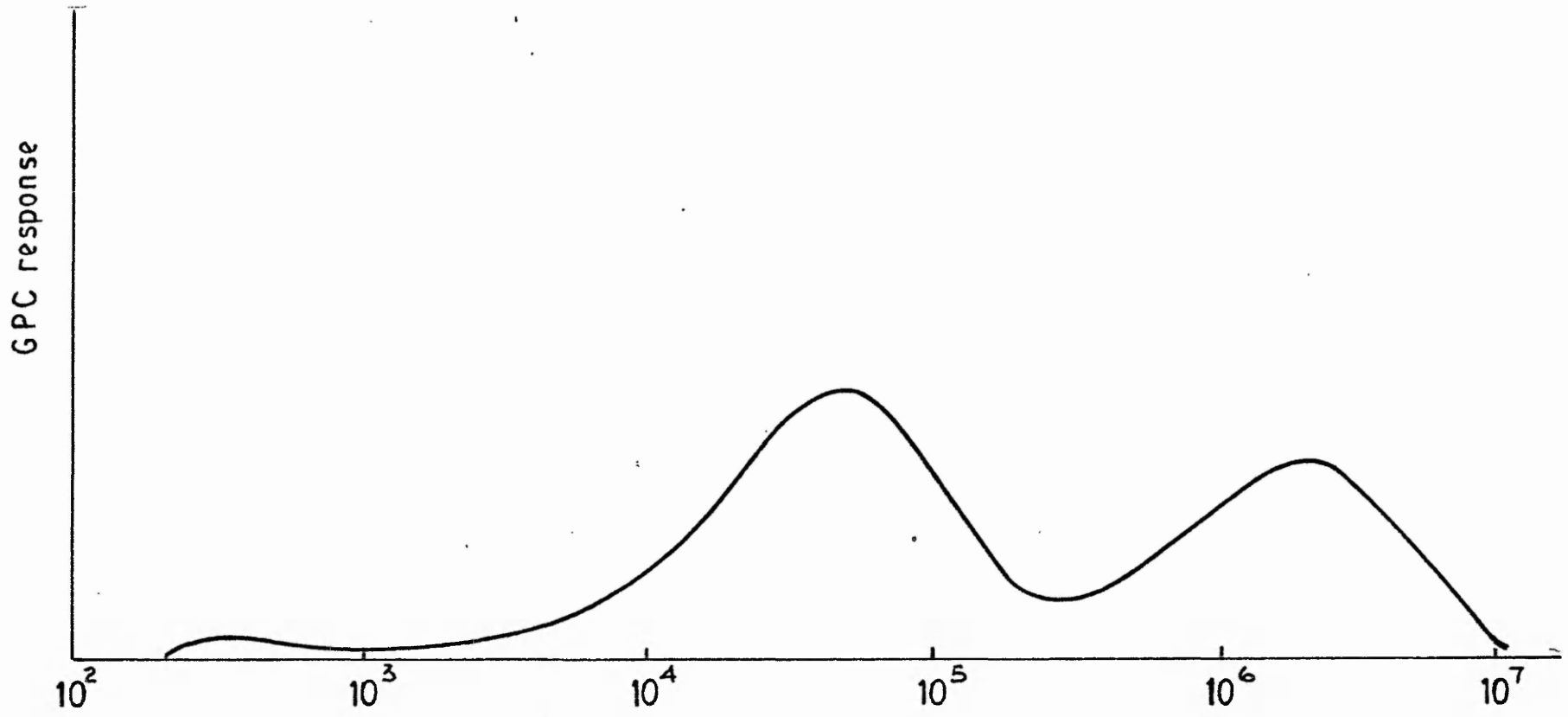

FIG A:8 GEL PERMEATION CHROMATOGRAPH FOR SAMPLE M C 69/8

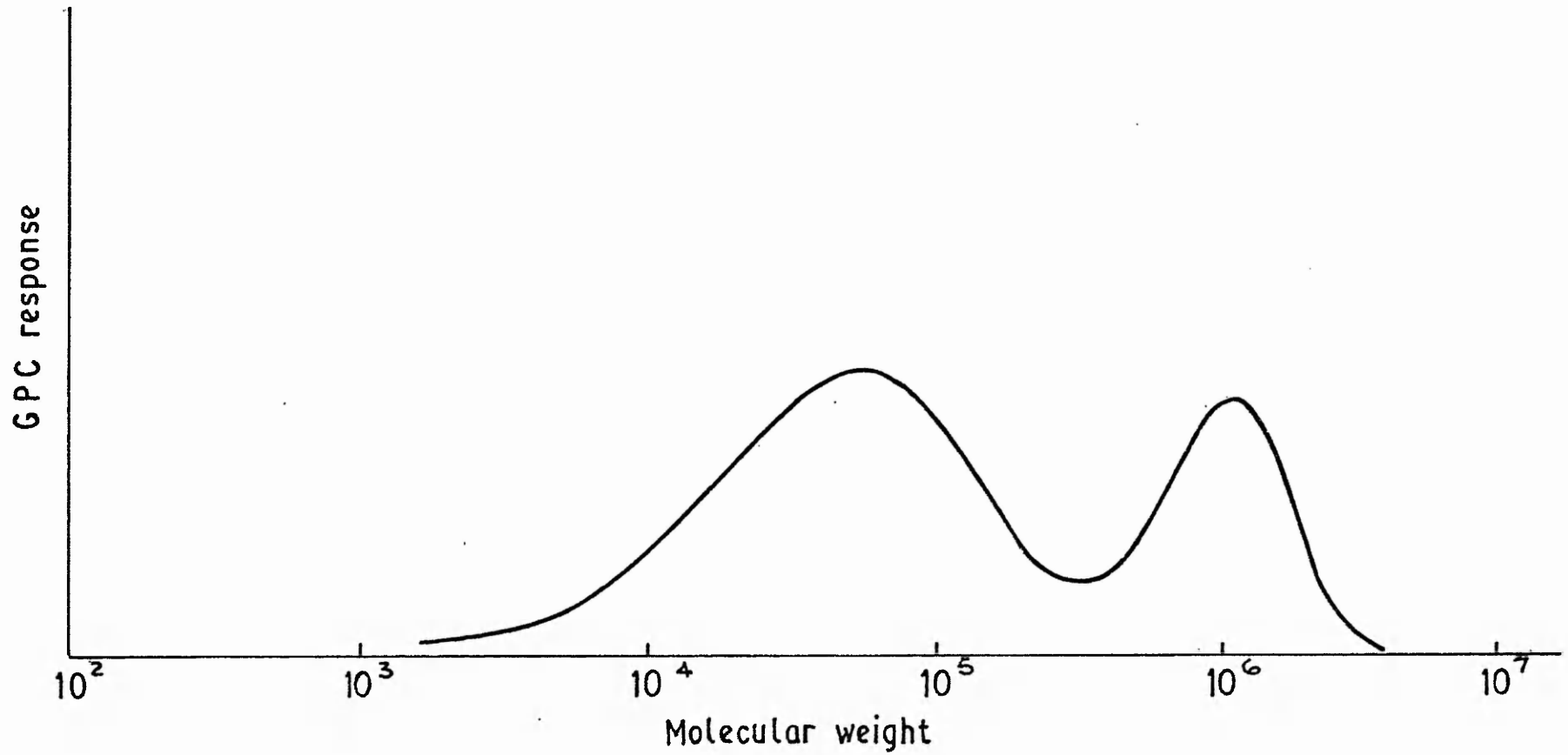

FIG A:9 GEL PERMEATION CHROMATOGRAPH FOR SAMPLE MC 69/9

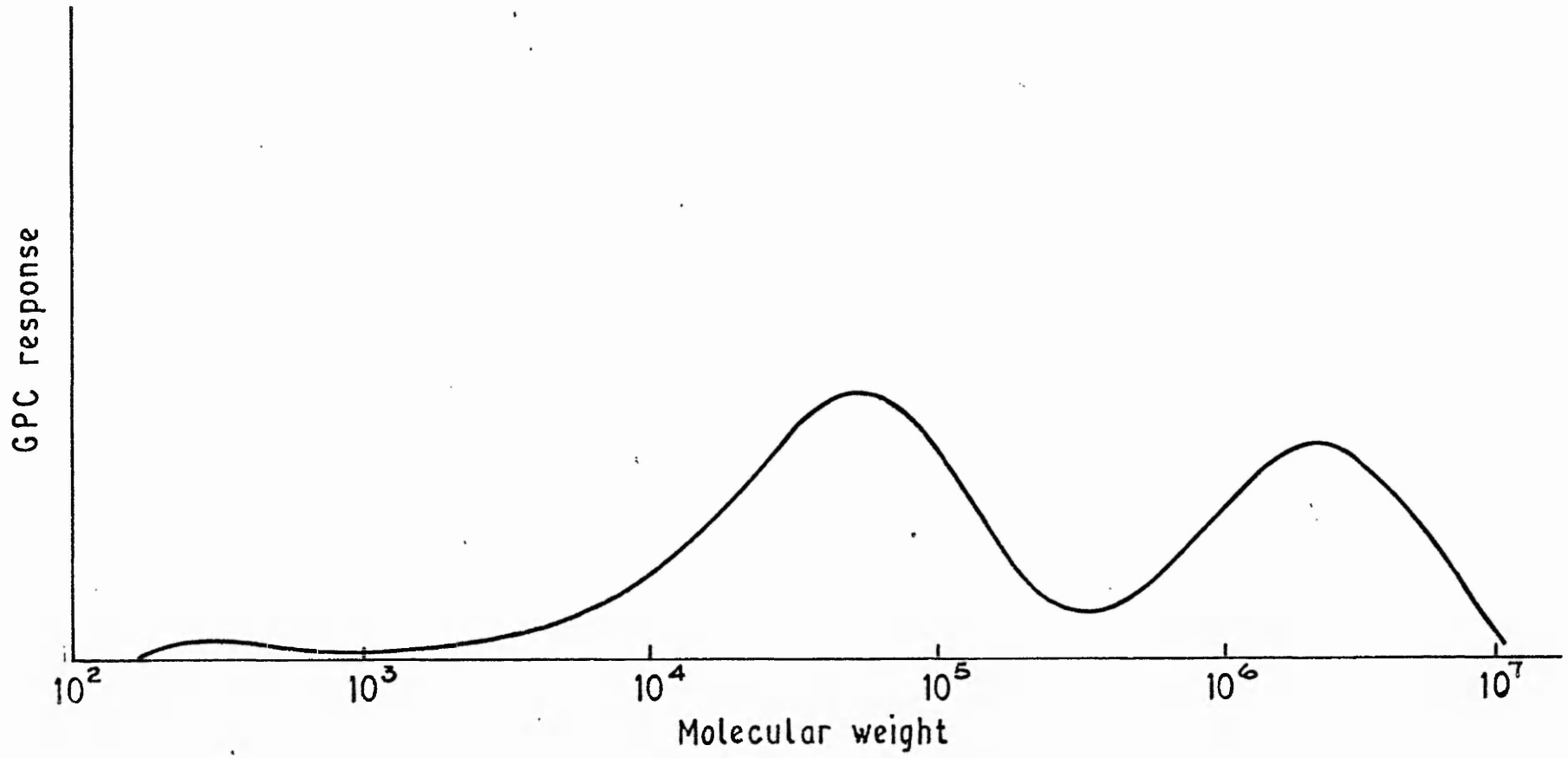

FIG A:10 GEL PERMEATION CHROMATOGRAPH FOR SAMPLE MC 69/10

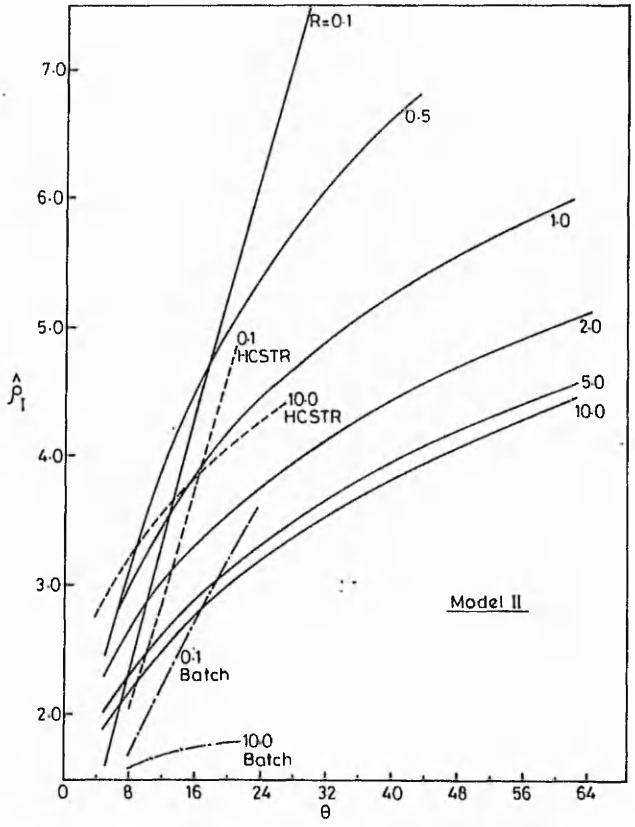

Fig.7 Polydispersity index for Model II.

Figures 8 and 9 show cross plots of ρ_I vs monomer conversion for different values of R and $\mu_{n,I}$. Such plots would be of significant engineering interest since they show the relationship between the three important parameters characterising the product from a reactor. For both the kinetic model, it is observed that at the same conversion, the polydispersity index falls as R increases. The graphs are closer together for Model I than for Model II, i.e. the results are more sensitive to the value of R for Model II because of the fact that more reactions are associated with the rate constant k_{11}.

4. CONCLUSIONS

MWDs and moments have been computed for condensation polymerisation of ARB type monomers violating the equal reactivity hypothesis in a segregated, continuous-flow,

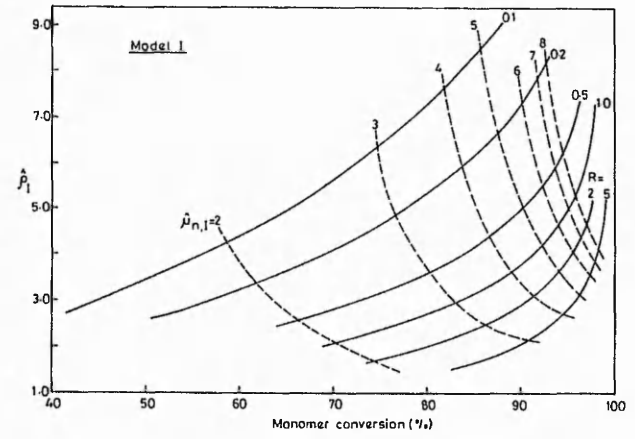

Fig.8 Cross plots of ρ_I vs monomer conversion for Model I for various R and $\mu_{n,\ I}$.

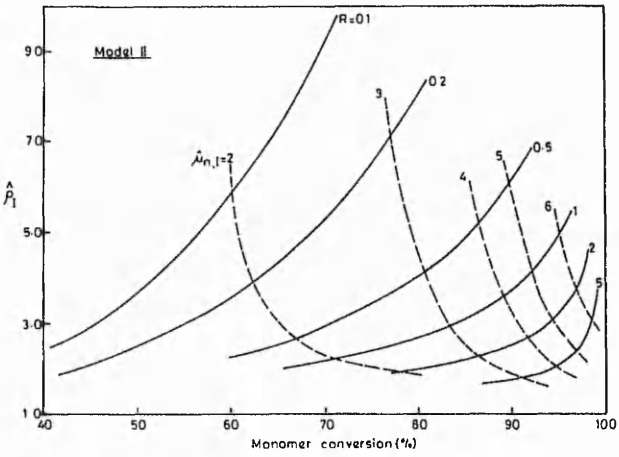

Fig.9 Cross plots of ρ_I vs monomer conversion for Model II for various values of R and $\mu_{n,\ I}$.

stirred tank reactor. Results for two kinetic schemes, representing limiting cases of actual polymerisations, are found to lie intermediate between earlier results on batch reactors and homogeneous, continuous-flow, stirred tank reactors.

References

1 Flory, P. J., *J. Amer. chem. Soc.*, 1936, **58**, 1977.
2 Schultz, G. V., *Z. Phys. Chim.*, 1935, **B30**, 379.
3 Stockmayer, W. H., *J. Polym. Sci.*, 1952, **9**, 69.
4 Flory, P. J., *Principles of Polymer Chemistry*, 1st ed., 1953, *Ithaca, New York: Cornell University Press.*
5 Kumar, A. & Gupta, S. K., *Fundamentals of Polymer Science and Engineering*, 1st ed., 1978, *New Delhi: Tata McGraw Hill*
6 Lenz, R. W., Handlovitz, C. E. & Smith, H. A., *J. Polym. Sci.*, 1962, **58**, 351.
7 Challa, G., *Makromolek. Chem.*, 1960, **38**, 105.
8 *Idem, ibid*, 1960, **38**, 123.
9 *Idem, ibid*, 1960, **38**, 138.
10 Bailey, M. E., Kriss, V. & Spaunburgh, R. G., *Ind. Engng. Chem.*, 1956, **48**, 794.
11 Lyman, D. J., in *Step Growth Polymerisation* ed. Solomon, D. J., 1972, *New York: Marcel Dekker.*
12 Drumm, M. F. & LeBlanc, J. R., in *Step Growth Polymerisation* ed. Solomon, D. J., *New York: Marcel Dekker.*
13 Kumar, A., Kulshreshtha, A. K. & Gupta, S. K., *Polymer*, 1980, **21**, 317.
14 Kumar, A., Kulshreshtha, A. K., Gupta, S. K. & Phukan, U. K., *Polymer*, in press.
15 Pal, P. K., Kumar, A. & Gupta, S. K., *Brit. Polym. J.*, 198, **12**, 121.
16 Hodgkin, J. H., *J. Polym. Sci., Polym. Chem. Edn.*, 1976, **14**, 409.
17 Kronstadt, M., Dubin, P. L. & Tyburczy, J. A., *Macromolecules*, 1978, **11**, 37.
18 Nanda, V. S. & Jain, S. C., *J. Chem. Phys.*, 1968, **49**, 1318.
19 Miller, D. R. & Macosko, C. W., *J. Polym. Sci.*, 1958, **29**, 455.
20 Gandhi, K. S. & Babu, S. V., *A. I. Ch. E. J.*, 1979, **25**, 266.
21 Goel, R., Gupta, S. K. & Kumar, A., *Polymer*, 1977, **18**, 851.
22 Gupta, S. K., Kumar, A. & Bhargava, A., *Polymer*, 1979, **20**, 305.
23 Gupta, S. K., Kumar, A. & Bhargava, A., *Eur. Polym. J.*, 1979, **15**, 557.
24 Levenspiel, O., *Chemical Reaction Engineering*, 2nd edn., 1972, *New York: Wiley.*
25 Biesenberger, J. A., *A. I. Ch. E. J.*, 1965, **11**, 369.
26 Tadmor, Z. & Biesenberger, J. A., *Ind. Engng. Chem., Funda.*, 1966, **5**, 336.
27 Hicks, J., Mohan, A. & Ray, W. H., *Can. J. Chem. Eng.*, 1969, **47**, 590.
28 Gupta, S. K., Kumar, A. & Saraf, R., *J. Appl. Polym. Sci.*, 1980, **25**, 1049.
29 Kumar, A., Gupta, S. K. & Saraf, R., *Polymer*, 1980, **21**, 323.
30 Ray, W. H., *J. Macromolec, Sci., C*, 1972, **8**, 1.
31 Abraham, W. H., *Ind. Engng. Chem., Funda.*, 1963, **2**, 221.
32 Kilkson, H., *Ind. Engng. Chem., Funda.*, 1964, **3**, 281.

A Microfiltration Technique for Cleaning Polymer Latices

M.C. Wilkinson, J. Hearn,* P. Cope* & M. Chainey*

A microfiltration technique for cleaning polymer latices is evaluated. The modified millipore microfiltration cell employed is described and optimum operating conditions given: the cell consists of a 47 mm diameter millipore filter supported on a stainless steel mesh and contained within a PTFE body. Double distilled water is pumped through the cell, removing impurities from the latex. The latex particles are retained by the filter: pore blockage is prevented by PTFE coated magnetic stirrer bar. The nature and location (water or polymer phases) of the major impurities encountered with polystyrene latices are identified. The efficiency with which microfiltration removes these impurities is compared with dialysis and ion exchange. Monomer, low molecular weight oligomer, benzaldehyde, and surface active agent are completely removed. However, electrolytic material associated with the polymer phase is not completely removed by this technique. Microfiltration may also be used to concentrate a latex and separate latex particles of different sizes.

1. INTRODUCTION

A wide range of narrow size distribution inorganic and polymeric sols can now be prepared by well-established techniques.[1–6] These have been used in a wide variety of applications [7,8] especially in fundamental studies of the interactions between particles. Model colloids for this latter purpose need to be well characterised and an important part of this process is the technique of cleaning. The cleaning process should be capable of removing impurities from both the bulk phase and the suspending medium (usually water) as well as that associated with the particle/suspending medium interface, without affecting the true nature of the sol (e.g. particle size, nature and concentration of surface groups, particle morphology).

The cleaning process can only be properly evaluated after the nature of the impurities have been identified. The major impurities encountered with polystyrene latices, which are probably the most widely studied 'model' sols, have been identified and methods for their removal have been studied by Wilkinson *et al*, [9–14] Everett *et al* [15] and others, [2,16] and details are given in Table 1. The ease of removal of these impurities varies widely; for example, electrolyte material is removed readily by conventional dialysis or ion exchange whereas styrene monomer and oligomeric material are only slowly removed by these techniques.[9,11,15]

Dialysis and ion-exchange have been used for many years as cleaning techniques but the problems associated with these have only recently been identified. Different techniques are now being developed. These include hollow-fibre dialysis, [17] ultra-filtration [18] and the use of activated charcoal.[19] Hollow-fibre dialysis and ultra-filtration are similar to dialysis, although far more rapid, for they rely for their effectiveness on the exchange of materials across a membrane or filter. Activated charcoal in the form of a wovencloth material is similar in action to ion-exchange resin and comes into direct contact with the sol.

Labib and Robertson [20] have recently given a brief description of a dia-filtration device which gave a significant reduction in the time taken for cleaning a latex, compared with dialysis. The efficiency of removal of impurities was measured by monitoring the eluent wash water conductance, determining the change in surface charge on the latex and by TEM examination. This showed the removal of small particles, capable of passing through the pores in the filter, and also of a 'gel-like' material, often obversed in TEM's of latices, and ascribed to monomer or oligomeric materials.

Table 1. Impurities Found in Polystyrene Latices

Impurity	*Location*		
	Water Phase	*Polymer Phase*	*Particle Water Interface*
Styrene monomer	√	√	√
Oligomers	√	√	√
Thermally polymerised styrene	√	√	√
Sulphuric acid	√	–	–
K+	√	–	√
Na+	√	–	√
Benzaldehyde/formaldyhyde	√	–	√
Benzoic acid	√	–	√
Microbiological material	√	—	√

This paper describes a microfiltration device, similar to that recently discussed by Ahmed *et al*, [21] which has been independently evaluated. Particular attention has been paid to its efficiency in removing residual monomer, emulsifier, electrolyte, benzaldehyde, benzoic acid and microbiological materials; contaminants whose presence has been shown to be important when attempting to prepare model colloids.[14] A wide range of filters can be employed and samples from 10 cm^3 to 1000 cm^3 easily cleaned within a day.

2. EXPERIMENTAL

2.1 Microfiltration Unit

A schematic diagram of the unit is shown in Fig. 1. It is a modified version of a commercially available unit made in

Chemical Defence Establishment, Porton Down, Salisbury, Wilts.
**Dept Physical Sciences, Trent Polytechnic Burton St, Nottingham*

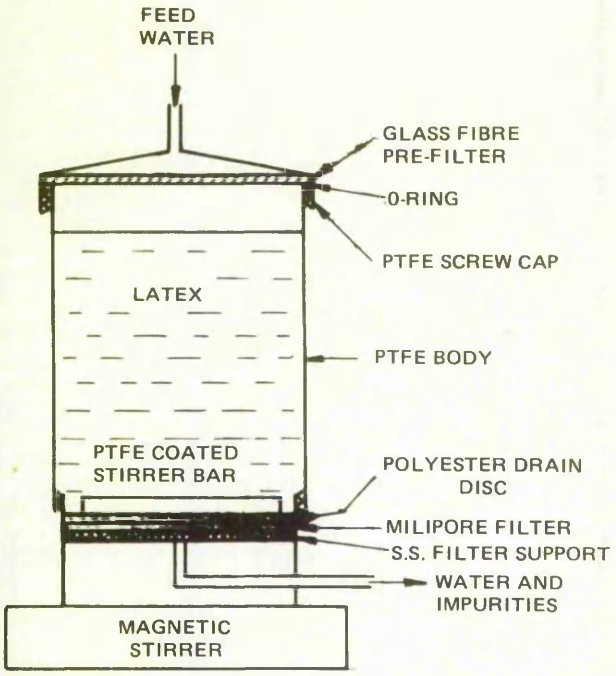

Fig.1 Schematic design of microfiltration unit

polycarbonate and marketed by Millipore Ltd.** The main components of the cell were machined out of PTFE to avoid attack of the polycarbonate by various monomers. The cell capacity was 80 cm^3 and a standard 47 mm diameter filter was employed (a larger cell could be employed with an appropriately larger filter – up to 293 mm diameter). Prior to use it was disassembled and all parts boiled in double distilled water for 30 min. The unit was then assembled and double distilled water passed through (80 $cm^3\ h^{-1}$) until the surface tension and conductance were the same as the feed water. This process was then repeated with the filter in position.

Both Nuclepore† and Millipore filters can be used in the cell. The former consist of a polycarbonate disc (10 μm thick) which has been bombarded with α-particles to produce the pores. The manufacturers claim that there are no pores larger than the nominal size stated. The membranes are very delicate and require careful handling in the cell. A similar filter is marketed by Bio-Rad* under the name Uni-Pore.

Millipore filters are composed of cellulosic fibres. They are much thicker (150 μm) and consequently much more robust. Retention of particles larger than the rated pore size results from random entrapment within the filter. The greater tortuosity of this type of filter results in a lower flow rate (normally of the order of 50% lower) for a given pressure. However, the Nuclepore filter has only about 15% open area (depending on pore size) – compared with the Millipore filter (Plates 1 and 2) – and it readily becomes blocked by latex particles. Ahmed *et al*, [21] who worked exclusively with this type of filter, found that latices of 10–15% solids filtered at 5 psi clogged the filter and formed enough coagulum to stop the stirrer.

** Millipore UK Ltd, Millipore House, Abbey Road, London NW10 7SP.

† Sterilen Ltd, 43–45 Broad Street, Teddington, Middlesex TW11 8QZ.

* Bio-Rad Laboratories Ltd, Caxton Way, Holywell Industrial Estate, Watford, Herts WD1 8RP.

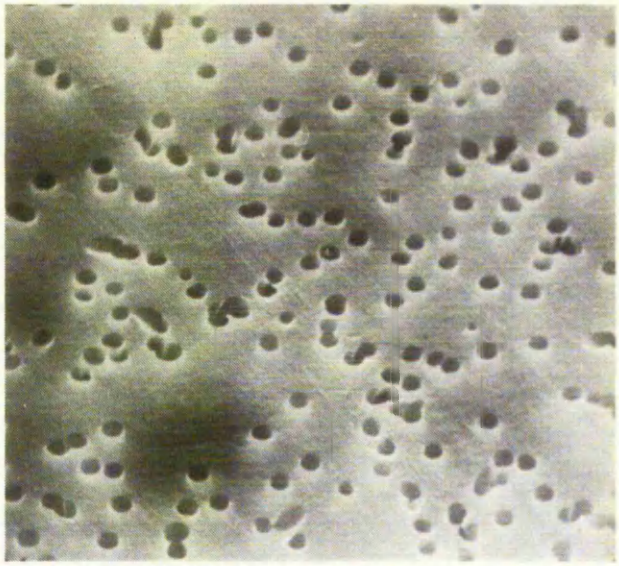

Plate 1 0.8 μm Nuclepore membrane

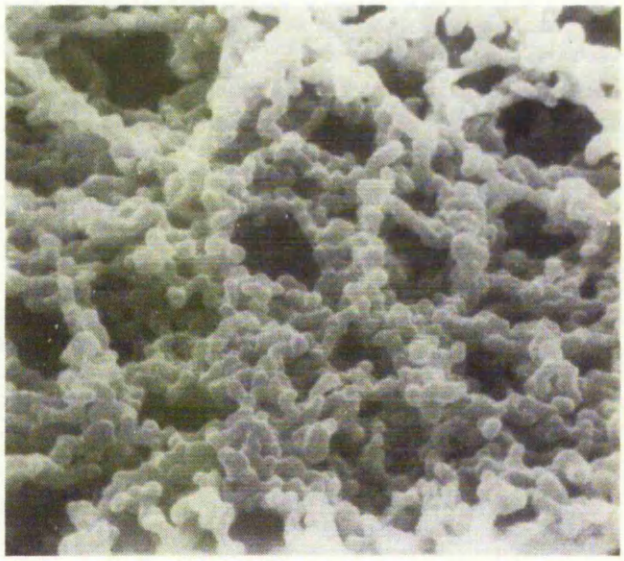

Plate 2 0.8μm Millipore membrane

Both types of filter were evaluated initially. However, the Nuclepore filters invariably allowed the passage of latex particles: after about 10 cell changes, all the latex had passed through the filter. The most likely explanation fo for this was leakage through the filter caused either by distortion during mounting or attrition of the surface by the stirrer bar. Special precautions were taken to try to prevent this, including an experiment in which a 0.2 μm Nuclepore filter was sandwiched between two 0.8 μm Millipore filters.

In addition to mechanical wear of the polycarbonate filter, chemical attack by impurities, especially residual monomer, is possible. Tests showed that styrene did not etch the filters, although acrylate monomers did. Many other monomers might be expected to attack polycarbonate. It is now possible to obtain Nuclepore filters made from polyester, but since they were not available unti this study was substantially complete, they have not been evaluated.

Because of the problems of leakage encountered with Nuclepore filters, most of the work reported here is restricted to Millipore filters.

Although Millipore filters rely on the trapping of larger particles within the membrane, no problems with blockage were encountered unless a large amount of residual monomer was present. This could be prevented by the use of a 'Drain disc' (polyester, non-woven fabric construction; manufactured by Bio-Rad) which was placed above the Millipore filter. In extreme cases the drain disc became clogged with a monomer/polymer coagulum and had to be replaced. The original Millipore filter was unaffected.

Ahmed *et al* [21] do not report the effect of residual monomer concentration on the efficiency of cleaning.

2.2 Latices

Polystyrene latices used in this work were prepared by the emulsifier-free technique and their preparation has been described in detail elsewhere.[22] The particle sizes and solids contents are listed in Table 2.

Table 2. Details of Polystyrene Latices

Latex	*Diameter/nm*	*% Solids*	*Surface Area in 80^3 Latex/cm^2*
A	440	7.30	9.6×10^5
B	490	2.29	2.7×10^5

2.3 Water

Double distilled water from an all pyrex glass still was used. It was flushed with oxygen-free nitrogen to remove dissolved gases (carbon dioxide in particular) before use, and then stored in a 10 dm^3 aspirator in a sealed system. The surface tension at 298K was 72.0 mNm^{-1} and the conductivity $\leqslant 1$ μS.

2.4 Determination of Styrene and Benzaldehyde

Styrene and benzaldehyde (method sensitivity 5×10^{-5} mol dm^{-3} and 10^{-5} mol dm^{-3}, respectively) were determined with a PYE 104 gas chromatograph. A 1.5 m x 4 mm ID column packed with 5% carbowax 20 M on chromo-sorb W (80–100 mesh) was employed. The nitrogen carrier gas flow rate was 50 cm^3 min^{-1} and the oven temperature 373K. Samples for analysis were diluted 4 times with tetrahydrofuran and mechanically shaken for 30 min.

2.5 Ion-Exchange Materials

Four ion-exchange media were employed:

Dowex 50 X8 and 1 X8

Bio-Rad AE1X–4 + AG50W–X4

\+ AIEC (Advanced Ion Exchange Cellulose)

Amberlite XAD12

The resins were cleaned according to the manufacturers recommendations and were employed as a 5x excess (based on ion-exchange capacity).

2.6 Determination of Sodium and Potassium

An EEL flame photometer was used to measure sodium and potassium levels in water and polymer. Sensitivities were: Sodium, 10^{-3} ppm (at 589.3 nm) and potassium 5×10^{-2} ppm (at 766.5 nm).

#British Drug House, Poole, Dorset BH1Z 4NN

+ Whatman Laboratory Sales Ltd, Springfield Mill, Maidstone, Kent ME1X 2LE

2.7 Conductometric Titrations

The latices were characterised by conductometric titration which was carried out on 30–35 cm^3 samples of latex at 25 ± 0.1°C in a nitrogen atmosphere (sample preflushed) with 10^{-2} mol dm^{-3} sodium hydroxide solution.

2.8 Surface Tension Measurements

Surface tensions were determiend useing the Du Nouy ring technique.

3. RESULTS AND DISCUSSION

3.1 Factors Affecting Water Flow Rate

3.1.1 Latex Particle Diameter/Filter Pore Size

A filter was chosen such that the average pore size was 50 to 75% of the latex particle diameter.

3.1.2 Stirrer Speed

The speed of the magnetic stirrer bar was kept to a minimum, typically to 100 rpm. This was sufficient to keep pore blockage to a minimum.

3.1.3 Latex Concentration

The latex concentration was usually 3 to 5% although the optimum solids content was less than 20% (Fig 2). Much higher solids contents could be cleaned but the eluent rate dropped with increasing solids content. The unit could be used to concentrate a latex to as much as 50% solids. This process is particularly useful where the solids content is too low (< 2%) for a reliable conductometric titration to be carried out.[12]

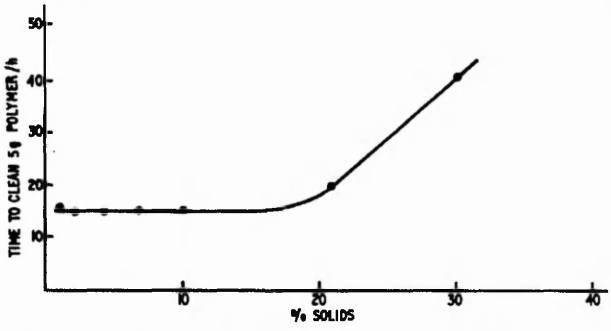

Fig.2 Time to clean 5g of polymer at different solids contents. This includes the stages (i) filtration (ii) acid wash (iii) cleaning wash to remove acid

3.1.4 Water Pressure

The elution rate could be varied by pressurising the water supply in the aspirator via a nitrogen (0_2–free) cylinder. The elution rate varied with applied pressure but was approximately linear between 1 and 2.2 psi (Fig. 3). Most of the work was carried out at pressures between 1 and 3 psi.

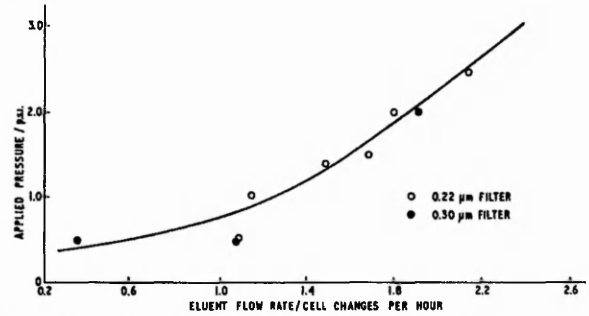

Fig.3 Variation in eluent rate with applied pressure

3.2 Cleaning of Latex

3.2.1 Rate of Removal of Electrolyte

A sample of freshly prepared and untreated latex was centrifuged and the centrifugate and mother liquor analysed by flame photometry. The centrifugate was found to contain 180 μg cm^{-3} potassium; the mother liquor contained 25 μg cm^{-3} potassium and 16 μg cm^{-3} sodium. The sodium was derived from the impurity in the potassium persulphate (measured by flame photometry to be 0.002% w/w).

The latex was microfiltered using double distilled water and samples of the eluent water analysed after various volumes had been passed. The results in Fig. 4 show that both potassium and sodium levels in the aqueous phase were reduced to negligible levels after approximately 5 cell changes. However, this was no indication as to the level of sodium and potassium left associated with the polymer phase (i.e. in the electrical double layer), which as shown by acid washing and ion-exchange techniques can be significant (refer Section 2.2). Thus, this technique, in common with dialysis and similar methods is not capable of ensuring complete removal of electrolytic material associated with the polymer phase.

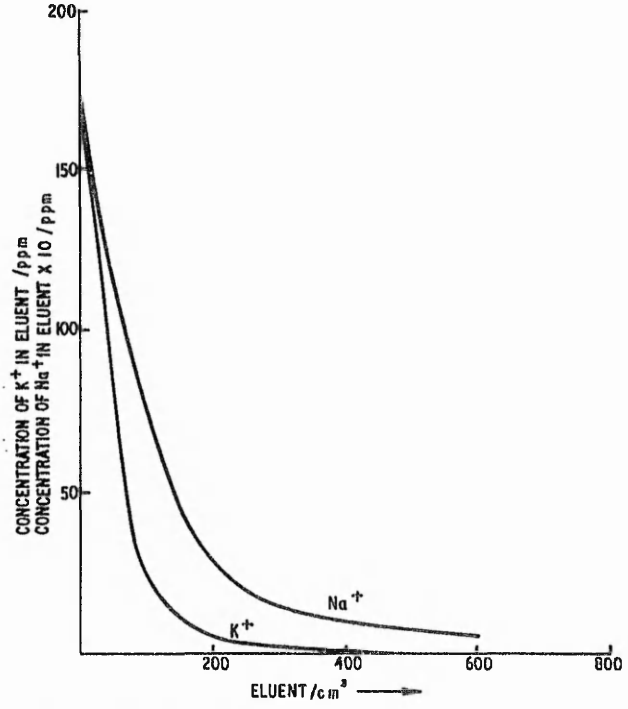

Fig.4 Efficiency of removal of sodium and potassium ions

3.2.2 Effect on Surface Charge

Samples of latex were taken during elution and titrated against 10^{-2} mol dm^{-3} sodium hydroxide solution. The surface charge fell rapidly such that after ca 10 cell changes (800 cm^3 of eluent) the surface charge was very similar to that recorded after 28 days dialysis, ie 2.31 μeq g^{-1} and 2.20 μeq g^{-1}, respectively. This then varied little during further elution (after 16 cell changes a value of 2.44 μeq g^{-1} was recorded).

A sample of latex cleaned according to Vanderhoff *et al* [21] with a mixed bed ion-exchange resin gave a significantly higher surface charge of 14.1 μeq g^{-1} (Fig. 5). It was thought that the low value on dialysis and microfiltration was due to the incomplete exchange of cations for protons.[2] To test this hypothesis the latex was washed

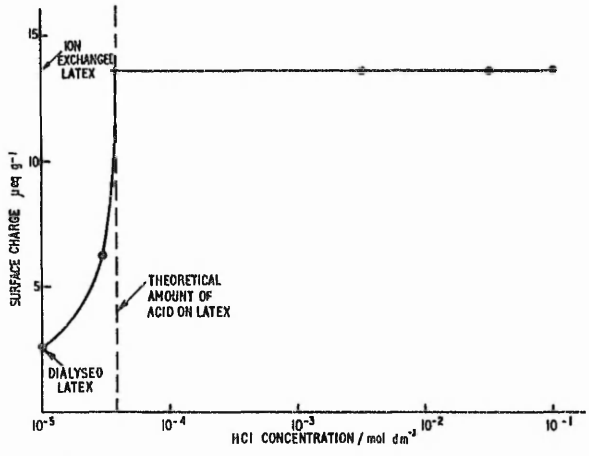

Fig.5 Effect of acid washing on surface charge

in the cell with various concentrations of hydrochloric acid. This was followed by distilled water elution until the conductivity of the eluent was the same as that of distilled water. It was noted that the surface charge changed little until a concentration of ca 6 x 10^{-5} mol dm^{-3} acid was reached, whereupon it increased rapidly to ca 13.5 μeq g^{-1} and remained constant as the acid concentration was increased to 10^{-1} mol dm^{-3} (Fig. 5). The value of 13.5 μeq g^{-1} agreed well with the ion-exchanged value of 14.1 μeq g^{-1} and it was assumed that this corresponded to the state where all cations had been replaced by protons.

The sharp increase in surface charge at ca 5 x 10^{-5} mol dm^{-3} acid concentration agreed well with the calculated amount of cations required to be exchanged (i.e. 6 x 10^{-5} mol dm^{-3}). A 24h dialysis of the acid washed sample (6 changes of dialysate at 400:1 exchange ratio) did not result in any change of this value (13.6 μeq g^{-1} being recorded). This finding is in agreement with the results of Ahmed *et al* [21].

3.2.3 Removal of Styrene and Benzaldehyde

Labib and Robertson [20] found that a 'gel-like' material could be removed from a polystyrene latex when filtered using a diafiltration technique. This resulted in a 'clean' latex with an almost complete absence of 'bridges' between contacting latex particles. They did not analyse for this material but it was almost certainly styrene monomer and low molecular weight oligomers.[9] The microfiltration unit employed in this work was equally as effective in removing monomer, low molecular weight oligomers and also benzaldehyde (Table 3). The efficiency of removal of these materials can be compared with that of dialysis and ion-exchange, which were found to be generally ineffective (Table 3).

3.2.4 Removal of Benzoic acid

Previous work [10] has shown that benzoic acid is formed during the emulsion polymerisation of styrene and this is adsorbed at the polymer latex/water interface and is difficult to remove by conventional dialysis. The presence of even small amounts of benzoic acid can have a significant effect on the conductometric titration curve, contributing to an increase in the titratable strong acid at low concentrations ($< 10^{-3}$ mol dm^{-3}) and only appearing as a weak acid species in concentrations above this.

Significant oxidation of styrene can occur during an emulsion polymerisation, even in a nitrogen atmosphere – presumably by oxidation via the persulphate free radical

Table 3. Efficiency of Removal of Styrene and Benzaldehyde by various Techniques

	% Styrene Removed	*% Benzaldehyde Removed*
Microfiltration (10 x vol exchange)	> 99	> 99
Amberlite XAD–2	58	50
AIEC	8	75
Mixed Dowex	75	85
Dialysis (1 day)	6	–
Dialysis (20 days)	90	–

Notes

Original concentrations: styrene 71 mg/g polymer
benzaldehyde 8 mg/g polymer

Ion-exchange resins used on a 5 x excess (based on exchange capacity.) Contact time 5h.

Dialysis carried out at 20:1 ratio.

initiator. For example, it was found that benzoic acid was being generated at 1.95 mmol dm^3h^{-1} in a stirred system consisting of 2 cm^3 of benzaldehyde in 100 cm^3 of 11 11 mmol dm^{-3} potassium persulphate solution at 343K under nitrogen. Although the levels of benzaldehyde present during a polymerisation will be very much less than this, there is still sufficient to radically affect the nature of the surface charge if converted to benzoic acid.[10]

To determine the efficiency of removal of benzoic acid by the microfiltration technique a clean sample of latex A was dosed with 2% w/w polymer and this was eluted in the usual manner. Samples were taken and titrated conductometrically during elution (Fig. 6). The surface charge decreased from an initially high value of 68 μeq g^{-1} (an apparent strong acid: ref 10) to a constant value of ca 13.9 μeq g^{-1} after 25 changes of cell content. It is of note that almost 3 times as many exchanges were required to remove the benzoic acid (7 mmol dm^{-3}) as the equivalent concentration of hydrochloric acid. This demonstrates the strong adsorption of benzoic acid on the latex particles.[10]

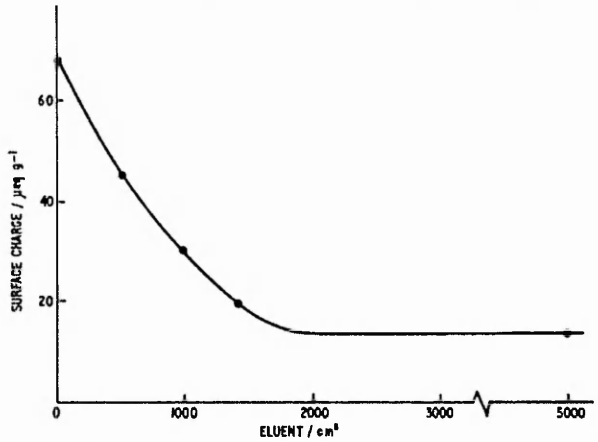

Fig.6 Efficiency of removal of benzoic acid from latex by elution

The surface charge did not drop to that of the original clean sample (2.4 μeq g^{-1} – not acid washed, refer Fig. 5); but reached a constant value of 13.9 μeq g^{-1}. This agrees well with the acid washed sample and may not be unexpected since benzoic acid is partially dissociated at room temperature (6.3 x 10^{-5} mol dm^{-3} in the dissociated form) and could therefore enable complete exchange of cations for protons to be achieved.

3.2.5 Removal of Surface Active Agent

The large majority of emulsion polymerisations involve the use of a surface-active agent [25,26] and it is important to evaluate the microfiltration technique in this context. This is particularly pertinent since there are conflicting views on the efficiency of removal of certain surface active agents by the dialysis technique.[27–29] Since most of the work in this area has been concerned with sodium dodecyl sulphate this was chosen for study in the present work.

A solution of a pure sample of sodium dodecyl sulphate and a sample of latex A were mixed. The concentration of sodium dodecyl sulphate in the latex was 12.5 mmol dm^{-3}: this concentration was chosen because it is above the critical micelle concentration and was capable of reducing the concentration of the latex to a constant low value (38.8 mNm^{-1}). This latex was then eluted continuously in the usual manner until the surface tension and conductivity of the eluent were the same as those of the feed water (Fig. 7). A sample of the cleaned latex A was titrated against 10^{-2} mol dm^{-3} sodium hydroxide solution and this gave an endpoint of 19.4 μeq g^{-1} (cf acid washed latex). A second sample of the cleaned latex was back titrated with sodium dodecyl sulphate solution according to the technique of Maron *et al* [31] until the surface tension decreased to a minimum (Fig.8). The endpoint was used to calculate the critical micelle concentration after allowing for the amount which would be adsorbed on the latex particles. This was 7.9 mmol dm^{-3} compared with the literature value of 8.0 mmol dm^{-3}.[30] If the uncertainty in the cirtical micelle concentration is 5%, then the minimum detectable surface coverage is ca 10%.

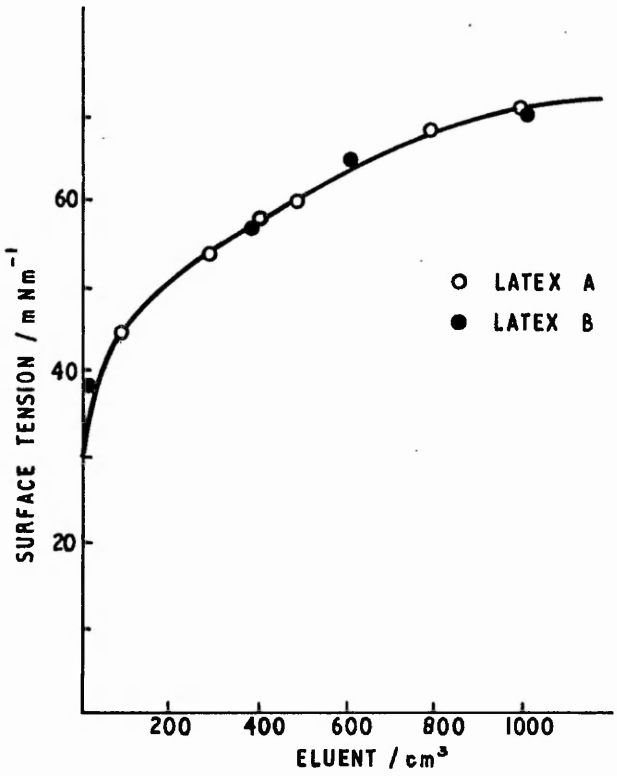

Fig.7 Rate of removal of sodium dodecyl sulphate from latex

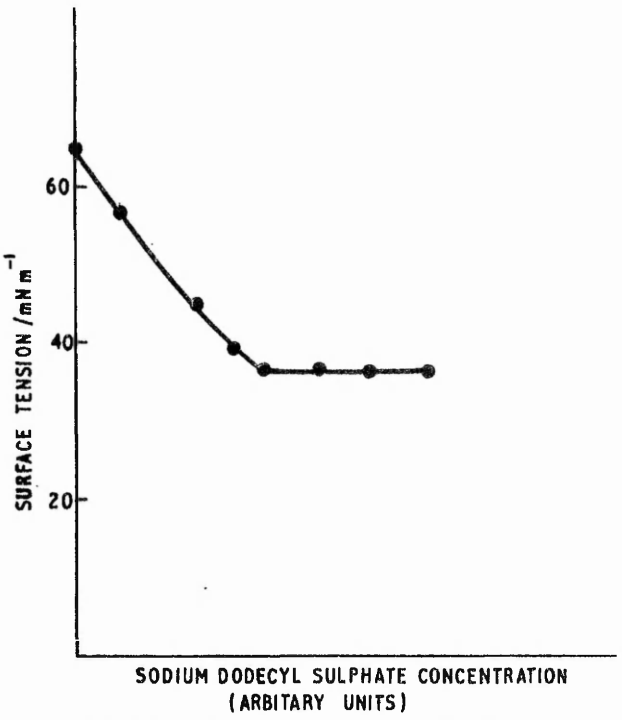

Fig.8 Variation in surface tension of latex B with added sodium dodecyl sulphate.

In order to check that all the sodium dodecyl sulphate is recovered by microfiltration, when it can no longer be detected by its effect on the conductivity and surface tension of the eluent water, a further experiment was conducted. A fresh mixture of latex B and sodium dodecyl sulphate solution was prepared and a portion of this was eluted as before. When the conductivity and surface tension had reached the same vlaues as those of the feed water, elution was halted and the cell left stirring overnight. Elution was continued 13 hours later, and there was no change in the values of conductivity and surface tension of the eluent. This microfiltered latex was then left standing for one week so that equilibrium between sodium dodecyl sulphate molecules in the aqueous phase and those adsorbed on the latex particles could be reachieved. The method of Barr *et al* [32] was used to determine whether or not any sodium dodecyl sulphate was present in the aqueous phase. A known volume of latex was diluted with 100 cm^3 of distilled water. Five drops of bromophenol blue indicator and 50 cm^3 of chloroform were added. The mixture was then titrated with cetyl trimethyl ammonium bromide solution (10^{-3} mol dm^{-3}) the flask being shaken vigorously after each addition. The endpoint was marked by the appearance of a blue colouration in the lower chloroform layer.

Varying concentrations of sodium dodecyl sulphate solution were titrated for calibration: these showed that concentrations as low at 10^{-6} mol dm^{-3} could be detected easily. One percent of the monolayer coverage of the total surface area of 100 cm^3 of latex B was equivalent to 9.3×10^{-7} mol of sodium dodecyl sulphate. Thus, it can be seen that this is a very sensitive test for this emulsifier.

There is a measure of disagreement between the results presented above and those reported by Ahmed *et al* with regard to the rate of removal of sodium dodecyl sulphate. The results of the experiments reported here suggest that complete removal of adsorbed surface-active agent is achieved rapidly. For example 12½ cell changes (ca 6h at 2.2 cell changes h^{-1}) were required to reduce the concentration of sodium dodecyl sulphate in the eluent from 12.5×10^{-3} mol dm^{-3} to a negligible level: this is to be compared with the 29h taken to reduce the concentration from 3.35×10^{-4} mol dm^{-3} to 0.17×10^{-4} mol dm^{-3} by Ahmed *et al*. It seems likely that equilibrium removal of solute and adsorbable species applies at quite rapid elution rates, and it therefore follows that to delay elution to ensure the equilibrium desorption of these species (the technique used by Ahmed *et al*) is unnecessary.

3.2.6 Removal of Inhibitors

Wilkinson *et al* [11] have shown that microbiological activity in a latex can lead to serious contamination. Surface sulphate groups can be rapidly hydrolysed and weak acid metabolites can be formed in advanced stages of growth; thus, the latex loses stability and flocculates. Microbiological contamination can occur very readily (e.g. from glassware, airborne material) and is difficult to identify until an advanced stage of growth is reached.

Various inhibitors are available commercially, and several of these were evaluated with regard to their effect on latex stability and ease of removal (Table 4). None of the inhibitors proved suitable since they either had a destabilising effect on the latex or were impure and led to an irreversible change in surface characteristics which could not be reversed by extensive microfiltration.

Since no satisfactory inhibitor could be found it is essential to ensure purity of materials used in polymerisations and care should be exercised in their storage. An analysis at various periods during storage should be carried out for the presence of microbiological activity.[11]

3.3 Separation of Different Particle Sizes

The microfiltration unit was capable of separating two different sized latices, if a Millipore filter was employed where the pore size was greater than the smaller of the two. For example a latex mixture consisting of 1000 nm and 100 nm particles in a ratio of 1:40000 was successfully separated within several hours.

3.4 Comparison of Microfiltration and Dialysis Techniques

The experiments described show that microfiltration will remove all the adsorbed surface-active agent from a polystyrene latex, in as little as six hours. Dialysis, however, is a slow process and frequently only incomplete removal is achieved.[27,28] This is principally due to the slow rate of diffusion of large molecules resulting in a rapid increase in concentration just inside the surface of the dialysis membrane. Edelhauser [27] found that the rate of dialysis of surface-active agent solutions was increased by stirring the inside solution, which would minimise this effect. Industrially, dialysis tubes containing latices are rotated or agitated in some way, to achieve the same end. Nevertheless, this slow diffusion will result in latex particles being in a region of high concentration unless they are close to the surface of the dialysis membrane and therefore the extent of desorption of surface-active agent will be small.

Contrast this situation with that inside the microfiltration cell, where the aqueous suspending medium is being changed every 30–60 minutes. Here, the latex particles are in a region of low concentration, and the adsorbed surface-active agent will desorb much more quickly.

Table 4

Inhibitor Concentration	Latex	Surface Charge[c] ($\mu eq\ g^{-1}$)	Surface Charge ($\mu eq\ g^{-1}$) After Addition of Inhibitor	Surface Charge ($\mu eq\ g^{-1}$) After Microfiltration (1000 ml eluent)	Surface Charge ($\mu eq\ g^{-1}$) After Dialysis	Notes
0.3% 3-methyl 4-chloro hydroxy-benzene	*A (acid washed)*	13.50	8.9	6.5	6.5[a]	Probably imputity
0.001% thiomesal[b] (morthiolate)	"	19.2	5.4(8.0)	18.9[d]	—	Destabilised Redispersed Ultrasonically
0.0001% Phenyl mercuric acetate	"	19.2		19.4[e]	—	Destabilised

[a] 6 x 3000 ml in 24h

[b] Thiomesal — supplied by ICI

[c] After acid washing

[d] After acid washing (0.125 m HCL)

[e] After acid washing (0.05 m H_2SO_4)

Note In addition to the above the following inhibitors were also evaluated. However, none were found suitable due to either irreversible contamination of the latex or to their destabilising effect.

4-chloro m-cresol, chlorohexidine diacetate, sulphur dioxide, chlorine, sodium azide and formaldehyde.

If, for any reason the concentration of surface-active agent in the aqueous phase is above the critical micelle concentration, then its removal by dialysis is certain to be incomplete. This has been attributed by various authors [27] to materials originally present in the dialysed latex being incorporated in the micelles, thereby stabilising them.[27] Since dialysis relies on diffusion of monomeric species through the dialysis membrane (the micelle being larger than the pores) removal of surface-active agent from the aqueous phase becomes negligible after a certain point. The pore sizes of the filters used in microfiltration are much larger than the micelles and therefore this problem does not arise. The micelles are simply washed out of the latex, after which the process reverts to the type described earlier.

4. CONCLUSIONS

The microfiltration technique has several advantages over other methods for the cleaning of latices. It avoids the prolonged preparation associated with the purification of ion-exchange resins, and it permits the rapid removal of adsorbed surface-active agent from the latex, something which may require prolonged periods of dialysis to achieve. The apparatus is simpler and hence cheaper than that required for diafiltration or hollow-fibre dialysis. A further advantage of this microfiltration technique is its versitility: apart from cleaning latices, the solids content may be adjusted easily, and a choice of filters of differing composition and construction may be employed to suit varying circumstances.

Nuclepore filters have the advantage of being a much better substrate for electron microscope analysis. However, as a routine method for cleaning latices for characterisation and other purposes, Millipore filters are more suitable, being more robust and easier to handle, able to cope with residual monomer, higher solids contents and greater pressures.

References

1 Matejevic, E., Preprints, NATO Adv. Study Inst. *'polymer Colloids'*, 1975, Univ. Trodheim, Norway.

2 Vanderhoff, J.W., Van der Hul, H.J., Tausk, R.J.M. & Overbeek, J.Th.G., *'Clean surfaces; their preparation and characterisation for interfacial studies'*, Goldfinger, G. (Ed), 1970, p15, *New York: Marcel Dekker.*

3 Goodwin, J.W., Hearn, J., C.C. Ho & Ottewill, R.H., *Brit. Polym. J.*, 1973, **5**, 347.

4 Chung-Li, Y., Goodwin, J.W. & Ottewill, R. H., *Origr. Colloid & Polym. Sci.*, 1976, **60**, 163–175.

5 Wright, H.J., Bremmer, J.F., Bhimani, N. & Fitch, R.M., US Patent 3, 501, 432.

6 Ugelstad, J., Kaggerud, K.H., Hansen, F.K. & Berge, A., *Makromol. Chem.*, 1979, **180**, 737–744.

7 Vanderhoff, J.W., *Preprints Org. Coating & Plastics Chem. Div., ACS*, 1964, **24(2)**, 223.

8 Stone-Masui, J. & Watillon, A., *J. Colloid & Inter. Sci.*, 1975, **52**, No. 3, 479–502.

9 Goodall, A.R., Hearn, J. & Wilkinson, M.C., *J. Polym. Sci. Polym. Chem. Ed*, 1979, **17**, 1019–1037.
10 Goodall, A.R., Wilkinson, M.C., Hearn, J. & Cope, P., *Brit. Polym. J.*, 1978, **10**, 205.
11 Wilkinson, M.C., Sherwood, R., Hearn, J. & Goodall, A.R., *ibid*, 1979, **11**, 1–6.
12 Hearn, J., Wilkinson, M.C. Goodall, A.R. & Cope, P., *'Polymer colloids II'*, Fitch, R.'., (Ed), 1979, p379.
13 Wilkinson, M.C., Hearn, J., Goodall, A.R. & Cope, P., *J. Colloid & Inter. Sci.*, in press.
14 Hearn, J., Wilkinson, M.C. & Goodall, A.R., *J. Colloid & Inter Sci.*, **1981**, **14**, 173.
15 Everett, D.H., Gultepe, M.E. & Wilkinson, M.C., *J. Colloid & Inter Sci.*, 1979, **71(2)**, 336–349.
16 Yates, D.E., Ottewill, R.H. & Goodwin, J.W., *ibid*, 1977, **62(2)**, 356–358.
17 McCarvill, W.T., & Fitch, R.M., *J. Colloid & Inter Sci.*, 1978, **64(3)**, 403-411.
18 Vanderhoff, J.W., *Proc. 4th Int. Conf. Organic Coating Sci. & Tech.*, 1978, 447–83.
19 Wilkinson, M.C. & Fairhurst, D., *J. Colloid & Inter, Sci.*, **1981**, **79**, **272**.
20 Labib, M.E. & Robertson, A.R., *J. Colloid & Inter Sci.*, 1978, **67(3)**, 543–547.
21 Ahmed, S.M., El-Aasser, M.S., Pauli, G.H., Poehlein, G.W. & Vanderhoff, J.W., *ibid*, 1980, **73(2)**, 388.
22 Goodall, A.R., Wilkinson, M.C. & Hearn, J., *J. Polym. Sci.*, 1977, **15**, 2193.
23 Everett, D.E. & Gultepe, M.E., Preprints NATO Advanced Study Institute: *'Polymer colloids'*, 1955, Univ. Trondheim, Norway.
24 Vanderhoff, J.W., *'Characterisation of metal & polymer surfaces,'* 1977, Vol 2, *'Polymer surfaces'*, Lee, L-H, (Ed), *London: Acadmic Press.*
25 Blackley, D.C., *'Emulsion polymerisation'*, 1975, *London: Applied Science.*
26 Warson, H., *'The applications of synthetic resin emulsions'*, 1972, *London: Ernest Benn Ltd.*
27 Edelhauser, H.A., *J. Polym. Sci.*, 1969, (C), **27**, 291.
28 *'Colloid science'*, Kruyt, H.R. (Ed), 1952, Vol 1, p68, *'Irreversible systems', Amsterdam: Elselvier.*
29 Shaw, J.N., *J. Polym, Sci.*, 1969, (C), **27**, 237.
30 Elockhark, B.D. & Ubblehode, A.R. *J. Colloid Sci.*, 1953, 8, 428.
31 Maron, S.H., Elder, M.E. & Ulevitch, I.N., *J. Colloid Sci.*, **1954**, **9**, 89.
32 Barr, T., Oliver, J. & Stubbings, W.V., *J. Soc. Chem. Ind.*, 1948, **67**, 45.

Calendar of Meetings

Macro Group UK

January 6–7, 1982. The University of Birmingham. In association with the Polymer Physics Group and The University of Birmingham a conference on 'Thermal and mechanical properties of polymers'.

This Conference is in honour of Professor R. N. Haward who will then, have retired from the Chair of Industrial Chemistry. The University of Birmingham, and is intended to follow new developments in several research interests of Professor Haward.

(a) the structure and properties of polymers,

(b) the glass transition and physical ageing, and

(c) polymer fracture

with introductory lectures by Professor E. Baer, Case Western Reserve University, Professor A. Keller, The University of Bristol, Professor G. Rehage, The Technical University of Clausthal, Professor J. G. Williams of Imperial College, London and Professor I. M. Ward of The University of Leeds.

Full particulars and Registration Forms can be obtained from Dr. J. N. Hay, The Department of Chemistry, The University of Birmingham, P.O. Box 363, Birmingham B15 2TT.

(when 5% mole ratio of LiH_2PO_4 is added) and rising to a maximum of 28.9% wt (at 40% mole ratio).

Elemental analysis of the soluble products are consistent with polyphenylphonosiloxanes modified with lithium phosphate groups. The amount of lithium in the soluble product rises to a maximum value of 0.2% wt attained at about 10% mole LiH_2PO_4 which corresponds approximately to 4% of modifying groups of the total Si and P groups in the polymer.

For the reaction in which 10% mole ratio of LiH_2PO_4 is used, the Si/P ratio of the soluble product is close to unity indicating a structure as in (I) with a ratio for X of Li/Ph approximately 1:9. As more LiH_2PO_4 is incorporated into the reaction the ratio Si/P increases. Since the analyses show that each residue is mainly lithium metaphosphate (Li 8.1%: P, 36.1% required for $LiPO_3$ it is concluded that self condensation [2] between LiH_2PO_4 molecules occurs releasing water which gives rise to condensation between chlorosilane groups (e.g. 3) to yield products soluble in chloroform.

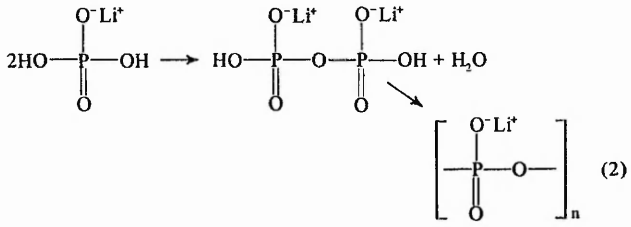

(2)

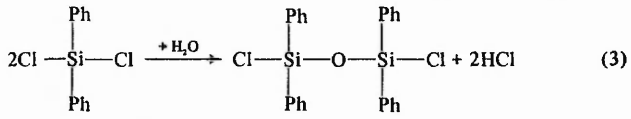

(3)

In the reactions involving NaH_2PO_4 near quantitative collection of hydrogen chloride was obtained for 5% mole ratio of NaH_2PO_4 but became lower than expected as more of the phosphate is added. However, in contrast to the Li series, significant amounts of chlorine are found in the insoluble residues indicating the formation of NaCl; also none of the soluble products contain any sodium. Thus reaction (4) contributes alongside (1) to the formation of polyphosphonasiloxanes.

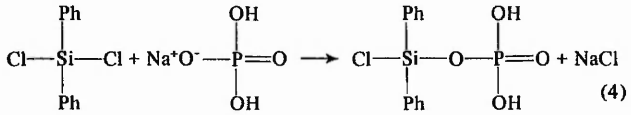

(4)

Products will therefore contain cross-linking groups of the type.

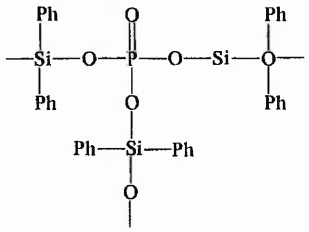

Formation of these units would account for the observed rise in $\bar{M}n$ from about 800 to 1257. Further evidence for cross-linking comes from the infrared of the soluble products which shows a decrease in the intensity of the absorption at 930 cm^{-1} (associated with linear P–O–P bonds) and an increase in the intensity of the band at 480 cm^{-1} (attributed to the cross-linked phosphorus atom).[9]

In the Li series the soluble products show an increase of *Tg* with increase of Li content. In the Na series, since no sodium was incorporated in the polymer, the increase in *Tg* obtained is due to a combination of increased molecular weight and the presence of cross-linking.

3.2 Interaction of Me_2SiCl_2, $MePO(OH)_2$ and LiH_2PO_4 or NaH_2PO_4

Again in each experiment the relative proportions of reactants were such that the total number of OH groups was always equal to the number of Cl groups.

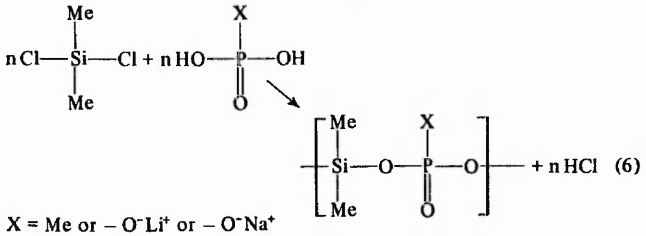

(6)

X = Me or $-O^-Li^+$ or $-O^-Na^+$

Results are given in Tables 3 and 4. Note that total phosphorus figures could not be obtained because of the difficulty of oxidising methyl phosphonate groups, the figures given are for phosphorus as phosphate.

The reaction sequences are similar to those obtained for the phenyl series. The reaction of a 1:1 mixture of Me_2SiCl_2 and $MePO(OH)_2$ gives a clear, viscous liquid, which is a polymethylphosphonasiloxane probably a mixture of short chains and cyclics with average $n = 2–3$.

Thus in the Li series soluble polymers of the general type shown in (6) are obtained, a maximum Li content being obtained when equimolar quantities of $MePO(OH)_2$ and LiH_2PO_4 were used. The molecular weights vary from 400 to 600 indicating an average $n = 3–4$. In constrast to the $LiH_2PO_4/Ph_2SiCl_2/PhPO(OH)_2$ reactions, there is evidence that Me_2SiCl_2 and LiH_2PO_4 interacts to give formation of LiCl and cross-linking groups in the soluble product (cf, reaction 5). Thus as the proportion of LiH_2PO_4 in the reaction mixture is increased the elemental analysis of the insoluble residue indicates formation of LiCl and there is also an excess in the soluble product of phosphate over Li^+. In the Li series there is again an increase in the Tg with Li content. Analysis of the insoluble residue also indicates the formation of a lithium phosphate (cf reaction 2).

As in the phenyl series little sodium is incorporated in the soluble products due to the formation of NaCl which appears in the insoluble residue together with sodium phosphate. But unlike the phenyl series there is no significant increase in the molecular weight of the product.

References

1 Currell, B. R., Grzeskowiak, R. & Lynn, M.E., *Brit. Polym. J.* **1981, 13,** 117.
2 Currell, B. R., Grzeskowiak, R. & Lynn, M. E., *Brit. Polym. J.*, **1981, 13,** 122.
3 Voronkov, M. G. & Zgonnik, V. N., *Zh. Obshch. Khim.*, 1957, **27,** 1483.
4 Alfrey, T., Hohn, F. J. & Mark, H. F., *J. Polym. Sci.*, 1946, **1,** 102.
5 Goubeau J., Wilborn, W. & Kerger, K., *Mitteilungsblatt. Chem. Ges. D.D.R.*, **1963, 10(3),** 47.
6 Kerger, K. & Kohlhaas, R., *Z. Anorg. Allg. Chem.*, 1967, **354,** 44.
7 Andrianov, K. A., Vasil'eva, T. V. & Khananashivili, L. M., *Izv. Akad. Nauk. SSR, Otdel, Khim. Nauk,* **1961,** 1030.
8 Andrianov, K. A., Vasil'eva, T. V. & Kozolova, L. V., *Izv. Akad. Nauk. SSSR, Ser. Khim.*, 1965, 381.
9 Corbridge, D. E. C., 'The infrared spectra of organophosphones compounds' in *Topics in phosphorus chemistry,* Eds. Grayson, M., & Griffith, M., Vol.6, 1969, *London: John Wiley.*

Preparation of Overcoated Polymer Latices by a 'Shot Growth' Technique

Malcolm Chainey, John Hearn and Michael C. Wilkinson

A 'shot growth' technique has been developed which enables a monodisperse polymer latex to be overcoated with a range of coating thicknesses by a different polymer. This has enabled a range of polymer latices to be produced which have mechanical and diffusional characteristics which are very different from either the seed latex or the coating polymer.

1. INTRODUCTION

This paper describes a surfactant-free polymerisation technique which has been used to prepare a series of monodisperse latices, whose particles consist of a polystyrene core overcoated with an acrylate polymer shell. When the coating polymer has a minimum film formation temperature (MFT) below room temperature and the coat is of sufficient thickness (normally >50 nm), the latex will be film forming. Films cast from such latices have an interesting range of mechanical properties, from brittleness to toughness and flexibility with increasing coat thickness.

The production of overcoated polymer latices is an important industrial process and many examples are to be found in the patent literature.[1–7] This topic has also attracted the attention of workers in the field of emulsion polymerisation, as a means of producing either larger particles than can be achieved in a single-stage reaction [8] or controlled surface charge densities in 'model' systems.[9] It is anticipated that films cast from surfactant-free preparations may constitute model films' for permeability studies, which is the main aim of the current work, and further, that the omission of the surfactant 'impurity' in the cast film may give improved film characteristics.

A variety of methods have been used for preparing overcoated latices: these fall essentially into three categories:

(a) 'initial charge' where (i) the comonomers are both charged at the start of the reaction or (ii) the second monomer is fed in slowly right from the start and throughout the course of the reaction;

(b) 'seeded growth' where the second monomer is added initially with an already polymerised core latex;

(c) shot addition' which is a compromise between the previous two approaches where the seed latex is allowed to reach a fairly high conversion (>60%) before the second monomer is charged.

The most commonly adopted procedure in industrial practice is a.(ii) where surfactant is also progressively added. The locus of the polymerised second monomer, ie aqueous phase, bulk polymer or at the interface between them has been shown [10] to be dependent in part on the affinity of the monomer for these loci and its reactivity, and may be further influenced by the core-shell mechanism believed by Williams [11] to operate even for compatible monomers. In seeded growth systems it has been shown [12] that the number density of seed particles is an important parameter in determining whether secondary nucleation of a new crop of stable particles occurs, ie polymer not bound to the core particles. Chung Li *et al* [13] have discussed the occurrence of secondary nucleation in terms of heterocoagulation of a new polymer, formed in the aqueous phase, with the seed particles relative to its homocoagulation which can result in stable nuclei.

The shot growth process has been investigated by Sakota and Okaya [14] with regard to the efficiency of incorporation of carboxyl groups on the surface of styrene/isoprene copolymer latices. They found that 60% incorporation of carboxylic groups at the surface could be achieved by adding at 80% conversion – this increasing to 80% incorporation at 95% conversion.

In this work, techniques (ii) and (iii) are compared for the production of polystyrene latices overcoated with methyl acrylate, methyl methacrylate, ethyl acrylate and n-butyl methacrylate. The basis of the shot growth technique is to polymerise styrene by the usual surfactant-free emulsion polymerisation process until the reaction reaches about 80% conversion. At this point, the reaction starts to slow and the second monomer is added. Normally, no additional initiator is necessary, since the half life of potassium persulphate is sufficiently long that there will be an ample supply of free radicals. The reaction is allowed to proceed to completion.

2. EXPERIMENTAL

2.1 Materials

The monomers used were BDH laboratory reagent grade containing a small quantity (ca 0.002% v/v) of inhibitor. This was removed by distillation under reduced pressure of nitrogen at between 293–313K. The distilled monomers were stored at 268K until use.

Potassium persulphate, Fisons Analytical Reagent grade was used as supplied.

Water was doubly distilled from an all pyrex apparatus and stored in pyrex glass aspirators.

2.2 Procedure for Shot Growth Reactions

The polymerisations were carried out in 500 cm^3, three-necked, round bottomed flasks, equipped with a reflux condenser, nitrogen inlet and stirrer. The flasks were immersed in a water bath at 353K. The stirrer speed was maintained at 300 rpm.

The styrene and most of the water were placed in the flask and left for about 20 minutes to come to temperature.

Chemical Defence Establishment, Porton Down, Salisbury, Wiltshire and Department of Physical Sciences, Trent Polytechnic, Burton Street, Nottingham.
(Manuscript received 27 May 1981)

During this time, the contents of the flask were stirred and flushed with nitrogen, via a long inlet tube. The initiator was dissolved in the remaining water, flushed with nitrogen and heated to the reaction temperature. Addition of the initiator marked the start of the reaction. A short gas inlet tube was substituted from the long one, and a slow current of nitrogen passed above the aqueous phase.

At the appropriate time, a sample of latex was withdrawn and the second monomer added. Half the sample was dialysed for subsequent electron microscope examination; the remainder was used for a gravimetric solids content determination. The reaction was allowed to proceed to completion.

In order to assess the effect of particle concentrations on the tendency to form secondary growth particles, some reactions were diluted prior to addition of the second monomer. The diluent, potassium persulphate solution at the initial concentration, was flushed with nitrogen and preheated before addition.

2.3 Seeded Growth Reactions

Polystyrene seed latices were prepared by the normal surfactant-free process [15] and extensively dialysed before use. The latex, monomer and water (if necessary) were placed in the flask as before. The mixture was left to attain the temperature of the bath, whilst being flushed with nitrogen. The initiator was dissolved in water, sparged and heated, and added to the reaction.

2.4 Electron Microscopy

A Philips EM600 electron microscope was employed for transmission electron microscopy (TEM). The latex sample was diluted down to about 10 ppm, and one drop placed onto a 20 μm Formvar film-coated grid and allowed to air-dry at room temperature in a dust-free box. Usually, three grids were prepared and six electron micrographs of different regions taken. In order to obviate the effects of electron beam damage, the operating conditions were so chosen that any beam damage was minimal, e.g. 80 kV accelerating potential at 3–4 μA beam current.

The latex particle size distribution was carefully determined by sizing about 250 particles if relatively monodisperse (standard deviation $<10\%$) and about 600 if polydisperse. Measurements were taken from different regions of all the electron micrographs.

To overcome the problem of particle deformation of soft latices freeze drying (typically 193K) was employed. A carbon replica was then made of the dried frozen particles. The technique involved pipetting a drop of suspension onto a formvar coated grid and removing excess liquid with filter paper leaving just a smear of suspension. The grid was immersed in melting liquid nitrogen to achieve rapid cooling. It was then transferred to a suitable freeze dry unit and freeze dried at 193K for 30–60 min to remove residual moisture. It was then cooled to approx 123K. The specimen was tilted to 45° and a Pt/C mixture evaporated to provide shadows to the particles. The C was then evaporated normally. The specimen was allowed to return to room temperature, the grid removed and (a) the formvar film dissolved in chloroform (b) the latex dissolved in a suitable solvent (eg toluene for polystyrene). The replica was then examined by TEM.

2.5 Film Casting

Films were cast in shallow silicone rubber dishes and dried at 333K and atmospheric pressure.

3. RESULTS

Seeded and shot growth methods were used to overcoat polystyrene with poly (methyl acrylate), poly (methyl methacrylate), poly (ethyl acrylate) and poly (n-butyl methacrylate). Typical results are summarised in Tables 1 and 2. It was possible to prepare monodisperse overcoated latices reproducibly by both methods with all but poly (ethyl acrylate) as the coating polymer. However, if the number density of core particles was below a critical value, small (60–150 nm) secondary growth particles were produced, and the final product had a bimodal size distribution. The advantage of the shot growth technique is that this critical value is lower than for the seeded growth method.

Table 1 Results of seeded growth reactions

Latex	*MC4*	*MC9*	*MC31*	*MC11*
Seed latex	MC1	MC1	MC26	MC8
Size/mm	480	480	440	440
σ/nm	7.0	7.0	8.3	6.6
Solids content (%)	8.0	8.0	6.9	2.7
Volume/cm^3	50	250	425	500
Particle No Density/cm^{-3}	$1.3.10^{11}$	$6.5.10^{11}$	$1.4.10^{12}$	$5.3.10^{11}$
Monomer	*MMA*	*MMA*	*MMA*	*EA*
Volume/cm^3	16	11	50	15
Initiator/g	0.16	0.25	0.25	0.25
Water/cm^3	450	250	50	50
Temp/K	353	353	353	353
Total Polymerisation Time/min	180	180	1385	180
Product				
Particle size/nm	530,140	500,65	470	440–450, 10
σ/nm	5.7, 6.3	7.2, 4.1	3.6	
	Bimodal	Bimodal	Monodisperse	Polydisperse
Solids content (%)	3.6	5.6	9.2	7.2
Conversion (%)	94	77	25*	92

* Latex had coagulated during reaction.
σ's for large and small particles of bimodal size distribution reported separately.

For example with methyl methacrylate as the second monomer, the critical number densities were approximately 1.10^{12} cm^{-3} and 1.10^{11} cm^{-3} for seeded and shot growth methods, respectively.

Another advantage of the shot growth method was that the resultant particles were spherical, whereas the seed grown particles were rather irregular in shape (compare Figs. 1 and 2).

With poly (ethyl acrylate) as coating polymer, both methods gave a polydisperse product, i.e. one in which there was variable coating thickness as well as the formation of secondary

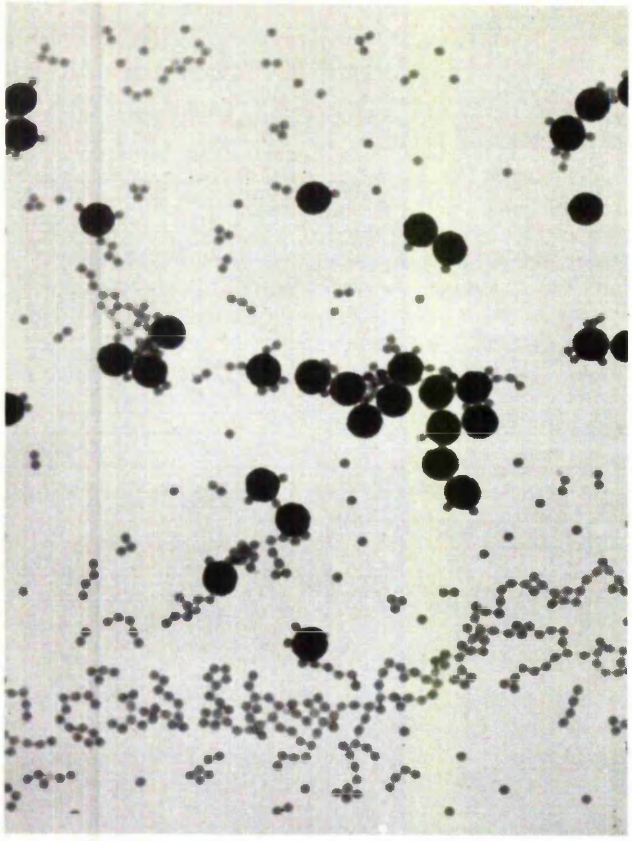

Fig.1 MC4 Poly (methyl methacrylate) coated polystyrene prepared by seeded growth method. Magnification 20,845.

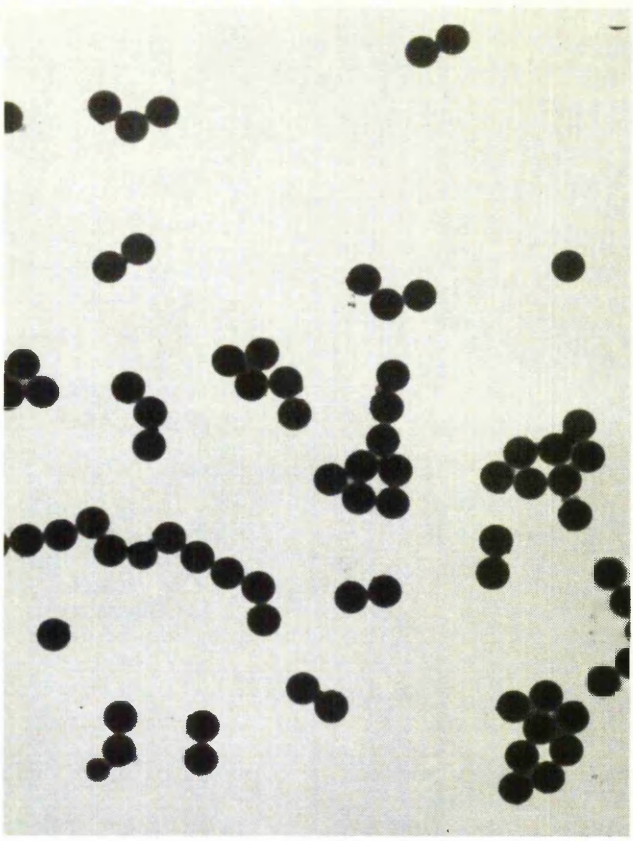

Fig.2 MC5 Poly (methyl methacrylate) coated polystyrene prepared by shot growth method. Magnification 20,845.

Table 2 Results of Shot Growth Reactions

Latex	*MC5*	*MC45*	*MC19*	*MC10*	*MC56*	*MC20*	*MC24*	*MC42*
Core latex								
Size/nm	400	410	370	460		330	420	420
σ/nm	7.0	4.3	6.1	6.2		8.2	35.2	6.7
Solids content (%)	5.9	0.69	4.92	6.74	9.0	4.1	5.4	7.7
Particle No Density /cm^{-3}	$1.7.10^{12}$	$1.7.10^{11}$	$1.9.10^{12}$	$1.3.10^{12}$		$2.2.10^{12}$	$1.4.10^{12}$	$2.0.10^{12}$
Monomer	*MMA*	*MMA*	*MA*	*EA*	*EA*	*BMA*	*BMA*	*BMA*
Volume/cm^3	16	12	7	16		12	85	20
Initiator/g	0.5	0.12 + 0.95	0.5	0.5		0.5	9.5	0.5
Temp/K	353	353	353	353	353	353	353	353
Polymerisation Time/min	300	250	290	295	243	300	200	180
Product								
Particle Size/nm	490	540	530	480–510 3–10		500	580	560
σ/nm	7.7	6.8	3.6	–	–	6.9	11.4	7.4
Solids content (%)	11.4	2.7	11.34	12.0	8.9*	13.0	22.8	15.2
Conversion (%)	55	24	–	–	–			
Particle No Density/cm^{-3}	$1.9.10^{12}$	$3.1.10^{11}$	$1.45.10^{12}$	–	–	$2.1.10^{12}$	$2.0.10^{12}$	$1.8.10^{12}$

* Latex had coagulated.

growth particles. These secondary growth particles were much smaller (usually ca 10 nm) (see Fig. 3) and more numerous than those formed with other acrylates although in terms of mass, the amounts were about the same.

Fig.3 MC11 Poly (ethyl acrylate) coated polystyrene prepared by seeded growth method. Magnification 10,050.

3.1 Efficiency of Coating

Secondary growth particles, where obtained, were immediately apparent by their small size. It was possible to prove, by a mass balance calculation, that all the monomer added could be accounted for, within experimental error, by the increase in size of the particles. By performing this calculation in reverse, it would be possible to calculate the amount of monomer required to produce a given coat thickness, and thus to tailor make overcoated latices.

4. DISCUSSION

The principal object of this study has been the preparation of overcoated polymer latices for subsequent film casting work. Nevertheless, it is interesting to interpret the results in terms of existing theories concerning emulsion polymerisation.

The factors which favour a secondary nucleation include:

(i) a high polymer concentration in the aqueous phase

(ii) a low total surface area per unit volume, and

(iii) a low capture efficiency of core particles.

That the shot growth process will still produce a monodisperse latex at lower core particle number densities, under otherwise equivalent conditions of core particle size, initiator concentration, ionic strength and temperature, is presumably related to the capture efficiency of the core particles for polymer from the aqueous phase. The significant difference between the shot and seeded growth methods is that in the former case the core particles will contain some residual monomer, plasticising them, whereas in the latter (providing the latex has been properly cleaned) they will not. It has been shown that the rate of swelling of dialysed polystyrene latex particles by styrene monomer is slow.[13] It is suggested that the higher capture efficiency of the shot growth process is due to the shell monomer actively polymerising at the core particle surface, becoming entwined in the polymer matrix, and unable to transfer back out of the particle. In contrast, in the seeded growth process, there can be no direct binding of shell polymer to the core particle. The rigid, unplasticised nature of the core particles is reflected in the irregular shape of the overcoated particles, compared with the perfectly spherical shape of those obtained by the shot growth process.

Films cast from latices having a thin polyacrylate coat (ca 20 nm thick) have mechanical properties intermediate between the opaque, discontinuous and clear, continuous films resulting respectively from non film forming and film forming latices. The SEM's of the top and bottom surfaces of these films (Figs. 4–6) show the hexagonal close packing first observed by Bradford and Vanderhoff.[15] The fracture cross section shows clearly the polystyrene core particles

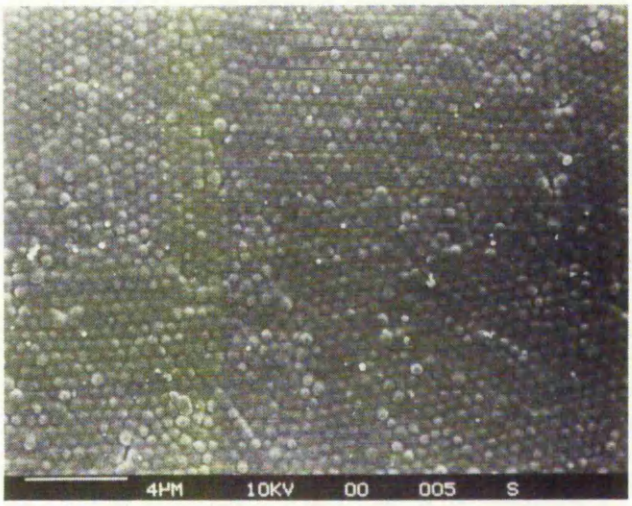

Fig.4 SEM of bottom surface of film cast from latex MC10 – poly (ethyl acrylate) coated polystyrene prepared by shot growth method. Magnification 6.000.

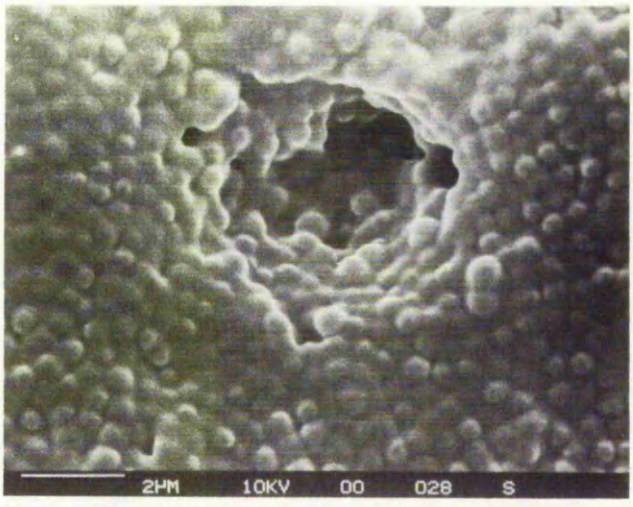

Fig.5 SEM of bottom surface of film cast from latex MC10 – poly (ethyl acrylate) coated polystyrene prepared by shot growth method. Magnification 12,000.

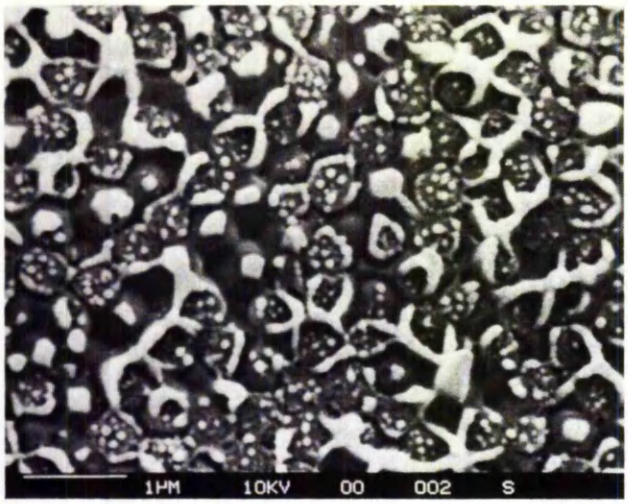

Fig.6 SEM of broken edge of film cast from latex MC10. Magnification 24,000.

and the coalesced coating polymer. Complete phase separation does not take place upon fracture – small globules of acrylate can be seen on core particle surface – and this is taken as evidence of direct bonding of acrylate polymer chains to the polystyrene surface.

References

1 Hahn, F. J. & Heaps, J. F., US Patent 3, 256, 233, **1966**.
2 Herman, D. F., Resnick, A. L. & Simone, D., US Patent 3, 265, 644, 1966.
3 Pfluger, H. L. & Gebelein, C. G., US Patent 3, 291, 768, 1966.
4 Settlage, P. H., US Patent 3, 309, 330, 1967.
5 Goodman, D., Isgur, I. E. & Wacome, D. M., US Patent 3, 397, 165, 1968.
6 Ryan, C. F. & Crochowski, R. J., US Patent 3, 426, 101, 1969.
7 Meier, G. L., US Patent 3, 575, 913, 1971.
8 Goodwin, J. W. Ottewill, R. H., Pelton, R., Vianello, G. & Yates, D. E., *Brit. Polym. J.*, 1978, **10,** 173.
9 Hearn, J., Wilkinson, M. C. & Goodall, A. R., *Adv. Colloid and Interface Sci.*, 1981, **14,** 173.
10 Greene, B. W., *J. Colloid and Interface Sci.*, 1973, **43,** 449, 462.
11 Williams, D. J., *J. Polym. Sci., Polym. Chem. Ed.*, 1974, **12,** 2123. and refs cited therein.
12 Hearn, J., PhD Thesis, Bristol Univ., 1971.
13 Chung-Li, Y., Goodwin, J. W. & Ottewill, R. H., *Progr. Colloid and Polym. Sci.*, 1976, **60,** 163.
14 Sakota, K. & Okaya, T., *J. Appl. Polym. Sci.*, 1976, **20,** 1735.
15 Bradford, E. B. & Vanderhoff, J. W., *J. Polym. Sci.*, (C), **1963, 3,** 41.

Preparation of Overcoated Polymer Latices by a "Shot-Growth" Technique

Malcolm Chainey,[1] Michael C. Wilkinson,[2] and John Hearn*[1]

Trent Polytechnic, Burton St., Nottingham, England, and Chemical Defence Establishment, Porton Down, Salisbury, Wiltshire, England

A surfactant-free emulsion polymerization technique for the preparation of "overcoated" polymer latices is described. Particles consist of a polystyrene core coated with an acrylate (methyl acrylate, methyl methacrylate, ethyl acrylate, *n*-butyl methacrylate) shell. Latices are prepared by a "shot-growth" process whereby the styrene is polymerized to approximately 80% conversion before the second monomer or mixture of monomers is added. An advantage of the shot-growth technique is that a lower number density can be employed without the occurrence of secondary growth. There is evidence that the acrylate coat is more strongly bound to the core particles than is the case for "seeded-growth" products. Neither process produced a monodispersed product when ethyl acrylate was the coating monomer and this was ascribed to homocoagulation (secondary growth) rather than heterocoagulation with the core particles. Films cast from "overcoated" latices have properties intermediate between those of a discontinuous film and a continuous film.

Introduction

Previous work by Chainey et al. (1981) has described a surfactant-free polymerization technique which has been used to prepare a series of monodisperse latices, whose particles consist of a polystyrene core overcoated with an acrylate polymer shell. When the coating polymer has a minimum film formation temperature (MFT) below room temperature and the coat is of sufficient thickness (normally >50 nm), the latex will be film forming. Films cast from such latices have an interesting range of mechanical properties, ranging from brittleness to toughness and flexibility with increasing coat thickness (Figure 1).

The production of overcoated polymer latices is an important industrial process and many examples are to be found in the patent literature (Goodman et al., 1968; Herman et al., 1966; Meier, 1971; Pfluger and Gebelin, 1966; Ryan and Crochowski, 1969; and Settlage, 1967). This topic has also attracted the attention of workers in the field of emulsion polymerization, as a means of producing either larger particles than can be achieved in a single-stage reaction (Goodwin et al., 1978) or controlled surface charge densities in "model" systems (Hearn et al., 1981). It is anticipated that films cast from surfactant-free preparations may constitute "model films" for permeability studies and that the omission of the surfactant "impurity" in the cast film may give improved film characteristics.

A variety of methods have been used for preparing overcoated latices. These fall essentially into three categories: (a) "initial charge" where (i) the comonomers are both charged at the start of the reaction or (ii) the second monomer is fed in slowly right from the start and throughout the course of the reaction; (b) "seeded growth" where the second monomer is added initially with an already polymerized core latex; (c) "shot addition", which is a compromise between the previous two approaches where the seed latex is allowed to reach a fairly high conversion (>60%) before the second monomer is charged.

The most commonly adopted procedure in industrial practice is (a. ii), where surfactant is also progressively added. The locus of the polymerized second monomer, i.e., aqueous phase, bulk polymer or at the interface between them has been shown by Greene (1973) to be dependent in part on the affinity of the monomer for these loci and its reactivity, and it may be further influenced by the core-shell mechanism believed by Williams (1974) to operate even for compatible monomers. In seeded growth systems it has been shown by Hearn (1971) that the number density of seed particles is an important parameter in determining whether secondary nucleation of a new crop of stable particles occurs, i.e., polymer not bound to the core particles. Chung Li et al. (1976) have discussed the occurrence of secondary nucleation in terms of heterocoagulation of new polymer, formed in the aqueous phase, with the seed particles relative to its homocoagulation which can result in stable nuclei.

The shot growth process has been investigated by Sakota and Okaya (1976) with regard to the efficiency of incorporation of carboxyl groups onto the surface of styrene/isoprene copolymer latices. They found that 60% incorporation of carboxylic groups at the surface could be achieved by addition at 80% conversion and this increased to 80% incorporation upon addition at 95% conversion.

The purpose of this work was to compare the shot growth technique with the more usual seeded growth method and to try to gain a better understanding of the role of particle swelling. Both techniques have been employed to prepare latices of polystyrene coated with a range of acrylate monomers. Photon correlation spectroscopy (PCS) and light-scattering, which has been used previously by Goodall et al. (1980) and Munro et al. (1979) to study particle nucleation and growth occurring in the initial stages of the emulsifier-free emulsion polymerization of styrene, has been used to observe the swelling of polystyrene latices by styrene and butyl methacrylate. A comparison of the rates of particle swelling and growth throws some light on the mechanism of the shot growth process. Further information was obtained from scanning electron micrographs of the films cast from overcoated latices.

Experimental Section

1. Materials. The monomers were distilled twice under nitrogen at 293–313 K to remove inhibitor before use. Potassium persulfate (Fisons Analytical Reagent grade)

[1] Trent Polytechnic.
[2] Chemical Defence Establishment.

Reprinted from I&EC PRODUCT RESEARCH & DEVELOPMENT, 1982, 21, 171.

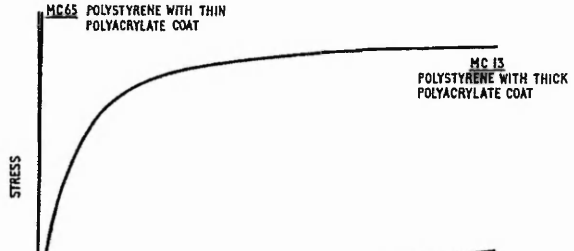

Figure 1. Mechanical properties of films.

was used as supplied. Water was doubly distilled from an all-Pyrex apparatus.

2. Shot Growth Reactions. The polymerizations were carried out in 500 cm^3 or 1 dm^3, three-necked, round-bottomed flasks, equipped with a reflux condenser, nitrogen inlet, and stirrer. The flasks were immersed in a water bath at 353 K. The stirrer speed was maintained at 300 rpm.

The styrene and most of the water were placed in the flask and left for about 20 min to come to temperature. During this time, the contents of the flask were stirred and flushed with nitrogen, via a long inlet tube. The initiator was dissolved in the remaining water, flushed with nitrogen, and heated to the reaction temperature. Addition of the initiator marked the start of the reaction. A short gas inlet tube was substituted for the long one, and a slow current of nitrogen passed above the aqueous phase.

At the appropriate time, a small sample of latex was withdrawn for subsequent analysis and the second monomer added. Half the sample was dialyzed prior to electron microscope examination; the remainder was used for a gravimetric solids content determination. The reaction was allowed to proceed to completion.

In order to assess the effect of particle concentration on the tendency to form secondary growth particles, some reactions were diluted prior to addition of the second monomer. The diluent, potassium persulfate solution at the initial concentration, was flushed with nitrogen and preheated before addition.

3. Seeded Growth Reactions. Polystyrene seed latices were prepared by the normal surfactant-free process and extensively dialyzed before use. The latex, monomer, and water (if necessary) were placed in the flask as before. The mixture was left to attain the temperature of the bath while being flushed with nitrogen. The initiator was dissolved in water, sparged and heated, and added to the reaction.

4. Electron Microscopy. A Philips EM600 electron microscope was employed for transmission electron microscopy (TEM). The latex sample was diluted down to about 10 ppm, and one drop was placed onto a 20-μm Formvar film-coated grid and allowed to air-dry at room temperature in a dust-free box. Usually, three grids were prepared and six electron micrographs of different regions were taken. In order to obviate the effects of electron beam damage, the operating conditions were so chosen that any beam damage was minimal, e.g., 80 kV accelerating potential at 3–4 μA beam current.

The latex particle size distribution was carefully determined by sizing about 250 particles if relatively monodisperse (standard deviation <10%) and about 600 if polydisperse. Measurements were taken from different regions of all the electron micrographs.

To overcome the problem of particle deformation of soft latices, freeze drying (typically 193 K) was employed. A carbon replica was then made of the dried frozen partic The technique involved pipetting a drop of suspens onto a Formvar coated grid and removing excess liq with filter paper thereby leaving just a smear of suspens The grid was immersed in liquid nitrogen to achieve ra cooling. It was then transferred to a suitable freeze- unit and freeze-dried at 193 K for 30–60 min to rem residual moisture and then cooled to approximately K. The specimen was tilted to 45° and a Pt/C mixt evaporated to provide shadows to the particles. The C then evaporated normally. The specimen was allowe return to room temperature, the grid was removed, (a) the Formvar film was dissolved in chloroform or the latex was dissolved in a suitable solvent (e.g., tolu for polystyrene). The replica was then examined by T or SEM.

5. Film Casting. Films were cast in shallow silic rubber dishes and dried at 333 K and atmospheric pr sure.

6. Laser Light Scattering/P.C.S. A 25-mW h um/neon laser provided coherent illumination for pho counting and photocount autocorrelation and was e ployed to measure swelling rates of latices. Observati were carried out on monomer saturated, oxygen-free, wa contained in Teflon capped 10-mm quartz or silica gl cuvettes. A small amount of monomer was present on water surface and measurements were made within 1 r of this layer to minimize problems of diffusion to swelling particles.

Results

Both seeded and shot growth methods were used overcoat polystyrene with poly(methyl acrylate), po (methyl methacrylate), poly(ethyl acrylate), poly(*n*-bu acrylate), and poly(*n*-butyl methacrylate). Typical resu are summarized in Tables I and II. It was possible prepare monodisperse overcoated latices reproducibly both methods with all but poly(ethyl acrylate) as coating polymer. However, if the number density of c particles was below a critical value, small (60–150 r secondary growth particles were produced, and the fi product had a bimodal size distribution. The advant of the shot growth technique is that this critical num density value is lower than for the seeded growth meth For example, with methyl methacrylate as the seco monomer, the critical number densities were appro mately 1×10^{12} and 1×10^{11} cm^{-3} for seeded and s growth methods, respectively.

Another advantage of the shot growth method was t the resultant particles were spherical, whereas the se grown particles were rather irregular in shape (comp Figures 2 and 3).

With poly(ethyl acrylate) as the coating polymer, b methods gave a polydisperse product, i.e., one in wh there was a variable coating thickness as well as the f mation of secondary growth particles. These second growth particles were much smaller (usually ca. 10 nm) Figure 4) and more numerous than those formed w other acrylates, although in terms of mass, the amou were about the same.

Secondary growth particles, where obtained, were mediately apparent by their small size. In the absenc secondary growth it was possible to prove, by a m balance calculation, that all the monomer added could accounted for, within experimental error, by the incre in size of the particles. By performing this calculation reverse, it would be possible to calculate the amoun monomer required to produce a given coat thickness, a thus to "tailor-make" overcoated latices.

Table I. Results of Seeded Growth Reactions

	Latex			
	MC4	MC9	MC31	MC11
seed latex	MC1	MC1	MC26	MC8
size/nm	480	480	440	440
σ/nm	7.0	7.0	8.3	6.6
solids content, %	8.0	8.0	6.9	2.7
volume/cm^3	50	250	425	500
particle no. density/cm^{-3}	1.3×10^{11}	6.5×10^{11}	1.4×10^{12}	5.3×10^{11}
	Monomer			
	MMA	MMA	MMA	EA
volume/cm^3	16	11	50	15
initiator/g	0.16	0.25	0.25	0.25
water/cm^3	450	250	50	50
temp/K	353	353	353	353
total polymerization time/min	180	180	1385	180
	Product			
particle size/nm	530, 140	500, 65	470	440–450, 10
σ/nm[b]	5.7, 6.3	7.2, 4.1	3.6	
	bimodal	bimodal	monodisperse	polydisperse
solids content, %	3.6	5.6	9.6	7.2
conversion, %	94	77	25[a]	92

[a] Latex had coagulated during reaction. [b] σ's for large and small particles of bimodal size distribution reported separately.

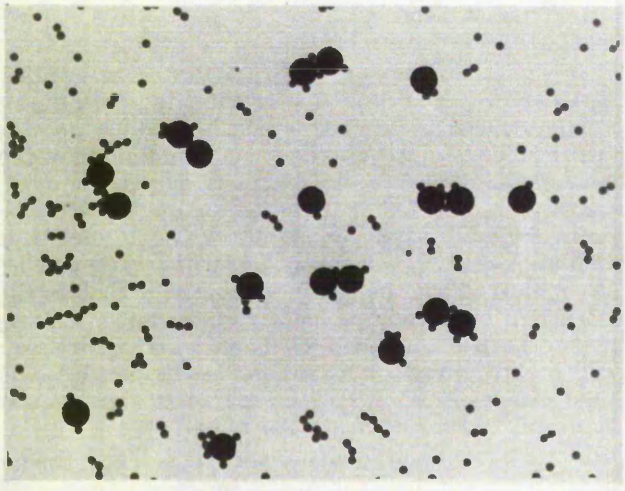

Figure 2. MC4 poly(methyl methacrylate) coated polystyrene prepared by seeded growth method. Magnification, 6950.

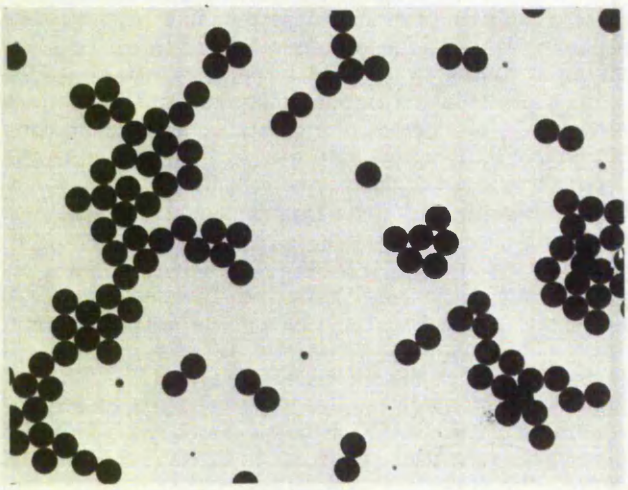

Figure 3. MC5 poly(methyl methacrylate) coated polystyrene prepared by shot-growth method. Magnification, 6950.

Discussion

1. Role of Swelling. Although outwardly similar to the seeded growth method, it is apparent from the above

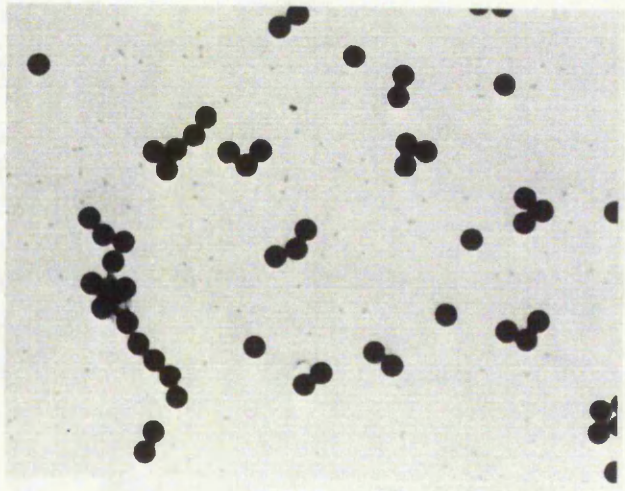

Figure 4. MC11 poly(ethyl acrylate) coated polystyrene prepared by seeded growth method. Magnification, 6700.

results that the shot growth technique operates via a somewhat different mechanism to the heterocoagulation mechanism proposed by Chung-Li et al. (1976) for seeded growth. The principal difference between the two methods is, of course, the presence or residual monomer in the core particles at the stage at which the coating monomer is added. This residual monomer has been shown to have a profound effect on the rate of swelling (Table III).

Different aspects of swelling have been studied by Morton et al. (1954), Chung-Li et al. (1976), Ugelstad and Mørk (1980), and Goodwin et al. (1980). However, the systems studied varied widely and no clear picture emerges. Morton et al. derived an equation showing that equilibrium uptake varied with particle size. They confirmed the validity of their treatment with swelling experiments on polystyrene latices with a range of particle size 37–173 nm and molecular weights 10^5–10^7. They also showed that the equilibrium uptake of toluene was rapid, being attained within 30 min. Ugelstad and Mørk, working with low molecular weight oligomer, were able to achieve large uptakes very rapidly. Chung-Li et al. found that the swelling of large particles (>2 μm) took place very slowly

Table II. Results of Shot-Growth Reactions

	Latex										
	MC5	MC45	MC19	MC10	MC64	MC78	MC42	MC71	MC92	MC65	
core latex size/nm	400	410	370	460	414	417	420	436	238	446	
σ/nm	7.0	4.3	6.1	6.2	10.3	6.8	6.7	8.3	19.9	14.7	
solids content %	5.9	0.69	4.92	6.74	7.38	67.6	7.7	8.4	1.6	8.4	
particle no. density/cm^{-3}	1.7×10^{12}	1.7×10^{11}	1.9×10^{12}	1.3×10^{12}	1.9×10^{12}	1.7×10^{12}	2.0×10^{12}	1.84×10^{12}	2.1×10^{12}	1.7×10^{12}	
	Monomer										
	MMA	MMA	MA	EA	EA	BA	BMA	BMA	BMA	33% MMA/ 67% EA	
volume/cm^3	16	12	7	16	10[a]	20	20	40	10	30[a]	
initiator/g	0.5	0.12 + 0.95	0.5	0.5	0.5	0.5	0.5	0.5	0.5	0.5	
temperature/K	353	353	353	353	353	353	353	353	353	353	
polymerization time/min	300	250	290	295	315	340	180	795	230	270	
	Product										
size/nm	490	540	530	480–510	471	526	560	512	333	497	
σ/nm	7.7	6.8	3.6	3–10	15.4	21.4	7.4	22	68.1	14.7	
solids content, %	11.4	2.7	11.34	12.0	11.4	13.7	15.2	14.7	5.16	13.5	
conversion, %	55	24	92	95	117	117	106	88.1	85.9	91.3	
particle no. density/cm^{-3}	1.9×10^{12}	3.1×10^{11}	1.45×10^{12}		2.0×10^{12}	1.7×10^{12}	1.8×10^{12}	2.0×10^{12}	2.5×10^{12}	2.0×10^{12}	

[a] Monomers added at constant low rate of 0.2 cm^3 min^{-1}.

(Table III), even when the polymer was freshly forme and contained residual monomer. Goodwin et al. ha recently studied the rate of swelling as a function of t cleaning technique. They found that swelling occurr quite rapidly, irrespective of cleaning technique (dialys ion exchange, and steam-stripping). Unfortunately, th do not report the monomer contents of the latices pri to swelling.

The rate of swelling of polystyrene by styrene, as d termined by PCS, was greater in the presence of residu monomer (6.6%) than in its absence (Table III) as mig be expected. However, both results were lower than t rate obtained by Goodwin et al. for a steam-stripped late which should contain no monomer (Table III). A low result was observed for the swelling of polystyrene co taining residual monomer with butyl methacrylate and th is presumably due to the greater incompatibility of t more polar monomer.

Comparison of the rate of swelling of polystyrene l styrene and the rate of growth indicates that the diffusi of monomer into the particle is not rate determinin However, the propagation rate of butyl methacrylate (a of other acrylate monomers) is faster than that of styren and this, coupled with a lower swelling rate, suggests th absorption into the particle is the limiting step. Hence neither case is there any need to postulate a heter coagulation mechanism for the shot-growth process.

2. Overcoating of Core Polymer Particles. Neith TEM nor PCS would be able to show the presence secondary nuclei prior to heterocoagulation with the co in the former case because their size would be below t limit of resolution of the instrument, and in the latt because their contribution to the light scattering would swamped by that of the larger particles. In principle, should be possible, by assuming a constant particle numb density throughout the coating reaction, to deduce t presence or absence of secondary nuclei by calculati whether the increasing solids contents during the reacti could be accounted for by the increasing particle siz Unfortunately, the errors inherent in the size measureme render this test insufficiently sensitive.

Besides increasing the rate of particle swelling, the r sidual monomer will also influence the polymerization the coating monomer. In this respect, it is interesting note the results of Mangeraj and Rath (1972), in particul the effect of a small amount of styrene increasing the ra of polymerization of acrylate monomers, in emulsion c polymerization systems. Thus, the overcoating reacti is very sensitive to the amount of styrene remaining in t particle. In some cases, the reaction had reached co pletion in a shorter time than was predicted from the ra of pure acrylate emulsion polymerization.

It has been argued above that the locus of polymeriz tion of the coating monomer is likely to be at the par cle/water interface whereas the residual styrene will p lymerize within the core. However, consideration has be given to the fact that a large amount of the monom remains in the aqueous phase, and its behavior there w strongly influence the outcome of the reaction. The so ubilities in water, and rates of polymerization, of acryla monomers are greater than those of styrene. This w promote the formation of oligomeric radicals, which wou normally be expected to micellize or coagulate to for secondary growth. That this does not occur is presumab due to a high capture efficiency of the core particles. is suggested that this high capture efficiency is due to t shell monomer actively polymerizing at the particle/wat interface and thus becoming covalently bound to the co

Table III. Rates of Swelling and Growth

A. Styrene/Polystyrene

	latex			Chung-Li et al., flask B	Goodwin et al., steam-stripped
	MC88	MC85	ARG62A		
monomer content, %	6.6	0	growth	not stated	0[a]
initial size/nm	160	572	222	2890	425
final size/nm	182	588	290	2930	512
time/min	10	10	28	60	10
temperature/K	353	353	353	333	298
10^3 rate/cm^3 min^{-1} cm^{-3}	47.2	8.63	4.39	1.50	7.48

B. Butyl Methacrylate/Polystyrene

	latex			latex	
	MC89	MC92		MC89	MC92
monomer content, %	6.6	growth	time/min	10	10
initial size/nm	160	259	temperature/K	353	353
final size/nm	173	282	10^3 rate/cm^3 min^{-1} cm^{-1}	26.4	29.1

[a] Assumed, since latex steam-stripped.

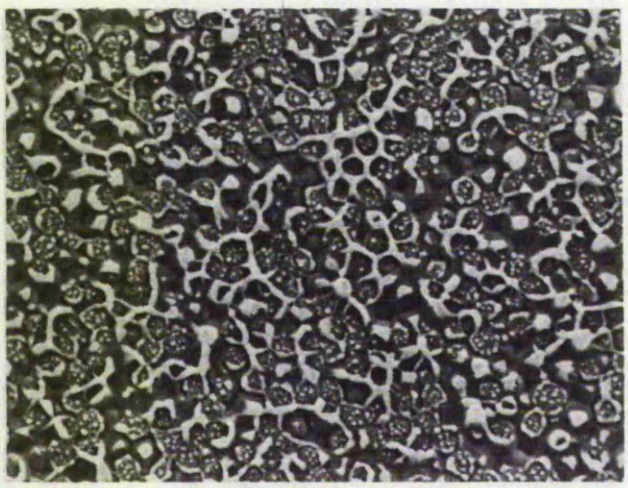

Figure 5. SEM of fracture cross section of film cast from latex MC10 (prepared by shot-growth method). Magnification, 6165.

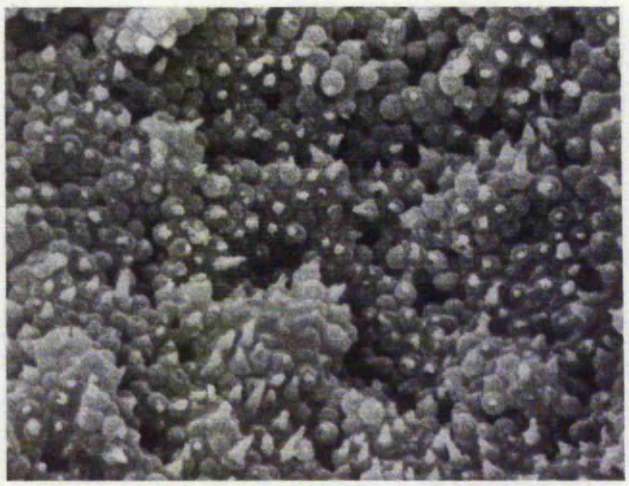

Figure 6. SEM of fracture cross section of film cast from latex MC11 (prepared by seeded growth method). Fractured at 293 K. Magnification, 6165.

particle and thereby unable to transfer back out of the particle.

Evidence for the direct combination of acrylate monomer units with free radicals at the core particle surface comes from a comparison of scanning electron micrographs of films cast from overcoated latices. Figure 5 shows the fractured edge of a film cast from latex MC10 (prepared by the shot-growth technique). There is a clear contrast between the polystyrene core particles (dark) and the polyacrylate coat (light) which has presumably been stripped off the polystyrene core and then has collapsed back on fracture. The small globules adhering to the core particles have been interpreted as polyacrylate chains directly bound to the core particle surface. Clearly, this direct combination cannot occur during a seeded growth reaction, and this is confirmed by Figures 6 and 7, which show fractured edges of a film cast from latex MC11 (prepared by the seeded growth technique). Figure 6 shows an edge fractured at room temperature, revealing a separation of the acrylate coat from the underlying seed particles, some of which have anomalous regions observed by Cox et al. (1977). None of the exposed core particles shows the small globules of acrylate polymer.

Figure 7 shows an edge which was fractured at liquid nitrogen temperature in order to retard the flow of coating polymer as much as possible. Here, some of the coating polymer remains attached to the seed particles. Where this occurs there is only one globule per seed particle (cf. Figure 5, where several small globules are attached to each core particle) and no globules are visible on seed particles displaying anomolous regions. This indicates that at room temperature, extensive coating polymer flow occurs on fracture and that polymer contained in the anomolous regions is removed. This suggests that direct binding of

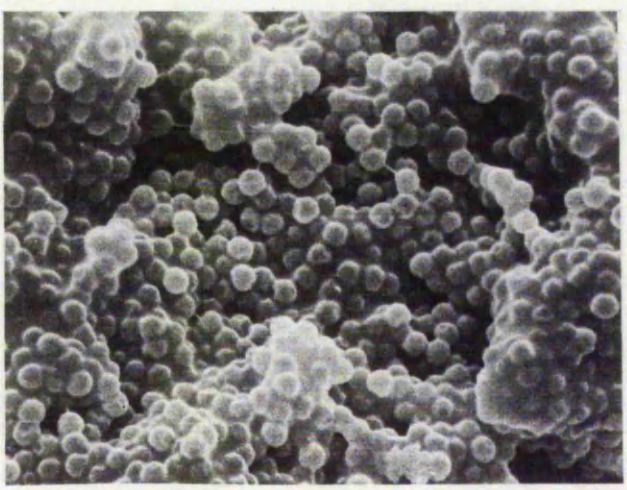

Figure 7. SEM of fracture cross section of film cast from latex MC11. Fractured at 77 K. Magnification, 6165.

coating polymer to core particles occurs in the shot-growth process, as is demonstrated by the retention of acrylate polymer on the core particles for the "shot-growth" fracture section at room temperature.

Literature Cited

Chalney, M.; Hearn, J.; Wilkinson, M. C. *Br. Polym. J.* **1981**, *13*, 132.
Chung-Li, Y.; Goodwin, J. W.; Ottewill, R. H. *Progr. Colloid Polym. Sci.* **1976**, *60*, 163.
Cox, R. A.; Wilkinson, M. C.; Creasey, J. M.; Goodall, A. R.; Hearn, J. *J. Polym. Sci.* **1977**, *15*, 2311.
Goodall, A. R.; Randle, K.; Wilkinson, M. C. *J. Colloid Interface Sci.* **1980**, *75*(2), 493.
Goodman, D.; Isgur, I. E.; Wacome, D. M. U.S. Patent 3 397 165, 1968.
Goodwin, J. W.; Ottewill, R. H.; Harris, N. M.; Tabony, J. *J. Colloid Interface Sci.* **1980**, *78*, 253.
Goodwin, J. W.; Ottewill, R. H.; Pelton, R.; Vianello, G.; Yates, D. E. *Br. Polym. J.* **1978**, *10*, 173.
Greene, B. W. *J. Colloid Interface Sci.* **1973**, *43*, 449, 462.
Hearn, J. Ph.D. Thesis, Bristol University, Bristol, England, 1971.
Hearn, J.; Wilkinson, M. C.; Goodall, A. R. *Adv. Colloid Interface Sci.* **1981**, *14*, 173.
Herman, D. F.; Resnick, A. L.; Simone, D. U.S. Patent 3 265 644, 1966.
Mangeraj, D.; Rath, S. B. *Polym. Prepr., Am. Chem. Soc., Div. Poly Chem.* **1972**, *13*(1), 349.
Meier, G. L. U.S. Patent 3 575 913, 1971.
Morton, S.; Kiazerman, S.; Altier, M. W. *J. Colloid Interface Sci.* **1954**, 300.
Munro, D.; Goodall, A. R.; Wilkinson, M. C.; Randle, K.; Hearn, J. *J. Col Interface Sci.* **1979**, *68*(1).
Pfluger, H. L.; Gebelin, C. G. U.S. Patent 3 291 763, 1966.
Ryan, C. F.; Crochowski, R. J. U.S. Patent 3 426 101, 1969.
Sakota, K.; Okaya, T. *J. Appl. Polym. Sci.* **1976**, *20*, 1735.
Settlage, P. H. U.S. Patent 3 309 330, 1967.
Ugelstadt, J.; Mørk, P. C. *Adv. Colloid Interface Sci.* **1980**, *13*, 101.
Williams, D. J. *J. Polym Sci., Polym. Chem. Ed.* **1974**, *12*, 2123, and references cited therein.

Received for review August 24, 19
Accepted March 2, 19

Paper presented at the 4th International Conference on Surfa and Colloid Science, Jerusalem Israel, July 5–10, 1981.